Institut für Produktionstechnik

Forschungsberichte aus dem
wbk Institut für Produktionstechnik
Karlsruher Institut für Technologie (KIT)

Fabian Johannes Ballier

Systematic gripper arrangement for a handling device in lightweight production processes

Band 222

Research report from
wbk Institute of Production Science
Karlsruhe Institute of Technology (KIT)

Editor: Prof. Dr.-Ing. Jürgen Fleischer
Prof. Dr.-Ing. Gisela Lanza
Prof. Dr.-Ing. habil. Volker Schulze

Research report
Fabian Johannes Ballier

Systematic gripper arrangement for a handling device in lightweight production processes

Volume 222

Systematic gripper arrangement for a handling device in lightweight production processes

Zur Erlangung des akademischen Grades eines / einer

DOKTORS / DOKTORIN DER INGENIEURWISSENSCHAFTEN (Dr.-Ing.)

von der KIT-Fakultät für Maschinenbau des

Karlsruher Instituts für Technologie (KIT)

genehmigte

DISSERTATION

von

Dipl.-Ing. Fabian Johannes Ballier

Tag der mündlichen Prüfung:	03.12.2018
Hauptreferent:	Prof. Dr.-Ing. Jürgen Fleischer
Korreferent:	Prof. Dr.-Ing. Jill Urbanic

Bibliographic information published by the Deutsche Nationalbibliothek
The Deutsche Nationalbibliothek lists this publication in the Deutsche Nationalbibliografie; detailed bibliographic data are available in the internet at http://dnb.d-nb.de.

Zugl.: Karlsruhe, Karlsruher Institut für Technologie, Diss., 2018

Copyright Shaker Verlag 2019
All rights reserved. No part of this publication may be reproduced, stored in a retrieval system, or transmitted, in any form or by any means, electronic, mechanical, photocopying, recording or otherwise, without the prior permission of the publishers.

Printed in Germany.

ISBN 978-3-8440-6704-0
ISSN 0724-4967

Shaker Verlag GmbH • Am Langen Graben 15a • 52353 Düren
Phone: 0049/2421/99011-0 • Telefax: 0049/2421/99011-9
Internet: www.shaker.de • e-mail: info@shaker.de

Preface by editor

The fast and efficient implementation of innovative technologies is supported by the following factors. The globalization of the economy is the decisive economic factor for manufacturing companies. As "value-added partners", universities can make a significant contribution to the competitiveness of industry by developing scientific foundations, new methods and technologies as well as actively supporting the implementation process in practical applications. Against this background, this series of publications will report the current research results of the Institute of Production Engineering (wbk) at the Karlsruhe Institute of Technology (KIT). Our research work is concerned with increasing the performance of manufacturing processes, associated machine tool and handling technologies as well as with the holistic consideration and optimization of the entire production system. On the same time technological and organizational aspects are considered here.

Prof. Dr.-Ing. Jürgen Fleischer

Prof. Dr.-Ing. Gisela Lanza

Prof. Dr.-Ing. habil. Volker Schulze

Preface by author

This work was created during my work as a research associate at the wbk Institute for Production Engineering of the Karlsruhe Institute of Technology (KIT) since March 2014.

First of all, I would like to thank Prof. Dr.-Ing. Jürgen Fleischer for taking over the main referent and for five years of successful cooperation. The freedom of decision that he grants to his research associate is one of the reasons why they have the opportunity to develop themselves professionally and personally. I would also like to thank my co-referent Prof. Dr.-Ing. Jill Urbanic for constructive discussions and the productive visit that I was able to experience in Canada, which helped me a lot in my dissertation.

My institute colleagues were an important support for me in the creation of this work, taking time for me despite having a full schedule. The friendly and open atmosphere of our institute is an important aspect of our success and I hope it will be preserved. I would also like to express my special thanks to the numerous staff members at the institute who make it possible for the research associates to work scientifically to this extent in the first place. In addition, I would like to thank the workshop employees, all colleagues in the IT, secretariats and finance department who take over a lot of the organizational work from us, which enables us to carry out our research. I think we all know that the scientific staff sometimes causes more chaos than necessary.

I would also like to mention my students who contributed to the success of this work. I would especially like to mention Michael Steinlein, Moritz Gegenbauer, Tobias Dmytruk, Uli Hörmann and Amal Abderrahman for their support.

Writing a dissertation always involves a great deal of time, which has a considerable influence on leisure activities. For this reason, such work is only possible if friends and family support this project which is not self-evident.

I would like to thank my friends for understanding that I did not always have time for them. Furthermore, I have to thank my wife for the time she gave me to write my thesis and most importantly I would like to thank my parents who have always given me the right measure of freedom and support so that I can write these lines today. You have all been directly or indirectly involved in this work and have been an important part of my life. Thanks to all of you.

Karlsruhe, Dezember 2018

Fabian Johannes Ballier

wbk
Institute of Production Science

KIT
Karlsruhe Institute of Technology

Abstract

Handling devices are an integral part of automated production processes. Nevertheless, they are generally regarded as non-value-adding and therefore their planning and projecting should be as effective as possible, with only a small amount of time and personnel expenditure. Still, they remain an important part of the process chain and they must meet certain conditions in this context. In order to ensure their functionality and invest little time in their project planning, handling devices are often oversized. Especially for flat parts, this results in heavy handling solutions where the weight of the object and the handling device are in a disproportionate relationship.

The objective of the present work is to automate the project planning of handling devices as much as possible. This process is presented using the example of the process chain for the production of lightweight parts using the sheet molding compound (SMC) and resin transfer molding (RTM) processes.

As a first step, a modular handling device is developed and built-up, which enables a large number of gripper arrangements. This device then makes it possible to measure the resulting deflection of flat parts in the handling process. In order to ensure that it is not always necessary to measure the deflections, a model is built-up with ABAQUS to enable a simulated estimation. Using this simulation model, a design logic for the arrangement of the grippers on any shaped parts is presented.

This design logic works in two steps and is based on the approach of growing neural gas (GNG), which is adapted to the problem by implementing additional rules. First, an initial gripper configuration is created based on the geometry of the object, which is then improved by an iterative process of simulation and adaptation. Since the production of lightweight parts often requires more than just one type of sheet, various solutions for the different sheets are combined systematically at the end to form one gripper arrangement and a method is shown concerning how this can be implemented using the previously developed modular handling device.

Kurzfassung

Handhabungsgeräte sind ein integraler Bestandteil automatisierter Produktionsprozesse. Dennoch werden sie in der Regel als nicht wertschöpfend angesehen, weshalb ihre Planung und Projektierung mit geringem Zeit- und Personalaufwand so effektiv wie möglich sein sollte. Gleichzeitig bleiben sie ein wichtiger Teil der Prozesskette und müssen in diesem Zusammenhang bestimmte Bedingungen erfüllen. Um ihre Funktionalität zu gewährleisten und wenig Zeit in die Projektierung zu investieren, sind Handhabungsgeräte oft überdimensioniert. Insbesondere bei flachen Teilen führt dies zu schweren Handhabungslösungen, bei denen das Gewicht des Handhabungsobjekts und des Handhabungsgerätes in einem Missverhältnis zueinander stehen.

Ziel der vorliegenden Arbeit ist es, die Projektierung von Handhabungsgeräten so weit wie möglich zu automatisieren. Dieser Prozess wird am Beispiel der Prozesskette zur Herstellung von Leichtbauteilen mit den Verfahren „sheet molding compound“ (SMC) und „resin transfer molding“ (RTM) dargestellt.

In einem ersten Schritt wird ein modulares Handhabungsgerät entwickelt und aufgebaut, das eine große Anzahl von Greiferanordnung ermöglicht. Mit diesem Handhabungsgerät kann dann die resultierende Durchbiegung von flachen Bauteilen mit verschiedenen Greiferanordnungen gemessen werden. Um sicherzustellen, dass es nicht immer notwendig ist die Durchbiegungen zu messen, wird mit ABAQUS ein Modell aufgebaut, das eine Simulation der Durchbiegung ermöglicht. Anhand dieses Simulationsmodells wird eine Designlogik für die Anordnung der Greifer entwickelt.

Diese Designlogik arbeitet in zwei Schritten und basiert auf dem Ansatz des „growing neural gas“ (GNG), das durch die Implementierung zusätzlicher Regeln an das Problem angepasst wird. Zuerst wird eine erste Greiferkonfiguration basierend auf der Geometrie des Objekts erstellt, die dann durch einen iterativen Prozess aus Simulation und Anpassung verbessert wird. Da die Herstellung von Leichtbauteilen oft mehr als nur einen Zuschnitt erfordert, werden am Ende systematisch verschiedene Lösungen für die verschiedenen Zuschnitte zu einer Greiferanordnung zusammengefasst und ein Verfahren gezeigt, wie dies ‚mit dem zuvor entwickelten modularen Handhabungsgerät realisiert, werden kann.

Table of contents

Table of contents **I**

Table of abbreviations **IV**

1 Introduction **1**

1.1 Motivation 1

1.2 Structure of the thesis 3

2 Background **4**

2.1 Terms and definitions 4

2.2 Materials for lightweight production processes 5

2.2.1 From Co- to Dico- to CoDico-material 5

2.2.2 Dry fiber textiles 6

2.2.3 Pre-impregnated materials 7

2.3 Representation of a handling process by VDI 2860 8

2.4 Machine learning 10

2.4.1 Basic concepts of unsupervised machine learning 10

2.4.2 Self-organizing maps 12

2.4.3 Neural gas 13

2.4.4 Growing cell structure 13

2.4.5 Growing neural gas 14

3 State of the art **17**

3.1 Lightweight production processes 17

3.1.1 RTM process 17

3.1.2 SMC process 20

3.2 Gripper technologies for flat non-rigid parts 21

3.2.1 Introduction of gripper technologies for flat non-rigid parts 21

3.2.2 Conclusion on gripper technologies for flat non-rigid parts 24

3.3 Energy consumption of handling processes 25

3.4 General classification of gripper arrangements 27

3.5 Research fields for handling flat non-rigid parts 27
3.5.1 Development and dimensioning of grippers 28
3.5.2 Selecting gripper technology 29
3.5.3 Handling device design/ conception 29
3.6 Conclusion from the state of the art 32
4 Objective and own approach 35
4.1 Objective 35
4.2 Own approach 35
4.3 Thesis procedure 38
5 Experimental setup for handling processes 40
5.1 Handling device 40
5.1.1 Requirements for handling devices in lightweight production processes 41
5.1.2 System design of the modular handling device 48
5.2 Test setup for reproducible handling operations 56
5.3 Test procedure and systematic description 58
5.4 Use-cases for handling tests for RTM and SMC process 60
5.4.1 Use-cases for SMC 60
5.4.2 Use-cases for dry fiber textiles in the RTM process 60
6 Simulation and measurement of material deflection 62
6.1 Definition of the system boundaries 62
6.1.1 Acceleration and velocity in a vertical handling process 62
6.1.2 Experimental analysis of time behavior 65
6.2 Simulation model and acquisition of material data 67
6.2.1 Selection of a simulation model 68
6.2.2 Material data for the simulation 73
6.3 Comparison of simulation results and scan results 77
6.3.1 Configuration of the simulation 78
6.3.2 Processing of scan data 78
6.3.3 Comparison of measured scan data and simulated data 83

7 Gripper configuration 90

7.1 Concepts for an initial gripper configuration process 90

7.1.1 Initial gripper configuration by full-body gripper 91

7.1.2 Initial gripper configuration by pre-simulated basic geometries 91

7.1.3 Initial gripper configuration by self-organizing maps algorithm 95

7.1.4 Conclusion of the different approaches 98

7.2 Initial gripper configuration without specific deflection data of the shape 99

7.2.1 Modification of GNG for initial gripper configuration 99

7.2.2 Influence of parameters on the initial gripper configuration 104

7.2.3 Initial gripper configuration for use-cases 118

7.2.4 Conclusion for initial gripper configuration 122

7.3 Adjustment of gripper configuration with deflection data 122

7.3.1 Modification of GNG for the gripper configuration adjustment 123

7.3.2 Gripper configuration for use-cases 130

7.3.3 Conclusion for gripper configuration adjustment 135

7.4 Number of grippers to maintain a user defined deflection 135

8 Solution composition 136

8.1 Combination of solutions to one gripper configuration 136

8.2 Implementation on the modular handling device 141

9 Summary and Outlook 148

9.1 Summary and conclusion 148

9.2 Outlook 151

10 References I

List of figures XIV

List of tables XX

List of source code XXI

Appendix XXII

Table of abbreviations

Symbol	Measurements	unity
CAD	Computer-aided design	
CCU	Central control unit	
CFD	Computer fluid dynamics	
CNC	Computerized numerical control	
Co	Continuous	
Dico	Discontinuous	
CoDico	Continuous-discontinuous	
DCU	Decentral control unit	
FEA	Finite element analysis	
FRP	Fiber reinforced polymers	
GNG	Growing neural gas	
GCS	Growing cell structure	
GUI	Graphical unit interface	
JSON	Java script object notation	
LOS	Line of sight	
NG	Neural gas	
ODP	Open document presentation	
RC	Robot control	
RTM	Resin transfer molding	
HP-RTM	High-pressure RTM	
SMC	Sheet molding compound	
SOM	Self-organizing maps	
STL	Standard tessellation language	
TCP	Tool center point of the industrial robot	
UD	Unidirectional	

Symbol	Measurements	unity
A	Area	[mm^2]
a	Acceleration	[mm/s^2]
B	Bending stiffness	[N*mm^2]
c_w	Drag coefficient	[-]
d	Distance between neuron and input data point	[mm]
D_Z	Deflection of an object in Z-direction	[mm]
D_{Z_MAX}	Maximum deflection in Z-direction of a part	[mm]
ER	Error GNG	[mm]
E_1, E_2	Elasticity modulus	MPa
ΔE_{Crit}	Error criterion	[mm]
G_{12}	Shear modulus	MPa
g	Acceleration due to earth's gravity	[m/s^2]
$Grid_{Spacing}$	Discretized representation of parts parameter	[mm]
I	GNG: Iteration counter	[-]
I_{max}	GNG: Maximum iterations	[-]
K	Counter reference vectors / neurons	[-]
L	GNG: Criteria for adding new neurons	[-]
$l_{Ü}$	Overhang	[mm]
M_{ϵ_n}	Multiplier for ϵ_n	[-]
m	Mass	[g]
N_{max}	GNG: Maximum number of neurons	[-]
$Point_{Weight}$	Weighting factor	[-]
$\boldsymbol{REF_1}, \boldsymbol{REF_2}, \dots$	Reference object center	[mm]
$\boldsymbol{REF_{Center}}$	Center of experiment setup calculated	[mm]
$\boldsymbol{REF_{Vector}}$	Reference vector in experiment setup	[mm]
tex	Weight of a roving	[g/km]

Symbol	Measurements	unity
v	Velocity	[mm/s]
$\boldsymbol{w}$	Neurons in SOM or SOM derivates	[mm]
α	GNG: Reduction coefficient of error	[-]
ϵ_b	GNG: Adjustments to the winner	[-]
ϵ_n	GNG: Adjustments to the neighbor	[-]
ϵ_{b_FEA}	GNG: Adjustments to the winner using FEA	[-]
ϵ_{b_Final}	Adjustments to the winner using in final round	[-]
ϵ_{n_FEA}	GNG: Adjustments to the neighbor using FEA	[-]
ϵ_{n_Final}	Adjustments to the neighbor using in final round	[-]
$\boldsymbol{\xi}$	Input data set for SOM or SOM derivates	[mm]
ρ_{Air}	Air density	[g/mm^3]
$\rho_{Textile}$	Weight per area of textile	[g/mm^2]
v_{12}	Poission’s ratio	[-]
τ	Error reduction parameter of GNG	[-]
ω	Longitudinal force	[N/mm]

1 Introduction

1.1 Motivation

The automation of production processes caused by the industrial revolution is crucial for economic production in high developed countries (Marsh 2012, p 182; Allen 2017, p 323). Usually a product must pass through several process steps that add value to it by generating features (Arnold & Furmans 2009, p 20). Such process steps are executed by different machines and can include an assembly step, milling, welding, heat treating, painting and many others (Stephens & Meyers 2013, p 20). On the other hand automated production also needs systems, which link the different value-adding machines together (Diebold 1952).

This process is called handling, whereby Hesse (2016) defines the handling operation by creating, modifying or temporarily maintaining a pre-defined spatial arrangement of geometrically-determined bodies in a reference coordinate system, without any intended changes to the object itself. Handling is an operation occurring in workstations and production facilities. Other conditions can be specified, such as time, quantity and the movement path. (Hesse 2016, p 11)

The handling system normally includes a kinematic device like an industrial robot and a gripping mechanism to fulfill this task (Hesse 2016, p 11). Since this thesis only considers the device on the tool center point (TCP) of the robot the term “handling device” will be used as an identical definition. The handling device can be realized with a wide range of different gripper technologies. Which gripper technology should be used, how many grippers are necessary and where the grippers should hold the object is mostly influenced by the geometry and properties of the object (Fantoni et al. 2014, p 684). The selection of a gripper technology is mostly influenced by the material properties only and thus is often solved by a selection matrix considering the material properties (Fantoni, Capiferri & Tilli 2014, p 331; Gutsche 1993, p 34; Stephan 2001, p 21; Reinhart, Straβer & Ehinger 2009, p 185).

The number and arrangement of grippers is also influenced by the geometry of the object. The larger the object and the lower the stiffness of the used material, the more easily it can lead to deflections in the handling process. This is especially the case with flat objects like textiles, since they have only a small expansion in thickness direction. As a result, the arrangement of the grippers on such an object is important to avoid unwanted deflections of the object which could lead to collisions with the surrounding, folding edges or unexpected releasing from the gripper (Fantoni et al. 2014, p 686; Biermann, Hufenbach & Seliger 2008, p 22). Such handling operations hold interest in the production of fiber reinforced polymers (FRP) parts or the normal textile industry (Reinhart & Straßer 2011, p 303; Tai et al. 2016; Saadat & Nan 2002).

These effects can be avoided if the flat non-rigid object is held at several points. Different solutions are possible. The first solution can be defined as full-body gripping concept. This could be achieved by using one huge gripper surface or the combination of multiple individual gripping elements close together (Gutsche 1993, p 19). Such a handling device can handle different shapes without the need of a hardware reconfiguration. Hereby, the device is attractive for small production quantities (Reinhart & Straßer 2011, p 302). The downside of having this flexibility without the need of a hardware reconfiguration is having an oversized handling system. It has more gripper elements or a larger gripper surface than it needs most of the time and thus it consumes more energy by using more grippers in comparison with a customized solution. Furthermore, more grippers or a larger gripper surface as necessary also result in more weight and have a direct impact on the energy consumption of the robot holding the handling device (Rassõlkin, Hõimoja & Teemets 2011, p 3; Paryanto et al. 2014, p 132). Figure 1-1 shows an example of an oversized and customized handling solution holding a triangle part.

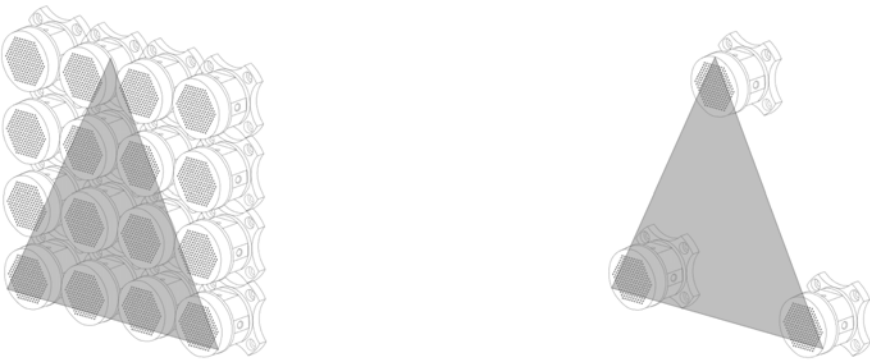

Figure 1-1: Example of an oversized (left) and a customized handling solution (right)

This increased energy consumption becomes interesting in mass production application (Mohammed et al. 2014, p 400; Chemnitz, Schreck & Krüger 2011, p 1). One solution for this is the design of customized handling devices for handling tasks. It is important that these solutions are not oversized or there will be no benefit at all. The problem is that a customized solution requires an engineering process involving human creativity and experience.

Therefore, this thesis aims to develop a systematic and programmable approach to generate customized handling solutions that takes the material behavior and the geometry of the objects into account. The examinations are carried out using the examples of lightweight production processes. These processes using flat and non-rigid objects like dry carbon fiber textiles or SMC and are thus a challenge in handling operations.

1.2 Structure of the thesis

Beginning with the technical background for this thesis in **chapter 2**, **chapter 3** will then present the state of the art of handling devices for flat non-rigid parts. Furthermore, existing systematic approaches for the design of such handling devices will be presented to identify the open research issue for this thesis. **Chapter 4** will explain the further approach in this thesis. This approach starts in **chapter 5** with the development of an experimental setup to enable reproducible handling operations for further investigations. One element of this experimental setup is a modular handling device. Furthermore, the boundary conditions for the handling process of flat non-rigid parts will be defined. In order to take the deformation in the handling process into account, a simulation model is set up and tested in **chapter 6.** The approach for the design of the handling device is separated into different steps, which will be discussed in **chapter 7.** First, in **chapter 7.1** different possible methods are introduced and it is discussed how a gripper arrangement can be generated automatically. **Chapter 7.2** presents a method for the distribution of the grippers without initially considering the deformation of the part. In **chapter 7.3**, this approach is extended, taking the deformation of the part into account. Since a handling device must often be able to handle different kinds of shapes, **chapter 8** will present the combination of gripping solutions for different parts to one. Moreover, the implementation of a modular handling device will be discussed. These steps will be conducted on an example task, which should validate the whole approach in this thesis.

2 Background

This chapter aims to summarize the basics necessary for understanding this thesis. First of all, the terms used in this dissertation will be defined more precisely to distinguish them more clearly from other work. Subsequently, a brief explanation of materials that are used will be provided. In order to approach the topic of the handling process systematically, the procedure is described by using the VDI 2860. Because of that, the basics of the VDI 2860 will also be explained in this chapter. Finally, a brief introduction to the topic of machine learning is given. The explanations focus on unsupervised algorithms, since they will be used in this thesis to arrange grippers on different flat parts.

2.1 Terms and definitions

The terms “handling device” and “handling system” are widely used, colloquially known and thus often only blurredly defined. Hesse (2016, p 11) defines the gripper itself and a robot or other kinematics for the realization of movements as essential components of a handling system. What is not mentioned here are the additional supporting structures between the gripper and the robot, which connect them together.

Such support structures are an integral part of every handling device and are often assembled from simple modular aluminum structures, which can be seen in many publications as well as in practice (M. Kordi, M. Hüsing, B. Corves 2007, p 3; Glorieux 2017, p 22; Gerngross & Nieberl 2016, p 8). This definition can be clarified by Figure 2-1 based on Hesse (2011, p 16).

The representation of Hesse (2011, p 16) was extended by the force flow from the robot via the quick-change system and the supporting structure to the gripper, ensuring that the gripper is held by the robot (Figure 2-1). According to the illustration, the robot holds the handling device via the quick-change system. All other resources such as electrical energy, information and pneumatic pressure are brought into the handling device in the same way. The support structure is normally permanently connected to the quick-change system and it also connects all individual components of the handling device. Information is also exchanged, which then controls an electric motor via a drive control system or switches a valve, which is then a type of energy converter.

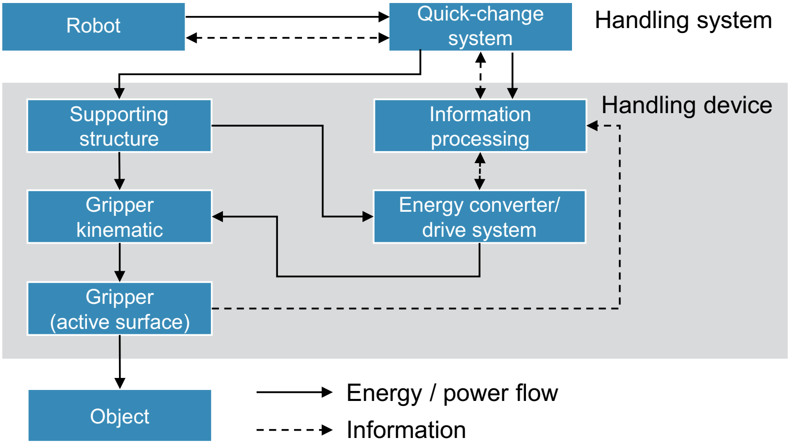
Robot
Quick-change system
Handling system
Supporting structure
Information processing
Handling device
Gripper kinematic
Energy converter/ drive system
Gripper (active surface)
Object
Energy / power flow
Information

Figure 2-1: Own extended representation of force, information and energy flow based on Hesse (2011, p 16)

If multiple individual grippers are used on a handling device to transport a part, these grippers must placed in specific positions. Their number and positioning will therefore be referred to in the following as the gripper configuration.

2.2 Materials for lightweight production processes

FRP - as the name indicates - are always made of a fiber material surrounded by a polymer matrix system (Ishikawa et al. 2018, p 223; Friedrich 2016, p 1). Differences in FRP exist with respect to fiber material, matrix material, fiber length and fiber orientation (Assmann & Witten 2013, p 295; Cherif 2016, p 14; Assmann & Witten 2013, pp 38–107). Depending on these parameters, different processes exist for the production of a part. Whether the fibers are already pre-impregnated with matrix system (prepreg) or dry (not pre-impregnated) has a major influence on the manufacturing process. In addition, both categories can be distinguished according to whether they are FRP with continuous (Co) or discontinuous fibers (Dico). These decisive differences will be explained further.

2.2.1 From Co- to Dico- to CoDico-material

The length of the fibers in FRP has a major influence where the components can be used. When using Co-fibers the length of the fibers is matched with the dimensions of the part, which results in higher mass specific properties in the finished components

(Friedrich 2017, p 407; Henning & Moeller 2011, p 379; Cherif 2016, p 30). The Co-fiber material can be provided in various textile forms. Figure 2-2 shows a unidirectional (UD) arrangement for Co-fiber material as an example. Here the continuous fibers are aligned all in the same direction. However, processing Dico-fiber material into a finished product is already a production technique that is used for mass production and thus it has already demonstrated a certain economic efficiency (Assmann & Witten 2013, p 290; Witten & Schuster, p 37). The length of the fibers in the Dico material can vary between different applications.

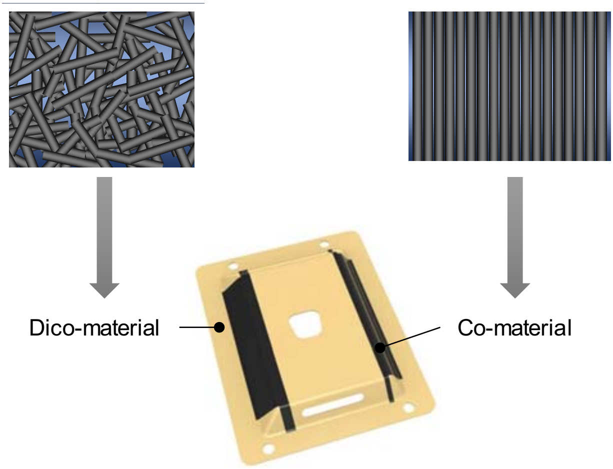

Figure 2-2: Co- and Dico-material in the demonstrator of GRK 2078

Normally, components are unevenly loaded. Depending on the application, certain areas are exposed to higher loads than others. Therefore, it can make sense to combine Co-materials with Dico-materials. An example of this is the demonstrator developed within the international research and training group GRK 2078 (Figure 2-2). A Dico-material SMC is used as a flat structure and reinforced at specific points with a Co-prepreg. The result can be called a Co-Dico-material.

2.2.2 Dry fiber textiles

Dry semi-finished fiber products like woven fabrics can be purchased on the market with different materials and different fiber orientations. They are usually available on rolls and the standard roll width is round about 1000 mm (Dickert 2014, p 44;

Siebenpfeiffer 2014, p 62). Of course, also unusual roll widths are possible, from a few millimetres to 30 metres (Cherif 2016, p 160). Apart from the type of fiber, the main difference is probably in how the fibers are aligned and what length they have. Accordingly, the dry textiles can be divided into four groups nonwoven, woven fabric, weft-knitted fabric and warp-knitted fabric (Assmann & Witten 2013, pp 224–229). They represent the materials for all processes that use dry textiles. In this dissertation, a woven fabric is used to represent the dry textiles.

The most common pattern for two-dimensional woven fabrics are plain weave, twill weave and satin weave (Cherif 2016, p 162). The properties change depending on the type of weaving. A plain weave (Figure 2-3) is generally considered to be easy to handle, but the large number of roving undulations in the textile has a slight negative effect on the mechanical properties of the infiltrated part than with other weaves (Neitzel 2014, p 78).

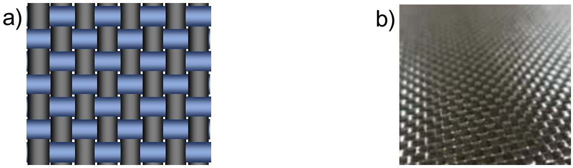

Figure 2-3: Structure of a plain weave fabric (a) and real fabric (b)

2.2.3 Pre-impregnated materials

Prepregs are a finished mixture of fibers and matrix material. Since the fibers are already impregnated with the matrix, this step no longer has to take place in the production process.

Both, thermoplastic and thermoset matrix systems are commonly used. For endless fibers UD fabrics dominate in thermoset matrix material, while in thermoplastic woven fabrics are more likely to be found (Assmann & Witten 2013, p 233). Prepregs with a thermoplastic matrix are also often called organo-sheet (Friedrich 2017, p 398; Siebenpfeiffer 2014, p 23).

Another kind of prepreg is the so-called SMC (Figure 2-4). This is a material made of thermoset polyester or vinylester resins, textile glass fibers, mineral fillers and necessary additives (Assmann & Witten 2013, p 245). The fibers are cut to a specific length for this process and then fall randomly into the prepared resin paste (Bücheler

2018, p 21). Due to the production machines of this material, material widths of 1000 mm to 1500 mm are common (Siebenpfeiffer 2014, p 62; Magnaud 2016, p 11).

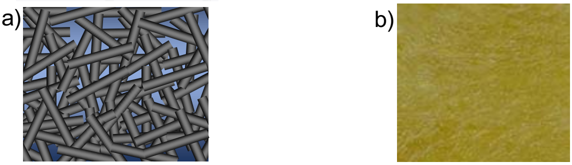

Figure 2-4: Structure of a sheet molding compound(a) and real material (b)

2.3 Representation of a handling process by VDI 2860

All necessary processes which occur within a handling step can be described with the help of VDI 2860. Although the directive was withdrawn in June 2016 because it was not often used, here it is nevertheless suitable for a systematic presentation. The method provides seven elementary functions and 27 compound functions overall, each assigned to five different sub-functions. Figure 2-5 gives an overview of all functions and their classification. However, only the functions that will be used in the next chapters will be briefly explained.

VDI 2860 Handling

Storing	Change quantity	Moving	Securing	Testing	
	- Splitting - Merge	- Move - Rotate	- Hold - Release	- Checking	**Elementary function**
- Fully ordered - Partially ordered - Disordered	- Divide - Assign - Split - Combine - Sort	- Pivoting - Orienting - Positioning - Arranging - Guiding - Passing	- Clamp - Loosen	- Identity - Presence - Shape - Dimension - Color - Wight - Position - …	**Compound function**

Figure 2-5: Functions of the VDI 2860

Compound functions are combinations of other compound functions and/or elementary functions. On the other hand, elementary functions are the smallest possible unit and can no longer be subdivided. In chapter 5 the VDI 2860 will be used to identify the different subsystems which are necessary for the investigations. The functions that will be used are explained in the table below.

Table 2-1: A small selection of function from VDI 2860

Symbol	Description
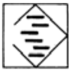	*Partial ordered storage:* The position of an object in three-dimensional space can generally be completely described with three translations and three rotations. In a partial state of a storage at least one of these six variables is known or defined, but not all.
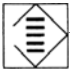	*Fully ordered storage:* In a fully ordered storage, all six variables are known or defined to describe the location of the object. However, it makes no statement about the accuracy with which these variables are set.
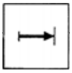	*Move:* Describes the movement of an object from position A to position B. Both positions must be known.
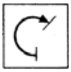	*Rotate:* Describes the rotation of an object from orientation A to orientation B. Both orientations must be known.
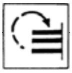	*Arranging:* Arranging is a combination of orienting and positioning. The object is moved from unknown orientations and positions to known states and thus usually passes from partially storage to fully ordered storage.
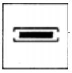	*Hold:* Temporarily securing an object in its position and/or orientation.
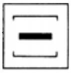	*Release:* Causes the resolution of *Hold*.
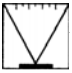	*Checking:* Generally, represents the acquisition or measurement of a characteristic.

2.4 Machine learning

The term machine learning initially includes a wide range of different approaches to solve problems. Usually, all of these approaches are assigned to one of two categories. These categories are called supervised and unsupervised learning (Christiano Silva & Zhao 2016, p 71; Kohonen 1990, p 1464).

During supervised learning, a training set of data is used to generate a predictive function. The goal is that this predictive function can derive generally valid rules from the training data which are applicable to the problem and provide good results for new data sets (Christiano Silva & Zhao 2016, p 72). However, if supervised algorithms are used, this also means that a sufficient number of results must be available to train them. This is not always the case for every problem. In such cases, unsupervised learning is an option. These algorithms are seeking for trends in the data set and try to group the data points considering similarities (Christiano Silva & Zhao 2016, p 72). Such algorithms can therefore be used for clustering, detection of features and multidimensional data visualization tasks (Christiano Silva & Zhao 2016, p 79; Zhang et al. 2009, p 545; Chen et al. 2013; Kruse et al. 2016, p 109). A further classification can be made with the unsupervised and supervised algorithms on whether they form a network or not (Christiano Silva & Zhao 2016, p 81).

2.4.1 Basic concepts of unsupervised machine learning

The unsupervised learning algorithms in chapter 2.4.2 to chapter 2.4.5 are using different basic concepts to select and fit their reference vectors $\boldsymbol{w}$ to a given input data set containing multiple inputs points $\boldsymbol{\xi}$. These basic concepts will be explained first in this chapter before the different unsupervised learning algorithms are explained in chapter 2.4.2 to chapter 2.4.5.

Competitive learning: All algorithms in the following chapter are working in iterations. In every iteration every input point $\boldsymbol{\xi}$ is selected once and the reference vectors $\boldsymbol{w}$ are adjusted. Competitive learning is one of the main concepts for unsupervised learning (Christiano Silva & Zhao 2016, pp 241–242). A system evaluates a winner reference vector $\boldsymbol{w}_s$ for the selected input point $\boldsymbol{\xi}$, which will then be updated. Therefore, an input data point $\boldsymbol{\xi}$ does not influence all reference vectors $\boldsymbol{w}$. (Uchiyama & Arbib 1994, p 1199; Martinetz & Schulten 1994, p 509; Kohonen 1990, p 1465). The algorithms in chapter 2.4.2 to chapter 2.4.5 determine the winning reference vector by the smallest distance to the selected input point ξ. An example for this process is illustrated in Figure 2-6.

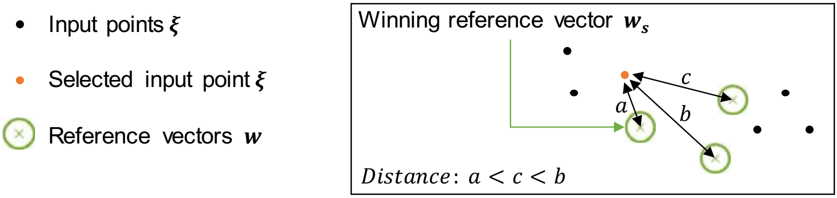
Input points ξ
Selected input point ξ
Reference vectors $\boldsymbol{w}$
Winning reference vector $\boldsymbol{w}_s$
c
a
b
$Distance: a < c < b$

Figure 2-6: Example for competitive learning

Vector quantization: This basic concept was originally invented for data reduction (Makhoul, Roucos & Gish 1985, p 1551). Kohonen (1990, p 1465) explains that a number of input data ξ should be represented by a specific number of reference vectors $\boldsymbol{w}$. The number of reference vectors $\boldsymbol{w}$ should of course be smaller than the number of input data ξ so that a reduction takes place. The general goal is to arrange the reference vectors in such a way that they represent the actual inputs points ξ well. This is the case when the error between the difference of ξ and $\boldsymbol{w}$ is minimized. It is achieved by iterative stepwise adaptation of the reference vectors $\boldsymbol{w}$ to the input data ξ. This is done by calculating an adjustment vector between ξ and $\boldsymbol{w}_S$ (Figure 2-7). The reference vector is then moved along the adjustment vector towards the selected input point. The procedure already includes the approach of competitive learning, since only the reference vector is influenced which is closest to the selected input point. (Kohonen 1990, p 1465)

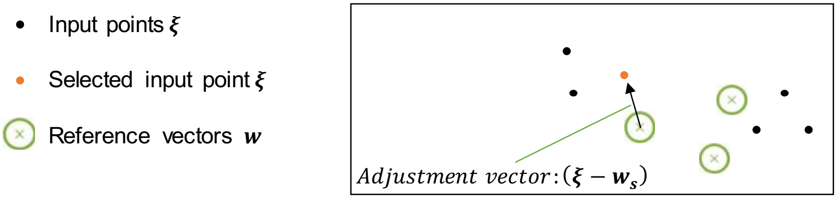
Input points ξ
Selected input point ξ
Reference vectors $\boldsymbol{w}$
$Adjustment\ vector: (\boldsymbol{\xi} - \boldsymbol{w}_s)$

Figure 2-7: Example of vector quantization

Hebbian learning: Hebb (1949) already proposed in 1949 a mechanism about reference vectors bound together by associative learning. This principle is also used in machine learning algorithms by implementing a connection between different reference vectors under certain conditions (Fritzke 1998, p 67; Martinetz & Schulten 1994, p 509). This condition is for example the ranking of the different reference vectors towards an input point. A connection is established or renewed every time two reference vectors are the closest ones to one input data point. In addition, if a connection is not renewed after a certain amount of steps, the connection will be deleted (aging of connections) (Fritzke 1998, p 69). An example for this process is illustrated in Figure 2-8. If two reference vectors share a connection, they are called neighbors.

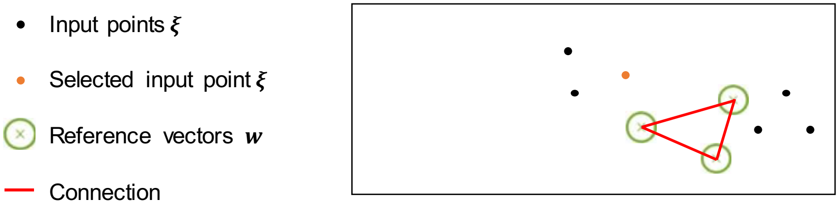
● Input points ξ
● Selected input point ξ
Reference vectors $\boldsymbol{w}$
Connection

Figure 2-8: Example of Hebbian learning

2.4.2 Self-organizing maps

In the field of unsupervised learning there is a range of different approaches and algorithms that have established themselves for various problems. One category of these is the self-organizing map (SOM), also called Kohonen map (Kruse et al. 2016, p 103; Kohonen 1982, p 59).

In SOM, reference vectors $\boldsymbol{w}$ are arranged in a regular pattern and connected to their neighbors (Kohonen 1982, p 59). These connections are fixed for the whole procedure. In this context “competitive learning” and “vector quantization” are now relevant. A SOM is now using these techniques to match the reference vectors $\boldsymbol{w}$ to the input data ξ. As described above in chapter 2.4.1, each ξ influences its nearest reference vector $\boldsymbol{w_S}$, which position is then adjusted by Equation 2-1. Due to the connections between the reference vectors, the adjustment now affects not only the nearest reference vector $\boldsymbol{w_S}$, but also its designated neighbors which have a connection to this reference vector $\boldsymbol{w_S}$. The adaptation of these neighbors follows the same logic as in Equation 2-1, whereby the factor $\alpha(t)$ depends on how far the neighbor reference vector was from the nearest reference point in the starting topology. (Kohonen 1990, p 1467)

$$\boldsymbol{w_{i+1}} = \boldsymbol{w_i} + \alpha(t) * (\boldsymbol{\xi} - \boldsymbol{w_i})$$

Equation 2-1

The properties of a SOM can therefore be summarized as following. A structure with a defined number of reference vectors, which are in a fixed relation to each other and are adapted to the input data according to a competitive learning and vector quantization. Many other works have now taken up this principle and have developed variations that are presented in the following sections.

2.4.3 Neural gas

In contrast to SOM, the neural gas (NG) works without a fixed structure. If an input data point $\boldsymbol{\xi}$ is selected, it creates a ranking of the nearest reference vectors and then adjusts them similar to the Equation 2-1. However, another factor ($k(\boldsymbol{\xi}, \boldsymbol{w_i})$) is inserted depending on a ranked order (Equation 2-2). (Martinetz, Berkovich & Schulten 1993, p 559)

$$\boldsymbol{w_{i+1}} = \boldsymbol{w_i} + * k(\boldsymbol{\xi}, \boldsymbol{w_i}) * (\boldsymbol{\xi} - \boldsymbol{w_i}) \qquad \text{Equation 2-2}$$

Additionally, a Hebbian learning element is added, which creates a structure between the refences but has no influence on the adaptation process above.

2.4.4 Growing cell structure

In contrast to the NG, the growing cell structure (GSC), like the SOM, has a network structure. However, in comparison with SOM, the number of reference vectors and the structure are variable. In addition, the network structure also has an influence on how the reference vectors are adjusted. Similar to the previous approaches, the adjustment distinguishes between the winner reference vector and its neighbors. Winners will be adjusted by the rule of Equation 2-3 and their neighbors by Equation 2-4, if there is a connection between the reference vectors. The adjustment depends on the static value ϵ_b for the winner and on ϵ_n for all its neighbors. The effects of these two values are explained in detail in chapter 7.2.2. The structure of the network, similar to SOM thus has an effect on the adaptation of the system.

At the same time, a new mechanism is introduced to implement new reference vectors into the existing structure. Each reference vector calculates and accumulates its error based on its closest input data points. If the overall error value does not fall below a certain target value, a new reference vector is inserted. For the position of the new reference vector, the existing reference vector with the largest accumulated error is searched for first. Next, the system searches for its neighbor with the largest distance. Subsequently, the new reference vector can be implemented exactly between these two reference vectors. Fritzke (1994) also refers to the elements previously called reference vectors as neurons in this context, and this designation will be used in the further course of this dissertation. (Fritzke 1994, p 1442)

$$\boldsymbol{w_{i+1}} = \boldsymbol{w_i} + * \epsilon_b * (\boldsymbol{\xi} - \boldsymbol{w_i})$$ Equation 2-3

$$\boldsymbol{w_{i+1}} = \boldsymbol{w_i} + * \epsilon_n * (\boldsymbol{\xi} - \boldsymbol{w_i})$$ Equation 2-4

2.4.5 Growing neural gas

The growing neural gas (GNG) is very similar to the principle of GCS but adopts the basic idea of Hebbian learning from NG that connections between neurons can arise and also be deleted again. Figure 2-9 illustrates the exact procedure of a GNG as Fritzke (1995) has introduced it.

The procedure runs for a defined number of iterations I_{max}. In an iteration I, each entry of the input data $\boldsymbol{\xi}(\boldsymbol{K})$ is selected once, whereby the sequence is random. If a data point is selected, all distances $d(\boldsymbol{\xi}(\boldsymbol{K}), \boldsymbol{w})$ between this point and the existing neurons $\boldsymbol{w}$ are calculated. Based on this, the first and second winning neurons $\boldsymbol{w}_{S1}$ and $\boldsymbol{w}_{S2}$ can be determined. Furthermore, the distance between the first winning neuron $\boldsymbol{w}_{S1}$ and the input data $\boldsymbol{\xi}(\boldsymbol{K})$ is added to the error sum $ER(\boldsymbol{w}_{S1})$ of the winning neuron and any connection the winning neuron has is aged. This is followed by the adjustment of the winning neuron and its neighbors by Equation 2-3 and Equation 2-4. In this adjustment step the winning neuron and its neighbors are moved closer to the position of the selected input point. In addition, the connection between the two winning neurons $\boldsymbol{w}_{S1}$ and $\boldsymbol{w}_{S2}$ will be renewed. Connections that are too old in the meantime are then dissolved and if neurons do not have any connections, they are deleted.

Finally, new neurons are added to the system if two conditions are met. First, the maximum number of neurons N_{Max} is not reached yet. Secondly, the number of iterations must reach a multiple of a user-defined value T. After each iteration, the total error for each neuron is also reduced by a factor τ. The process is finished when the maximum number of iterations is reached.

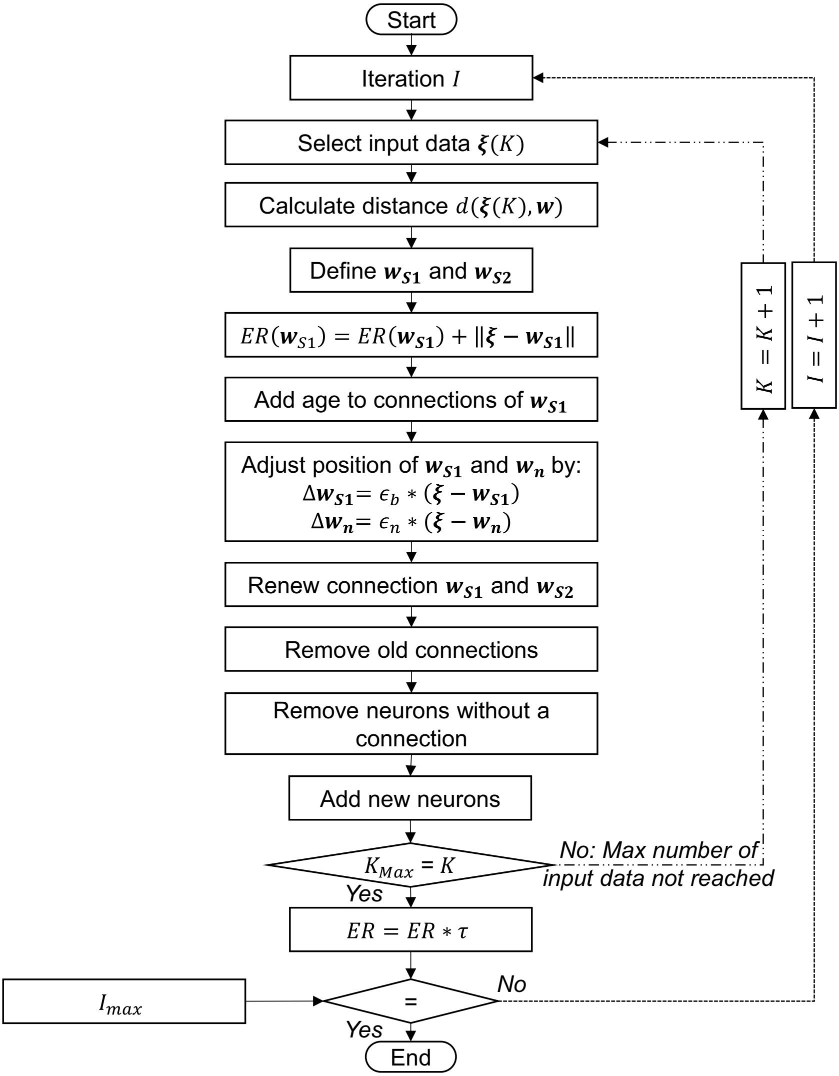
Start
Iteration I
Select input data $\boldsymbol{\xi}(K)$
Calculate distance $d(\boldsymbol{\xi}(K), \boldsymbol{w})$
Define $\boldsymbol{w}_{S1}$ and $\boldsymbol{w}_{S2}$
$ER(\boldsymbol{w}_{S1}) = ER(\boldsymbol{w}_{S1}) + \|\boldsymbol{\xi} - \boldsymbol{w}_{S1}\|$
Add age to connections of $\boldsymbol{w}_{S1}$
Adjust position of $\boldsymbol{w}_{S1}$ and $\boldsymbol{w}_n$ by:
$\Delta\boldsymbol{w}_{S1} = \epsilon_b * (\boldsymbol{\xi} - \boldsymbol{w}_{S1})$
$\Delta\boldsymbol{w}_n = \epsilon_n * (\boldsymbol{\xi} - \boldsymbol{w}_n)$
Renew connection $\boldsymbol{w}_{S1}$ and $\boldsymbol{w}_{S2}$
Remove old connections
Remove neurons without a connection
Add new neurons
$K_{Max} = K$
No: Max number of input data not reached
Yes
$ER = ER * \tau$
I_{max}
=
No
Yes
End
$K = K + 1$
$I = I + 1$

Figure 2-9: Algorithm of GNG

A simple adjustment process is illustrated for a better understanding in Figure 2-10.

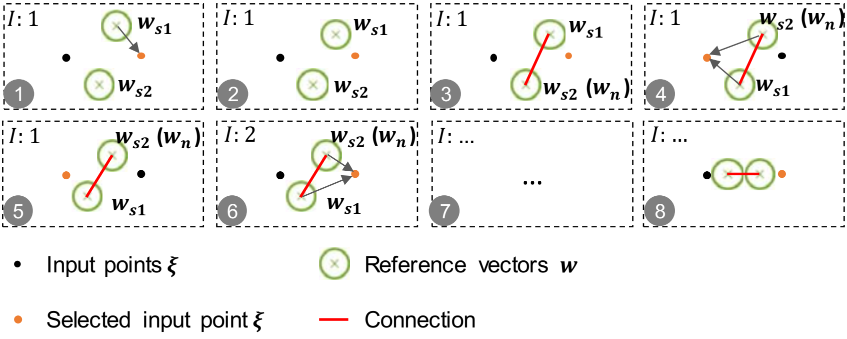

Figure 2-10: Example of the GNG algorithm for two neurons and two input points

Figure 2-10 “1”→”2”: The first two neurons in a GNG algorithm are always placed at first randomly without any connection. Then the first input point is selected and the distance to the existing neurons is calculated. Based on this distance calculation $\boldsymbol{w}_{S1}$ and $\boldsymbol{w}_{S2}$ are identified. Since no connections are existing at the start, only $\boldsymbol{w}_{S1}$ is performs an adjustment step according to Equation 2-3.

Figure 2-10 “3”: Then a connection is created between $\boldsymbol{w}_{S1}$ and $\boldsymbol{w}_{S2}$. Only from this point on the two neurons called neighbors.

Figure 2-10 “4”→”5”: Now, the second input point is selected and $\boldsymbol{w}_{S1}$ and $\boldsymbol{w}_{S2}$ are identified and the position of both neurons are adjusted. $\boldsymbol{w}_{S1}$ according to Equation 2-3 and $\boldsymbol{w}_{S2}$ according to Equation 2-4 because it is a neighbor of $\boldsymbol{w}_{S1}$. If there would be a third neuron that also has a connection to $\boldsymbol{w}_{S1}$, this would also be adjusted according to Equation 2-4.

Figure 2-10 “6”: Since only two input points are available the first input point is selected again and the process starts all over again.

Figure 2-10 “7”→”8”: If this process is repeated several times the neurons will line up between the both input data points. How many iterations are necessary and how close the neurons will be at the input data points depends on the parameters of the GNG. These parameters are explained in more detail in the chapter 7.1.3.

3 State of the art

This chapter aims to provide a brief overview of other works in the field of handling devices. Since this work is also related to the field of lightweight production processes, a brief overview of respective production processes using dry semi-finished textiles and SMC will also be given. Since the materials used here are very special, the grippers to handle such materials must fulfill special criteria and are therefore introduced too. Finally, an overview of other works in the area of handling non-rigid parts is given, from which this work must be distinguished.

3.1 Lightweight production processes

According to the Composites Market Report 2017, the SMC process has the largest production share in Europe. In the processing of continuous fibers, the manual process in open mold as well as the automated close mold like the resin transfer molding (RTM) process dominate. (Witten & Schuster, p 35)

Since these procedures make up such a large part, it seems appropriate to integrate both procedures into the considerations and pay attention accordingly to their boundary conditions.

3.1.1 RTM process

The RTM process is used to produce FRP with continuous fibers. The special feature of the RTM process is its high potential to enable an automated infiltration and thus to fully automate the production of FRP for short cycle times (Bergmann, Dörmann & Lange 2015, p 2399; Stewart 2009, p 17). In the actual RTM infiltration process, so-called preforms are infiltrated. These preforms are dry textile structures made of single- or multi-layer fiber textiles (Cherif 2011, p 30).

The production of these preforms is an integral and necessary part of the process chain and may require a lot of work because often different layers of textiles are necessary for one part (Gebauer et al., p 1). Since this work is focused on the automatic design of handling devices, the RTM process will be considered from this perspective in the following. Figure 3-1 gives an overview of the layout for the RTM process and the necessary handling operations. The first step of the RTM process chain is cutting the dry fiber textiles. This is done usually in an automated process with a computerized numerical control (CNC) cutting table using a laser or knife. Therefore, the task for the first handling system I (in Figure 3-1) is to grab the different shapes from the cutting table (Cherif 2011, p 25).

From here onwards, there are different possibilities in terms of how the production process can be designed. The cut-out shapes can first be temporarily stored in a magazine or immediately assembled into a finished stack (Ochs 2013, p 16). For preforming, it is very important that the individual layers of the stack no longer shift. This can be ensured in various ways.

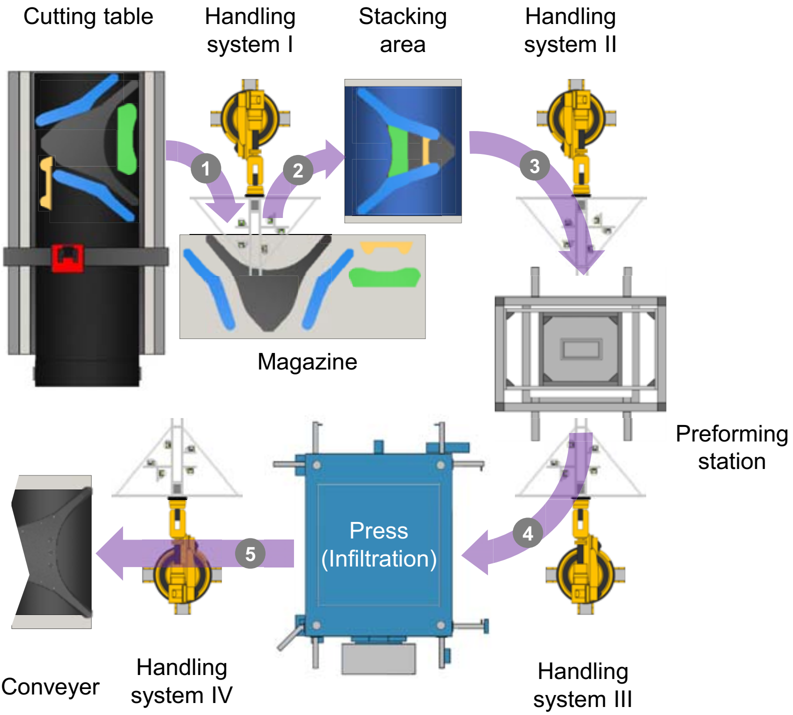
Cutting table
Handling system I
Stacking area
Handling system II
1
2
3
Magazine
Preforming station
Press (Infiltration)
4
5
Conveyer
Handling system IV
Handling system III

Figure 3-1: Layout of an automated RTM process chain

The handling system II can be designed in such a way that the layers are not displaced or different measures can be carried out, such as melting or activating a binder, the use of spray adhesive or sewing of the textiles to ensure that the layers are aligned with one another (Dickert 2014, p 11).

Once appropriate measurements have been taken, the stack is inserted into a preforming station and reshaped. Here at last, the individual layers of the stack are joined together with the aid of a previously applied binder (Wagner 2016, p 46). This can be a thermoplastic binder that connects the layers together by melting and cooling or a reactive binder that undergoes a curing process after heating (Klingele 2014, p 35). In any case, the properties of the object considerably change as a result of preforming. Handling systems I and II are required to handle loose textile layers. By joining the individual layers and forming the stack, the preform now has a considerably higher rigidity and can thus be handled more easily (Dickert 2014, p 8). However, two-dimensional structures will be transformed into a three-dimensional one by preforming. Therefore, the requirements between handling system II and III are changing considerably. Due to the changing properties of the object, the gripping principle can also change between handling system II and handling system III. Possible gripping principles for flat textile layers are low-pressure surface grippes as well as electrostatic and needle grippers (Förster 2016, p 28; Angerer et al. 2010, p 864; Reiff-Stephan 2006, p 282). Preforms, on the other hand, can have such a good rigidity and low air permeability that normal suction grippers such as those used for handling metal sheets can also be used (Klingele 2014, p 153).

The actual RTM process is the infiltration of the dry preform with the matrix. For this purpose, the preform is placed in a closable mold. This is often realized by the fact that an upper and a lower mold are mounted on a press. Once the mold is closed with the help of the press, the infiltration process begins. For this purpose, resin and hardener are mixed together in a mixing head and injected into the cavity under high pressure. For automated processes, the so-called high-pressure RTM (HP-RTM) is preferred. The reason for this is that the dry preform should remain as short as possible in the mold. This requires a very fast curing resin-hardener system to be used. (Ishikawa et al. 2018, p 223; Klingele 2014, p 150)

A fast resin-hardener system also changes its viscosity very quickly, thus making infiltration more difficult (Koch 2017, p 51). The high pressure of the HP-RTM should therefore enable the preform to be completely infiltrated with the matrix, so that the matrix can cure. Even larger preforms can be infiltrated in less than a minute. However, the mold must remain closed until the resin has a sufficient state of curing, which can take up to one or two minutes (Rosenberg et al. 2014, p 465). If this state is reached the finished part can be taken out of the mold. In the next process step, the finished component is machined and the mold is cleaned. The infiltrated part then has a solid surface.

3.1.2 SMC process

The SMC process also starts with cutting the required layers from the material, which are then picked up by a handling system (Figure 3-2).

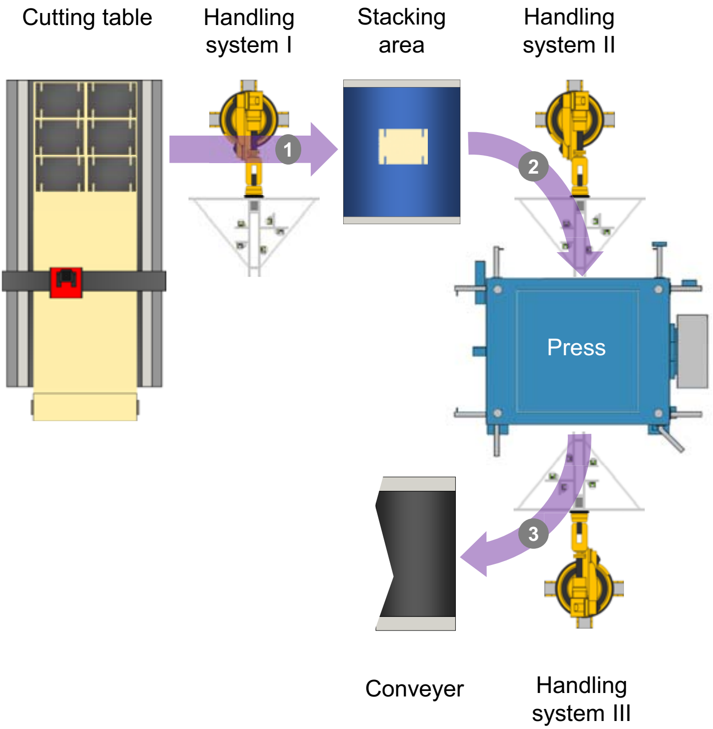
Cutting table
Handling system I
Stacking area
Handling system II
1
2
Press
3
Conveyer
Handling system III

Figure 3-2: Layout of an automated SMC process chain

Often, the protective film with which the SMC is stored is first removed in an additional step before the cutting, so that only a small amount of sytrol can escape during storage. However, the shapes of these cut-outs can be less complex, as the SMC material is flowable (Assmann & Witten 2013, p 251). On the stacking area, handling system I stacks several layers of the SMC on top of each other to achieve the necessary mass of material. Different cuts may be necessary depending on how much material is required at specific points of the component (Henning & Moeller 2011, p 612; Cherif 2011, p 386). It can be advantageous to work with short flow paths, as these influence the orientation of the fibers in the material (Hua-tie 1987, p 82). The flowability also leads to the fact that the components for handling system III are larger than for handling systems I and II.

By pressing the material at temperatures around 150 C°, the reaction starts in the SMC and it cures (Henning & Moeller 2011, p 612). The characteristics of the handling object between handling systems II and III change accordingly. The grippers used for these handling systems are normally based on the properties of the object to be handled (Fantoni et al., 2014b, p. 684; Fantoni et al., 2014a, p. 331; Gutsche, 1993, p. 34; Reiff-Stephan, 2006, p. 284; Reinhart et al., 2009, p. 185; Stephan, 2001, p. 21; Straßer, 2012). The good surface of the components after pressing enables the use of vacuum grippers for handling. Mechanical finger grippers, vacuum grippers and needle grippers can be used for handling the SMC layers when they are not yet fully hardened. However, the use of finger grippers requires the possibility of coming to the side of the blanks, which does not always have to be the case. In such cases, the needle or vacuum grippers enable gripping the blanks from above.

3.2 Gripper technologies for flat non-rigid parts

A classification of existing gripper technologies has been developed and can be found in a large number of different publications. In this case, the gripper technologies are classified according to their gripper principle positive locking, material locking or frictional locking. (Angerer et al. 2010, p 864; Gutsche 1993, p 27; Förster 2016, p 28; Reiff-Stephan 2006, p 282; Stephan 2001, p 17; Hesse 2011, p 10; Ochs 2013, p 20)

3.2.1 Introduction of gripper technologies for flat non-rigid parts

In the following, various representatives of these three gripper technologies will be presented.

Positive locking gripper technology

With positive locking grippers, a holding force is generated by the gripping partners forming undercuts to each other. In the case of flat and thin parts such as dry textiles or SMC, this means that elements holding the material are inserted by the gripper.

Primarily thin metal elements are used for this. The largest difference between the two representatives to be presented here lies in the actuation of this metal element.

The scraper gripper is a normal parallel finger gripper that injects small metallic wire chippings into the material to be gripped, by the relative movement of its two fingers (Hesse 2011, p 98). Especially in the case of textile, this inevitably leads to a change or damage of the textile (Szimmat 2007, p 45; Jodin 1992, p 27). Gutsche (1993) has carried out various experimental tests for this type of gripper and derived criteria for the design (Gutsche 1993, p 83).

The second representative is the needle gripper. Here, needles penetrate directly driven by a pneumatic actuator into the object (Böger 1997, p 71). It is important that they do this under a certain angle so that a positive locking can be generated.

This principle is one of thSe few that enables multiple layers to be gripped at once and need only at the same time accessibility from above. Disadvantageous is the possibility of damaging the handling part by piercing of the needles (Biermann, Hufenbach & Seliger 2008, p 22).

Material locking gripper technology

Material locking grippers use an additional material between the gripper and the object to generate the gripping force.

One possibility to produce a material locking is by using adhesives like polyisobutylene, plasticized synthetic rubbers, isocyanate elastomers or vinyl-based adhesives (Monkman & Shimmin 1991, pp 7–8). Such an adhesive surface is then used for gripping the textiles. However, this can lead to several problems. Textiles release dirt and dust to the adhesive surface during the gripping process, so that it can produce less gripping force (Monkman 1995, p 147). Adhesive residues may also remain on the object or damage may occur during removal (Szimmat 2007, p 91).

In addition to the use of chemical adhesives, freezing water can also be used. The material locking is created by first applying liquid water to the object surface. A cooling gripper surface is then brought into contact with the water on the textile, which then freezes and creates the material locking (Hesse 2011, p 14). The cooling is generated by a so-called Peltier-element (Szimmat 2007, p 92). Stephan (2001, p 54) has developed a process model for the process of freezing and the time it takes. Times of around 40 seconds are specified for establishing a connection between the freezing gripper and the object (Stephan 2001, p 90).

Frictional locking gripper technology

The frictional grippers are the largest group of grippers and provide a variety of technical possibilities for implementing.

This group also includes all types of finger grippers. These are mainly used for handling three-dimensional parts but also can be used for two-dimensional parts under certain boundary conditions. The accessibility of the part plays an important role here. Due to their geometry, flat parts are best gripped from above, as they offer the largest contact surface. Finger grippers can only be used here if it is allowed to bend the material (Fantoni et al. 2014, p 686). However, this is hardly desirable, which is why it is often attempted to access the material from the sides with this type of gripper. However, it is not always possible to reach the side of the material, especially with flat parts, which makes the use of this type difficult. Nevertheless, there are some works using this method (Zhu 2015, p 93; Zoumponos & Aspragathos 2008, p 185; Karakerezis, Doulgeri & Petridis 1994, p 595). Beside of the finger grippers the group of frictional grippers also includes electrostatic grippers, vacuum grippers, low-pressure surface grippers and Bernoulli grippers (Reiff-Stephan 2006, p 282).

Electrostatic grippers generate an adhesion by electrodes in a dialecticism. An electric field is created by applying a high voltage to the electrodes (Monkman 2003, p 327; Mohammad Dadkhah et al. 2016, p 1007). A positive aspect of this principle is the very gentle handling of the part. A disadvantage is the long release time, as the charges degrade only slowly. (Hesse 2011, p 103)

The remaining grippers are now based on the same basic principle. Vacuum grippers, low-pressure surfaces grippers and the Bernoulli grippers generate their gripping force by building up a lower internal pressure than the external atmospheric pressure. The main difference between the grippers is how they generate this negative pressure.

Bernoulli grippers generate a negative pressure between the gripper and the component which should be transported. For this purpose, an overpressure is blown in between the gripper and the component and sent through a tapering gap. Following the Bernoulli effect, the air is thereby further accelerated and generates a negative pressure which then holds the component. Theoretically this effect can be implemented in contactless handling processes, but the component should also not be deformed so that the gap is not changing. (Hesse 2011, p 136)

Vacuum grippers are designed to build up as much negative pressure as possible in their interior. It is often assumed that the surface of the part together with the sealing lip of the gripper generates a sufficiently good sealing effect so that only low leakage flows occur (Hesse 2011, p 108). Accordingly, such grippers only hold interest for air-impermeable materials like glass, metal or even SMC (Szimmat 2007, p 118).

Low-pressure surface grippers work with the same principle as vacuum grippers, but are not intend to generate large negative pressures due to the vacuum generator. Instead, the focus is on achieving a high air flow rate at all times so that leakage flows can be compensated. This is done for example by using ejectors which can generate large amounts of volume flow by a low weight of the vacuum generator (Hesse 2011, p 135; Lien & Davis 2008, p 34). However, there are also other principles to generate the necessary vacuum (Hesse 2011, p 113; Jodin 1992, p 75; Straßer 2012, p 105). The high air flow rate enables the handling of air-permeable materials such as textiles. As a result, it is usually possible to work without a sealing lip between the material and the gripper. Given that high volume flows have to be generated and leakage flows are accepted, the low-pressure surface gripper consumes a lot of energy (Lien & Davis 2008, p 34). Overall, they are very flexible in use, as they are suitable for both air-permeable and impermeable materials (Stühm et al. 2014, p 161). In addition, they handle the materials very gently (Angerer et al. 2010, p 864). It is also possible to control the force generated by these grippers. Förster (2016, p 169) was able to integrate sensors into low-pressure surface grippers and use them to set up a control loop for the separation of textile blanks with a very high degree of process reliability.

3.2.2 Conclusion on gripper technologies for flat non-rigid parts

The presentation of the different gripper technologies shows that each technology has advantages and disadvantages. Many grippers can damage the integrity of the material, such as needle and scraper grippers, or may take a long time to remove the object, such as the electrostatic gripper or the freezing gripper. For the use of finger grippers there must be certain possibilities to grip the part and many vacuum grippers need materials that are air-impermeable. Which technology is used, is therefore often linked to the exact conditions of the handling task and must be decided from case to case.

Many others have already tried to link the selection of the gripper to the properties of the material (Stephan 2001, p 21; Gutsche 1993, p 34; Reiff-Stephan 2006, p 284). This thesis will deal with the arrangement of grippers. For this purpose, one of the existing gripping technologies must be selected for further consideration. None of the technologies presented is perfect. A decision is therefore always a compromise.

Biermann, Hufenbach & Seliger (2008) have created an overview which grippers are used in the production process of fiber lightweight parts (Biermann, Hufenbach & Seliger 2008, p 38). The most common grippers are those that work with negative pressure, but it is not specified whether they mean vacuum grippers, low-pressure surface grippers or Bernoulli grippers. Next are needle grippers followed by finger grippers in this ranking. Grippers using low-pressure thus seem to be the right of choice for many applications in this area. The same statement is also made by Reinhart, Straβer & Ehinger (2009, p 185) who look at the gripper selection from the perspective of flexibility and commit themselves to low-pressure surface grippers. Not least due to the work of Förster (2016, p 169)), these grippers can function as part of intelligent production through an extension with sensors.

For this reason, in the further course of this thesis primarily low-pressure surface grippers are considered.

3.3 Energy consumption of handling processes

Handling systems are part of an automated process and are used for this reason especially when larger quantities have to be produced. Such systems are particularly economical when they are in operation for a long time. After a handling system has been put into operation, the running costs are primarily determined by maintenance and energy consumption. The energy consumption of the whole handling process is therefore defined by the energy for the gripper, any electronics to control the grippers and the energy for the kinematic to move the handling device (Straßer 2012, p 169). This kinematic is mostly an industrial robot. Ehinger (2013) and Straßer (2012) have made measurements on their respective handling systems and have come to the following results in Table 3-1. Both are using low-pressure surface grippers.

Table 3-1: Energy consumption of handling systems

Handling system	Robot movement (Standby 100 Wh)	Gripper	Control	Other subsystems
Straßer (2012)	92.5 % (83.3 Wh)	6.3 % (5.7 Wh)	1.2 % (1 Wh)	-
Ehinger (2013)	37.6 % (62 Wh)	12.1 % (20 Wh)	-	50,3 % (83 Wh)

Ehinger (2013, p 177) states that the robot's standby consumption is 100 Wh. Thus a total of 62 Wh decay on the actual energy for the movement. Straßer (2012) uses very little energy to generate the vacuum in his handling system by using radial fans (Straßer, 2012, p. 107). However, his robot system tends to consume more energy, which can be mainly due to the size and weight of its handling device, whose weight is unfortunately not specified. Energy consumption of a robot is defined by speed, path, and payload (Rassõlkin, Hõimoja & Teemets 2011, p 3; Paryanto et al. 2014, p 132). Speed and path are defined by the production process and are thereby not directly influenced by the design of the handling device. The minimization of the energy consumption by the robot through adjusting process and path planning is an independent research field (Glorieux 2017, p 61). The payload on the other side is the direct result of the design of the handling system. As with normal lightweight construction, a distinction can be made here between by design and by material. Here, there are also interesting approaches to reduce the weight of handling devices by using lightweight materials (Wulfsberg et al. 2015, p 456).

In general, however, it can be assumed that the weight of the handling device can be reduced from the design perspective by using only as many grippers as necessary. This will then result in a reduction of the energy consumption of the grippers as well as of the robot, which is an additional benefit of a customized handling device.

3.4 General classification of gripper arrangements

Existing handling devices can be classified according to whether parts are gripped over their entire surface or only held at specific positions by several individual gripper elements (Gutsche 1993, p 18; Seliger, Gutsche & Hsieh 1992, p 35). The arrangement and positioning of individual gripper elements at specific points can also called a configuration. This gripper configuration contains therefore the number as well as the position of the used gripper elements on the handling device.

There are various examples from the state of the art for full-body gripping (Straßer 2012, p 136; Kolluru, Valavanis & Hebert 1998, p 484; Angerer et al. 2011, p 559), grippers arranged in a regular pattern (Förster et al. 2017, p 40; Körber & Frommel 2018; Gerngross & Nieberl 2016, p 247) and special arranged gripper configuration (Glorieux 2017, p 51; Flixeder, Glück & Kugi 2017, p 250; Körber, Gänswürger & Gerngross 2014, p 4).

3.5 Research fields for handling flat non-rigid parts

Several works have already been conducted in the research field of handling devices, with a different background or focus. There are also different aspects that can be studied in the context of automated handling. Straßer (2012, pp 38–39) already developed categories for the different investigation in the handling process of flat non-rigid parts. The following chapter deals with the work mentioned in Figure 3-3 and will then be supplemented by other work that can be assigned to these categories.

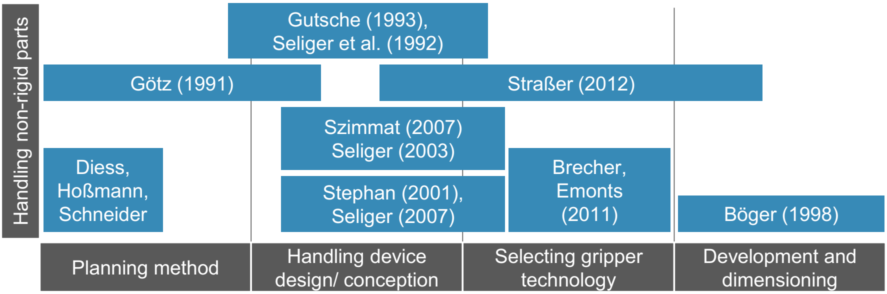
Handling non-rigid parts
Gutsche (1993), Seliger et al. (1992)
Götz (1991)
Straßer (2012)
Szimmat (2007) Seliger (2003)
Diess, Hoßmann, Schneider
Stephan (2001), Seliger (2007)
Brecher, Emonts (2011)
Böger (1998)
Planning method
Handling device design/ conception
Selecting gripper technology
Development and dimensioning

Figure 3-3: Different investigations in the field of handling devices according to Straßer (2012, pp 38–39)

3.5.1 Development and dimensioning of grippers

Papers and dissertations assigned to the area of dimensioning often deal with the design of a gripper technology, e.g. the influence of the hole diameter for a low-pressure surface gripper or the expansion and improvement of this technology. A characteristic of this category is that the focus is usually on a single gripper element.

Jodin (1992) has conducted research under what conditions a round leather part will fall off a low-pressure surface gripper. In his investigations, he varies the diameter, amount and shape of the intake holes. (Jodin 1992, p 138)

Böger (1997) developed a method for dimensioning a low-pressure surface gripper for the handling of leather sheets. Through experimental investigations, he has designed a set of characteristic lines to define the required vacuum inside a low-pressure surface gripper depending on the acceleration of the handling process, the center of gravity, material overhang and more. His approach only covers rectangular shaped parts. Furthermore, only one gripper holding the part is considered in his investigations. (Böger 1997, pp 129–131)

Stephan (2001) has developed an analytic model of the gripping process for hydro-adhesive grippers. The model can calculate the resulting gripping force depending on process parameters like the amount of applied liquid. Furthermore, an FEA model of the cooling process is part of the development (Stephan 2001, pp 108–109).

Ochs (2013) developed a gripping element that combines the advantages of adhesive principles with the advantages of vacuum-based systems in one gripper. A vibration-supported release is also used. This principle is based on specifically applied ultrasonic oscillations, which excite the component adhering to the gripper to release the adhesive contact.

Förster (2016) and Förster et al. (2017) extend a low-pressure surface gripper by a sensor principle, which enables the separation of carbon fiber textiles. This is made possible by integrating brass electrodes into the suction surface of the gripper. Due to the electrical properties of carbon fiber, the contact resistance between electrode and textile can be measured. An important aspect here is that the gripping force of the low-pressure surface gripper can be adjusted very quickly, thus making control possible.

3.5.2 Selecting gripper technology

The selection of a gripper technology depending on different properties of material and process can be part of a dimensioning or design/conceptions work. Therefore, some work will reappear in different chapters.

Reiff-Stephan (2006, p 284) has evaluated several gripping techniques based on different aspects of the material and the process. The non-rigid behavior of the material, the flexibility of the process and the holding force of the gripper are considered. In addition, there is the aspect how quickly the gripper can build up the gripping force, but also the susceptibility to external influences.

Reif-Stephan already carried out a similar evaluation under the name Stephan (2001, p 21) 2001, but focuses very strongly on textiles and deals more closely with their specific properties. The grippers, as explained in chapter 3.2, are evaluated here regarding the thickness of material, texture, weight per area, thread density and ondulations.

Fantoni, Capiferri & Tilli (2014, p 331) present an expert system for selecting a gripping technique. The system should explicitly pay attention to the compatibility of the gripping and releasing process. A series of parameters is passed to the expert system to describe the problem.

Fantoni et al. (2014, p 684) present an evaluation of different gripper technologies for different materials. Two-dimensional and three-dimensional objects are distinguished. However, it is not explained on which rules this classification is based.

Furthermore, Straßer (2012) and Reinhart, Straβer & Ehinger (2009, p 185) select at first a gripper technology for the development of their handling device. The main aspect here is the greatest possible flexibility and decisions are made based on a utility value analysis. The result of this analysis is the use of low-pressure grippers and they select a radial fan generator to generate the vacuum.

3.5.3 Handling device design/ conception

Gutsche (1993) and Seliger, Gutsche & Hsieh (1992) present a development method for a flexible handling device for technical textiles in an assembly process. A gripper technology selection is part of this process which considers the material properties. Furthermore, the basic principle of the gripper arrangement on the part is discussed based on material properties and the assembly process is set. Considering these data, a decision for a full-body or multiple gripping device is made. They also present an finite element analysis (FEA) of a cantilever beam to simulate the deflection of the part. However, the simulation data are not used for the design of the handling device. (Gutsche 1993, p 73)

Szimmat (2007) and Seliger et al. (2003) developed a process model of the separation process for textiles using a hydro-adhesive gripper. They also propose a first idea for the arrangement of the grippers on the outer contour of the part. This idea uses geometry marks on the outer contour of the sheet, for example edges, to define the position of the grippers. They also mentioned that it could be necessary to place some grippers inside the sheet's geometry to prevent large deformation, although they did not present an approach concerning how this should be done. (Seliger et al. 2003, p 23; Szimmat 2007)

Furthermore, Straßer (2012) sees parts of his work in this field and concentrates on the flexibility of the handling system for technical textiles. His own approach also includes a selection of a gripper technique considering the gripper force and the effect of the gripping process on the textile. The result of this approach is a handling device with low-pressure surface gripping technique. The gripper surface is made of 4320 actuators which are arranged in a matrix. These actuators control, if a specific part of the gripper surface holds a textile sheet or not. Therefore, the handling device can hold a wide range of different shapes and is reconfigurable just by editing the software program. The geometric shape of the handling part specifies which areas should be used in the gripping process. Any deformation of the part is prevented by a more or less full-body gripping principle controlled by the actuators. (Straßer 2012, p 187)

At this point other papers and dissertations will be added to this category that are not mentioned so far in Figure 3-3.

Ehinger (2013) develops a handling and assembly device to drape a technical textile on a metal mold. It is designed to work together with the handling device of Straßer (2012). Her focus on the development of the handling function for this device is to fit the needs of the assembly process. To achieve this, she generates a systematic approach to satisfy the requirements of every process step. The geometry of the part only plays a minor role for the handling function. (Ehinger 2013, p 189)

Kolluru et al. (2000) have developed a reconfigurable gripper system with a cross-bar structure. Four vacuum grippers can take individual positions, each actuated by an electrical drive and then grip two-dimensional parts. The paper is focusing the investigations on the static and dynamic properties of the handling device's mechanical construction. A direct handling application or a systemic way how the grippers should be arranged depending on the tasks is not presented.

Kordi, Husing & Corves (2007) have built a handling device which uses multiple gripping techniques. Needle, hydo-adhasive and low-pressure surface grippers are arranged on a frame to handle a technical textile and enable deformations by a kinematic build in the handling device itself. The distance between the gripping devices defines the possible deformation of the textile. (Kordi, Husing & Corves 2007, p 4)

Mantriota (2007) investigated a cross-bar structure handling device with four vacuum grippers. Like Kolluru et al. (2000), the arrangement of the grippers can be changed only manually. Based on the static mechanics, a model for the necessary vacuum in the four vacuum grippers is calculated here. The example of a simple square plate also shows that this analytical description form can be used to find the ideal location on the component where the least vacuum is required for a fixed arrangement of the grippers relative to each other. Any deflection of the component is not taken into account.

Bruns et al. (unpubl. 2018) are investigating the handling of organo-sheets. Since these parts are mostly transported hot, clamping grippers are often used to hold the parts. The handling device plays an important role in forming the finished part, because it drapes the initially gripped two-dimensional blank into the mold. Bruns et al. (unpubl. 2018) are simulating this draping process and the influence of the gripper configuration of their modular handling device in this context. They also mention in the outlook to use the simulation results to adapt the configuration of their handling device.

Schmalz et al. (2016) discuss an approach for the placement of finger grippers as well as vacuum grippers. It is not completely clear whether this consideration only addresses flat or also three-dimensional parts. The procedure for placing the vacuum grippers is to record all possible gripper positions based on the computer-aided design (CAD) data of the object. A ranking should then be created for these, in which the gripping force is also taken into account. It is also planned to include an FEA tool to check the stability of the component and gripper. It is explained which parameters are included in the ranking, but a more detailed explanation is not given.

Hoffmann & Kohnhäuser (2002) introduce an algorithm for creating gripper configurations for handling sheet metal parts in transfer presses. The focus here is that any vacuum gripper should carry too much load. For this purpose, the center of mass of the part is first calculated and the part in turn simplified by a two-dimensional image. Now this surface is divided by a straight line through its center of gravity and again the new centers of gravity are calculated. The focal points of these segments are then the theoretical points at which the grippers are to be placed. If the gripper force exceeds the actual applicable force, the segment is divided again using the same method.

The handling of metallic sheets in the automotive production is also investigated by Ceglarek, Li & Tang (2001). These metallic sheets are handled by a set of vacuum grippers. With an interactive FEA simulation and use of Powell's algorithm, an optimum gripper arrangement is found. The optimum arrangement should fulfill different goals. The deformation of the part in the handling process should be as close as possible to a given contour and the dynamic deformation due to acceleration should be as close as possible to the static. The authors also mention the need for an initial gripper arrangement but did not present a concept how this first configuration could be achieved. (Ceglarek, Li & Tang 2001)

3.6 Conclusion from the state of the art

In the state of the art it could be shown that it has energy and economic advantages to design handling devices in such a way that they are not oversized. The development of customized handling devices, however, is always associated with additional personnel costs and requires creativity and technical expertise from people. The planning of such handling devices can also become very complex if several different parts must be transported by one handling device one after another. In addition, the planning of handling devices is not only about planning the position of grippers, but also about being able to implement them later on a real device. From these problems, requirements can be derived which a systematic or method has to fulfill in order to plan customized handling devices for lightweight production processes.

Gripper arrangement: A solution is customized for an individual handling task if individual grippers can be used and freely positioned. The use of a full-surface gripping principle restricts this adaptability in any case.

Custom solution: A solution is customized for an individual handling task if it takes its boundary conditions into account. In the case of the transport of flat, non-rigid parts, this means that the geometry and material properties are considered.

Automated configuration: In order to limit the time and effort required to solve a problem, an automated method is necessary.

Several parts: During the RTM or SMC process, one and the same handling device must transport different parts one after another (Figure 3-1, handling system I). This point must therefore also be taken into account.

Hardware implementation: The planning of the necessary grippers required for handling must also cover the implementation on an actual handling device. For this a method is necessary to convert the gripper arrangements from theory into reality.

The criteria defined above are now applied to the approaches from chapter 3.5.3 to check if the existing approaches meet these requirements (Table 3-2).

Table 3-2 shows that many approaches already integrate geometry and material data into the development of the handling device. This is particularly the case with the work that deals with the handling of sheet metal (Hoffmann & Kohnhäuser (2002), Ceglarek, Li & Tang (2001), Li, Ceglarek & Shi (2002)). Here, the approaches are mostly systematized in such a way that they can run automatically. In the field of textile handling, the methods often involve creative steps that cannot be automated (Gutsche (1993), Szimmat (2007), Straßer (2012), Ehinger (2013). Kordi, Husing & Corves (2007)). The handling of several parts with one handling device is often only considered if a fully-body gripping principle is used. If several individual grippers (customized gripper arrangement) are used, this point is ignored. Furthermore, the implementation or configuration of the hardware of the handling device is also ignored in most work.

Table 3-2: Evaluation of existing approaches

Method/ Approach	**Gripper arrang.**	**Custom solution**	**Automated config.**	**Several parts**	**Hardware imp.**
Gutsche (1993)	Individual grippers	◑	◔	○	○
Szimmat (2007)	Individual grippers	◑	◔	○	◔
Straßer (2012)	Full-body gripping	◑	◔	●	◔
Ehinger (2013)	Full-body gripping	◔	◔	●	○
Kolluru et al. (2000)	Individual grippers	○	○	◔	◔
Kordi et al. (2007)	Individual gripper	○	◔	○	◔
Mantriota (2007)	Individual grippers	○	◕	○	○
Bruns et al. (unpl.2018)	Individual grippers	●	◑	○	○
Schmalz et al. (2016)	Individual grippers	●	●	○	○
Hoffmann & Kohnhäuser (2002)	Individual grippers	●	●	○	◔
Ceglarek, Li & Tang (2001)	Individual grippers	●	●	○	○
Legend	100 % ●	75 % ◕	50 % ◑	25 % ◔	0 % ○

4 Objective and own approach

4.1 Objective

The following conclusion can be drawn from the state of the art. There are already approaches that deal with the automatic generation of customized handling devices. These approaches come from the field of sheet metal handling and in this context do not deal with the handling of different parts on one and the same handling device. A systematic implementation of the handling devices hardware is also missing here.

If the development of handling devices in the field of fiber-based lightweight production processes is considered, it becomes apparent that several parts on one device are only considered if a full-body gripping principle and therefore an oversized handling device is used. Their development also often contains methods that are difficult to automate. A systematic implementation of the gripper devices is also rare or only partially developed.

Thus, it can be concluded that there is no systematic and programmable approach in the field of fiber-based lightweight production processes to generate customized handling devices. The aim of such an approach would be to take into account the shape and material properties when designing the handling device and to keep the number of grippers used small. It is also important for the RTM and SMC process that several different parts can be transported one after the other with one and the same handling device (Figure 3-1, handling system I). Finally, a systemic for generating customized handling devices must also consider how these can be implemented on a real handling device.

4.2 Own approach

A customized handling device should only use as much active grippers than necessary to transport a part. Therefore, it will be built-up of different individual grippers which are fastened on a frame structure, so they could be placed all over the part (Figure 4-1). The handling device will therefore have a gripper configuration which defines the number and the position of the individual grippers.

Since a handling device should be able for the RTM and SMC process to handle multiple parts a lot of boundary conditions arise. In order to reduce the complexity of the problem, a gripper configuration should first be found for each part individually. These individual gripper configurations should be combined later.

A disadvantage of a customized handling devices is the occurring of deflections in the handling process. To generate a customized handling device with a good gripper configuration these deflections must be kept in defined limits. To enable the evaluation of a gripper configuration in an automated way it is necessary to simulate the deflection of the non-rigid part. If the gripper configuration does not fit the needs of the handling process the gripper configuration can then be adjusted until the deflection does not exceed a defined value. It is important to mention that such a simulation and adjustment step can only be performed on an existing or initial gripper configuration which already ideally considers the shape of the part.

If all individual gripper configurations are found and combined the final gripper configuration must be implemented on the frame structure.

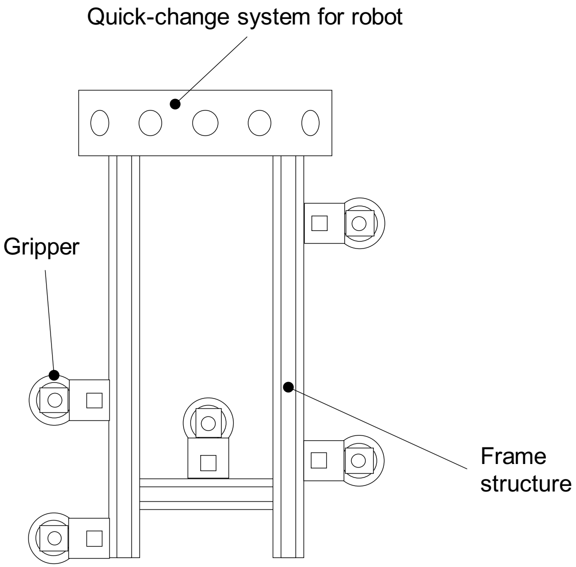

Figure 4-1: Example of a customized handling device

Considering all these points the approach must cover the following objectives.

Generate initial gripper configurations for each part which consider the shape.

Adjust the initial gripper configurations based on simulation data so the deflection does not exceed a given value.

Combine different gripper arrangement solutions for different parts so they could be handled by one handling device.

Plan the implementation of the solution on a real handling device.

Figure 4-2 presents the systematics of a programmable approach to carry out the steps above.

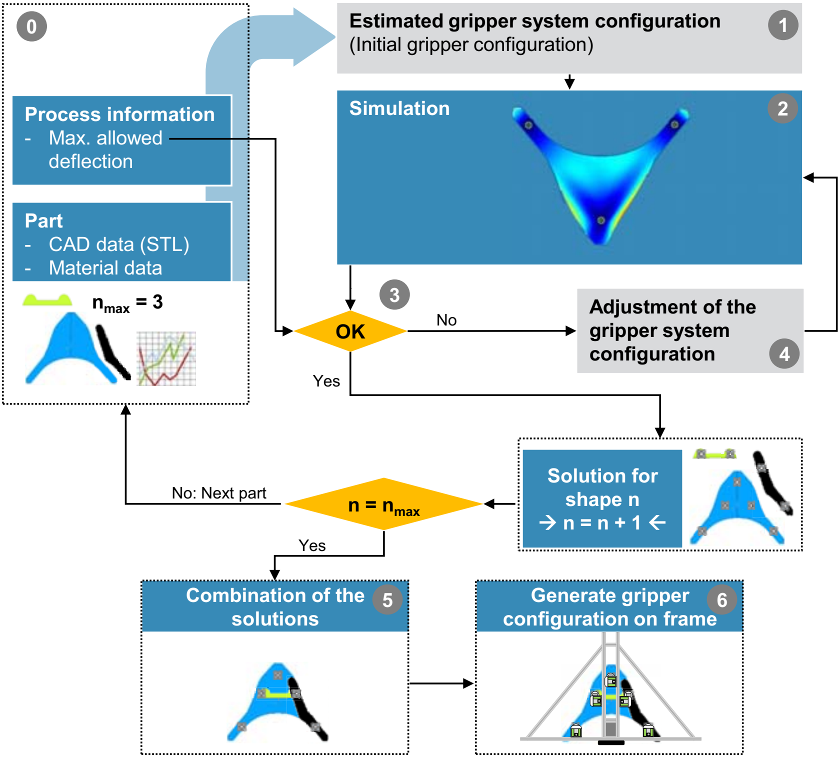
0
Process information
- Max. allowed deflection
Part
- CAD data (STL)
- Material data
n_{max} = 3
Estimated gripper system configuration
(Initial gripper configuration)
1
Simulation
2
3
OK
No
Yes
Adjustment of the gripper system configuration
4
Solution for shape n
→ n = n + 1 ←
$n = n_{max}$
No: Next part
Yes
Combination of the solutions
5
Generate gripper configuration on frame
6

Figure 4-2: Systematic for the design of handling device for lightweight production processes

The method will at a first receive a set of input data (“0” in Figure 4-2). These input data are the information of the material data, the shape of the part and an acceptable deflection of the part in the handling process. Therefore, it must be manually chosen which deflection is acceptable in this context.

With this input data a first gripper arrangement so-called “initial gripper configuration” has to be generated (“1” in Figure 4-2). This configuration enables a first simulation of the resulting deflection when the part is gripped by the handling device (“2” in Figure 4-2). It has to be checked if the occurring deflection of the part exceeds the acceptable deflection defined by the input data (“3” in Figure 4-2).

Now two different cases can occur. If the gripper configuration satisfies the process requirements for maximum deflection a solution for a shape is found otherwise an adjustment must be performed like adding a new gripper or just repositioning the existing ones (“4” in Figure 4-2). This proceedure is repeated for every shape until a acceptable solution exist. In the next step (“5” in Figure 4-2) the different solutions are combined to one gripper configuration. This enables the handling device to grip the different shapes which are necessary for the production of one lightweight part. The last step (“6” in Figure 4-2) will generate an implementable solution based on a modular handling device.

4.3 Thesis procedure

The different investigations and developments which are necessary to implement such a systematic but also programmable gripper configuration process are presented in Figure 4-3.

The first step is the development of an experimental setup to investigate handling processes in a reproducible way in chapter 5. For this purpose, it is important to first compose all requirements of a handling system in a production process. Based on this information, a modular handling device is designed which will enable a high range of different gripper configurations. In order to enable reproducible investigations, the final step in chapter 5 is the design of a setup to provide textile parts for the handling test.

One of the key concerns for the design of the handling device is the deflection of the part in the handling process. Because this approach should cover arbitrary geometry, a simulation model is necessary to predict the deflection of the part without performing experiments all the time. For this purpose, chapter 6 presents the model for the simulation based on an FEA. First, the boundary conditions for the simulation are defined and the material data are collected. Also, the simulation model and its simplification are presented. These steps are performed for textile and SMC material separately. The chapter ends with a comparison of practical experiments and simulation results of the deflection.

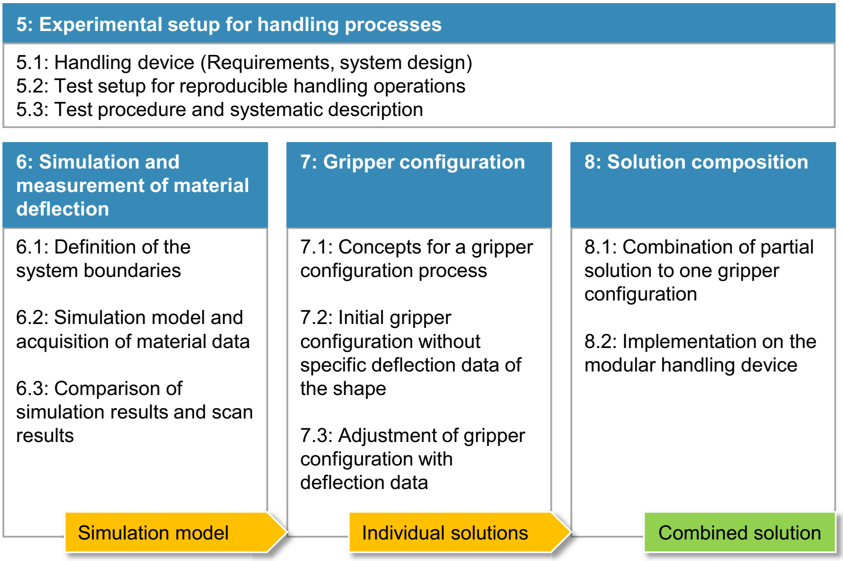
5: Experimental setup for handling processes
5.1: Handling device (Requirements, system design)
5.2: Test setup for reproducible handling operations
5.3: Test procedure and systematic description
6: Simulation and measurement of material deflection
6.1: Definition of the system boundaries
6.2: Simulation model and acquisition of material data
6.3: Comparison of simulation results and scan results
7: Gripper configuration
7.1: Concepts for a gripper configuration process
7.2: Initial gripper configuration without specific deflection data of the shape
7.3: Adjustment of gripper configuration with deflection data
8: Solution composition
8.1: Combination of partial solution to one gripper configuration
8.2: Implementation on the modular handling device
Simulation model
Individual solutions
Combined solution

Figure 4-3: Approach for the design of handling device in lightweight productions

Chapter 7.1 will initially discuss several possibilities how a gripper configuration could be achieved for arbitrary geometries. Based on this discussion a suitable method is selected and examined. The investigation in chapter 7.2 first covers the initial gripper configuration whereas chapter 7.3 addresses the adjustment of the gripper configuration and use the models from chapter 6. Both methods will be evaluated at the end of each chapter by testing them on a range of different geometries.

Chapter 8 will address the combination of the different gripper arrangements to one solution and a systematic planning of the implementation on a handling device. As a proof of concept, the gripper configuration for a use-case is than implemented on the real modular handling device.

5 Experimental setup for handling processes

In this chapter an experimental test setup will be developed. The test setup should enable a reliable and reproducible way to perform handling test with different gripper configurations, shapes and boundary conditions. Furthermore, it should be possible to measure the deflection of the part on the handling device. This procedure is represented in Figure 5-1 by the symbols and method according to the VDI 2860. The figure also suggests a device assignment (Figure 5-1: 1, 2, and 3).

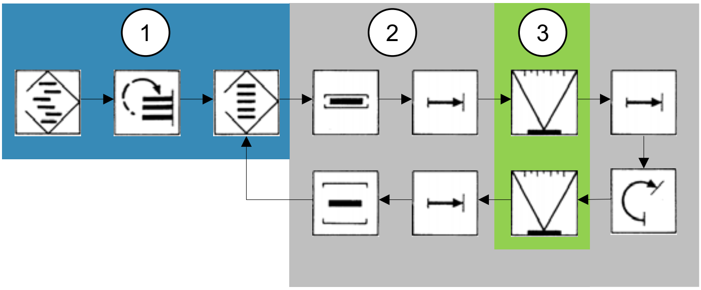

Figure 5-1: Procedure of a handling test illustrated by VDI 2860

In order to ensure the reliability of the tests, it is important to assure the correct positioning of the grippers on the part. Hence, the first step of a test procedure is the alignment of grippers and the part that should be handled on a reference (Figure 5-1: 1). After this alignment the actual handling operation can start by the activation of the grippers and the execution of the movements with the handling system (Robot + handling device) (Figure 5-1: 2). The movements are interrupted by the measuring of the deflection of the part on the handling device (Figure 5-1: 3). The following chapters will now discuss the solutions for the device assignments in Figure 5-1.

5.1 Handling device

In this chapter a solution is developed for the tasks in the device assignment “2” in Figure 5-1. The functions this device should be capable of based on Figure 5-1 are very simple and could be summarized by holding and moving the part. The movement is enabled by a robot, the holding of the part by a handling device on the robot.

The main components of a handling device are the grippers and the structure that connects these grippers to the robot. Besides these basic components, also control elements could be added on the handling device. Since the system will have all of these components the handling device will be a mechatronic system and the development will follow the systematic of VDI 2206 (Figure 5-2).

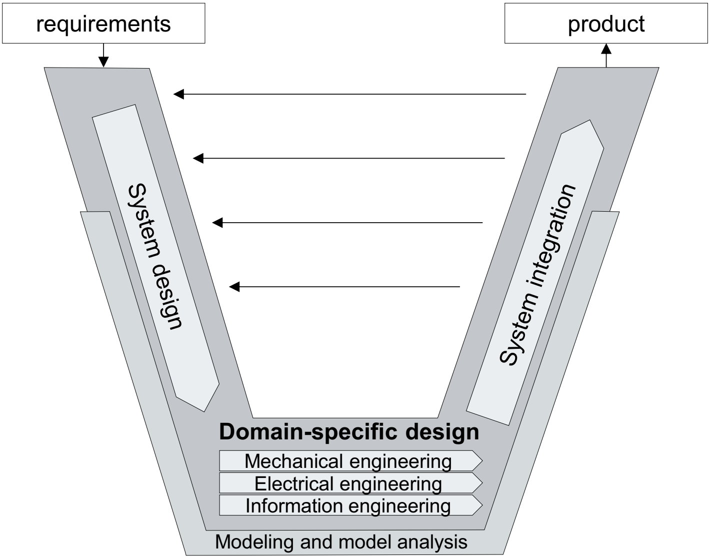
requirements
product
System design
System integration
Domain-specific design
Mechanical engineering
Electrical engineering
Information engineering
Modeling and model analysis

Figure 5-2: Design method of mechatronic systems by the V-model according to VDI 2206 (own representation)

The first step involves developing a summary of the requirements for the system. A key requirement is the possibility to enable various gripper configurations to implement customized arrangements for different use-cases, since these configurations could not be classified in advanced.

Nevertheless, the design of the handling system should also reflect the requirements of actual lightweight production processes. Consequently, first the requirements of the RTM and SMC lightweight production process must be summarized. In dependence of these findings, boundary conditions for the handling systems are defined.

5.1.1 Requirements for handling devices in lightweight production processes

The general criteria, which have an influence for the design of a handling device or the selection of a gripper, are almost constant in different research papers addressing this problem (Biermann, Hufenbach & Seliger 2008, p 22; Pham & Yeo S. H. 1991, p 309;

Straßer 2012, p 226; Seliger et al. 2003, p 23; Schmalz & Reinhart 2014, p 215). Figure 5-3 presents a summary of categories and criteria for handling devices by the state of the art.

Since these parameters are a summary of the state of the art and considering not a specific production process, not all are relevant for lightweight production processes. For example, humidity is mostly an unwanted element in lightweight production processes, since it has a negative influence (Ochs 2013, p 150). Furthermore, requirements by the environment are mostly special and could be ignored in the development of a first idea for a handling device.

Process

Type of process
Type of material provision
Shop floor layout
Number of different objects
Number of objects at the same time
Demanded accuracy
Process security
Cycle time
Cost

Part

Geometry dimensions
Geometry shape
Center of Gravity
Material properties
Surface quality
Temperature
Tolerance
Weight

Handling system

Carry capacity
Controlling interface
Actuation
Type of robot
Acceleration
Velocity
Accuracy

Environment

Temperature
Interference
Humidity

Legend:

- *Irrelevant parameter for a first concept for a modular handling device*
- **Relevant parameter**

Figure 5-3: Summary of parameters from the state of the art which have an impact on the design of a handling device

Furthermore, the parameters should be used to develop a concept for a modular handling device. As a result, a large number of parameters defined in section “Handling system” (Figure 5-3) will be defined by the configuration of the handling system/device and not by the general idea of the modular concept. The only remaining parameter in “Handling system” is therefore the robot which is holding the modular handling device. The same applies to most parameters in the "Part" area. Since the parts are not known yet at this time, many of the parameters cannot be determined. Because of that it is important to define rough guidelines that must to be met.

The RTM and SMC processes which were already described in chapter 3.1, will be analyzed to identify requirements. For this purpose, the parameters of the category “Process” should be considered first, starting with “Type of process” and “Shop floor layout”. The other parameters will be discussed after.

Process: Type of process, material provision and shop floor layout

For the RTM as well as the SMC process, the different stations which must be connected by the robot can be divided into material provision, preparation area and the hydraulic press. The general layout has already been presented in Figure 3-1.

The first step in both processes is the provision of the semi-finished material. One possibility is to cut the shapes on demand for the production out from an endless material roll. The cutting technology differs between SMC and RTM but this circumstance does not change the general way the cut out parts are provided for the next process steps. As a result of this cutting operation the parts are distributed by a fitting algorithm over the full width of the endless material roll to reduce the amount of wasted material. Due to this fitting algorithm, the orientation of the shapes on the cutting table could differ even for same parts if the fiber orientation for the parts itself keep constant. An alternative to the cutting table is a magazine for pre-cut parts. The handling device must then make sure only one part at the time is gripped out of this magazine.

From either of these devices the material is then transported to a preparation area. Depending on the type of process (SMC or RTM) the different parts are now stacked together as one component to weigh them and reach a target mass (SMC) or build up a combination of different dry textile parts with different fiber orientations (RTM). By SMC there is also the possibility to add Co-material prepreg to the Dico SMC to produce a CoDico part. In either case, the generated built-up contains multiple layers together. Through these steps in the preparation area, the conditions for the handling process considerably changes, whereby after this step a second handling device with other requirements is necessary to transport the stack into press for the infiltration (RTM) or forming (SMC).

> *Requirement:*
>
> The first handling step between the cutter or magazine and the preparation area has to handle different shapes by one handling device. Through the cutting process these different parts are in a well-defined position and orientation.

Process: Number of different objects

The number of different shapes used to build up a textile stack for an RTM process could theoretically reach any number. Examples could be found using one to 14 different cut outs to produce a preform (Gerngross & Nieberl 2016, p 3; Klingele 2014, p 93; Straßer 2012, p 169; Ehinger 2013, p 168). The number of different sheets in the SMC process is normally smaller, since the material can flow. Due to this ability, it is often sufficient to stack two sheets over each other or place them side by side in the mold (Fette et al. 2016, p 135; Castro & Griffith 1989, p 636).

> *Requirement:*
>
> It can be seen that several different cut outs are used in the production of FRP. A handling device which has to carry out the required handling steps automatically has therefore to be able to transport several different shaped parts from the cutting table. This thesis will focus on the handling of the different parts one after another. Accordingly, only one part at a time will be gripped by the handling device.

Process: Cycle time

Since the handling normally adds no value to the product, the handling steps must take place in tact to the value-adding process steps and should not add extra time to the production at all. In the RTM as well as in the SMC process the semi-finished part has to stay for a long time in the press. This is because the matrix material, which connects the load bearing fibers together needs to cure, before the mold could be opened. Together with the opening and closing of the mold, the removal of the finished part and a short cleaning step, this could take up between three or six minutes (Rosenberg et al. 2014, p 465).

Assuming for example that five cut out parts are necessary to form a textile stack to be further processed (for example Klingele (2014, p 93)) and the infiltration or pressing needs only three minutes, the handling step for one shape has to be completed within a time slot up to 36 seconds. This time slot includes the movement from the start to the target position and back. The time slot for one direction therefore is only 18 seconds.

> *Requirement:*
>
> A first estimation of the available transportation time for the handling process is 18 seconds for one part in one direction.

Part: Geometry dimensions

The dimensions of the parts that are possible depend in one direction on the dimensions of the endless roll material. For dry fiber textile materials widths of 800 mm or 1200 mm are common. SMC material rolls can be bought up to a size of 1500 mm (Lengsfeld et al. 2014, p 13; Magnaud 2016, p 11). On the other side the material also has to fit into the press, most of them have a square or near square layout.

The largest share of components will therefore have dimensions significant below 1500 mm.

> *Requirement:*
>
> A maximum dimension of the parts between 1200 mm and 1500 mm should be considered.

Part: Geometry shape

The geometry of the parts is not predictable in any way. Their shape is part of the dimensioning process and considers the load which should be handled by the finished part. This dimensioning step is influenced by a wide range of different aspects like cost, static or dynamic load or restrictions by the production process. Adding further restrictions to enable the automated handling in the production should be avoided.

> *Requirement:*
>
> The handling device must enable a high flexibility for the arrangement of the grippers to allow the handling of a great diversity of shapes.

Part: Weight

The maximum weight of the parts could be estimated by the size of the shapes and the typical weight per area of SMC material and dry fiber textile. Typical density of SMC is 1.9 g/cm^3. Assuming a material thickness of 1 mm and a rectangle shape of 1500 mm x 1500 mm, a maximum weight of 4.275 kg can be calculated. The typical weight per area of dry fiber textiles varies between 150 g/m^2 and 450 g/m^2 (Cherif 2011, p 388). A rectangle shape with the same dimensions as above but with textile material and not SMC would therefore be much lighter (1.0125 kg).

> *Requirement:*
>
> The maximum weight of a part on the handling device will be 4.275 kg.

Handling device: Type of robot

The use of vertical articulated arm robots is very widespread. They offer a huge motion range and a high degree of orientation freedom of the end effector. The motion radius varies between 1800 mm and 2700 mm. Typical carrying capacities are 120 kg and 180 kg. These capacities assume a center of gravity of the end effector near the robot flange. Quite often the motion range is more important or critical than the carry capacity. This is especially the case if it is necessary to consider the handling of large-scale parts. Large-scale parts like a textile with a dimension of 1200 mm x 1200 mm also need machines and stations with at least the same dimensions or even larger. Therefor a large amount of the robot movement range is necessary to reach into these large stations. Consequently, the end effector has to be designed in such a way that the movement range of the robot is not influenced negatively.

> *Requirement:*
>
> The handling device (often a vertical articulated arm robots) must be designed in such a way that the movement range of the robot is not influenced negatively.

Handling device: Acceleration

A first estimation showed that the robot has approximately 36 seconds to transport a part. The value can of course change if the production process is faster or the number of individual parts is larger. In these 36 seconds, the robot must perform both the transport movement with the part on the handling device and the return movement. It is possible to execute the back movement faster to have more time for the transport movement. Here, however, the less favorable case should be taken into consideration, the transport movement and return movement should be carried out at the same speed.

In the 18 seconds available for a transport or backward movement, the robot must lift the part, carry out a 180° swivel (in the case of handling system I in Figure 3-1) and deposit the part again. Based on the temporal estimation of individual movement sequences of a Kuka KR180 from A_Jenkel (2016, p 123), a time of 26 seconds would be required for this in T2 mode at 10 % maximum speed. Already at 30 % maximum speed only 12 seconds would be necessary. At this point, reference should be made to the forthcoming results in chapter 6.1.1. It shows a vertical acceleration of 0.35 m/s^2 will occur in T2 mode at a maximum speed of 30 %.

Requirement:

First estimation of vertical acceleration is 0.35 m/s^2.

The boundary conditions identified above are summarized in Table 5-1 for a better overview.

Table 5-1: Boundary conditions for the development of a modular handling device

Boundary conditions	
Type of process	RTM and SMC, gripping different parts from cutting table
Number of different objects	1 – 14 (based on examples), number can be larger
Cycle time	18 seconds
Geometry dimensions	Max. 1200 mm to 1500 mm
Geometry shape	Not predictable
Weight	Max. 4.275 kg
Type of robot	Vertical articulated arm robots, 120 kg – 180 kg, do not restrict handling range by handling device
Acceleration	0.35 m/s^2

5.1.2 System design of the modular handling device

The requirement should now be used in developing the handling device. The process by the V-model now suggests defining a system design. This system design aims "to establish a cross-domain solution concept which describes the main physical and logical operating characteristics of the future product" (VDI 2206 2004, p 29).

This system design should consider the three main components of the handling device:

1. the gripper(s)
2. the frame structures
3. the control elements

General idea for system design

The general idea for the system design is to use a modular concept to enable a high flexibility to implement different gripper configurations on the handling device. This concept is pictured in Figure 5-4.

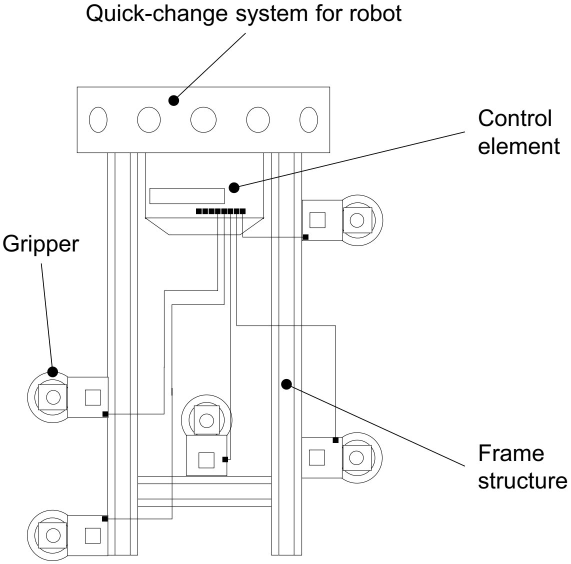

Figure 5-4: Three main components of the handling device

1. *Gripper (modules)*

In such a concept, the actual gripper is just one part of a whole gripper module. This gripper module should enable the fastening on the frame structure. The gripper module therefore provides the mechanical connection for the gripper to the frame. The position of the gripper is mainly defined by the position on the frame structure. The frame structure is often constructed from modular profiles. These profiles have inaccuracies that must be compensated.

2. *Frame structure*

The frame structure is the connection between the gripper and the robot. The connection to the robot could be realized by a quick-change system. The idea of modular building strategy is possible by defining a basic frame structure that will not be changed and an adjustable one. By using modular construction profiles to build this frame, adjustments become quite easy.

3. *Control*

Handling devices are often under the direct control of the robot. For instance, the robot control (RC) controls a valve terminal mounted on the robot through bus communication protocol and the gripper in turn is directly connected to the valve terminal. This means that if the gripper configuration on the handling device is modified the robot program must also be accordingly modified. This reprogramming in the robot can be avoided if the handling device itself has a separate control unit that represents an interface between the robot and the gripper module. This central control unit (CCU) should make it possible to configure the different grippers to action groups. The robot can than activate one or more gripper groups by one single signal.

The CCU needs the ability to activate and deactivate the grippers which is possible by turning on and off the supply of pressurized air. This could be done by a valve terminal that is under the direct control of the CCU. This valve terminal has a defined number of outputs and will therefore define the maximum number of possible grippers. Furthermore, if only a minor number of grippers is in use, some valves are useless. Accordingly, the idea is to decentralize the control of the pressurized air by adding a valve to every gripper module. If these modules also have a decentralized control unit (DCU), advanced features like the separation of sheets are possible as already shown by Förster et al. (2017, p 43).

All of these above described ideas for the system design are illustrated in a first concept (Figure 5-5) and the ideas will now be used in the domain-specific design.

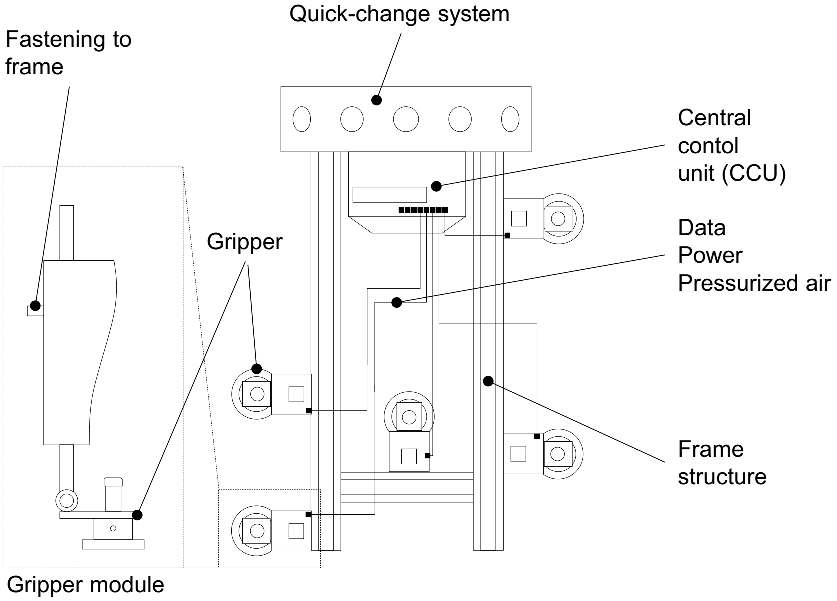
Quick-change system
Fastening to frame
Central contol unit (CCU)
Gripper
Data
Power
Pressurized air
Frame structure
Gripper module

Figure 5-5: Concept for modular handling system

Mechanical domain

The subject of the mechanical domain is mainly how to implement the frame structure and the gripper module. This domain must also address the mechanical connection to the robot. There is a wide range of modular systems to build up a frame structure for different applications. Irrespective of minor advantages and disadvantages the handling system will be built-up of Bosch compatible construction profiles with a side length of 30 mm x 30 mm, because they are widely used and available.

To realize the connection to the robot a quick-change system SWS-150 by Schunk is used. It enables a fast attachment and detachment from the robot end-effector. A set of construction profiles will be fastened on the quick-change system to provide a basic setup on which further construction profiles can be attached. This basic setup also contains a position for the CCU, which is a constant element for every configuration of the handling device. The difference between the basic setup frame and the adjustable elements is shown in Figure 5-6. In the analyzation of the requirements a maximum dimension of the parts of 1500 mm x 1500 mm was identified. The most parts will not need this maximum dimension. Therefore, the first setup of the variable frame structure is built-up with a dimension of 1200 mm x 1000 mm. An extension of these dimensions is possible without any problems.

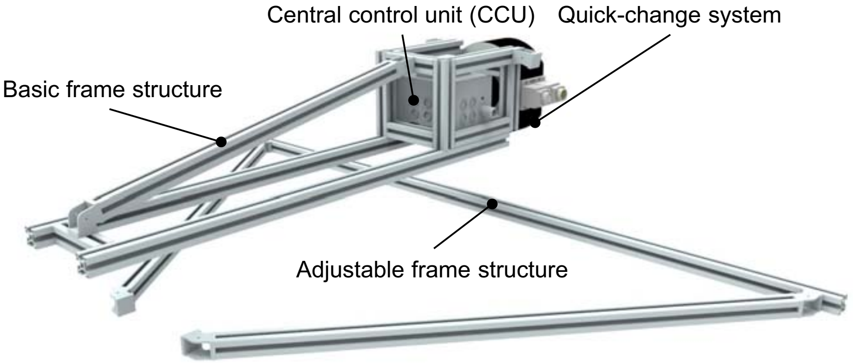

Figure 5-6: Basic frame structure and adjustable frame structure of the handling system

The gripper module is made of laser cut baseplate (Figure 5-7). With a standard corner element, it is connected to the frame structure. To compensate minor inaccuracies a mechanic adjustment with standardized, available and also cheap components is realized. It enables the adjustment of the height and also two different rotations. This baseplate also holds a valve which is capable to control a flow of pressurized air of 650 l/min. This is the maximum air flow that the low-pressure surface gripper (SCG 1xE100 A MA) used can handle. Due to the symmetry, an optional second valve could be placed in the gripper module. A DCU is placed on top of the valves. The last element is an optional proportional valve. These elements enable the regulation of the pressure between 0 bar and 6 bar and therefor the holding force of the gripper.

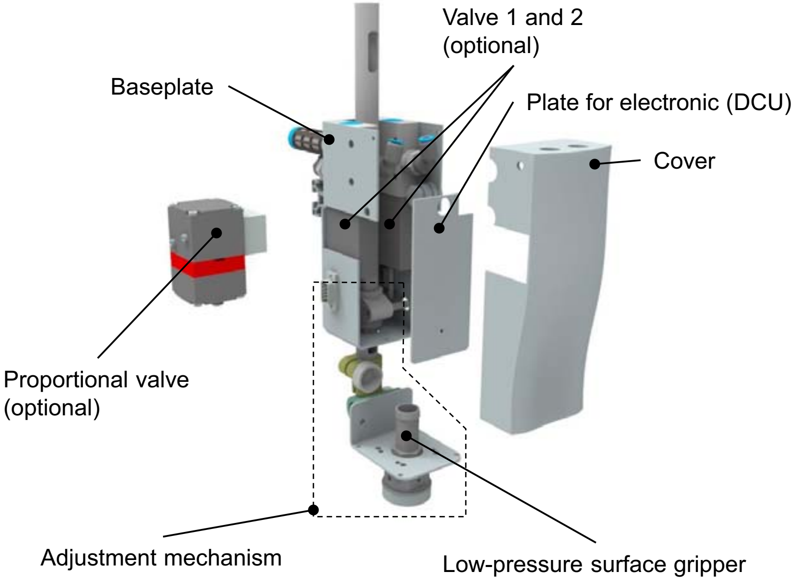
Valve 1 and 2
(optional)
Baseplate
Plate for electronic (DCU)
Cover
Proportional valve
(optional)
Adjustment mechanism
Low-pressure surface gripper

Figure 5-7: Mechanical elements of the gripper module

Electrical domain

The electrical domain must develop two main components for the handling device control. These components are the CCU in the center of the handling device and also the DCU in the gripper module. Both have different tasks.

The main tasks of the CCU is to configure the gripper modules and provide an interface between the RC and the DCU. Furthermore, the DCU must be supplied with voltage. The supply with electrical power is implemented by splitting the provided power from the robot to the gripper by the quick-change system. This quick-change system also provides the connection between the CCU and RC. Twelve digital inputs from the RC to the CCU enable a simple way for the robot to control the handling device (Figure 5-8).

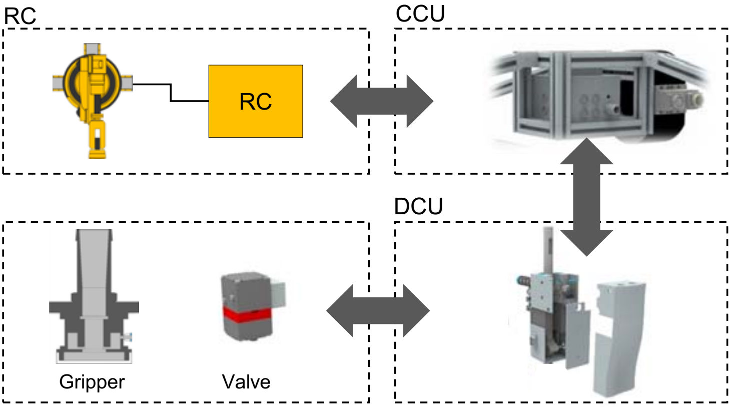

Figure 5-8: CCU to DCU communication and the control of the normal and proportional valves by the DCU in the gripper module (Own representation based on A_Steinlein (2017, p 53))

The CCU needs an electrical device that is capable of enabling a configuration of the handling device and the communication with the DCU. Increasingly more devices today try to implement the idea of industry 4.0 by providing a user-friendly way to enable an interaction between the user and the device. This reasonable aspect should be considered by a graphical user interface (GUI). This GUI should be runnable on a mobile device. The connection between the mobile device and CCU must use common types of communication like the connection through a USB or W-LAN. Since W-LAN has a higher comfort aspect for the user, because it doesn’t need to search for the physical connection plug, it is the preferred solution. Considering all these requirements the CCU is realized by using a Raspberry Pi 3 B.

The DCU now has to interact with the CCU, while it also has to control normal and proportional valves. The Raspberry Pi in the CCU already communicates with the mobile device to interact with the user. The communication with the DCU could now be implemented by the same way. For this purpose, an Arduino MKR1000 with a W-LAN module is used. The MKR1000 can control the valves with its digital and analog outputs.

Information domain

The information domain must now implement the communication and the setup through the GUI. The communication is managed by the Raspberry Pi in the CCU. It hosts a multi-client network. The gripper modules as well as the mobile device of the user act as clients. The server creates for every client a socket and establishes the connection. In every cycle of the main program on the server, the clients get a new data package which contains information for the gripper module configuration and orders. Detailed information regarding the development of the communication are given by A_Steinlein (2017).

As a result, every gripper module can be controlled by using a mobile device running a java application (Figure 5-9).

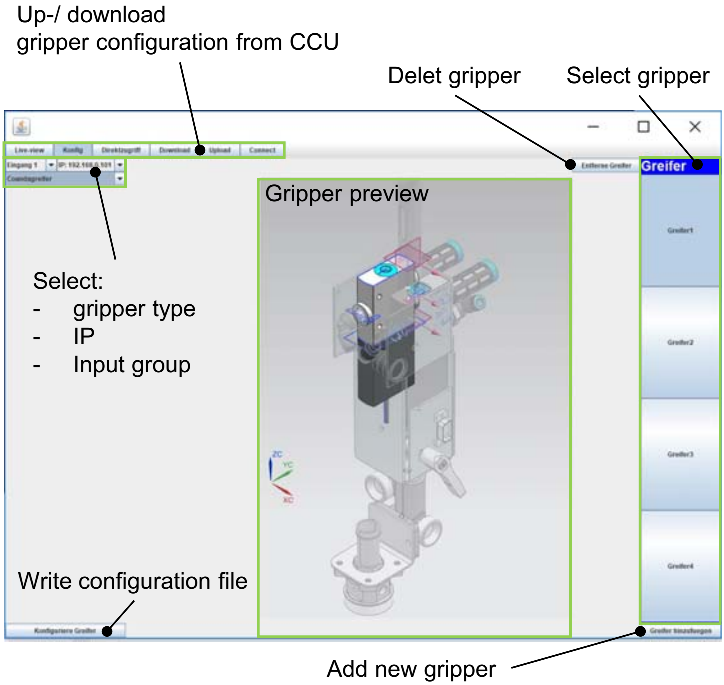
Up-/ download
gripper configuration from CCU
Delet gripper
Select gripper
Live-view
Konfig
Direktzugriff
Download
Upload
Connect
Eingang 1
Coandagreifer
Entferne Greifer
Greifer
Gripper preview
Greifer1
Greifer2
Greifer3
Greifer4
Select:
- gripper type
- IP
- Input group
Write configuration file
Konfiguriere Greifer
Greifer hinzufügen
Add new gripper

Figure 5-9: GUI for gripper configuration

In this application, the user can add or delete gripper modules. Every gripper module is identified by a unique IP address, which is stored in the DCU. When the GUI is connected to the CCU for the first time, the current gripper setup stored in the CCU can be downloaded. Changes in the setup only take effect when the new data set is uploaded to the CCU by the user. The application also offers the possibility to control the gripper modules directly. The gripper can be activated and the pressure is directly controllable if a proportional valve is mounted on the gripper module.

Final system design of the handling device

The overall result of the development process in this chapter is the handling device presented in Figure 5-10. It is capable of enabling various gripper configurations. This flexibility is possible by a modular frame structure which holds gripper modules. A gripper module itself contains the whole necessary periphery to operate the gripper and therefore helps to increase modular flexibility.

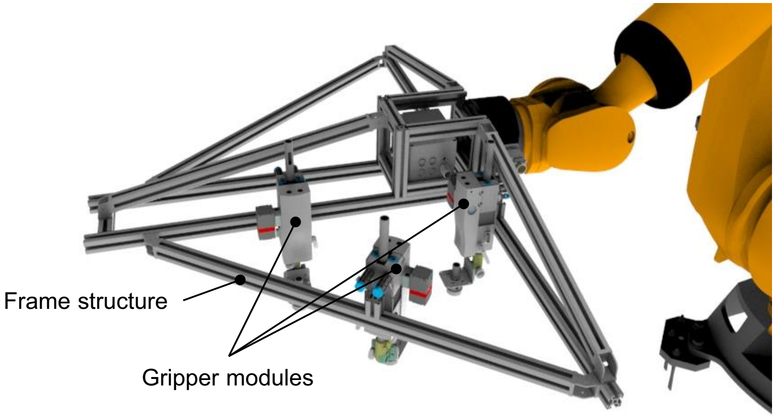

Figure 5-10: Final design for the handling device

5.2 Test setup for reproducible handling operations

This chapter will now develop a solution for the tasks in the device assignments 1 and 3 in Figure 5-1. The functions of this device should enable a reproducible execution of the handling experiments and the measurement of the deflection. Reproducibility in this context means ensuring the correct alignment of the gripper relative to the handling part. This could be achieved if the grippers as well as the part are aligned on one reference. This reference also needs the same flexibility as the handling device. This problem is solved by using a projector and a projection surface (Figure 5-11).

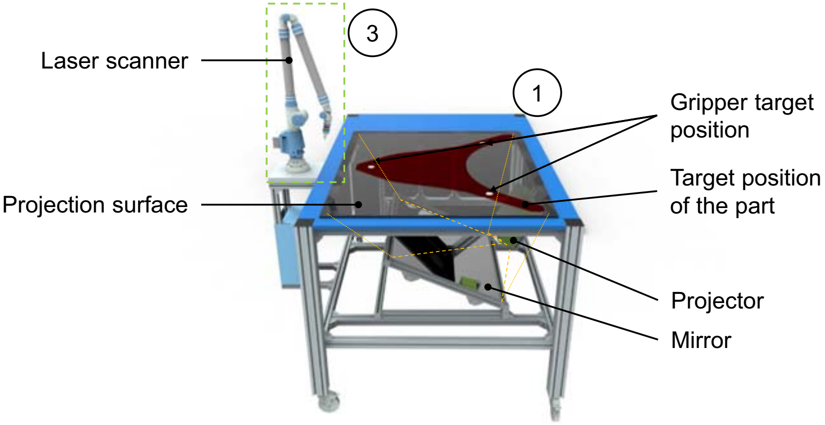

Figure 5-11: Test setup to project the shape of the part and the gripper onto a surface

Before the start of a handling test, shape and gripper positions are projected onto the surface. In a first step the handling device is positioned over the projection surface and the gripper on the gripper modules are aligned to fit the target positions. If the grippers are aligned correctly, a single sheet is placed on the same surface and aligned on the outer shape of the projected representation. Through this setup all functions for device 1 in Figure 5-1 are covered. The measurement of the deflection (3 in Figure 5-1) is implemented by a FARO ScanArm. With a laser scanner unit at the front of the end effector the deflection of the whole part can be measured. An outstanding issue is how to compare different scans to each other. This is possible by using reference objects that remain constant between the scans and serve as orientation for the alignment between the different scans. The elements are mounted on the handling device and must be aligned as well as the grippers like previously described. A PC provides the picture for the projector. The projector alone is incapable to displaying the dimensions of the part, grippers and references correctly. Distortions are caused by the redirection of the image via the mirror as well as the angle between the projector and the projection surface which cannot be compensated by the settings on the projector alone. For this reason, first a picture without compensations is generated. A calibration process implemented with MATLAB captures the X and Y values of the pixels which represent the corner of the real projection surface and generate a transformation matrix to correct the picture. The setup for the handling test is presented in Figure 5-12. In addition to the grippers so called reference objects are fastened on the frame. These reference objects are also scanned with the laser scanner device and allow an alignment of the scanned data to compare them to each other.

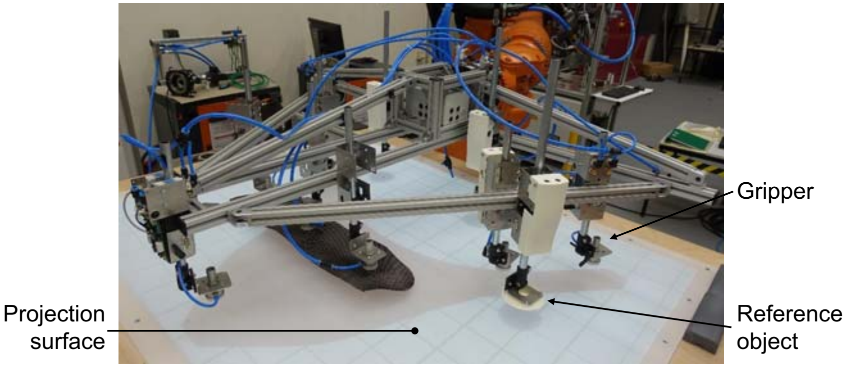

Figure 5-12: Complete setup for the handling tests

5.3 Test procedure and systematic description

The test procedure is illustrated in Figure 5-13. The first step is to load general setup data and display them on the projection surface. In the second step the handling device is placed on the projection surface and the gripper/reference objects are aligned to match the planned gripper/reference configuration. The reference objects are necessary, so that afterwards different scans can be aligned to each other. If this step is completed, the handling device is lifted off the surface by the robot and the part is aligned according to the projection. Now the robot program is loaded into the RC. This program defines which accelerations and velocity will occur in the handling process. The robot will then execute the handling operation by picking up the part and performing the planned motion. The last step is scanning the part and reference objects.

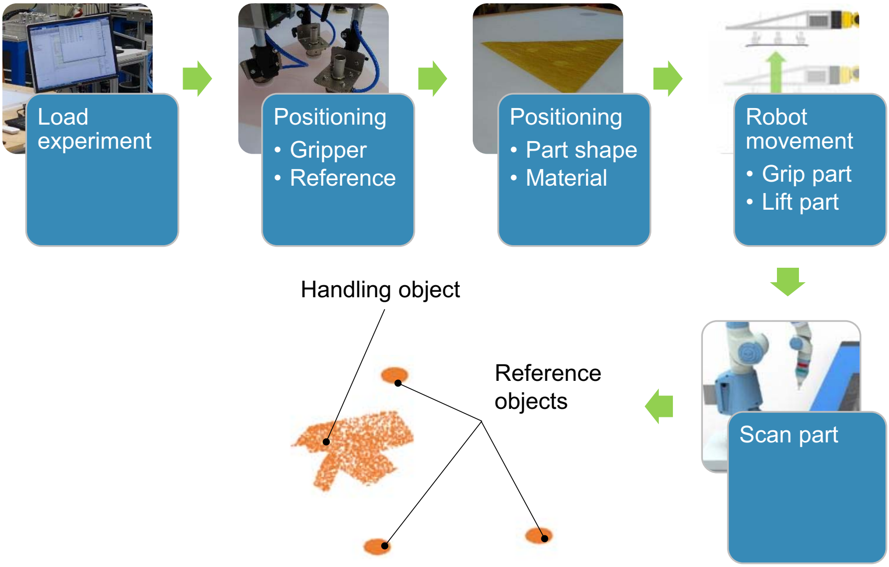
Load experiment
Positioning
• Gripper
• Reference
Positioning
• Part shape
• Material
Robot movement
• Grip part
• Lift part
Scan part
Handling object
Reference objects

Figure 5-13: Test procedure of a handling test to measure the deflection

The experiments should now get a unique and systematic description. This enables the later repetition of the experiments and an explicit description of the test parameters. The experiments are numbered consecutively. Every experiment must describe the grippers and reference configuration on the handling device, as well as the shape and the material of the handling part. Finally, the movement of the robot must be defined.

To describe these machine-readable data the data format java script object notation (JSON) is used. For every experiment a JSON file is created called e.g. “E001”. The letter “E” identifies the JSON file as a description of an experiment. A JSON file is a sorted list of names and values. The experimental file is designed as a collection of file names that describe the geometry of the part, the material, etc. (Source text 5-1).

Source text 5-1: JSON file describing an experiment

```
{"experimentSetup":[
{"name":"geometry","params":{"StlFile":"D300"}},
{"name":"material","params":{"JsonFile":"SigratexCW160PL110"}},
{"name":"gripper","params":{"JsonFile":"G001"}},
{"name":"reference","params":{"JsonFile":"R001"}},
{"name":"robotProgram","params":{"JsonFile":"P001"}}]}
```

Many of the files are JSON files themselves. Only the geometry of the part is stored as a standard tessellation language (STL) file and can be opened and created by most common CAD programs. This format has the advantage that it can also be opened with other programs such as MATLAB and thus enables analysis and further processing of the geometries. The other JSON files are adapted to the necessary variables to describe the gripper arrangement or the material. The description of the gripper and the references is for example very similar. The file names starts with “G” for gripper or “R” for references and define the arrangement by the X and Y value of center and the radius.

Source text 5-2: JSON file describing a gripper and a reference arrangement

```
{"gripper":[
{"name":"circular","params":{"center":[-34.64,-20],"radius":20}},
{"name":"circular","params":{"center":[0,40],"radius":20}},
{"name":"circular","params":{"center":[34.64,-20],"radius":20}}]}

{"reference":[
{"name":"circular","params":{"center":[-473,543],"radius":40}},
{"name":"circular","params":{"center":[21,536],"radius":40}},
{"name":"circular","params":{"center":[-149,-341],"radius":40}}]}
```

The program to create the projection for the table uses this description of the experiments to generate the projection image. This ensures that tests can be repeated at any time under the same boundary conditions.

5.4 Use-cases for handling tests for RTM and SMC process

This thesis will consider the handling of dry technical textiles in the RTM process as well as SMC material. For each of these processing technologies, a use-case will be presented to evaluate the findings of this thesis.

5.4.1 Use-cases for SMC

The use-cases for the SMC process is a part combining SMC with continuous and discontinuous fibers (Figure 5-14). Discontinuous SMC is used to generate the basic structure. At specific areas continuous UD tapes are used to reinforce the part. This thesis will focus on handling discontinuous SMC since the dimensions of the part are larger than the continuous ones.

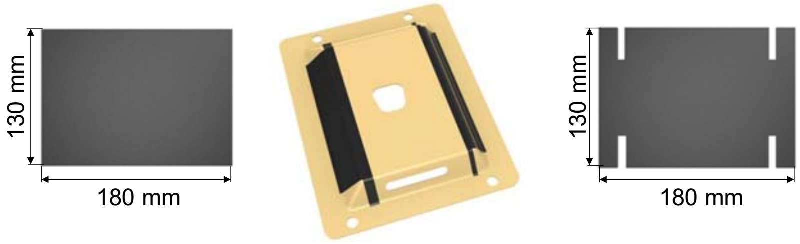

Figure 5-14: Two SMC sheets for the demonstrator of GRK 2078

5.4.2 Use-cases for dry fiber textiles in the RTM process

The use-case for a part made of dry textiles for the RTM process is a self-supporting rear diffusor used in the automotive industry. Four different textile shapes are used to generate the whole structure. The material used for this component is called Sigratex C W160-PL1/1. It is a plain weaved textile with an area weight of 160 g/m^2 using a 200 tex fiber (SGL Catalog 2016, p 6). Figure 5-15 pictures the rear diffusor and gives an overview of the different shapes.

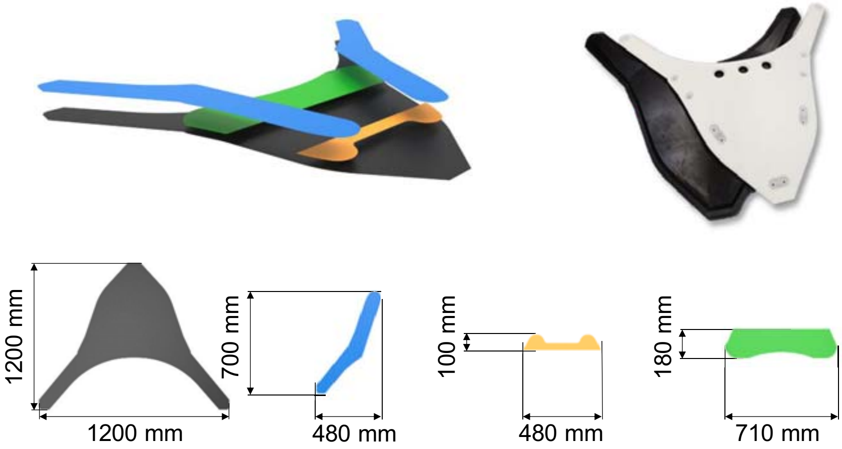
1200 mm
1200 mm
700 mm
480 mm
100 mm
480 mm
180 mm
710 mm

Figure 5-15: Self-supporting rear diffusor in the automotive industry

6 Simulation and measurement of material deflection

The adjustments of the gripper configurations in the further process in this thesis are based on simulation data which predict the deflection of the part in the handling process. In this chapter the simulation model for this approach is presented and discussed.

The mechanisms involved in the forming of textiles are complex and are the subject of numerous comprehensive investigations (Syerko, Comas-Cardona & Binetruy 2012, p 1365; Boisse et al. 2010, p 1229; Kang & Yu 1995; Hamila et al. 2009, p 1461; Fang & Liang 2011, p 2415; King, Jearanaisilawong & Socrate 2005, p 3867).

As a first step, the boundary conditions for the simulation are defined. The handling process can cause additional accelerations to the material. It is not clear how large these additional accelerations can be. Consequently, they will be measured. Also, not cured SMC has a viscoelastic behavior. This cause a deformation over time which is investigated. Based on these findings the simulation model will be chosen and necessary material parameters are determined. These steps will enable the simulation of the deflection of arbitrarily shaped handling objects. At the end of this chapter the simulated deflection is compared with experimental data.

6.1 Definition of the system boundaries

6.1.1 Acceleration and velocity in a vertical handling process

In this chapter the possible accelerations will be measured which can be applied on a part by a vertical handling process. The consideration of laterally occurring accelerations is not considered in the following and in all other considerations in this thesis.

To measure the accelerations the handling device is placed on the projection surface. It is then lifted by the robot in a vertical 600 mm movement using different modes of the robot. T1 is the set-up mode of the robot. In this mode the maximum velocity and acceleration is limited to one third. The T2 mode is also a set-up mode but has the same velocities and acceleration as the normal full-automatic operation mode that is normally used in an automated production. In every mode the maximum allowed velocity can be influenced by a 1 % to 100 % adjustment value. An acceleration sensor is installed on top of the CCU to measure the acceleration (Figure 6-1).

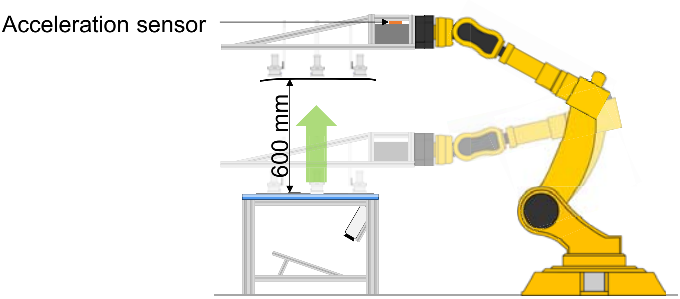

Figure 6-1: Vertical movement of the robot with the modular handling device

The measured values for T2 100 % are displayed in Figure 6-2. The movement is completed in almost 1.2 seconds. In this situation the robot can achieve a maximum acceleration of 2.68 m/s^2. By an integration over the time a maximum velocity of 1.12 m/s for the acceleration and 1.14 m/s for the deceleration can be calculated. The integration over the acceleration and deceleration should be equal in amount, because at the end the robot stops. However, such small errors are to be expected due to measurement uncertainties and the property of the integration to sum them up.

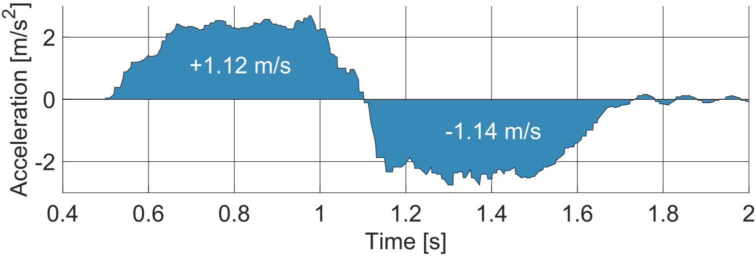

Figure 6-2: Acceleration and velocity of a vertical handling process (T2 100 %) of KUKA KR180

An acceleration of 2.68 m/s^2 is compared to the earth's gravity of 9.81 m/s^2 less significant. But it must be kept in mind that this is the fastest movement the robot can perform in this situation. A first estimation of the handling time was already done in chapter 5.1.1. A necessary robot mode of T2 30% was estimated based on experimental data. In Table 6-1 measured acceleration and calculated velocities for different robot modes are presented.

Table 6-1: Measured vertical acceleration and calculated vertical velocity for different robot modes

Robot mode	**Max Acceleration [m/s²]**	**Velocity [m/s]**
T1 10 %	0.35	0.04
T1 100 %	0.33	0.14
T2 33 %	0.35	0.36
T2 66 %	1.17	0.78
T2 100 %	2.68	1.12

For the T2 33 % mode the acceleration keeps small with 0.35 m/s^2. The earth's gravity will therefore dominate the behavior of the deflection with an acceleration of 9.81 m/s^2. Also the velocity has an influence on the deflection by draft. But if this aspect should also be simulated a computational fluid dynamic simulation (CFD) must be integrated. This will represent a major afford. To find out how large the influence can be, a rectangular sample of 25 mm times 250 mm is handled at T1 10 % and T2 100 % and scanned after the end of the movement (Figure 6-3).

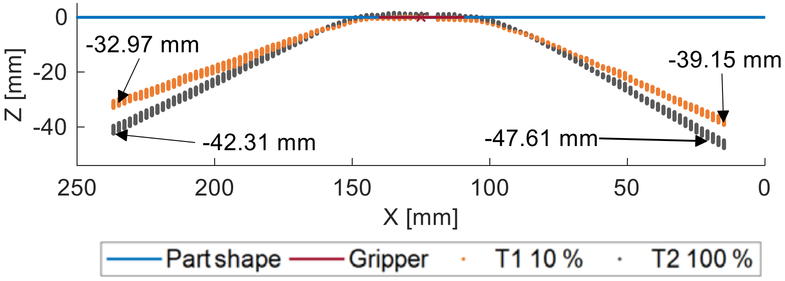

Figure 6-3: Deflection of a rectangle part after different vertical movements

The results in Figure 6-3 indicate that additional higher acceleration and also the velocity of handling have an influence on the final deflection when the handling process is completed and all movements are done. Also, it is unlikely that material has a complete elastic behavior. The exact calculation of draft forces causing this additional deflection will require a coupled CFD and FEA simulation. But since, the additional acceleration and velocity remain small for the relevant T2 33 % robot mode this thesis will only consider the influence of the acceleration and will also assume only a complete elastic behavior.

6.1.2 Experimental analysis of time behavior

The SMC material has a different behavior compared to a textile like the Sigratex C W160-PL1/1. First handling tests reveal a time depending deformation of the material. The goal of this first experimental analyzes is to get an idea about this time depending behavior. For this purpose, the test setup in Figure 6-4 is built-up.

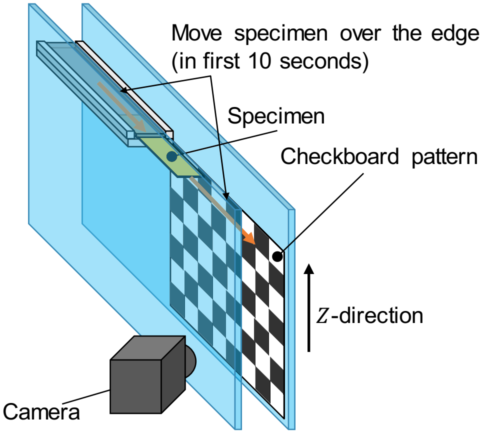

Figure 6-4: Schematic diagram of the test setup to measure the time behavior

The idea is to measure the tip of the specimen in the deformation process. Therefore, the specimen is pushed over the edge within a time frame of ten seconds. In addition, a camera is filming the whole measurement. A black and white checkboard pattern fills the background. This chess board pattern is crucial for the measurement process with the camera. The program to evaluate the measurement is implemented with MATLAB and it knows the exact dimensions of the checkboard. By comparing this data with the checkboard in the pictures, errors caused e.g. by the lens's distortion can be calculated and compensated. The corrected picture subsequently enables calculating the relative position between the camera and the chess board. The leading edge of the specimen is now detected by a set of different filters. These filters mainly use the different color of the specimen relative to the background to detect the specimen. A set of hole filling operations and Sobel filters ultimately enables detecting the specimen's leading edge, as shown in Figure 6-5. In order to measure the deflection, a deflection measure point is created, which is on the same level as the checkboard. Accordingly, the deflection of the specimen is detected.

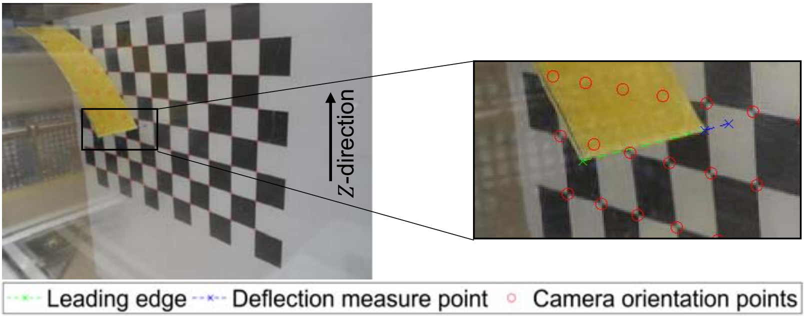

Figure 6-5: Measurement of the deflection over time by camera

In Figure 6-6 the deflection over time of three specimens is shown. Each specimen has a rectangular shape with a width of 25 mm according and a fix length of the rectangle of 10.5 mm is used. The specimen is pushed over the edge in the first 10 seconds of the measurement. This movement can be seen in Figure 6-6. Figure 6-6 shows the deflection in Z-direction of the “Deflection measure point” from Figure 6-5.

In the first 10 seconds the deflection value is mostly zero. Since this movement is performed manually, the movement does not always end at 10 seconds and can also spread. At the same time the specimen is at the beginning of the test procedure difficult to detect for the camera which results in incorrect measurements. The camera tends to measure slightly positive deflections in such a situation at the start. After 90 seconds most of the deflection has taken place.

The measurement of the deflection with the laser scanner later should therefore be taken after 120 seconds so that the sample does not deform anymore in the measurement process.

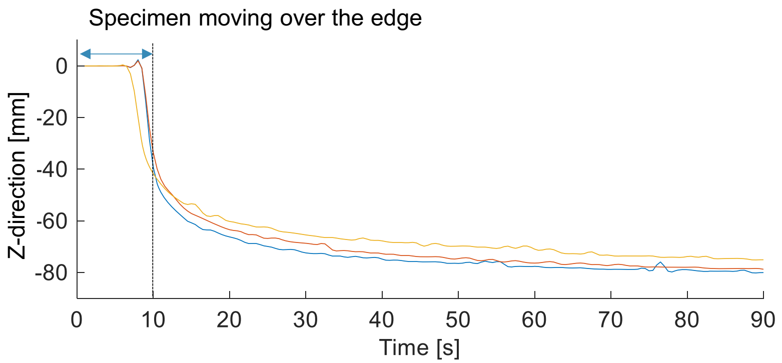

Figure 6-6: Deflection over time of three SMC specimens with a length of 10.5 mm

The same experiment is made with the textile Sigratex C W160-PL1/1. As expected the textile material did not have a critical time behavior and is no longer deformed after the 10 seconds defined by the experiment process.

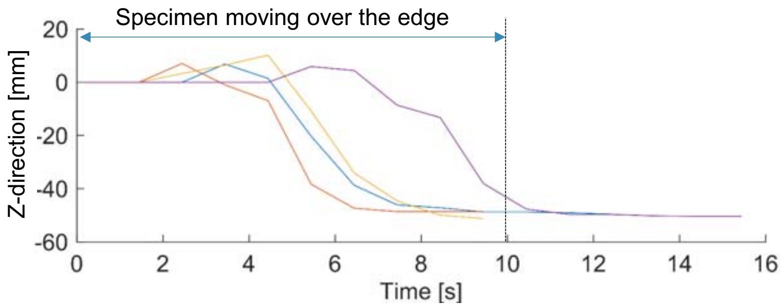

Figure 6-7: Deflection over time of four Sigratex C W160-PL1/1 textile specimens

6.2 Simulation model and acquisition of material data

The experiments in chapter 6.1.2 reveal a different time behavior of SMC and dry textile represented by the Sigratex C W160-PL1/1. This chapter will describe how the textile as well as the SMC material is simulated in ABAQUS. The material behavior in ABAQUS is defined by characteristic material values. These values are partly determined from the literature but also from experiments.

6.2.1 Selection of a simulation model

Both materials will have the assumption of a basic linear elastic material behavior in common. Furthermore, the geometry of the handling objects has a small and constant thickness in comparison with their other dimensions (Sigratex C W160-PL1/1: 0.3 mm and SMC: 0.9 mm). Therefore, S4R shell elements will be used in the simulation.

Textile:

The structure of the textile is initially assumed to behave orthotopically. In such a case, the description of the material behavior for the compliance matrix would include nine independent variables in Equation 6-1 (Kienzler & Schröder 2009, p 142). The parameters are the elastic modulus E, the shear modulus G and the Poission's ratio v in the different directions.

$$D = \begin{bmatrix} \frac{1}{E_1} & -\frac{v_{21}}{E_2} & -\frac{v_{31}}{E_3} & 0 & 0 & 0 \\ -\frac{v_{12}}{E_1} & \frac{1}{E_2} & -\frac{v_{32}}{E_3} & 0 & 0 & 0 \\ -\frac{v_{13}}{E_1} & -\frac{v_{23}}{E_2} & \frac{1}{E_3} & \frac{1}{G_{23}} & 0 & 0 \\ 0 & 0 & 0 & 0 & \frac{1}{G_{31}} & 0 \\ 0 & 0 & 0 & 0 & 0 & \frac{1}{G_{12}} \end{bmatrix}$$

Equation 6-1

Since the thickness of the textile is considerably smaller than the other dimensions, it is also assumed that the stress components in the thickness direction are small (Link 2014, p 33). This further simplifies the compliance matrix because all variables with a dependency of a parameter in Z-direction are no longer relevant ($E_3, G_{13}, G_{23}, v_{13}, v_{23}$) (Equation 6-2).

$$D = \begin{bmatrix} \frac{1}{E_1} & -\frac{v_{21}}{E_2} & 0 \\ -\frac{v_{12}}{E_1} & \frac{1}{E_2} & 0 \\ 0 & 0 & \frac{1}{G_{12}} \end{bmatrix}$$

Equation 6-2

Since the Sigratex C W160-PL1/1 is built up in the same way in 0° and 90° direction E_1 and E_2 will then also be identical. Furthermore v_{21} is equal v_{12}. In order to verify these assumptions, A_Hörrmann (2016) performed a sensitivity analysis. The nine engineering constants were systematically tested and examined in terms of the influence they have on the result. For this sensitivity analysis, a textile in the shape of an equilateral triangle was simulated (Figure 6-8).

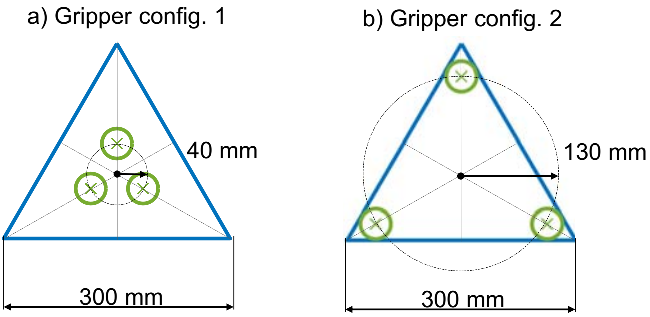

Figure 6-8: Gripper configuration 1 and 2

Two different gripper configurations are used. With “Gripper config. 1” (Figure 6-8, a), the grippers are deliberately placed far inside so that the corners can hang down. With “Gripper config. 2” (Figure 6-8, b) grippers are placed at the corners to capture effects in the middle of the shape. In “Gripper config. 1”, the deflection of the corners is used as a criterion for sensitivity. For “Gripper config. 2” the deflection is measured in the middle of the textile.

For the sensitivity analysis a fictional orthotropic material is assumed. Each of the nine independent parameters of Equation 6-1 is varied by reducing it by 20 % one after another while the others are kept constant. The change of the deflection caused by this parameter change is simulated. With these values the sensitivity is calculated by Equation 6-3. The result of this sensitivity analysis shows Figure 6-9.

$$Sensitivity = \frac{\Delta D_{Max}}{\Delta Value(E_1, E_2 E_3, G_{12}, G_{13}, G_{23}, v_{12}, v_{13}, v_{23})} \qquad \text{Equation 6-3}$$

In both configurations $E_3, G_{13}, G_{23}, v_{23}, v_{13}$ have no influence. This justifies the assumptions. However, there are different sensitivities between the two configurations regarding the remaining parameters E_1, E_2, G_{12} and v_{12}. If the grippers are placed inside, the elastic modules (E_1, E_2) are decisive. If, on the other hand, the grippers are at the outer edge in the corners, shear stiffness plays an important role. A description method called “Lamina” is used in ABAQUS to describe the material behavior with these remaing variables.

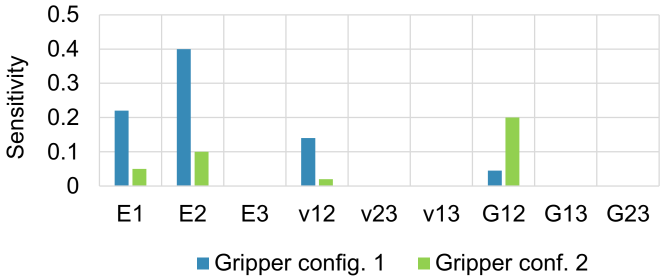

Figure 6-9: Results of the sensitivity analysis (A_Hörrmann 2016, p 50)

SMC :

The experimental analyses of the SMC material have already shown a time dependency of the deflection. The measurement of the deflection over time is a complicate process as can be seen in Figure 6-4. It is one thing to measure the deflection over time in the Cantilever test using a camera, but this method will not work if the deflection should be measured when a part is gripped by the handling device. Here the laser scanner should be used as already described in chapter 5.3. In order for to measure a part with the laser scanner, it is important that it does not deform anymore. As already discussed in chapter 6.1.2 no major deformation occurs after 120 seconds. So, this is the minimum amount of time a part must be hold on the handling device before the scanning and therefore the measuring of the deflection can begin.

For a transport movement a time of 18 seconds was estimated in chapter 5.1.2 which is significant smaller than 120 seconds. So, in a normal handling process the SMC material will not have the time to fully deform. Nevertheless, longer transport times could happen for example if a machine error occurs and the handling system must hold the part for a longer time. In such a case the SMC can deform completely. This will then be a worst-case handling situation and should therefore be considered here. So, the time behavior will be ignored, since a short transport time will always lead to better results than a SMC part that is hold on the handling device for a longer time.

SMC material was already explained in chapter 2.2.3. Due to the random orientation of the fiber in the plane, a material behavior can be expected that is independent of the direction in this plane. After the production process the material is rolled up. From this roll 25 mm wide and 200 mm long strips were cut in the rolling direction and across it. Strips with the longest dimension in the rolling direction are designated as 0° direction. Strips with the larger dimension across the rolling direction are designated as 90° direction. Figure 6-10 illustrates the arrangement of these different strips on the SMC roll.

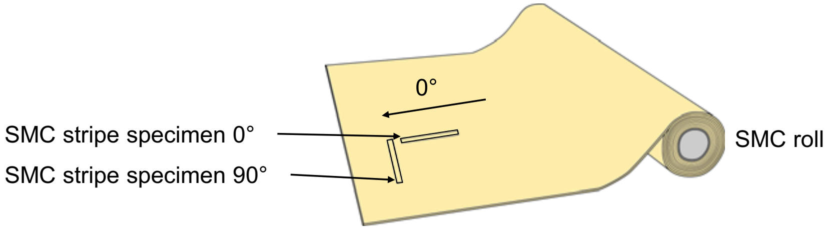

Figure 6-10: Cut out of stripes from SMC roll with different directions

These strips are now used in a Cantilever test to measure the deflection. The strips are pushed over the edge by 70 mm. Five different specimens for each direction are used. After 120 seconds the deflection is measured. The results of this measurement are presented in Figure 6-11 (left).

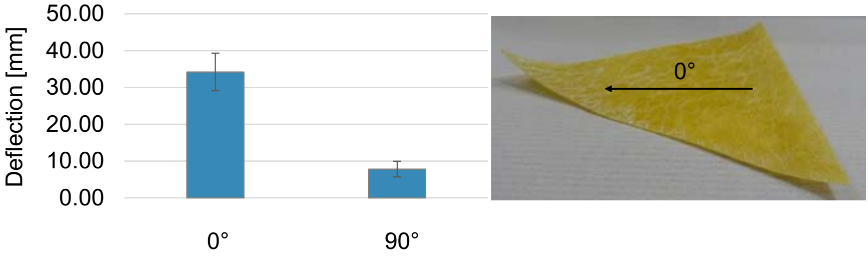

Figure 6-11: Maximum deflection of a Cantilever test of the SMC material in 0° and 90° direction (left) and resulting effect on a cut out triangle (right)

It is obvious that the material behaves significantly different in 0° and 90° direction. The specimens with 0° direction are deflecting more than in 90° direction. This is because the storage on the role has an influence on how the material is behaving. If a cut-out is placed on flat surface the outer way around this effect will cause the edges in 0° direction to lift up by themselves (Figure 6-11, right). The differences of the deflection in 0° and 90° direction are therefore the result of a pre-bending of the material caused by the storage conditions.

Gripper-Textile-Interaction:

The interaction between gripper and textile will be modeled in Abaqus using the “PINNED” boundary condition. Therefore, the shell elements of the simulation will be able to rotate but their nodes will be fixed to certain positions to simulate the grippers. Consequently, no material shifting on the gripper will be simulated using this kind of boundary condition.

6.2.2 Material data for the simulation

Textile:

As previously mentioned, the material model for the textile is using the material definition “Lamina” in ABAQUS. The modulus of elasticity can be easily determined by the experiment defined by DIN 53362. The setup is similar to the experiment in chapter 6.1.2 and is shown in Figure 6-12.

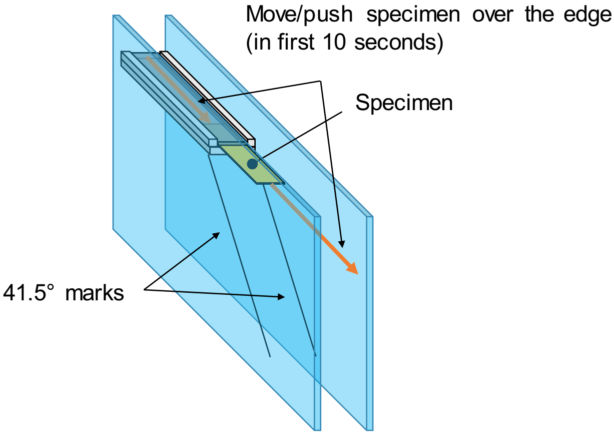

Figure 6-12: Test setup to measure the bending stiffness of fabrics an plastic materials defined by DIN 53362

In this test, a specimen with a width of 25 mm is pushed over an edge until it reaches the mark of 41.5°. The test specification also defines that the movement must be executed in 10 seconds. The rail in which the specimen is guided is slightly wider than the specimen, so that the deflection between the specimen and rail is not affected. A slider of 10 g per 10 mm length is placed on the sample itself to push the specimen forward. In this test, the overhang length $l_{ü}$ necessary for the sample to reach the 41.5° mark is measured. The measurement of this test setup is presented in Table 6-2.

Table 6-2: Measurement of bending stiffness of Sigratex C W160-PL1/1 (based on A_Hörrmann (2016, p 67))

Specimen name	**Mass m [g]**	**Longitudinal force ω [N/mm]**	**Overhang lü [mm]**	**Bending stiffness B [N*mm^2]**
1	0.97	3.80E-05	138.00	12.48
2	0.97	3.80E-05	136.00	11.95
3	0.90	3.55E-05	138.00	11.66
4	0.90	3.55E-05	135.00	10.92
5	0.91	3.58E-05	137.00	11.51
6	0.91	3.58E-05	140.00	12.28
7	0.97	3.79E-05	135.00	11.66
8	0.97	3.79E-05	143.00	13.85
9	0.91	3.58E-05	140.00	12.28
10	0.91	3.58E-05	140.00	12.28
Average value	**0.93**	**3.66E-05**	**139.60**	**12.09**
Standard deviation	**0.03**	**1.06E-06**	**2.36**	**0.71**

Since the simulation needs the elastic modulus and not the bending stiffness, the modulus is calculated based on the test results in Table 6-2. With the maximum deflection and the assumption that the textile acts like an elastic Cantilever beam. The relationship between the maximum deflection D_{Z_MAX} and the elastic modulus E is formulated in Equation 6-4 (Dubbel 2007, p 138).

$$D_{Z\_MAX} = \frac{\omega * {l_{\text{Ü}}}^4}{8 * E * I} \qquad \text{Equation 6-4}$$

Using the test results from Table 6-2 the elastic modulus E by using Equation 6-4 can be calculated. The results are summarized in Table 6-3. Based on the results in Table 6-3 a value of 240 MPa is selected for E_1 and E_2.

Table 6-3: Calculation of the elastic modulus for textile based on Equation 6-4

Specimen	**Maximum deflection** D_{Z_Max} **[mm]**	**Elastic modulus** $E_{1\&2}$ **[MPa]**
1	122	241.60
2	120	231.25
3	122	241.60
4	119	226.18
5	121	236.39
6	124	252.26
7	119	226.18
8	126	268.82
9	123	252.26
10	123	252.26
Average value	**121.9**	**242.9**
Standard deviation	**2.02**	**12.3**

The remaining parameters are G_{12} and v_{12}. For the Poisson's ratio v_{12} values from literature should be used. Common are values between 0.2 and 0.5. (Sirtautas, Pickett & Lépicier 2013, p 52; Lin et al. 2008, p 900; Lammering et al. 2018, p 271; Chen & Govindaraj 1996, p 21). Therefore, a value of 0.3 is chosen.

G_{12} is estimated based on testing results with the triangles from Figure 6-8. The sensitivity analyses in Figure 6-9 have revealed that G_{12} has a higher influence if the grippers are placed on the edges of the part. Because of that the gripper configuration two is used (Figure 6-8, right) to estimate G_{12}. A good match between simulation and test results is reached with a G_{12} of 0.07 MPa.

SMC:

The approach to define the simulation parameters for the SMC is now handled in the same way as for textiles. The first step is the measurement of deflection for the different direction since the material behaves very different in the defined 0° and 90° direction in Figure 6-10. This is now simplified in the simulation by assigning a lower modulus of elasticity to the material in 0° direction. For each direction five different specimens are pushed 70 mm over an edge and the maximum deflection after 120 seconds is measured. Table 6-4 presents the results of these measurements.

Table 6-4: Calculation of the elastic modulus for SMC based on Equation 6-4

Specimen	**Maximum deflection** D_{Z_Max} **[mm]**	**Elastic modulus** E_1 **[MPa]**
1 0°	31.00	18.63
2 0°	34.00	16.99
3 0°	31.00	18.63
4 0°	45.00	12.32
5 0°	30.00	18.48
Average value	**34.20**	**17.01**
Standard deviation	**5.08**	**2.21**
		E_2 **[MPa]**
1 90°	6.00	92.41
2 90°	5.00	110.89
3 90°	10.00	57.75
4 90°	7.00	82.50
5 90°	11.00	52.50
Average value	**7.80**	**79.21**
Standard deviation	**2.11**	**19.84**

From literature a Poisson’s ratio of 0.45 for the SMC is selected (Chen et al. 2014, p 157). G_{12} is estimated based on testing results with the triangles. A good match between simulation and test results is reached with a G_{12} of 150 MPa.

6.3 Comparison of simulation results and scan results

The simulation model for the deflection for textiles and SMC should now be evaluated. In order to enable comparisons of the simulation and test results, every test configuration receives its own test description. This description has already been introduced in chapter 5.3 and is used to support the correct alignment of the handling object, gripper and reference elements by a projection surface on a table. Chapter 6.3.1 will explain how this configuration description is used to ensure consistency of the boundary conditions between the simulation and the test by using the same description as an input file for the simulation. Furthermore, to compare simulation and scan data with each other both data sets must be loaded into a comparable data form. Chapter 6.3.2 will therefore introduce the necessary data processing steps to make the scan data comparable to the simulation data. These chapters enable then to compare the deflection of scan and simulation (chapter 6.3.3). An overview of the implemented program structure is given in Figure 6-13.

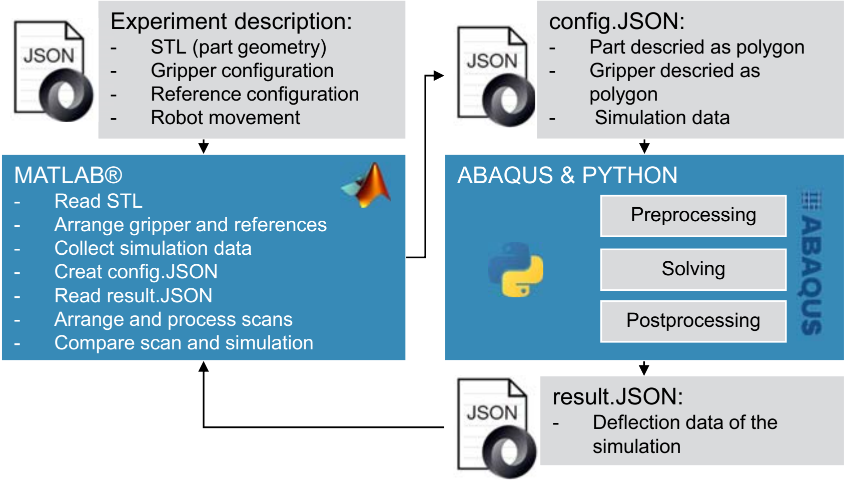
JSON
Experiment description:
- STL (part geometry)
- Gripper configuration
- Reference configuration
- Robot movement
JSON
config.JSON:
- Part descried as polygon
- Gripper descried as polygon
- Simulation data
MATLAB®
- Read STL
- Arrange gripper and references
- Collect simulation data
- Creat config.JSON
- Read result.JSON
- Arrange and process scans
- Compare scan and simulation
ABAQUS & PYTHON
Preprocessing
Solving
Postprocessing
ABAQUS
JSON
result.JSON:
- Deflection data of the simulation

Figure 6-13: Program structure for the simulation and comparison of simulation and scan data

6.3.1 Configuration of the simulation

The general idea is to create a well-defined interface for the simulation in ABAQUS. This will not only ensure the consistency between the test and simulation results but will also enable other programs to interact with the FEA simulation for the design of the handling device in the next chapters. Such an interface is implemented by using JSON files and PYTHON scripts for the communication between ABAQUS and MATLAB in Figure 6-13.

Since this thesis aims to develop a method to handle variable geometries, the description of the object geometry must also be flexible. Furthermore, it must be possible to analyses the geometries in an automated way. For this reason, the geometries are saved as STL files which is an established format in common CAD programs. Since ABAQUS cannot read the STL format a pre-processing step in MATLAB is implemented. A function “stlgeometry” by A_Dmytruk (2017, p 51) converts the three-dimensional description of the object in a two-dimensional description. The reduced dimension is the thickness of the material of the object. Together with other essential data from the experiment description (chapter 5.3) like the acceleration of the robot, the material data, shell element size and other simulation parameters a “config.json” file is generated by MATLAB. The model itself in ABAQUS is then built-up and run by a PYTHON script. The results of the FEA calculation are normally provided by ODB file, which cannot easily be read by other programs. Accordingly, that specific results like the deflection or the gripper force are extracted of the ODB file and written in the “results.json” file at the end of the simulation. The provision of the results in this format enables MATLAB to read and work with the data.

6.3.2 Processing of scan data

Through chapter 6.3.1 MATLAB can now run FEA simulations and access the results of these calculations. A comparison of the results is possible by performing the handling experiment with the developed handling device (chapter 5.1) and measuring the deflection with a laser scanner. This test procedure is already described in chapter 5.3. In order to analyze the data in MATLAB and compare it with the simulation, the following steps in Figure 6-14 are performed.

The scan data is exported from the scan device as a VTX file. This is also readable by text edit programs and describes the scan as a set of points with X, Y and Z coordinate information. The number of points the scan contains varies depending on the size of the scanned object and the work method of the person operating the scanner. The raw scan data often contains 27 points per square millimeters or more. This large number of data points make analysis difficult. Because there is no advantage in using such a high point density the point density is reduced to 0.25 points per square millimeters or even lower.

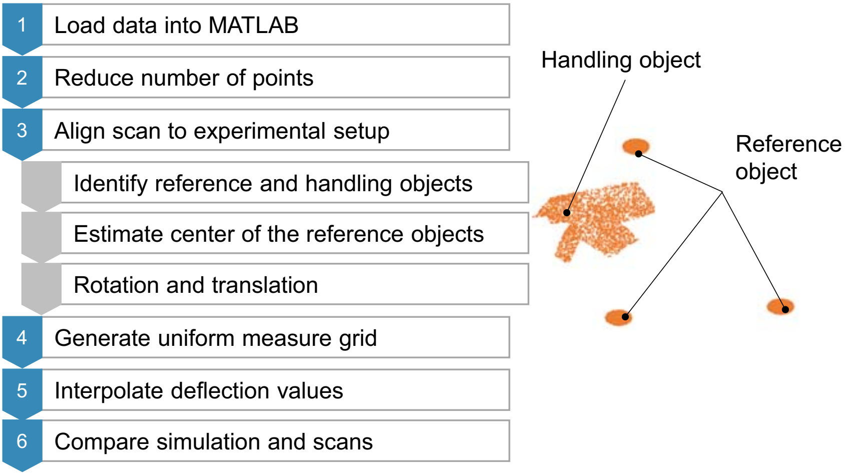
1 Load data into MATLAB
2 Reduce number of points
3 Align scan to experimental setup
Identify reference and handling objects
Estimate center of the reference objects
Rotation and translation
4 Generate uniform measure grid
5 Interpolate deflection values
6 Compare simulation and scans
Handling object
Reference object

Figure 6-14: Processing steps of deflection scans in MATLAB

The comparison of simulation and scan requires the alignment of both data sets. The simulation process (chapter 6.3.1) is using the same geometrical description of the object as the real handling test procedure provided by the experiment description from chapter 5.3. This description also includes the position of three reference objects. The reference objects are used to define a center point of the whole setup and a reference vector (Figure 6-15). The references are always positioned in such a way to form a scalene triangle. The two reference objects closest to each other are defined as $\boldsymbol{REF_1}$ and $\boldsymbol{REF_2}$. The remaining reference is defined as $\boldsymbol{REF_3}$. On the half distance between $\boldsymbol{REF_1}$ and $\boldsymbol{REF_2}$ an intermediate point is calculated. The $\boldsymbol{REF_{Center}}$ is located halfway along the connecting line between the intermediate point and $\boldsymbol{REF_3}$. Furthermore, a normalized $\boldsymbol{REF_{Vector}}$ is calculated between the intermediate point and $\boldsymbol{REF_3}$.

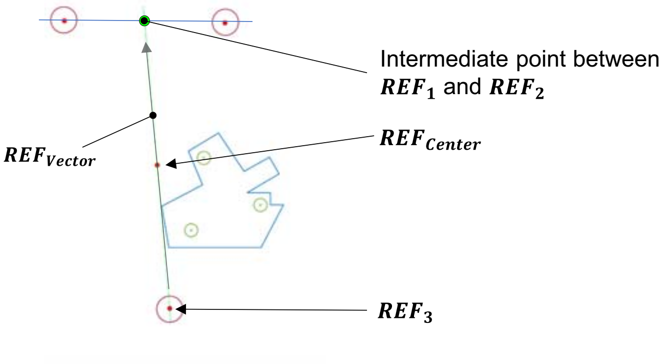

Figure 6-15: Definition of the reference objects (REF_1, REF_2, REF_3) and the reference vector (REF_{Vector}) in the experiment description

To align the scans, the same reference objects must be identified in the scans. Therefore, the captured scan points are clustered in a first step. For this purpose, the implemented “clusterdata” algorithm in MATLAB is used. This algorithm is using a hierarchical clustering method based on the Euclidean distance between objects. By using the prior knowledge that four different objects (REF_1, REF_2, REF_3 and the handling part) must be identified in the scan, the maximum number of clusters that must be identified can be set to four. The result of such a clustering is presented in Figure 6-16. Considering the distance between the individual scan points, increasingly larger clusters can be formed. Between a Euclidean distance of 13 mm and 150 mm, four separated clusters can be identified. The cluster containing the handling object often contains also a higher number of smaller sub-cluster. On the other hand, the reference objects comprise only one, even for smaller Euclidean distances. Furthermore, the handling objects contain the highest number of individual scan points. This circumstance is used to identify the handling object which makes it possible to separate the handling object from the references in further analysis.

The identification of the different reference objects now enables the alignment of the scan. For this the same characteristics (intermediate point between REF_1 and REF_2, REF_{Center}, REF_{Vector}) must be calculated in the scan. The calculation of these characteristics requires the determination of the centers of the reference objects.

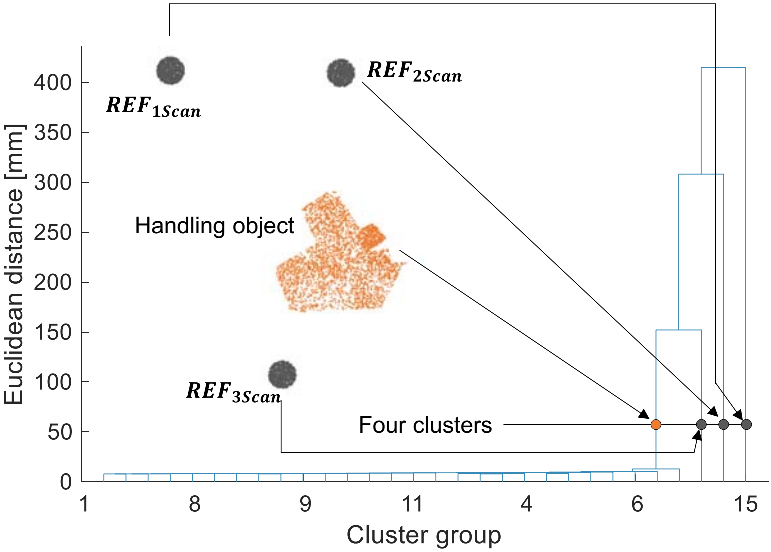

Figure 6-16: Result of a scan data clustering by the MATLAB function “clusterdata”

Since each reference object should have a circle shape this could be done by the calculation of the average X and Y values. Nevertheless, inhomogeneous point density and careless scanning could easily lead to inaccuracies in the detection of the center. Accordingly, a Hough transformation is used to identify the center of the reference objects in the scan $\boldsymbol{REF_{1Scan}}$ and $\boldsymbol{REF_{2Scan}}$, $\boldsymbol{REF_{3Scan}}$.

In Figure 6-17 the center of each reference object is identified and $\boldsymbol{REF_{CenterScan}}$, $\boldsymbol{REF_{VectorScan}}$ are already calculated. The goal now is to match $\boldsymbol{REF_{VectorScan}}$ with the $\boldsymbol{REF_{Vector}}$. Often only small tilts occur in the scan along the X and Y axis caused by deflection of the gripper frame or inaccuracies in the set-up process of the reference objects. The main tilt is around the Z axis because of variable orientation between the handling and scanning device (Figure 6-17). The alignment of the scan can now be done by a series of shifts and rotation transformations. The rotations should match $\boldsymbol{REF_{Vector}}$ and $\boldsymbol{REF_{VectorScan}}$. The shifts align $\boldsymbol{REF_{Center}}$ and $\boldsymbol{REF_{CenterScan}}$. To perform the rotations the center of the scan $\boldsymbol{REF_{CenterScan}}$ is moved to the coordinate origin. Subsequently, $\boldsymbol{REF_{CenterScan}}$ also became the pivot point for the rotations and the alignment of $\boldsymbol{REF_{VectorScan}}$with $\boldsymbol{REF_{Vector}}$ by the calculation of the angular difference. If the vectors have been matched a final shift operation moves the $\boldsymbol{REF}_{Center}$ to $\boldsymbol{REF}_{CenterScan}$.

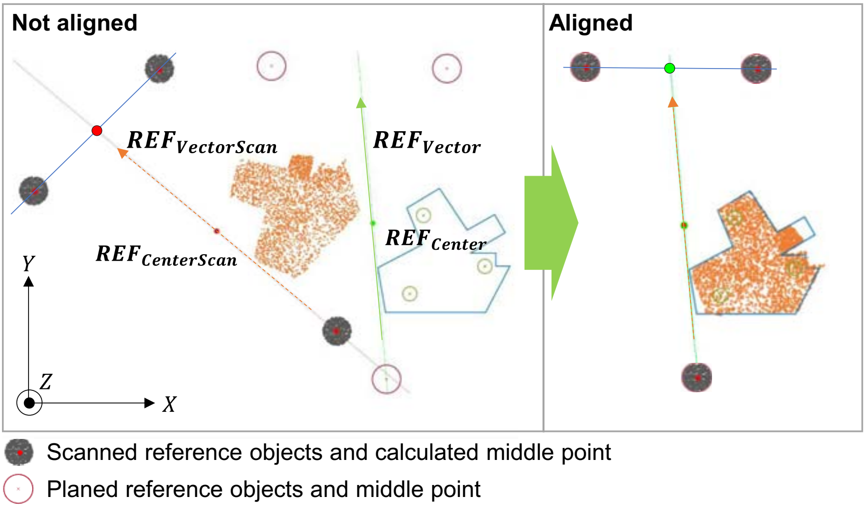
Not aligned
Aligned
$REF_{VectorScan}$
REF_{Vector}
REF_{Center}
$REF_{CenterScan}$
Y
Z
X
Scanned reference objects and calculated middle point
Planed reference objects and middle point

Figure 6-17: Matching of the scan data and the description of the experiment by aligning the $\boldsymbol{REF}_{Vector}$ and $\boldsymbol{REF}_{Center}$

Now the scan can be compared with the simulation. For this purpose the simulation is started by MATLAB using the experiment description (chapter 6.3.1). The problem is now that the scan data as well as the simulation data calculate the results only at discrete points. In the scan data these points are the individual scan points. In the simulation data the mesh structure with the S4R shell elements edges define these discrete points. However, the comparison of both requires the information of the deflection at exact the same location. This is achieved by creating a mesh grid that generates a regular distributed set of points in the shape of the part and then interpolates the data using cubic interpolation at the mesh grid points (Figure 6-18). After this the deflection from the simulation as well as from the scan is known at the same points. Based on this information the mean deflection of the scans and the standard deviation can be calculated.

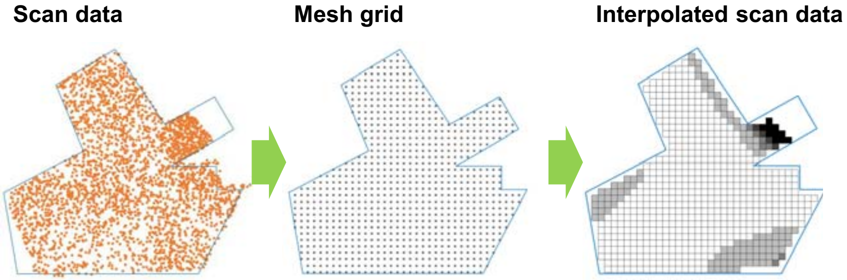

Figure 6-18: Example of the processing of scan or simulation data by interpolate data at the mesh grid points

6.3.3 Comparison of measured scan data and simulated data

The selection of the material models to simulate the deflection and the determination of material parameters are so far based on literature values and Cantilever beam measurements in chapter 6.2. This chapter will now introduce a new geometry to enable an evaluation of the implemented simulation. The geometry used is referred as RA001. “RA” in this context stands for randomized, because it is an arbitrarily-conceived geometry. Figure 6-19 shows the geometry.

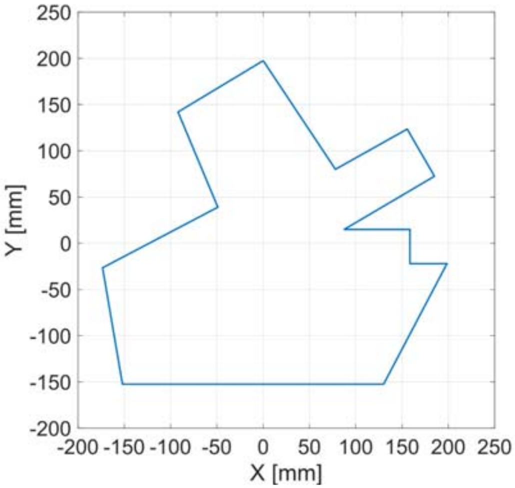

Figure 6-19: Geometry RA001

It also contains some difficult geometrical features like thin bridges and shape edges. For the evaluation of the simulated deflection, simulation and scans are now compared with each other.

SigratexCW160PL11

The comparison is done by two different diagrams presented in Figure 6-20. To measure the deflection of the scan for Figure 6-20 five different scans are performed, and a mean deflection is calculated.

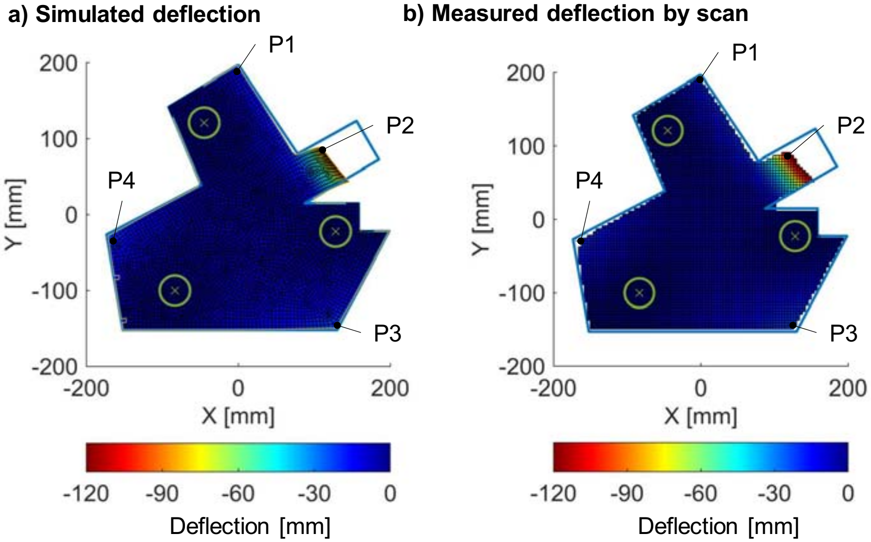

Figure 6-20: Simulated deflection (a) and measured deflection (b) for three grippers on RA001

For better comparison, Table 6-5 lists the deflections of the points P1 to P4 from the simulation and scan in Figure 6-20. A good match can be seen between real result and the simulation in the most areas of the geometry. The difference between the scans and the simulation is mostly small and the model predicts the deflection close to the reality. With large deflections, however, the error is getting larger too, which can be seen at P2 (Figure 6-20, P2 and Table 6-1, P2).

Table 6-5: Deflection of P1 to P4 in Figure 6-20

Points	**Simulated deflection (Figure 6-20, a) [mm]**	**Measured deflection (Figure 6-20, b) [mm]**
P1	-14.18	-20.52
P2	-102.2	-129.8
P3	-23.30	-23.69
P4	-22.17	-21.45

The model should now also be tested on a larger part. The part in Figure 6-21 was already presented in chapter 5.4.2 and is further referred to H003.

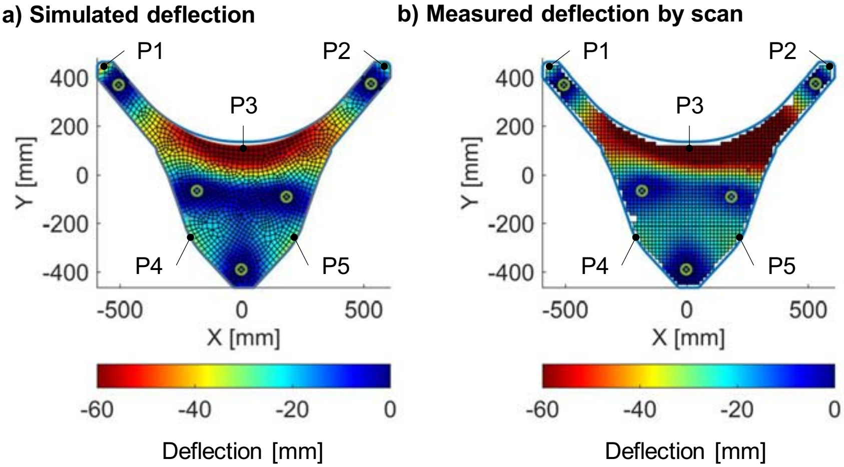

Figure 6-21: Simulated deflection (a) and measured deflection (b) for part H003

For better comparison, Table 6-6 lists the deflections of the points P1 to P4 from the simulation and scan in Figure 6-21. In comparison to the simulation of the smaller part RA001 in Figure 6-20 there are larger differences between the scan and the simulation. The deflection of the free hanging elements are predicted correctly. Also, the deflection of the material between the grippers is mostly correct simulated. The gripper arrangement in this test is slightly asymmetrical. This causes in the simulation also only a small asymmetrical deflection of the part. The real test results are more influenced by this asymmetrical arrangement than the simulation.

Table 6-6: Deflection of P1 to P4 in Figure 6-21

Points	**Simulated deflection (Figure 6-21, a) [mm]**	**Measured deflection (Figure 6-21, b) [mm]**
P1	-47.45	-43.9
P2	-77.41	-95.6
P3	-31.71	-31.93
P4	-30.72	-27.87
P5	-31.69	-29.47

Another interesting question is how good different fiber orientations are simulated. Figure 6-22 presents scan and simulation data for a triangle shaped part. Again, the values of certain points are summarized a table (Table 6-7). In general, the model predicts the deflection for the different fiber orientations correctly but also underestimated the amount of deflection.

Table 6-7: Deflection value for different points of a triangle with different fiber orientations

Points	**Simulated deflection 0° [mm] (Figure 6-22, a)**	**Measured deflection 0° [mm] (Figure 6-22, b)**	**Simulated deflection 30° [mm] (Figure 6-22, c)**	**Measured deflection 30° [mm] (Figure 6-22, d)**
P1	-42.43	-47.4	-28.69	-37.15
P2	-28.71	-38.93	-42.5	-43.63
P3	-42.43	-51.17	-42.41	-44.37

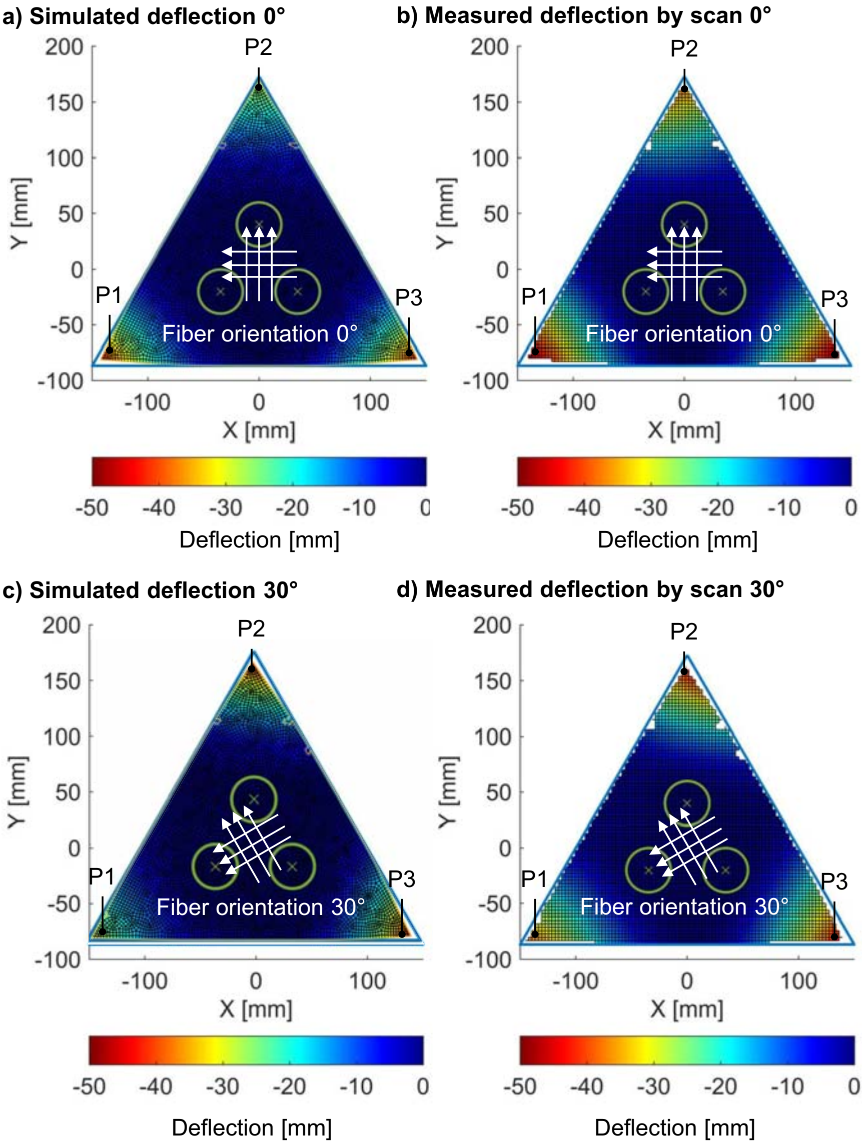

Figure 6-22: Simulated deflection (a) and measured deflection (b) for a triangle with different fiber orientations

SMC

The model for the SMC material is now to be evaluated. Larger differences between scan and simulation can be seen in Figure 6-23 than by the textile. But overall a matching between the simulated value and the results is achieved.

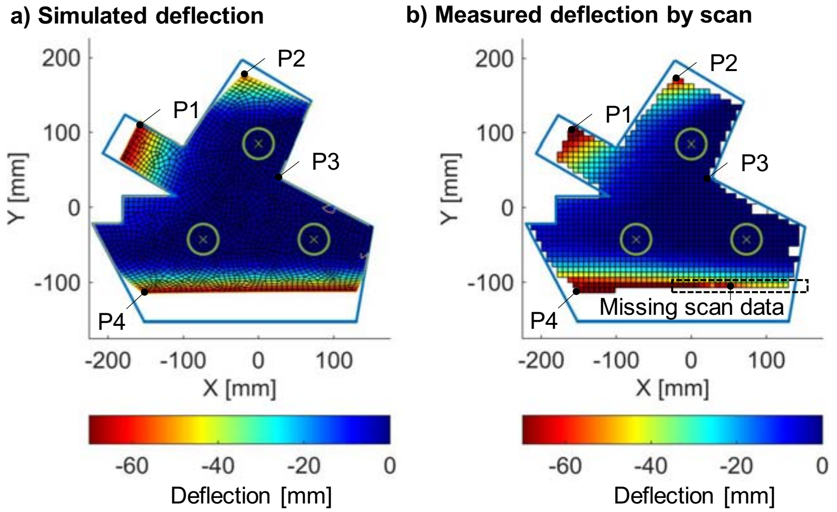

Figure 6-23: Simulated deflection (a) and measured deflection (b) for part RA001S

For better comparison, Table 6-8 lists the deflections of the points P1 to P4 from the simulation and scan in Figure 6-23.

Table 6-8: Deflection of P1 to P4 in Figure 6-23

Points	**Simulated deflection [mm]** **(Figure 6-23, a)**	**Measured deflection [mm]** **(Figure 6-23, b)**
P1	-67.55	-79.35
P2	-55.09	-65.12
P3	-0.996	-0.873
P4	-69.64	-82.77

Conclusion:

The simulation enables overall the correct prediction of deflections. For large deflections the difference between simulation and scan increase more and more. These differences are understandable since the assumption of a linear elastic behavior does not live up to the complexity of reality. Nevertheless, the presented simulation models are good enough because the bending characteristic is reproduced correctly.

7 Gripper configuration

This chapter will now discuss how a gripper configuration for different shapes could be generated. The first chapter will discuss therefore different approaches for this problem.

7.1 Concepts for an initial gripper configuration process

Chapter 6 introduced a simulation model for the deflection. The simulation model will enable predicting the deflection depending on the following input parameters: object geometry, material, gripper configuration and vertical acceleration. The first step (Figure 4-2) in the whole generation process of a gripper configuration already presented in chapter 4.2 is to find an initial gripper configuration to run a simulation at all. This initial gripper configuration can therefore be only created based on the geometry of the object, since simulation data will not be available in this first step. The general goal of the whole gripper configuration process is to find a solution which will cause only a specific maximum deflection and use only a minimum number of grippers to achieve this. For this it is advantageous if the initial gripper configuration is already very close to a configuration that fulfills these goals. At this point, it is still completely unclear how many grippers are necessary to maintain a maximum amount of deflection defined by the user. So a method to generate initial gripper configurations must be able to generate sensible solutions for different parts with different number of grippers. Figure 7-1 displays three different possibilities to generate an initial gripper configuration based on the geometry of the part. This chapter will now discuss these different concepts to find an initial gripper configuration.

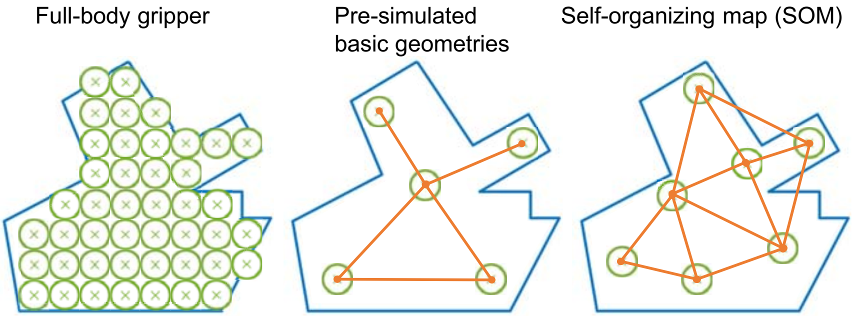

Figure 7-1: Different approaches to generate an initial gripper configuration

7.1.1 Initial gripper configuration by full-body gripper

The first idea is to place a tight mesh of grippers on the part, trying to cover as much of the part's area as possible. This approach will obviously result in an oversized initial gripper configuration. Accordingly, this approach will not generate a sensible solution, but serves as a starting configuration for the adaptation in the second step (Figure 4-2). Based on this tight mesh of grippers a sensible gripper configuration can then be found by using algorithms based on discrete combinatorial optimization.

The advantage of this approach is the very simple generation of the initial gripper configuration. The disadvantage is the fix positions of the grippers in the configuration. By this approach a possible gripper is set active (part of the configuration) of inactive (not part of the configuration) by the discrete combinatorial algorithm. Such a problem is then also called zero-one problem (Leung & Wang 2001, p 41). The fix positions of the grippers are thereby a restriction for the solution space since a better solution might require the position between two grippers. With combinatorial optimization many real problems can be addressed, but their solution can quickly mean exponential computational effort in relation to the problem size (Suhl & Mellouli 2013, p 10).

7.1.2 Initial gripper configuration by pre-simulated basic geometries

The next approach is based on the idea to use pre-simulated basic geometries like triangles, rectangles and Cantilever beams to estimate an initial gripper configuration. With this information the initial gripper configuration can rely on approximated deflection data.

Based on the material input data a specific set of simulations is performed and the results are summarized in a diagram (Figure 7-2). First Cantilever beam, rectangle and an equilateral triangle are simulated on their own, using different lengths l and fiber orientations. The rectangle as well as the Cantilever beam have a width of 40 mm. The simulation results in Figure 7-2 are created with the material model of the Sigratex C W160-PL1/1 from chapter 6. No additional acceleration by the handling process was assumed, so the deflection is only caused by earth's gravity. From these simulations results the maximum deflection for each basic geometry and different lengths l is then summarized in one diagram. This diagram now enables to select a maximum deflection on the X axis and the Y axis will then suggest a maximum length l for each basic geometry. Figure 7-2 also shows an example of a maximum deflection of 30 mm.

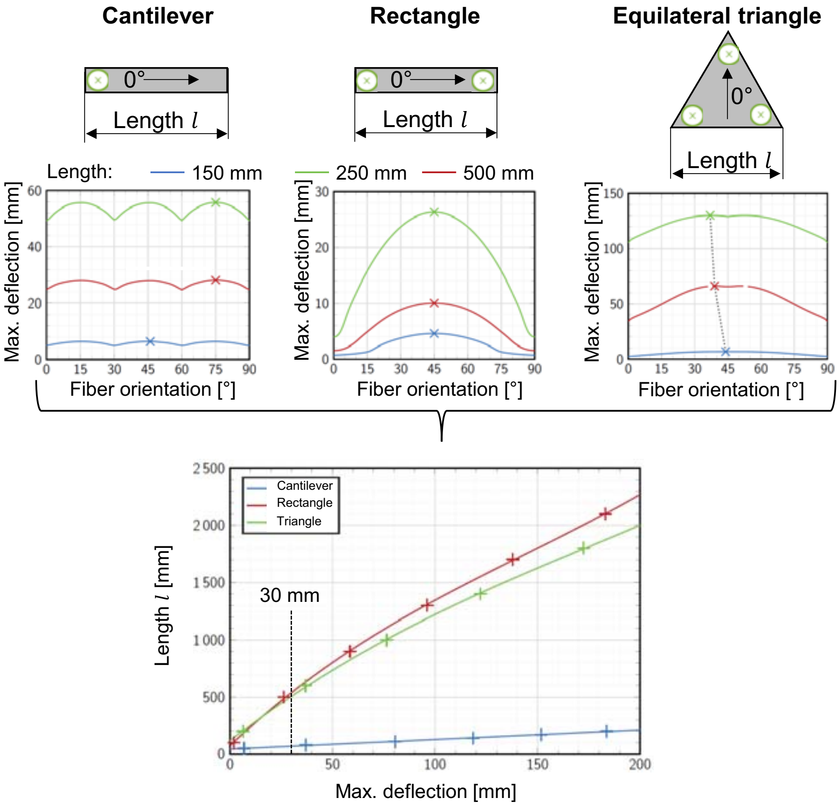

Figure 7-2: Design diagram for the arrangement of grippers based on pre-simulated basic geometries

Based on the example in Figure 7-2 the different geometries should have following maximum length l to achieve a maximum deflection of 30 mm (Table 7-1). The information from Table 7-1 should now be used to generate an initial gripper configuration. Therefore, the basic geometries (Cantilever beam, rectangle, equilateral triangle) should be placed on the handling part in such a way, that most of the part is covered. At the same time the maximum length l of the basic geometries which are placed on the handling part should not be exceeded.

Table 7-1: Maximum length l for the different geometries and a maximum deflection of 30 mm

Geometry	**Length l [mm] for a maximum deflection of 30 mm**
Cantilever beam	70
Rectangle	540
Equilateral triangle	510

In Figure 7-3, this arrangement of the basic geometries is done on the part manually to elaborate if this approach can generate good results. The grippers are arranged in such a way that the nearest edge of the part is 65 mm away.

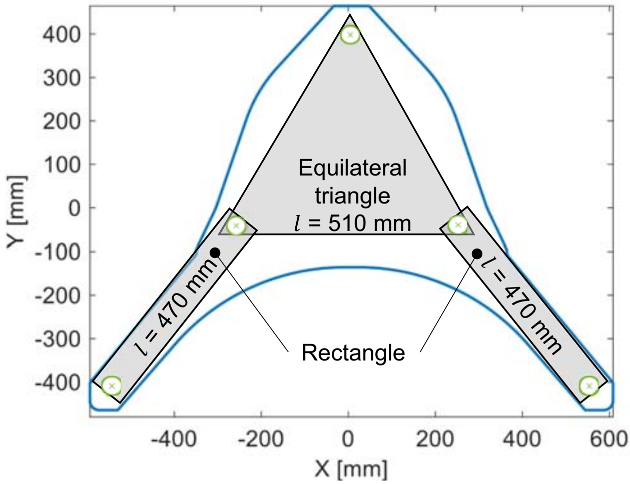

Figure 7-3: Arrangement of grippers on a part to achieve a maximum deflection of 30 mm

The equilateral triangle is at the maximum dimension of 510 mm. The rectangle on the other side has with a length of 470 mm some reserves and should not be a problem. Since this approach is always using the largest deflection of all fiber orientations for one basic geometry and length (Figure 7-2) the gripper arrangement should work for all fiber orientations of the handling part. Accordingly, this configuration is now simulated for a fiber orientation of 0 ° and 30 °. The occurring deflections are presented in (Figure 7-4).

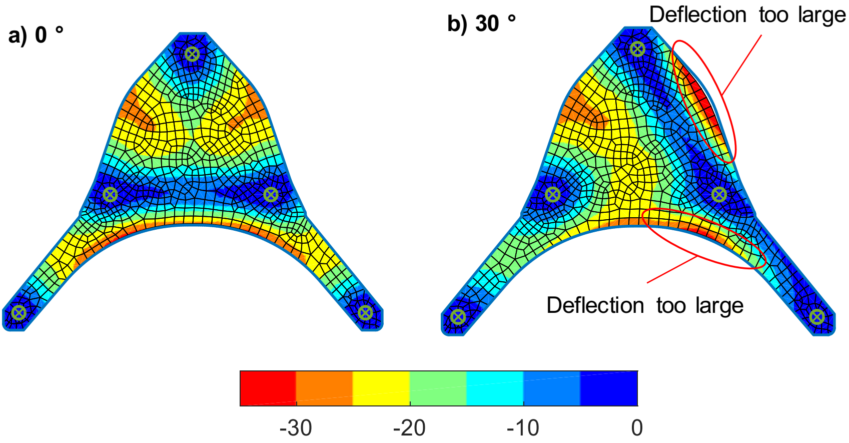

Figure 7-4: Deflection of an initial gripper configuration with a fiber orientation of 0° (a) and 30° (b)

The initial gripper configuration by pre-simulated basic geometries performs well for a fiber orientation of 0 ° (Figure 7-4, a). The deflection does not exceed the target value of -30 mm. For 30 ° (Figure 7-4, b) red zones appear in the simulation which indicate too large deflections. Primarily because these zones cannot be covered by the pre-simulated basic geometries. Nevertheless, the solution in Figure 7-4 is a good initial gripper configuration. It is very well conceivable that the result can now be further improved by adjusting the position of the grippers using the information of the simulation results.

A better initial gripper configuration without simulating the whole part would also be possible, if not only equilateral triangles are simulated but also triangles of any shape. With a major set of pre-simulated forms this approach would then also offer the possibility to perform the whole gripper configuration by using only pre-simulated geometries. This would also mean an increasing number of pre-simulated results which are necessary. The amount of simulations for the small example in this chapter were already 81 simulations. Nine simulations per basic geometry and length to simulate different fiber orientations, three different lengths (150 mm, 250 mm, 500 mm see in Figure 7-2) and three different basic geometries. One simulation run needs about 60 to 90 seconds depending on the size of the geometry. The next step would be to automate the process of arranging the basic geometry elements on arbitrary shaped parts.

7.1.3 Initial gripper configuration by self-organizing maps algorithm

The next approach is based on the principle of SOM or also Kohonen feature maps (Kruse et al. 2016, p 103). SOM are normally used to solve classification and clustering problems, but it is also possible to adjust them for optimization problems (Kruse et al. 2016, p 109; Chen et al. 2013; Kohonen 1990, p 1464). Every SOM or SOM derivate gets at the beginning an input data set and is placing then the neurons according to specific rules. The input data set for the gripper placement problem are the points defining the part. These points are further abbreviated with ξ. The gripper will take over the role of the neurons and are abbreviated with $\boldsymbol{w}$. Please note that the terms “gripper” and “neuron” will be used synonymously in the following. The mesh of points ξ defining the part is created by first generating a mesh with a specific grid spacing over the hole maximum dimension in the X and Y directions and then sort out points which are not in the shape defining the part. The result of this process is pictured in Figure 7-5.

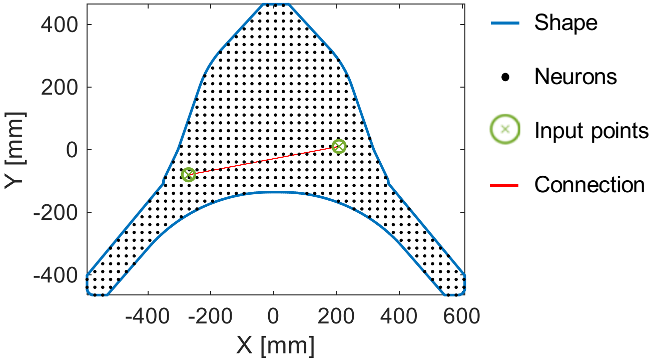

Figure 7-5: Points defining the geometry of the part

The normal SOM is just a mesh with a defined number of neurons (Kohonen 1990, p 1466). The general idea of SOM is then improved by different approaches. Derivative are for example neural gas (NG) by Martinetz, Berkovich & Schulten (1993), growing cell structure (GCS) by Fritzke (1994) and the growing neural gas (GNG) by Fritzke (1995). These different derivatives are elaborated and summarized in Table 7-2. Please note that the SOM, NG, GCS and GNG algorithm are also explained in detail in chapter 2.4. In the following only a short summary is given.

Table 7-2: Comparison of different derivates of SOM

	Flexible shape	**Parameter values**	**Flexible number of neurons**
SOM	-	+	-
NG	+	+	-
GCS	o	-	+
GNG	+	-	+

The classic SOM has a fix number of neurons which are connected by a pre-defined structure (Prudent & Ennaji 2005, p 1212). Especially the inflexible structure will make it unsuitable to fit on different shapes. Furthermore, they are often arranged two-dimensional (Kohonen 1982, p 61). However, since so many boundary conditions are already defined at the beginning, they have only a very small number of parameters.

The NG on the other side is just working with vector quantization and does not create any topology or structure between the neurons (Fritzke 1994, p 1212). This makes the algorithm very flexible. On the other side the number of neurons is defined already at the start and no new ones are added in the process (Martinetz, Berkovich & Schulten 1993, p 560).

The GCS starts with an initial network structure which corresponds to the input data (Fritzke 1994, p 1442). It can add and delete points, which makes it in general flexible to fit different shapes. By this process the algorithm always keeps the structure of the network with hyper tetrahedrons (Prudent & Ennaji 2005, p 1212). This circumstance reduces the flexibility slightly.

The GNG works in general like the GSC. The main difference is the structure of the network and the initial network at the start of the algorithm (Fritzke 1995, p 628). The algorithm starts always with two neurons. In contrast to the GSC the structure is not defined, so that individual neurons can also be created with only a single connection to other neurons. This makes the realizable structure of the network very flexible. Using a GNG as developed by Fritzke (1995) will produce the following initial gripper configuration in Figure 7-6. The following GNG parameter set in Table 7-3 was used which was already explained in chapter 2.4.5.

Table 7-3: Parameter set for GNG to generate gripper arrangement in Figure 7-6

Parameter	ϵ_b	ϵ_n	N_{max}	I_{max}	α	δ	L	T
Value	0.01	0.0001	5	200	0.9	0.9	10	10

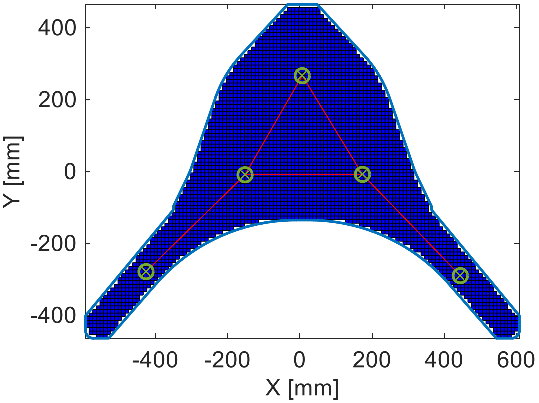

Figure 7-6: Initial gripper configuration generated by using the GNG algorithm by Fritzke (1995)

The initial gripper configuration generated by the GNG in Figure 7-6 looks generally similar to the solution in Figure 7-4. They differ mainly in the size of the triangle and rectangle. The GNG offers the possibility to create initial gripper configurations automatically, which can be similar to manually crated ones because the positions of the neurons depend on the geometrical input information of the part.

Pre-studies using this method to generate gripper configurations by A_Abderrahman (2017) also revealed some problems with this algorithm for such a task. Grippers (or neurons) have often large distances to the edges of the part. This can be a critical point, because these spots will act like Cantilever beams and tend to cause large deflections (see Figure 7-2). Another problem are inner cut-outs in shapes like the extreme example in Figure 7-7 (A_Abderrahman 2017, p 48). The algorithm tries to keep the distance to all points of the component as small in sum. This does not always lead to a good solution for the problem which should be solved here. Unfortunately, inner cut-outs are often to be found because they improve the drapability and lead to a low formation of wrinkles during this process (Potter 2002, p 678; Robertson et al. 2000, p

709). The GNG algorithm completely ignores such cut-outs and places the grippers in empty spaces, as shown in Figure 7-7.

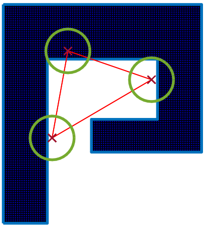

Figure 7-7: A shape with inner cut-outs causing problems for GNG

A last issue is the high number of parameters the GNG uses compared to other algorithms and how they affect the result (A_Abderrahman 2017, p 27). If this algorithm should be used for this problem the influence of the different parameters must be investigated.

7.1.4 Conclusion of the different approaches

The presented approaches above have different advantages and disadvantages. For example, using a full-body gripping approach and optimize the problem using a discrete combinatorial optimization algorithm is already a method to find a final gripper configuration. Nonetheless, the disadvantage of this approach are larger parts which must be covered with a great number of grippers. This will result in large solutions space which can get problematic for the discrete combinatorial optimization since it is normally important to reduce the number of possible combinations (Balas 1965, 517-546; Suhl & Mellouli 2013, p 10). Nevertheless, there are specialized algorithms for specific problems in combinatorial optimization that solve them with high efficiency (Korte & Vygen 2012, p 9). The real drawback is the need of discretization the problem. Especially for smaller parts the change in the deflection is huge when only one gripper alternates between two possible gripper positions. For smaller parts this approach will probably only generate inadequate solutions and for large parts there is the danger of long runtimes due to the large solution space.

Using pre-simulated basic geometries led to a good result with a manual placement of the basic geometries on the part. This placement would still have to be automated. The major drawback of this approach is the number of pre-simulations that has to be done. It would be an interesting approach if the same simulation results could be used over and over again. However, simply by changing for example the handling acceleration, it is necessary to calculate the whole set of simulations again.

The GNG approach on the other side does not need pre-simulations and offers the possibility to place the grippers not only on discrete positions. The algorithm tries to set the grippers based only on the geometric input of the parts shape and thus generates appropriate arrangements. Open issues are dealing with cut-outs in the shape and bringing the gripper closer to the edges of the part. However, all of these points make the approach very interesting, especially since it promises to deal with a wide variety of shapes. The results of the algorithm depend on the input parameters and this issue will need further investigations. However, due to the promising results in the pre-investigations by A_Abderrahman (2017), this approach will be further examined in the following chapters.

7.2 Initial gripper configuration without specific deflection data of the shape

This chapter will introduce necessary modifications to the standard GNG algorithm to adjust it for the generation of initial gripper configurations. After these adjustments are done an investigation on the different influences of the GNG parameters is performed. The general goal hereby is to identify values which perform well and will generate sensible solutions.

7.2.1 Modification of GNG for initial gripper configuration

As mentioned in chapter 7.1.3, the GNG algorithm generally performs well for creating initial gripper configurations but there are some issues:

1. Large distances to the edges of the part
2. Non-observance of cut-outs in parts
3. Result quality depending on the GNG parameter setting

Aside from the last point which will be discussed in chapter 7.2.2, adjustments must be made in the GNG to solve point one and two.

Large distances to the edges of the part

The normal GNG algorithm is based on Equation 7-1 or Equation 7-2 depending if a gripper $\boldsymbol{w}$ is the nearest gripper to the point $\boldsymbol{\xi}$ or just a neighbor.

$$\Delta \boldsymbol{w}_{\boldsymbol{S1}} = \epsilon_b * (\boldsymbol{\xi} - \boldsymbol{w}_{\boldsymbol{S1}}) \qquad \text{Equation 7-1}$$

$$\Delta \boldsymbol{w}_{\boldsymbol{n}} = \epsilon_n * (\boldsymbol{\xi} - \boldsymbol{w}_{\boldsymbol{n}}) \qquad \text{Equation 7-2}$$

Thereby every point $\boldsymbol{\xi}$ has the same weight and when a GNG is performed the grippers searching for a way to keep the smallest average distance to the points. Because the most points are located in the inner structure and not on the outside contour of the part, the grippers are placed also more towards the center.

One solution is to distinguish between the different points and weight them differently. Points defining the outside contour $\boldsymbol{\xi}_{\boldsymbol{OUT}}$ of the part will be assigned a higher weight than inner points $\boldsymbol{\xi}_{\boldsymbol{IN}}$. This is achieved by modifying Equation 7-1 or Equation 7-2 and adding a variable G which values depend on the point $\boldsymbol{\xi}_{\boldsymbol{IN/OUT}}$:

$$\Delta \boldsymbol{w}_{\boldsymbol{S1}} = \epsilon_b * G(\boldsymbol{\xi}_{\boldsymbol{IN/OUT}}) * (\boldsymbol{\xi}_{\boldsymbol{IN/OUT}} - \boldsymbol{w}_{\boldsymbol{S1}}) \qquad \text{Equation 7-3}$$

$$\Delta \boldsymbol{w}_{\boldsymbol{n}} = \epsilon_n * G(\boldsymbol{\xi}_{\boldsymbol{IN/OUT}}) * (\boldsymbol{\xi}_{\boldsymbol{IN/OUT}} - \boldsymbol{w}_{\boldsymbol{n}}) \qquad \text{Equation 7-4}$$

By using this, points defining the outer couture can get more weight and will attract the grippers (aka neurons) more. If the same GNG as in Figure 7-6 is repeated using the same values from Table 7-3 but different weights $G(\boldsymbol{\xi})$ for inner and outer points the result is changing significantly. In Figure 7-8 the points on the outer contour $\boldsymbol{\xi}_{\boldsymbol{OUT}}$ have a 120 times greater weight $G(\boldsymbol{\xi}_{\boldsymbol{OUT}})$ then the points $\boldsymbol{\xi}_{\boldsymbol{IN}}$ in the inside of the part and the points are nearer to the outer contour than in Figure 7-6**.** Therefore, this value controls how close the gripper is dragged to the outer couture. The ratio of $G(\boldsymbol{\xi}_{\boldsymbol{OUT}})$ to $G(\boldsymbol{\xi}_{\boldsymbol{IN}})$ should be represented by the parameter $Point_{Weight}$ and is defined by Equation 7-5, whereby $G(\xi_{IN})$ should always has a weighting of one. Hereby $Point_{Weight}$ is always equal $G(\xi_{OUT})$**.**

$$Point_{Weight} = \frac{G(\boldsymbol{\xi}_{\boldsymbol{OUT}})}{G(\boldsymbol{\xi}_{\boldsymbol{IN}})} \qquad \text{Equation 7-5}$$

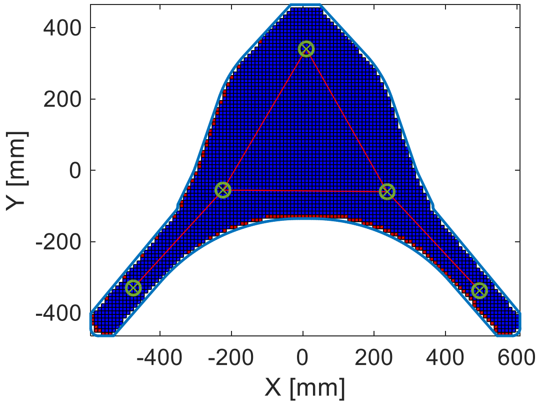

Figure 7-8: Gripper configuration with higher weight of points defining the outer contour of the part

Non-observance of cut-outs in parts

This problem mainly occurs because grippers are attracted by points even if there is an outer contour between them. This effect could be demonstrated if one gripper should be placed in a part with a huge cut-out in the middle displayed in Figure 7-9 (a). The gripper tries to achieve the minimum average distance to the points and the logical answer is somewhere in the middle of the part. Unfortunately, this ideal spot for the minimum average distance is also a cutout. The solution is therefore inviolable for this kind of application. In order to avoid such behavior, the simplest solution is to implement a line of sight (LOS) condition in the algorithm. Every gripper is only attracted by points or considered as nearest gripper of a point if a LOS rule is existing. Through this condition, an adjustment step performed according to Equation 7-3 and Equation 7-4 will never result in a gripper leaving the part (Figure 7-9, b).

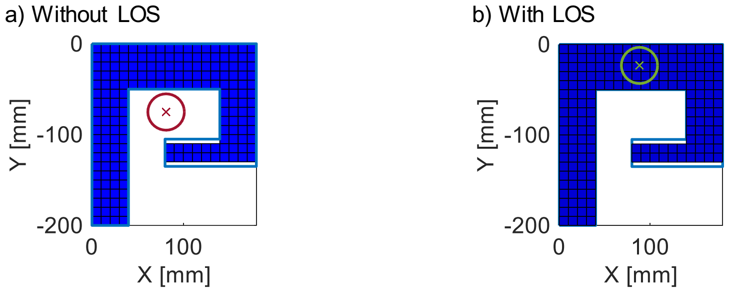

Figure 7-9: Gripper placed by standard GNG (a) and by implementing a line of sight (LOS) rule (b)

The same problem exists with the connection of two grippers. According to the rules of a normal GNG two neurons or grippers are connected to each other if they have at least one point in common where they are the closest or second closest grippers. This rule can result in a situation as displayed in Figure 7-10 (a). This becomes a problem if a new gripper should be added to the existing ones. This new gripper is placed between two existing ones with the highest error. If the position is not inside of the part the configuration will benefit from this gripper. To avoid this problem every step of a gripper is precalculated. If an adjustment step by Equation 7-3 and Equation 7-4 will result in breaking up the LOS between two grippers this adjustment step will be skipped. Due to this rule, the grippers will no longer move if their connection line is near the outer shape of the part. An example of this behavior is shown in Figure 7-10 (b).

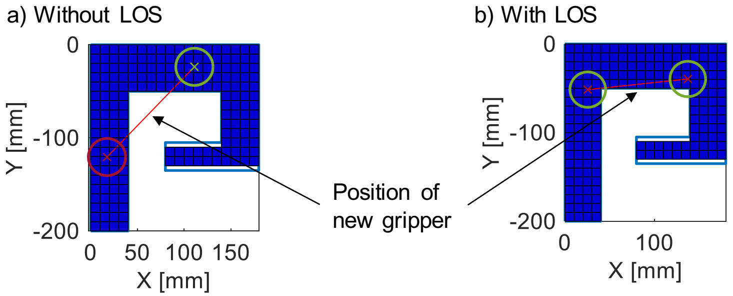

Figure 7-10: Connection of two grippers by standard GNG (a) and LOS rule (b)

This rule must be applied at least until the maximum number of grippers is reached. The rule can then be overridden, since no new grippers have to be integrated.

Abort criterion, error calculation and adding grippers

The classic GNG does not have an abort criteria in the usual way. At the start a maximum number of iterations is defined, which are then calculated. There are no criteria to terminate the calculation prematurely before this maximum number of iterations is reached. However, it is not possible to predict how many iterations are necessary to complete a gripper configuration, especially since this depends on the other GNG parameters. Accordingly, a criterion should be defined for canceling the process. The idea is to monitor the error of the gripper configuration and abort the process if no significant change between the iterations is detected anymore.

The error ER in a standard GNG is calculated by summarizing the closest square Euclidean distance between all neurons and its closest input points. This is done once for each point in an iteration. Hereby at the end of an iteration the total error of the current configuration is calculated. The algorithm to generate gripper configurations will use the rate of change of this total error in multiple ways. The normal GNG does not reset this error after an iteration run, but rather sums it up from one iteration to the next. To prevent the error from rising to infinity, this error is reduced in each iteration with the factor α. This procedure is discarded for the problem presented here.

As in the standard GNG in every iteration the error is calculated but it will start for every iteration at zero. The abort criterion will be depending on the change rate of the error between the different iterations. The idea is that a low error change rate indicates a stable gripper configuration solution. If the change rate will drop under a certain value ΔE_{Crit} the algorithm will stop and the configuration is complete. The standard GNG on the other side defines the moment a new neuron is added to the configuration with the factor L. Each time the number of iterations corresponds to a whole divisible of L a new neuron is inserted.

Furthermore, many iterations can be passed if the algorithm already starts with the final designated number of grippers. This is not a good idea for a standard GNG but for this problem here where a certain number of grippers is aimed for, it is a good possibility to reduce iterations. Accordingly, that all grippers start at the same position and thus lie on top of each other at the beginning. Nevertheless, the rules of integrating new neurons/grippers according to the standard GNG is maintained for the case in which a gripper is deleted in the process and must be integrated again.

7.2.2 Influence of parameters on the initial gripper configuration

Since several changes have been made to the existing GNG in the last chapter (7.2.1), this chapter will first provide a brief systematic overview of the procedure of the new algorithm to identify all relevant parameters for this chapter. This overview is presented in Figure 7-11.

The parameters should be commented briefly in the following:

Objekt.stl: Is the input file defining the geometry of the part by STL format.

$Grid_{Spacing}$: This parameter defines how fine the mesh representing the part will be. If this parameter is set to 14 it means a mesh with a grid spacing of 14 mm will be used. The further figures will no longer show the individual points, since the representation becomes confusing. Accordingly, only the outer shape of the component is represented. Exceptions are explicitly mentioned.

$Point_{Weight}$: In chapter 7.2.1 it was introduced to treat points on the outer shape of the part in another way than the inner points. An inner point has a weighting of 1. A point on the outer shape gets a higher weight by multiplying it with this factor.

ϵ_b: Is a parameter taken from the normal GNG. It has an influence how large an adjustment on a winner neuron $\boldsymbol{w}_{s1}$ is performed.

ϵ_n: Is a parameter taken from the normal GNG. It has an influence how much an adjustment on a neighbor neuron $\boldsymbol{w}_n$ is performed.

$Start_{Pos}$: Is just the start position of the grippers.

T: Is a parameter taken from the normal GNG. It represents a threshold after an existing link is deleted if it has not been renewed for a certain number of steps. A connection is always created or renewed if the two grippers connected by it still represent the two next neurons for an input point.

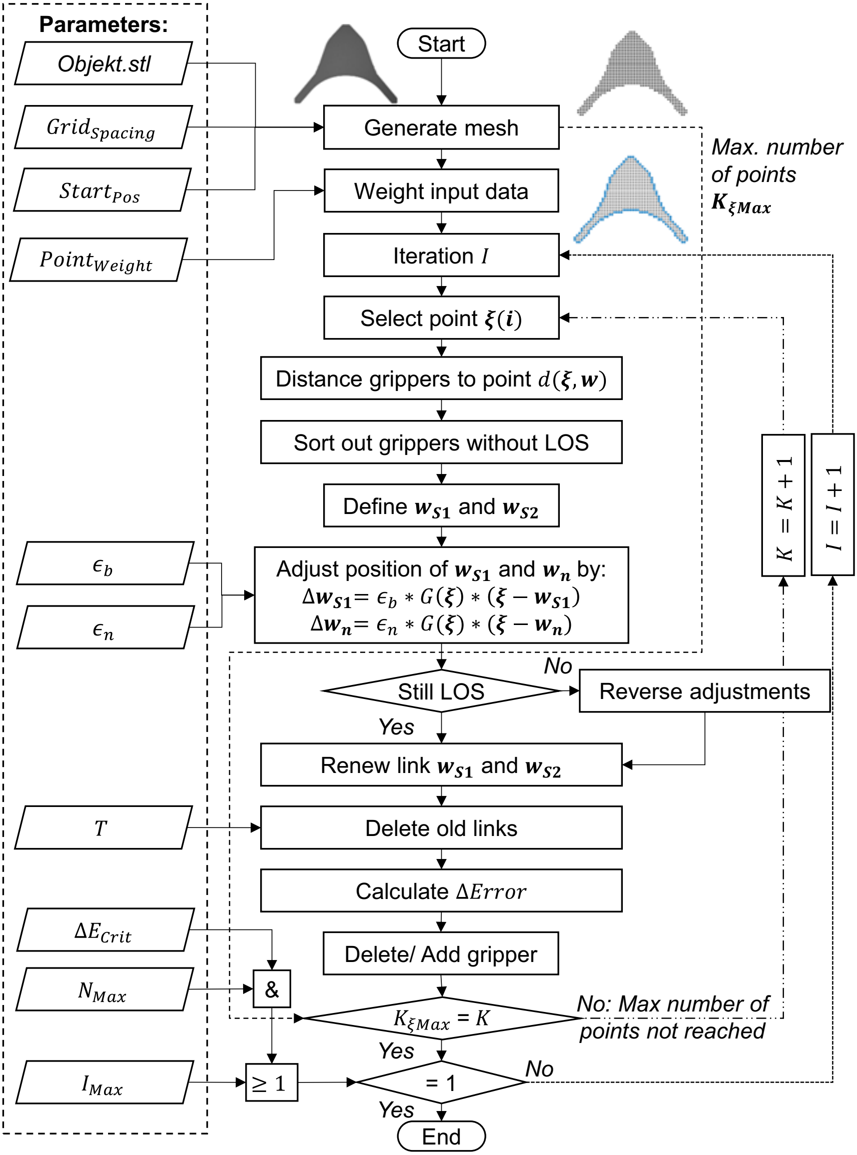
Parameters:
Objekt.stl
$Grid_{Spacing}$
$Start_{Pos}$
$Point_{Weight}$
ϵ_b
ϵ_n
T
ΔE_{Crit}
N_{Max}
I_{Max}
Start
Generate mesh
Weight input data
Iteration I
Select point $\boldsymbol{\xi}(\boldsymbol{i})$
Distance grippers to point $d(\boldsymbol{\xi}, \boldsymbol{w})$
Sort out grippers without LOS
Define $\boldsymbol{w}_{S1}$ and $\boldsymbol{w}_{S2}$
Adjust position of $\boldsymbol{w}_{S1}$ and $\boldsymbol{w}_n$ by:
$\Delta \boldsymbol{w}_{S1} = \epsilon_b * G(\boldsymbol{\xi}) * (\boldsymbol{\xi} - \boldsymbol{w}_{S1})$
$\Delta \boldsymbol{w}_n = \epsilon_n * G(\boldsymbol{\xi}) * (\boldsymbol{\xi} - \boldsymbol{w}_n)$
Still LOS
No
Reverse adjustments
Yes
Renew link $\boldsymbol{w}_{S1}$ and $\boldsymbol{w}_{S2}$
Delete old links
Calculate $\Delta Error$
Delete/ Add gripper
&
$K_{\xi Max} = K$
No: Max number of points not reached
Yes
≥ 1
= 1
No
Yes
End
Max. number of points $\boldsymbol{K}_{\boldsymbol{\xi Max}}$
$K = K + 1$
$I = I + 1$

Figure 7-11: Flowchart to create initial gripper configurations

ΔE_{Crit}: This is a new parameter. The change rate of the error ER in the gripper configuration is monitored every iteration step and an average error value is calculated over the last three iterations. If the change rate of this average error is falling below a certain value ΔE_{Crit} a new neuron is added. If the maximum number of neurons is already reached the whole process is completed. The process will also come to an end if the maximum number of iterations is reached. However, this should be avoided if possible.

N_{Max}: Is a parameter taken from the normal GNG. It defines the maximum number of neurons which can be used.

I_{Max}: Is a parameter taken from the normal GNG. It defines the maximum number of iterations. As already mentioned, it should only play a secondary role here and only serve as the last termination criterion if a solution does not converge.

It should now be investigated which different effects the parameters have on the result of the gripper configuration performed by the algorithm described in Figure 7-11.

Presetting parameter values

The first step is to reduce the number of parameters which have to be considered if meaningful values can be defined based on external boundary conditions. Such a value is for example the maximum number of iterations I_{Max}. The normal GNG aims to complete all iterations. By looking at the error development, it can be seen whether the distribution of the neurons can fulfill the self-imposed goals set by the parameter α. This will not work for the problem here. In this case a certain number of grippers/neurons should be placed. How many iterations it takes is not of primary interest. Accordingly, the I_{Max} is set for all configurations to a very high value (250). If this value is reached, the process is generally considered unsuccessful. This also limits the maximum time that can be used to generate a gripper configuration.

Another parameter is the $Grid_{Spacing}$ value. This parameter should be the same for all of following considerations. The question is what could be a good value. Generally, the algorithm will be more accurate if this value is small, because then the component is represented very detailed. This will also mean that the algorithm has to deal with a large amount of points, which will take some time. In chapter 5.1.1 it was specified that parts can have dimensions of 1500 mm x 1500 mm. If a $Grid_{Spacing}$ of 1 mm is used this will result in 2.250.000 input points in every iteration. A compromise is necessary. This can be developed by considering the size of the gripper. A gripper has a round gripper surface with a diameter of 40 mm. To grip parts with dimensions smaller than this gripper surface does not make sense. The value for $Grid_{Spacing}$ can therefore be as large as possible and still display the gripper surface in sufficient detail. In Figure 7-12 a part with the dimension equal to the gripper surface is meshed with a $Grid_{Spacing}$ value of 10 mm. Thereby the surface is still represented by nine points which should be enough for such a small object. With this $Grid_{Spacing}$ value the biggest part with 1500 mm x 1500 mm will still contain 22.500 points.

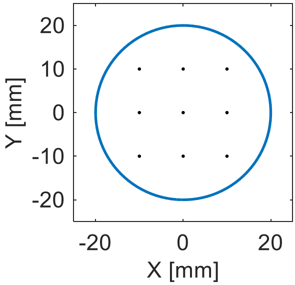

Figure 7-12: Gripper surface represented by nine points

Furthermore, the parameter ΔE_{Crit} will be a constant value for all investigations. This value defines when a configuration process is completed. It will be set to 1 mm. The average value of the last three iterations may therefore only change within one millimeter for a process to be considered complete. Such a change is very small and shows that a stable solution has been achieved.

Systematic analysis of parameters

The remaining values (*Object*, ϵ_b, ϵ_n, $Point_{Weight}$, T, N_{Max}, $Start_{Pos}$) are now to be systematically examined. The most important parameter is ϵ_b, as it directly controls the adjustment steps of the grippers/neurons. Therefore, the investigation will start with this parameter. The plan for the parameter variation is displayed in Figure 7-13. Furthermore, comments are added in Figure 7-13 to explain the values. Three different values for ϵ_b are chosen (0.5, 0.05 and 0.005). These different values for ϵ_b will all be tested with different $Point_{Weight}$ (1 and 10) and also different $Start_{Pos}$. The term "C" in Figure 7-13 indicate that the grippers are placed in the geometric center of the part at the beginning of the algorithm. It should be clarified once again that all grippers start at the same position and thus lie on top of each other at the beginning. The remaining parameters remain constant and are assigned only one value at a time.

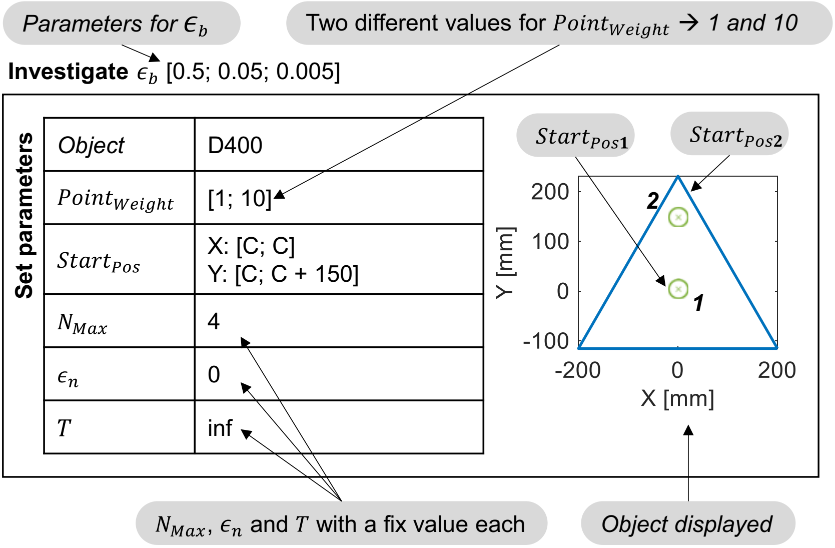

Parameters for ϵ_b

Two different values for $Point_{Weight}$ → *1 and 10*

Investigate ϵ_b [0.5; 0.05; 0.005]

Set parameters

Object	D400
$Point_{Weight}$	[1; 10]
$Start_{Pos}$	X: [C; C] Y: [C; C + 150]
N_{Max}	4
ϵ_n	0
T	inf

N_{Max}, ϵ_n and T with a fix value each

Object displayed

Figure 7-13: Variation of the parameters to investigate the influence of ϵ_b

The results of these parameter setup are displayed in Figure 7-14. In the first line, it can be seen that the results for smaller ϵ_b are becoming increasingly large. The fourth gripper moves to the middle of the part, which is certainly better for the gripper arrangement. This shows that ϵ_b must be sufficiently small to obtain a good result. In the second row, the $Point_{Weight}$ is set from one to ten, whereby all results consequently deteriorate. The result for ϵ_b 0.005 in row two looks now very similar to the formal result for ϵ_b 0.05 in row one.

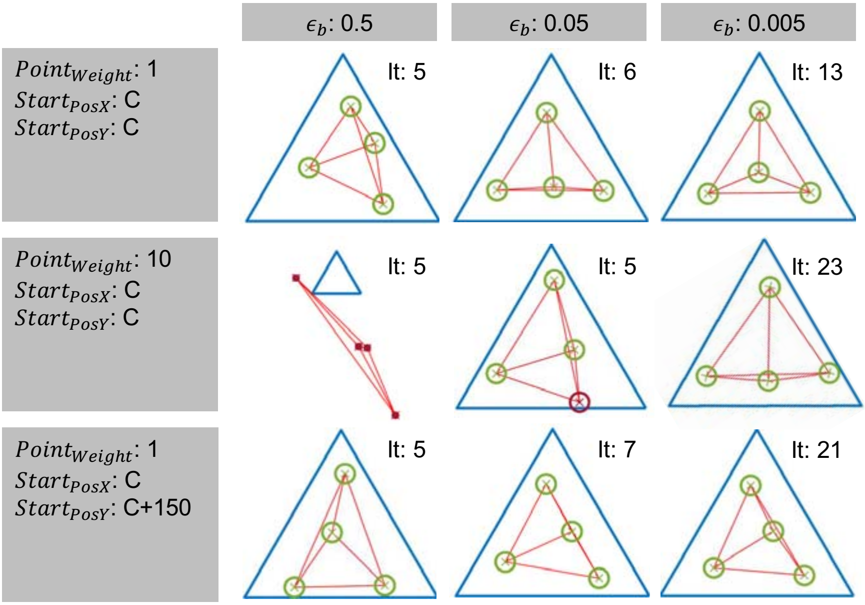
ϵ_b: 0.5
ϵ_b: 0.05
ϵ_b: 0.005
$Point_{Weight}$: 1
$Start_{PosX}$: C
$Start_{PosY}$: C
It: 5
It: 6
It: 13
$Point_{Weight}$: 10
$Start_{PosX}$: C
$Start_{PosY}$: C
It: 5
It: 5
It: 23
$Point_{Weight}$: 1
$Start_{PosX}$: C
$Start_{PosY}$: C+150
It: 5
It: 7
It: 21

Figure 7-14: Results for parameter setup in Figure 7-13 to investigate the influence of ϵ_b

This result is understandable, since in Equation 7-3 and Equation 7-4 the ϵ_b and $G(\boldsymbol{\xi})$, which is equal the $Point_{Weight}$ (see chapter 7.2.1), are calculated directly with each other. In order to obtain stable results, again it is necessary to divide the ϵ_b by the $Point_{Weight}$ factor. It can be shown that no reproducible results can be generated with too large ϵ_b values. This correlation can be shown by the resulting error in the gripper distribution ER. For this purpose, three gripper configurations are generated for each different ϵ_b. In each case it is recorded, how the error develops over the iterations. The curves are shown in Figure 7-15. The three attempts with a high ϵ_b (0.5) only needed five iterations, but they vary a lot regarding their find error. The other three attempts with a low ϵ_b (0.005) need longer but also lie closer together. They even overlap and, their error is significantly smaller. In this case a good gripper distribution and a small error correlate.

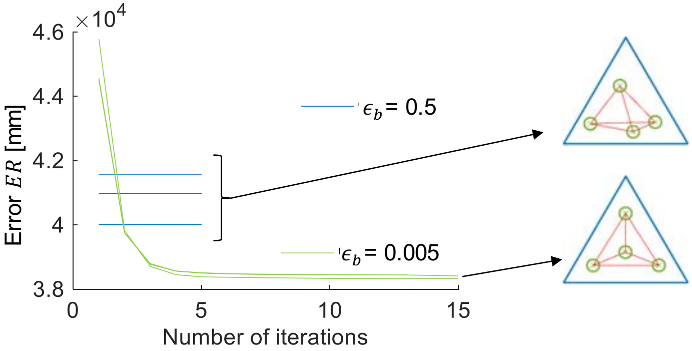

Figure 7-15: Error of gripper configurations generated ϵ_b= 0.5 and ϵ_b= 0.005 (Number of iterations cut by 15)

Conclusion from Figure 7-14 and Figure 7-15: From these first experiments it can be concluded that a low ϵ_b value is necessary to get stable results. Also, a higher $Point_{Weight}$ value has a destabilizing effect. In addition, the start position of the grippers has an influence on the results.

The next parameter that will be investigated is ϵ_n. ϵ_n is responsible for the fact that neighbors can influence each other in a GNG. An input point always draws the next gripper with ϵ_b towards its own position. The same point draws all neighbors of the gripper with ϵ_n. The general idea is that the gripper closest to the input point is also most affected. The effect on its neighbors, on the other hand, is expected to be less. For this reason, in the following ϵ_n should always be used depending of ϵ_b according to Equation 7-6.

$$\epsilon_n = M_{\epsilon_n} * \epsilon_b \qquad \text{Equation 7-6}$$

Correspondingly, not ϵ_n but rather M_{ϵ_n} must be examined. Since ϵ_n should always be smaller as ϵ_b, M_{ϵ_n} must have a value smaller one or even smaller.

To test M_{ϵ_n} a ϵ_b is defined with a value of 0.005 because this value has performed well so far. Weighting $Point_{Weight}$ is also kept constant at a value of one, because so far it is just destabilizing the results. However, in addition to a variation of M_{ϵ_n}, two different start positions are also used. They are the same as in the previous study of ϵ_b (Figure 7-14). It can be observed in Figure 7-16 that for a larger M_{ϵ_n}, the grippers move closer together than for a smaller M_{ϵ_n}. Furthermore, there is no difference between the different start positions. M_{ϵ_n} can therefore ensure that the solution no longer depends on the starting position. Moving the grippers together can have a negative effect, because the edges of the part will have large deflections.

Investigate M_{ϵ_n} [0.5; 0.25; 0.1]

Set parameters	*Object*	D400
	$Point_{Weight}$	1
	$Start_{Pos}$	X: [C; C] Y: [C; C + 150]
	N_{Max}	4
	ϵ_b	0.005
	T	inf

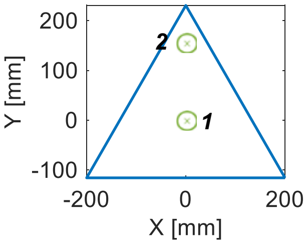

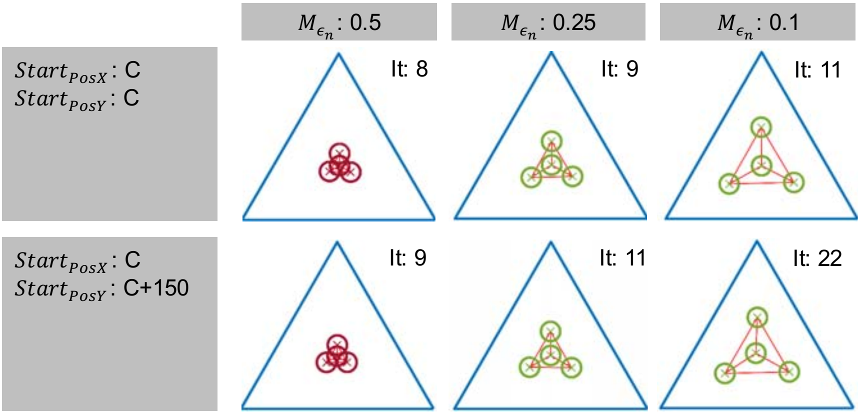
M_{ϵ_n}: 0.5
M_{ϵ_n}: 0.25
M_{ϵ_n}: 0.1
$Start_{PosX}$: C
$Start_{PosY}$: C
It: 8
It: 9
It: 11
$Start_{PosX}$: C
$Start_{PosY}$: C+150
It: 9
It: 11
It: 22

Figure 7-16: Variation of the parameters to investigate the influence of M_{ϵ_n}

It should now be analyzed how the error develops depending on M_{ϵ_n}. For this purpose, three configurations with an M_{ϵ_n} of 0 and three with an M_{ϵ_n} of 0.1 are calculated. Each time a ϵ_b of 0.005 is used. Furthermore, the start position is always the center of the part. Figure 7-17 shows the result. Using a M_{ϵ_n} actually has a negative influence on the error. It becomes larger by using it a larger M_{ϵ_n}, which can be explained by the fact that the grippers move closer together by M_{ϵ_n} and thus move away from their ideal position with respect to the distance to the input points.

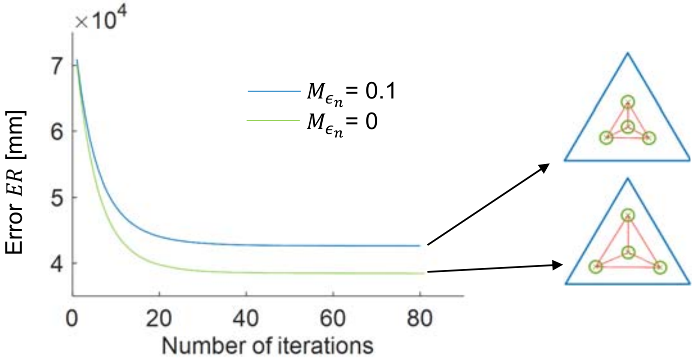

Figure 7-17: Error of gripper configurations generated M_{ϵ_n}= 0 and M_{ϵ_n}= 0.1

Conclusion from Figure 7-16 and Figure 7-17: From the variation of M_{ϵ_n} it can be concluded, that M_{ϵ_n} will make the results independent of the starting position. Furthermore, M_{ϵ_n} arrange the grippers more symmetrically but it will also increase the error of the final result.

So far it can be seen that $Point_{Weight}$ can destabilize the results because it indirectly increases ϵ_b. The general intention of $Point_{Weight}$ was to distinguish between inner and outer points. So, a negative effect on ϵ_b can be prevented if ϵ_b is divided by $Point_{Weight}$. Then $Point_{Weight}$ will still ensure that the inner points will have a smaller influence but it cannot destabilize the results anymore. Accordingly, Equation 7-3 and Equation 7-4 are adjusted. These adjustments can now be seen in Equation 7-7 and Equation 7-8. This adjustment ensures that the solutions do not escalate even with a larger $Point_{Weight}$ but it will reduce the influence of the inner points and will drag the gripper further outwards. This has already been shown in Figure 7-14.

$$\Delta \boldsymbol{w}_{S1} = \frac{\epsilon_b}{Point_{Weight}} * G(\xi_{IN/OUT}) * (\xi_{IN/OUT} - \boldsymbol{w}_{S1})$$ Equation 7-7

$$\Delta \boldsymbol{w}_{n} = \frac{\epsilon_n}{Point_{Weight}} * G(\xi_{IN/OUT}) * (\xi_{IN/OUT} - \boldsymbol{w}_{n})$$ Equation 7-8

However, now this correlation is to be studied in further detail with the parameters selected so far and how the adjustments in Equation 7-7 and Equation 7-8 affect each other. The adjustments in Equation 7-7 and Equation 7-8 make the results stable. Using a ϵ_b of 0.005 and a M_{ϵ_n} of 0.1 will result now for a $Point_{Weight}$ of 10 or 100 in a reproduceable result. This was not the case without the adjustments before.

Again, three passes were made of each configuration (Figure 7-18). Each result is now stable, which is a significant improvement relative to the first results in Figure 7-14. However, the gripper moves downwards in the middle for larger $Point_{Weight}$ values.

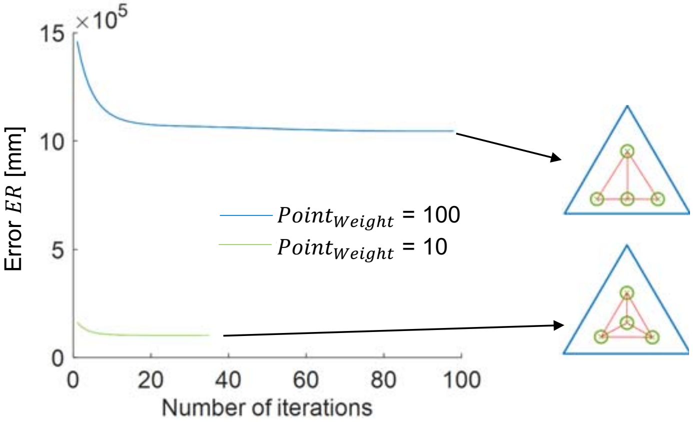

Figure 7-18: Error of gripper configurations generated by $Point_{Weight}$

The reason why the gripper moves out of the middle for large $Point_{Weight}$ is clearly visible in the Figure 7-19.

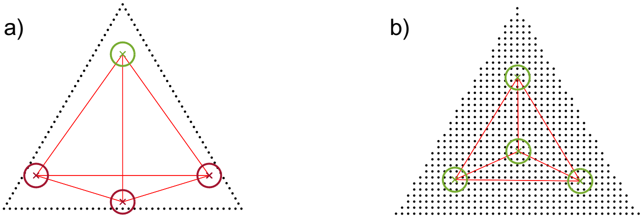

Figure 7-19: Gripper configuration using only points on the edge of the part (a) and all points (b)

Here a gripper configuration is generated only by the points at the edge (a) and by the points inside (b). Each gripper must move as close as possible to the points, which is only possible if the gripper moves away from the center. However, for the later gripper distribution it is certainly often important to have a gripper in the middle of the part. This aspect of $Point_{Weight}$ can therefore be a disadvantage.

Conclusion from Figure 7-18 and Figure 7-19: By the adjustments in Equation 7-7 and Equation 7-8 high $Point_{Weight}$ values can be used now without any destabilization. However, gripper from within the arrangement then also move to the edges for a large $Point_{Weight}$.

The problem in this situation is that the grippers on the outside should spread widely and be near the edges of the part but still some grippers should remain on the inside. By slight adjustment on ϵ_b and M_{ϵ_n} this is possible even with a large $Point_{Weight}$. This is done by decreasing ϵ_b (change from 0.005 to 0.0005) or slightly increasing M_{ϵ_n}. Just by testing values an increase of M_{ϵ_n} from 0.1 to 0.11 was found to be enough. However, all these measures come at the cost of an increasing number of iterations. This can be seen in Figure 7-20. From an economical perspective, the best result is the configuration in the middle of Figure 7-20. The grippers are already quite widely distributed and with a number of only 36 iterations the effort is manageable.

Investigate $Point_{Weight}$ [1; 16; 32]

Set parameters

Object	D400
$Start_{Pos}$	X: [C; C] Y: [C; C]
N_{Max}	4
ϵ_b	0.005; 0.0005
M_{ϵ_n}	0.1; 0.11
T	inf

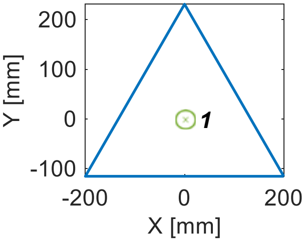

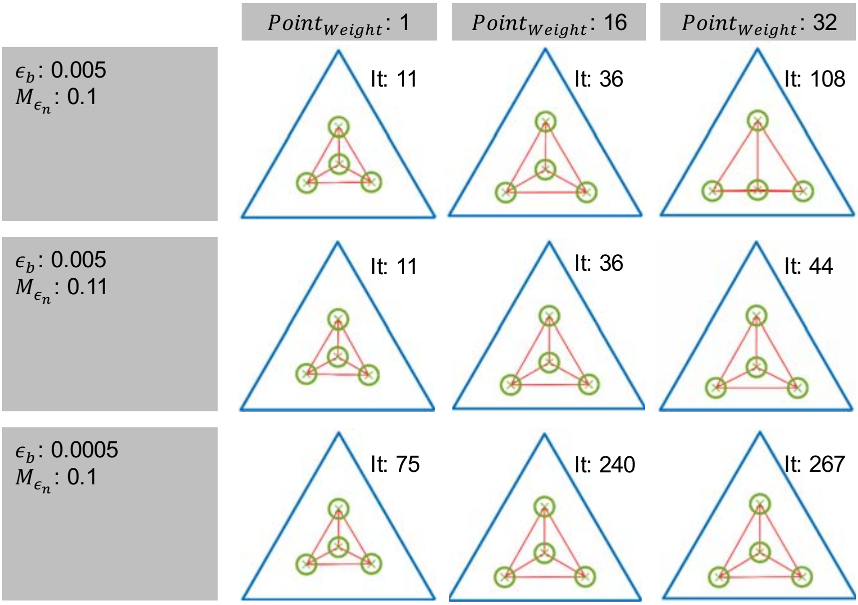

Figure 7-20: Variation of parameters to investigate the influence of $Point_{Weight}$

Conclusion from Figure 7-20: Ultimately it has to be said that the method of weighting the boundary points differently works but must be used with care. Good results will need a high number of iterations.

Accordingly, something else has to be done to bring the grippers closer to the edge. ϵ_n (M_{ϵ_n}) is primarily used to make the solution more independent of the starting position, but unfortunately also has the effect of bringing the grippers closer together. This also means that ϵ_n is necessary at the start of the configuration but not at the end. Instead of applying a higher weighting for the points at the edge it is also possible to reduce the parameter M_{ϵ_n} at the end of the process or even set it to zero. The end of the process is normally reached if the E_{Crit} is fulfilled the first time. However, instead of stopping the process at this time the M_{ϵ_n} will be manipulated. Using the same logical also ϵ_b will be reduced to ensure an accurate result. These parameters will be marked as ϵ_{b_Final} and $M_{\epsilon_{n\_Final}}$. As in the previous investigations good results were achieved with a ϵ_{b_Final} value of 0.005. A wider distribution is enabled when the $M_{\epsilon_{n\_Final}}$ value (and therefore ϵ_n) is set to zero at the end. This is tested in Figure 7-21 in the right configuration. $M_{\epsilon_{n\_Final}}$ starts with a value of 0.11 at is reduced at the end to 0. The left and middle gripper configuration have already been shown before in Figure 7-20 and are here in Figure 7-21 for a comparison to the one on the right. Of the three gripper configurations, the right one managed to spread the grippers the most. At the same time the number of iterations is only slightly increased with 73 iterations. At the same time the exact value of M_{ϵ_n} is now less important anymore as long as it is not to big (≤0.5) or too small (≥0.1).

	$Point_{Weight}$: 16 ϵ_{b_Final}: 0.005 M_{ϵ_n}: 0.11 $M_{\epsilon_{n\_Final}}$: 0.11	$Point_{Weight}$: 32 ϵ_{b_Final}: 0.0005 M_{ϵ_n}: 0.1 $M_{\epsilon_{n\_Final}}$: 0.1	$Point_{Weight}$: 1 ϵ_{b_Final}: 0.005 M_{ϵ_n}: 0.11 $M_{\epsilon_{n\_Final}}$: 0
ϵ_b: 0.005			

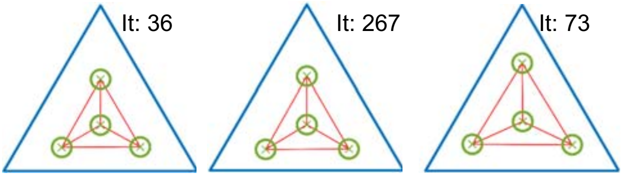

Figure 7-21: Test of the use of a final value ϵ_{b_Final} and $M_{\epsilon_{n\_Final}}$

The last parameter is T to analyse in this chapter. It defines when connections between the grippers have to be deleted. Previously, this value was set to infinity, which enabled this aspect to be omitted thus far. It should ensure that connections between two grippers are disconnected if they no longer have a common point. The value is set equal to the number of points for all considerations. This ensures that a connection is maintained even if only one single point connects two grippers. For the object D400 this will result in the following gripper configuration in Figure 7-22. The parameter values in Figure 7-22 will also represent the final values of the parameter investigation in this chapter. Through the influence of T, the connection between gripper one and two is deleted because gripper four is slightly too close to the lower edge and therefore there are no more common points for gripper one and two.

$Point_{Weight}$: 1
ϵ_b: 0.005
ϵ_{b_Final}: 0.005
M_{ϵ_n}: 0.2
$M_{\epsilon_{n\_Final}}$: 0
T: 713

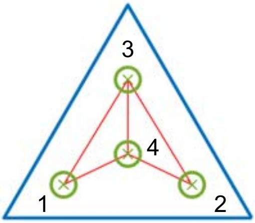

Figure 7-22: Final parameter setting of this chapter and influence of the T parameter

Since in the course of this chapter adjustments have again been made to the structure and sequence of the algorithm, the additions are shown in Figure 7-23 relative to Figure 7-11. The changes are marked in blue. If now all conditions are met to complete the process the first time ϵ_{b_Final} and $M_{\epsilon_{n\_Final}}$ are activated by just replacing the old ϵ_b and M_{ϵ_n} values. Also, the error of the configuration is manipulated so that the ΔE_{Crit} is not fulfilled anymore and a new adjustment process with the new values ϵ_{b_Final} and $M_{\epsilon_{n\_Final}}$ is executed.

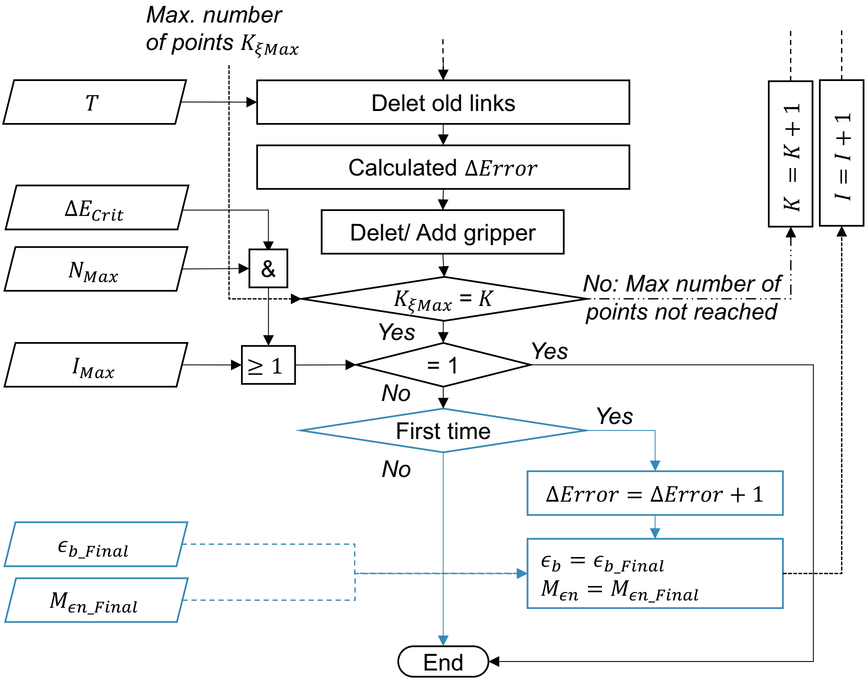
Max. number
of points $K_{\xi Max}$
T
Delet old links
Calculated $\Delta Error$
ΔE_{Crit}
Delet/ Add gripper
N_{Max}
&
$K_{\xi Max} = K$
No: Max number of
points not reached
$K = K + 1$
$I = I + 1$
Yes
I_{Max}
≥ 1
$= 1$
Yes
No
First time
Yes
No
$\Delta Error = \Delta Error + 1$
ϵ_{b_Final}
$M_{\epsilon n\_Final}$
$\epsilon_b = \epsilon_{b\_Final}$
$M_{\epsilon n} = M_{\epsilon n\_Final}$
End

Figure 7-23: Adjustments to the algorithm relative to Figure 7-23 (marked blue)

7.2.3 Initial gripper configuration for use-cases

The adjusted algorithm in Figure 7-23 with the final parameter set (Figure 7-22) will now be used to generate initial gripper configurations for the use-cases presented in 5.4. The different parts will be presented one after another with a different number of grippers (different N_{Max}). The aim is to reflect whether the gripper configuration is a sensible configuration for each component that can be further improved by integrating simulation data.

Use-case SMC: IR001

Figure 7-24 shows gripper configurations for the first SMC use-case part IR001. Most configurations are plausible, whereby exceptions are the configurations C2 and C4. The distribution of three grippers on a rectangle is generally a difficult task. Whether the distribution is so appropriate is difficult to answer and a human would probably tend to place one of the three grippers on the opposite side of the two grippers in the middle. However, in the C4 configuration it is definitely necessary to place one of the five grippers in the center and the others symmetrically around it in the corners. This can still happen through the integration of simulation data in the next step.

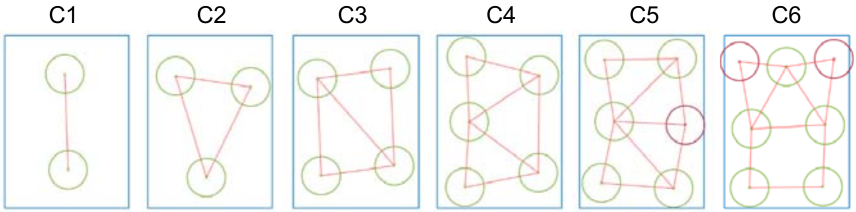

Figure 7-24: Generated initial gripper configurations for part IR001 with a different number of grippers

Use-case SMC: IR002

IR002 differs from IR001 only regarding the cuts-outs for a better draping behavior. The algorithm takes these differences into account by no longer arranging the grippers in a rectangle but in a diamond shape (C3) and then continuously expanding this (C4 - C6).

The adjustments in chapter 7.2.1 show effect and no gripper is placed in the cut-outs. It is to be expected that the distributions will give good results. However, with the form IR002 all configurations of IR001 could also work well because the cut-outs are very small, and the grippers could also bridge them.

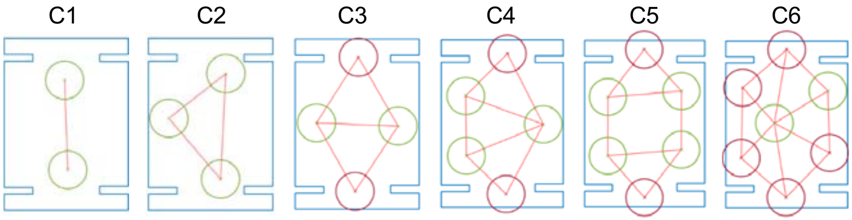

Figure 7-25: Generated initial gripper configurations for part IR002 with a different number of grippers

Use-case RTM: H003

The algorithm arranges the grippers for part H003 (Figure 7-26) in the configuration C3 to C7 well and in a symmetrical way. Only their spreading over the component can be mentioned here as something to be improved. Furthermore, in C1 the form is correct, but not the spreading. Asymmetric occurs only in C2. Here it is uncertain whether this distribution is worthwhile for a further improvement by a simulation.

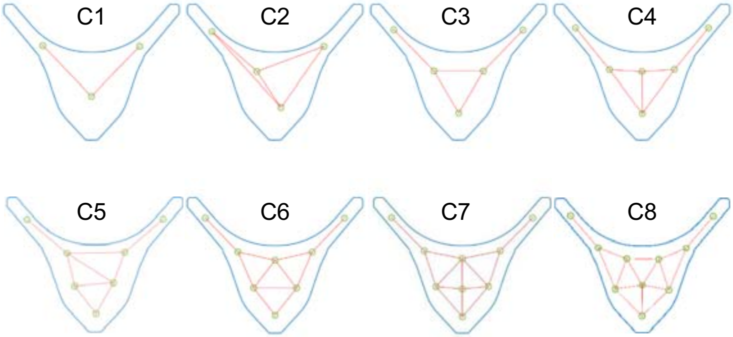

Figure 7-26: Generated initial gripper configurations for part H003 with a different number of grippers

Use-case RTM: H003_1L & H003_1R

The parts H003_1L and H003_1R are basically identical but are mirror-inverted to each other. For this reason, only the part H003_1L is shown here in Figure 7-27. Since the component is not very wide, the algorithm distributes all grippers to be distributed into one line. Each of the distributions therefore represents a useful initial gripper configuration.

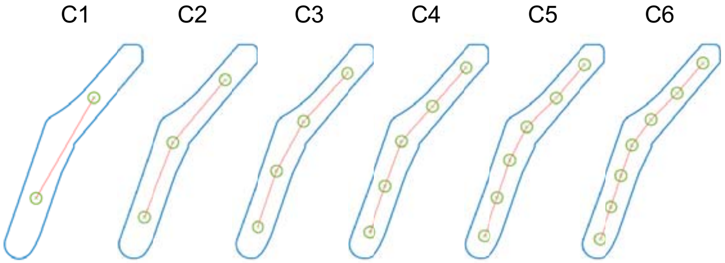

Figure 7-27: Generated initial gripper configurations for part H003_1L with a different number of grippers

Use-case RTM: H003_2 & H003_3

The last two parts H003_2 and H003_3 have the same characteristic as the previous part H003_1L. They are not wide and therefore only a gripper arrangement along a line makes sense (Figure 7-28).

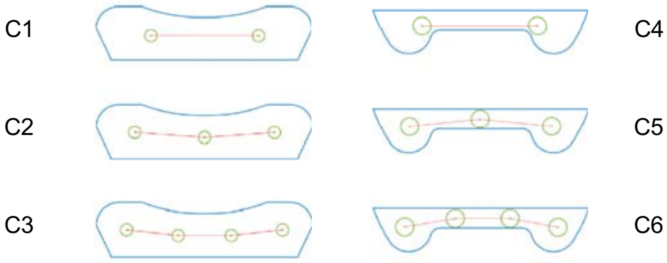

Figure 7-28: Generated initial gripper configurations for part H003_2 and H003_3 with a different number of grippers

“Randomized” part: RA001

The last part on which the algorithm is to be tested is not part of a use-case but has a balanced mixture of flat and thin geometric features. Figure 7-29 shows arrangements for a different number of grippers, all of which are all suitable as initial gripper configuration.

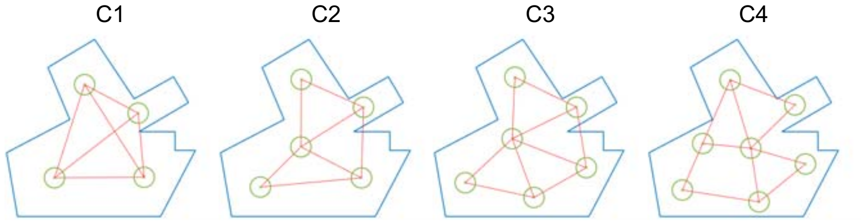

Figure 7-29: Geometry and generated initial gripper configurations for part RA001 with a different number of grippers

7.2.4 Conclusion for initial gripper configuration

In this chapter, an algorithm has been developed that aims to generate initial gripper configurations for two-dimensional parts using different numbers of grippers. For this purpose, the GNG approach was selected and adapted to the problem. As in chapter 7.2.3, the resulting algorithm produces good results in most cases and generates sensible gripper arrangements. Only one of 36 gripper arrangements is questionable (H003 C2 in Figure 7-26). However, it is quite conceivable that the systematics shown here can deliver good results for a variety of different forms. This should be shown especially by applying the algorithm to different shapes in chapter 7.2.3. The implementation of the widest possible distribution is still an issue for some shapes.

7.3 Adjustment of gripper configuration with deflection data

Since initial gripper configurations are available through chapter 7.1, they can now be simulated. The simulation results will provide information on where problem areas are. However, it is clear that the grippers are not yet correctly arranged in the initial gripper configurations. This cannot be the case because neither the material data or fiber orientation were taken into account during generation. The task is now to adjust the previously placed grippers in such a way that the deflection is reduced. Only if no improvement of the deflection can be achieved with the existing grippers anymore a statement can be made whether an additional gripper is necessary to achieve the target deflection or not. An approach is therefore needed to improve the existing gripper configuration.

A large deflection at a specific point can usually be reduced by bringing an existing gripper from the configuration closer to it. Intuitively, one would select the gripper that is closest to this point, as this would require the slightest change in the configuration. The systematic steps to make these adjustments are:

1. Identify points with a too large negative deflection
2. Select a gripper closest to this point and drag it towards this position
3. Check the result of the adjustment

This means that the same algorithm used to generate the initial gripper configuration can also be used to adjust it. However, there is a significant difference between the two tasks. The input data representing the part was previously only described in two dimensions (X and Y). Based on this information, the position of the grippers was then also determined in two dimensions. In addition, the information was previously static and thus unchanged throughout the entire process. Since simulations are now performed and the part is deformed, the positions of the input points describing the part will change therefore in three dimensions. Furthermore, the input data will no longer be static about the process, because with every small change in the gripper positions, the deformation of the component will also change. However, the grippers still only have to be arranged in two dimensions, given that the component is to be picked up on a flat surface. Accordingly, the third dimension (Z) must always be zero for the grippers.

7.3.1 Modification of GNG for the gripper configuration adjustment

Since the boundary conditions of the problem change, the algorithm must also be adapted again. The adjustments in the previous Equation 7-7 and Equation 7-8 were dependent on ϵ_b (or ϵ_n), the weighting $G(\boldsymbol{\xi})$ of the respective point and the distance between the gripper $\boldsymbol{w}$ and the point $\boldsymbol{\xi}$. The direction of the adaptation was defined by the vector between the input point $\boldsymbol{\xi}$ and the gripper $\boldsymbol{w}$.

The input points describing the part are shifted in three dimensions by the deformation in the simulation. For each undeformed point $\boldsymbol{\xi_0}$ it is calculated by the simulation how it is moved by the deflection in the different directions $D_X(\boldsymbol{\xi})$, $D_Y(\boldsymbol{\xi})$ and $D_Z(\boldsymbol{\xi})$. If these shifts are now applied to the point $\boldsymbol{\xi_0}$ to calculate a deformed $\boldsymbol{\xi}$, the gripper would also be shifted into three dimensions by the adaptation vector $(\boldsymbol{\xi} - \boldsymbol{w_{S1}})$. However, it has already been mentioned that only two-dimensional displacements are permissible for the grippers. Therefore, the displacements are not applied to the vector itself, but only the $D_Z(\boldsymbol{\xi})$, is calculated as a weighting like $Point_{Weight}$ before. The shifts $D_X(\boldsymbol{\xi})$ and $D_Y(\boldsymbol{\xi})$ should be ignored in this analysis. Large deformations in $D_Z(\boldsymbol{\xi})$ are often accompanied by large deformations in $D_X(\boldsymbol{\xi})$ and $D_Y(\boldsymbol{\xi})$. Accordingly, a deformed part has a different outer contour than the undeformed part when viewed from above. However, the aim is to bring the grippers to critical X and Y positions on the still undeformed part, to avoid these strong deformations later. Accordingly, $D_X(\boldsymbol{\xi})$ and $D_Y(\boldsymbol{\xi})$ must be ignored.

The direction of the adjustment should still be maintained, although the distance between the gripper $\boldsymbol{w}$ and the input point $\boldsymbol{\xi}$ is no longer important because the important value is now the deflection $D_Z(\boldsymbol{\xi})$. For this reason, the vector is now normalized by its magnitude in Equation 7-9 and Equation 7-10. Instead of the weight $G(\boldsymbol{\xi})$, the deflection of the part in Z-directions is considered in $D_Z(\boldsymbol{\xi})$.

$$\Delta\boldsymbol{w}_{\boldsymbol{S1}} = \epsilon_{b\_FEM} * D_Z(\boldsymbol{\xi}) * \left(\frac{\boldsymbol{\xi} - \boldsymbol{w}_{\boldsymbol{S1}}}{\overline{\boldsymbol{\xi} - \boldsymbol{w}_{\boldsymbol{S1}}}}\right) \qquad \text{Equation 7-9}$$

$$\Delta\boldsymbol{w}_{\boldsymbol{n}} = \epsilon_{n\_FEM} * D_Z(\boldsymbol{\xi}) * \left(\frac{\boldsymbol{\xi} - \boldsymbol{w}_{\boldsymbol{n}}}{\overline{\boldsymbol{\xi} - \boldsymbol{w}_{\boldsymbol{n}}}}\right) \qquad \text{Equation 7-10}$$

Another important fact is that the value of the input points change depending on the adjustment movements of the grippers. Therefore, after each adjustment step, a new simulation must be carried out. Each simulation can take a few minutes. This makes every step very time-consuming. Accordingly, it is important that there is always an improvement through the adjustment. Misadjustments must be avoided or their consequences reduced as far as possible. It is unlikely that an adjustment step takes exactly the right measure the first time. Generally, two scenarios can occur:

1. The adjustment step led to an improvement but did not go sufficiently far enough.

2. The adjustment step was too large. Although it was possible to eliminate a large deflection at a spot, but a new deflection was created due to the large adjustment step.

The first scenario is not a problem. The result was a step in the right direction and can therefore be accepted. Even the next step in this direction can be enlarged a little. In the second scenario, the adjustment has overstepped the mark. The result is therefore useless. Here, it becomes necessary to reload the initial situation and try again with a smaller step. All of these described adjustments can be seen in Figure 7-30.

The process is repeated until the rate of change deflection falls under a criterion D_{Crit}.The process starts with loading the initial gripper configuration and the first simulation of the deflection. The important values D_{Min} and D_{Mean} are stored and the abort criterion is checked. If there was already a previous step it will be checked whether it was good and could improve the result. The ϵ_{b_FEM} is then increased or reduced according to the evaluation. The increase or reduction of ϵ_{b_FEM} is done by multiplying ϵ_{b_FEM} by the factor $I_{\epsilon_{b\_FEM}}$ or $R_{\epsilon_{b\_FEM}}$. If the last step led to larger deflection, the last good configuration is loaded. As with the initial gripper configuration, the input data from the simulation are to weight, whereby this topic will be discussed in detail later. The following procedure for performing the adjustment steps corresponds exactly to the system already described for the initial gripper configuration (page 105). However, ϵ_n is no longer used in this process. This is to be justified by the fact that ϵ_n always leads to a reduction of the distribution and thus would prevent the grippers from migrating to the problem areas. This could already be shown in Figure 7-15.

A new element in Figure 7-30 is the decision concerning whether a step was good or not. Since the goal of the algorithm is to minimize the negative amount of deflection, a good step is logically associated with reducing the amount of deflection relative to the previous one. The goal is therefore generally always to take steps in the right direction. Adjustments that reduce the average deflection are also considered to be a step in the right direction, as there is a chance of reducing the amount of negative deflection in the next steps. Depending on this evaluation, the ϵ_{b_FEM} is enlarged or reduced in the next step. A value for $I_{\epsilon_{b\_FEM}}$ of 1.5 and $R_{\epsilon_{b\_FEM}}$ of 0.5 is specified for all considerations. Depending on the boundary conditions of the task, other values can lead to a good result more quickly. However, a more detailed examination should not be done, because it is assumed that it will only influence the number of iterations, but not on the final result.

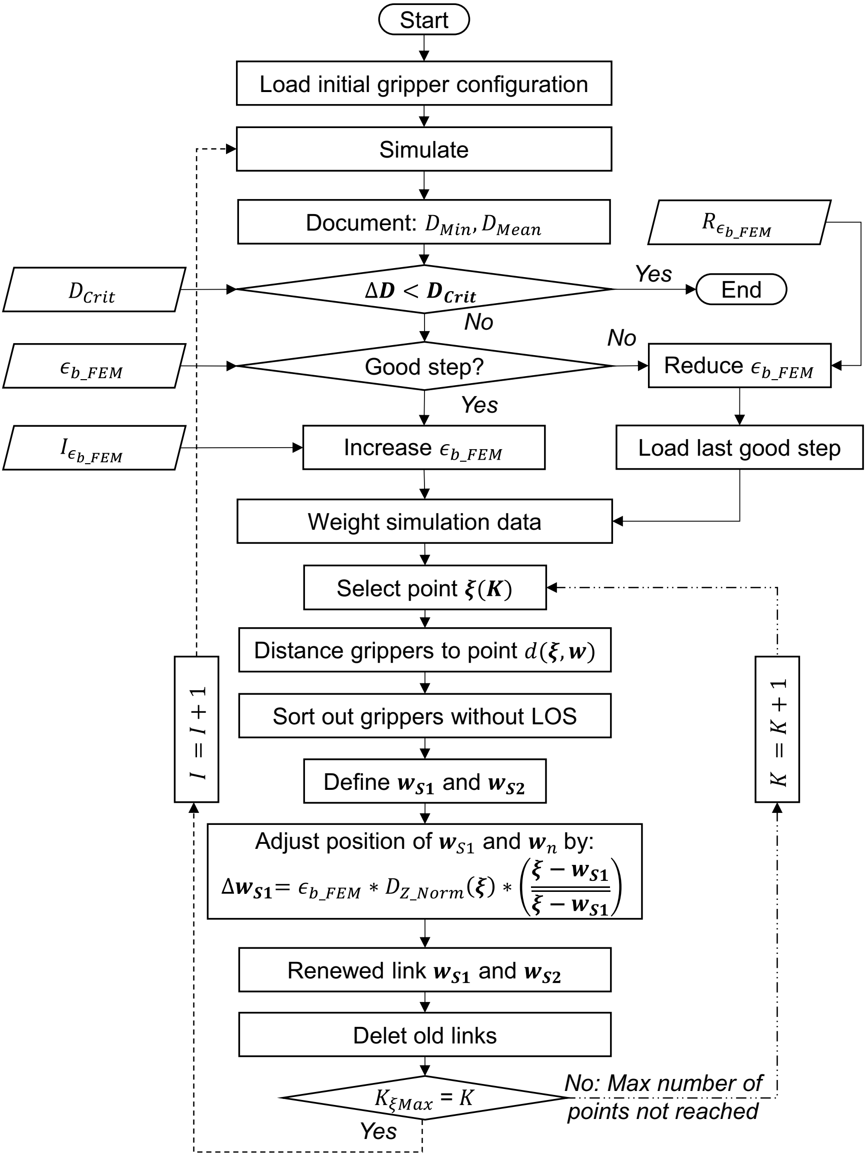
Start
Load initial gripper configuration
Simulate
Document: D_{Min}, D_{Mean}
$R_{\epsilon_{b\_FEM}}$
D_{Crit}
$\Delta \boldsymbol{D} < \boldsymbol{D_{Crit}}$
Yes
End
No
No
ϵ_{b_FEM}
Good step?
Reduce ϵ_{b_FEM}
Yes
$I_{\epsilon_{b\_FEM}}$
Increase ϵ_{b_FEM}
Load last good step
Weight simulation data
Select point $\boldsymbol{\xi}(\boldsymbol{K})$
Distance grippers to point $d(\boldsymbol{\xi}, \boldsymbol{w})$
$I = I + 1$
$K = K + 1$
Sort out grippers without LOS
Define $\boldsymbol{w_{S1}}$ and $\boldsymbol{w_{S2}}$
Adjust position of $\boldsymbol{w_{S1}}$ and $\boldsymbol{w_n}$ by:
$\Delta \boldsymbol{w_{S1}} = \epsilon_{b\_FEM} * D_{Z\_Norm}(\boldsymbol{\xi}) * \left(\frac{\boldsymbol{\xi} - \boldsymbol{w_{S1}}}{\|\boldsymbol{\xi} - \boldsymbol{w_{S1}}\|}\right)$
Renewed link $\boldsymbol{w_{S1}}$ and $\boldsymbol{w_{S2}}$
Delet old links
$K_{\xi Max} = K$
No: Max number of points not reached
Yes

Figure 7-30: Flowchart for making adjustments to gripper configuration

For the generation of the initial gripper configuration in chapter 7.2, the points at the edge of the part were weighted differently from those in the inner of the part. Such a distinction is no longer necessary here, but each point now has an individual weighting in the amount of D_Z. This D_Z can vary during the adjustment of the gripper configuration. Especially in the first simulation very large deflections of up to 250 mm and more can occur. If the gripper configurations are then adjusted, the deflections are also reduced. Nevertheless, the algorithm should be able to improve a configuration with only low deflections just as well as with large ones. To achieve this, the D_Z from the simulation is first normalized by the largest deflection in terms of amount (Equation 7-11).

$$D_{Z\_Norm} = \frac{D_Z}{max|D_Z|} \qquad \text{Equation 7-11}$$

In order to ensure that the algorithm can concentrate on the current problem areas in each iteration and is not held back by unproblematic points, a limit value filtering is also used. This limit filter sets any value zero whose value is greater than $D_{Z\_Threshold}$. $D_{Z\_Threshold}$ is calculated from the average deflection in Z-direction and the maximum value of D_Z in negative direction according to Equation 7-12.

$$D_{Z\_Threshold} = \mathrm{mean}(D_Z) - \frac{|(min(D_Z)| - |mean(D_Z)|}{2} \qquad \text{Equation 7-12}$$

A simple example illustrates the effects of the adjustments above. The example is a small rectangular blank with a dimension of 250 mm x 25 mm in Figure 7-31. When meshing the component, a grid spacing of 10 mm is still used, which is why the width of the component is not 100 percent correctly approximated through the grid. Subsequently, the initial gripper configuration for two grippers is calculated as a first step. Each point has a weighting of -1, which can be seen from the color coding. Step two in Figure 7-31 represents the result of the first simulation. There is a very small deflection between the grippers while the freely suspended ends of the part have the largest deflection. In the illustrations is marked with an **x** symbol which points fulfill the criterion $D_{Z\_Threshold}$ and therefore have an influence on the grippers.

In the third step, the grippers have obviously moved too far outwards and the largest deflection is now formed in the middle of the component. However, since the deflection has improved relative to step two, $D_{Z\_Threshold}$ has decreased and points with a deflection up to -0.45 mm are now also taken into account. This causes the grippers to move back again until a balanced condition prevails in the fourth step.

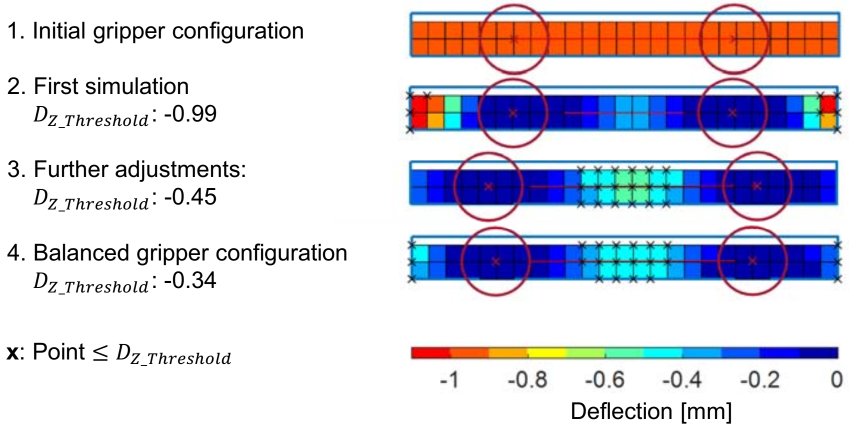

Figure 7-31: Adjustment steps to an initial gripper configuration

A deflection of approx. -0.5 mm now occurs on both insides at the freely-hanging edges. The color coding used in the MATLAB surf plot shows this only partially correct. The color of a rectangular area element is always selected based on the value of the lower left point. Due to the few rectangular surface elements, it may look as if the right side deflects slightly less than the left side in step four. To illustrate this, Figure 7-32 shows a side view of step four in Figure 7-31.

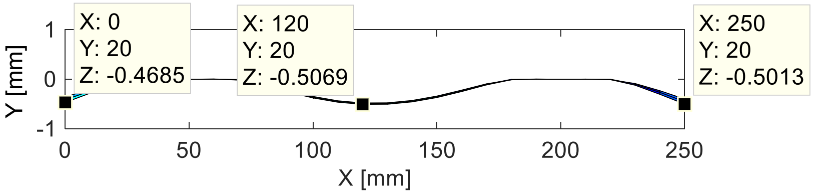

Figure 7-32: Side view on the part in Figure 7-31 step four

In the chapter before it was important to find a good value for ϵ_b. It could also be shown that a too large ϵ_b has a bad influence on the generated configurations. This can be explained by the fact that a non-standardized vector was used for the initial gripper configuration. If a non-standardized vector is used, an ϵ_b of one means that the gripper takes a complete step to the point to which it is to be adapted. The ϵ_b is also still used to adapt the gripper configuration. However, the vector between the input point and the gripper is only used in a normalized way and whether an adjustment was good or bad can be decided directly by a simulation. An adjustment of ϵ_{b_FEM} depending on the simulation result has already been introduced.

For these reasons, all gripper adaptations will therefore start with an ϵ_{b_FEM} of one. In Figure 7-33 it can be seen how the ϵ_{b_FEM} and the negative deflection between the different steps for the example from Figure 7-31 develop. Note that there is sometimes more than one simulation between the different steps. This is the case if a step has not led to an improved result and therefore the ϵ_{b_FEM} is reduced and the step must be repeated.

For example, it takes four simulations to get from step 3 to step 4. In Figure 7-33 the ϵ_{b_FEM} starts with the value 0.005 for the initial gripper configuration, since this was used for the creation of the initial gripper configuration. After the first simulation, the value of ϵ_{b_FEM} is then switched to 1 and the actual adjustment of the configuration begins. Since the adjustment between step 1 and 2 improved the result, the value for ϵ_{b_FEM} is increased to the value 1.5 by multiplication with $I_{\epsilon_{b\_FEM}}$. The next step between step 2 and 3 is then too large in a series of adjustments and lead to worse results. Therefore, the ϵ_{b_FEM} value is iteratively reduced with $R_{\epsilon_{b\_FEM}}$ until a good result is achieved with an ϵ_{b_FEM} of 0.1875. However, in the diagram at step 3 a value of 0.2813 is shown, since the successful value of 0.1875 is calculated immediately after the successful step with the $I_{\epsilon_{b\_FEM}}$. The same happens between step 3 and step 4.

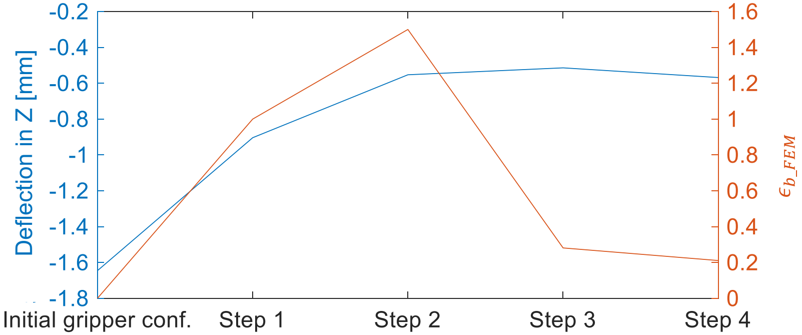

Figure 7-33: Development of ϵ_{b_FEM} and deflection in Z-direction

The benefit of $D_{Z\_Threshold}$ in the adjustment process can be shown when three grippers are arranged on a triangle (Figure 7-34). The gripper arrangement on the left triangle (Figure 7-34, a) in Figure 7-34 is using a $D_{Z\_Threshold}$ as described in Equation 7-12. By the adaption of the other gripper arrangement (Figure 7-34, b) all points have an influence.

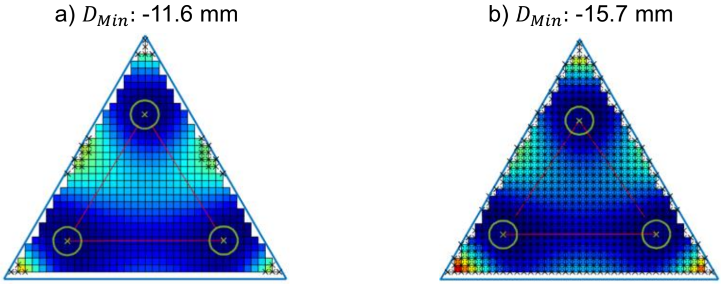

Figure 7-34: Gripper arrangement with the use of $D_{Z\_Threshold}$ (a) and without (b)

This also means that the point in the middle of the triangle try to pull the grippers to their own position. They may have only small deflection and have therefore only a small influence. However, their larger numbers compensate the few points on the edge with large deflections. This effect keeps the grippers closer to the middle of the part which causes higher deflections on the edges.

7.3.2 Gripper configuration for use-cases

The method presented in Figure 7-30 is now applied to improve the generated initial gripper configurations from chapter 7.2.3. As shown in Figure 7-30 the algorithm will not add new grippers but will try to arrange the existing grippers in such a way that the amount of deflection is reduced. The configurations for part H003 configuration C1 and C2 on page 120 can be described as difficult. Configuration C1 is symmetrical and makes sense in terms of the type of arrangement, but not sufficiently distributed over the part to be good. The question is now whether the algorithm for the adjustment manages to create a good configuration even from a less favorable initial gripper configuration. Figure 7-35 shows different steps of adjustment by the algorithm.

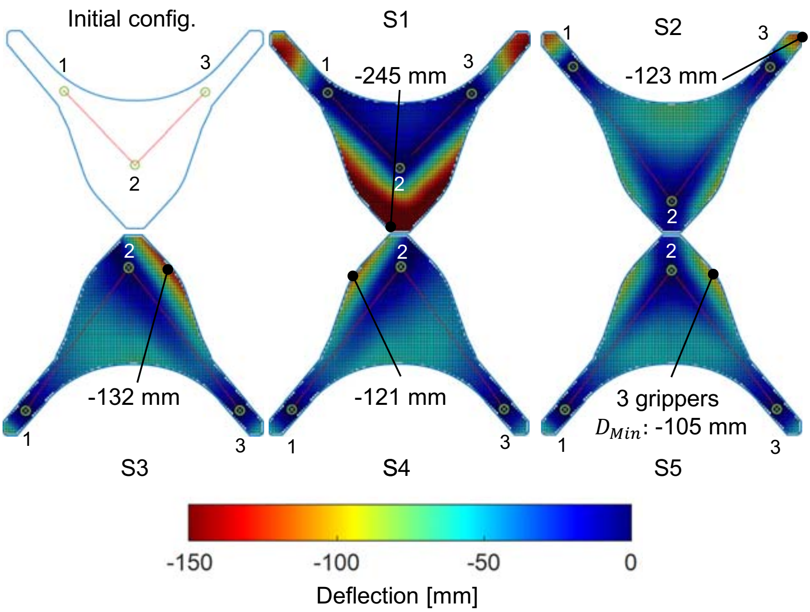

Figure 7-35: Adaptation of the gripper configuration for three grippers for part H003

S1 represents the first simulation of the initial gripper configuration. Black **x** symbols in each step indicate the points that meet the $D_{Z\_Threshold}$ criterion to which the grippers will respond. It should be noted that there are several simulations and adjustments between the different representations in Figure 7-35. A total of 39 adjustments and simulations were required to move from the initial gripper configuration to the result S5. First, between S1 and S2, the grippers spread in all directions. Gripper 2 in S2 is not positioned exactly in the middle, which means that the right side of the component is deflecting more. In S3, gripper 2 reacts to this deflection in S2 by moving there and creating a larger deflection on the other side. This shows a complexity with the part H003, even a slight non-symmetrical arrangement leads to a folding down of one of the edges. Nevertheless, after several adjustments of the step size, the algorithm finds a configuration with an equilibrium at both edges. After 39 adjustments and simulations, the maximum deflection in the negative Z direction is reduced to -105 mm.

Another difficult configuration is part H003 with four grippers (Figure 7-36). In the initial gripper configuration, the distribution of the grippers is already asymmetrical and too small distributed across the component.

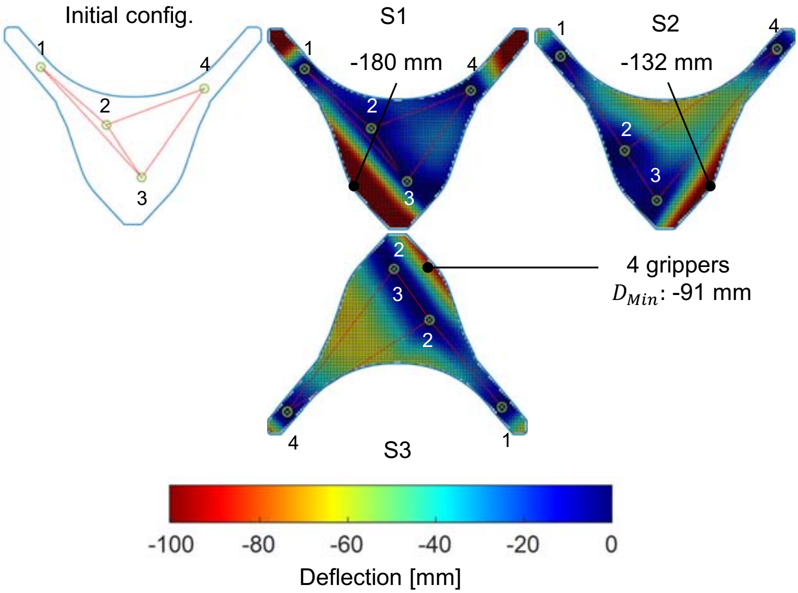

Figure 7-36: Adaptation of the gripper configuration for four grippers for part H003

Here too, the grippers are first distributed over the component from S1 to S2. In step S3 the configuration then comes to a stop. The configuration is very similar to the configuration before (Figure 7-35), only the gripper four was integrated between gripper 2 and 3, which corresponds to the internal logic. The additional gripper relative to Figure 7-35 reduces the deflection in the negative Z direction to -91 mm. The two lateral corners are still responsible for the major part of the deflection.

For the next configurations of H003, only the final results will be presented in Figure 7-37.

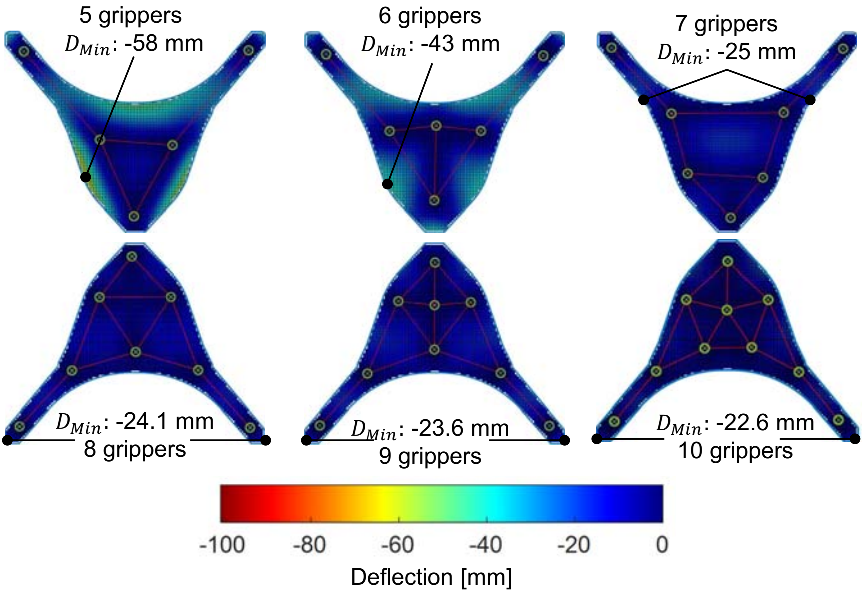

Figure 7-37: Adaptation of the gripper configuration for part H003 with different number of grippers

The arrangement of the grippers is reasonable. The gripper configuration with nine grippers the placement of the central gripper seems improvable. This gripper is stuck between two grippers. These two grippers deal with every critical deflection. Because of that the gripper in the middle does not move and stays at the same position. Furthermore, in the configuration eight, nine and ten grippers the largest negative deflections are always on the same spot and is not improving anymore. This is due to the fact that the gripper closest to these the largest negative deflections is held back by a large number of points with smaller deflections values. This effect was already explained and illustrated in Figure 7-34.

It is also important to mention that all improved gripper configurations are keeping the general shape of the initial gripper configuration. Every gripper in this configuration is adapting its position in order to reduce the deflection but there are no major shape changes relative to the initial gripper configuration in Figure 7-26. Therefore, the algorithm is optimizing the gripper configuration, but it is not clear if it is towards a global or local optimum. For a small number of grippers (five to eight) it is more or less obvious that the general arrangement of the grippers is the most efficient one. With an increasing number of grippers there are also more possibilities how this arrangement can be done.

Relative to H003 the remaining geometries do not have different ways to place the grippers. Because H003_1L, H003_2 and H003_3 have slim profiles grippers can just be arranged in one line (Figure 7-38). Here the algorithm is working towards a global optimum. How close the solution gets to the optimum is mainly depending on $D_{Z\_Threshold}$ as already described in chapter 7.2.1.

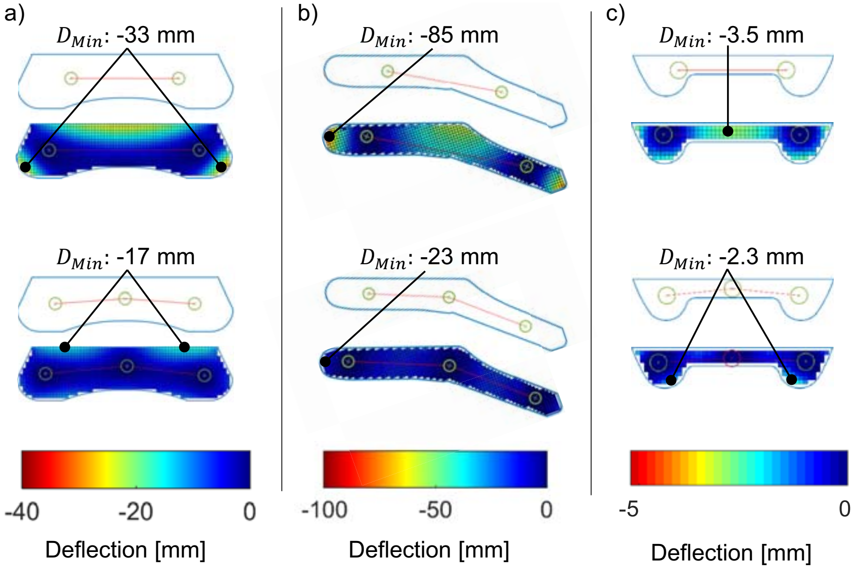

Figure 7-38: Adaptation of the gripper configuration for part H003_2 (a), H003_1L (b) and H003_3 (c) with different amount of grippers

Finally, the gripper configuration for the SMC material is displayed in Figure 7-39. The gripper arrangement for the IR001 part (Figure 7-39, a) performs well with -0.3 mm. Because of the cut-out in IR002 (Figure 7-39, b) the grippers are not placed like by IR001. This causes with -1.8 mm a slightly larger negative deflection. There is a light asymmetrical deflection for IR002 due to inaccuracies in the calculation. The color coding represents this circumstance more serious than it is, since the color of an element depends on the value of the lower left node.

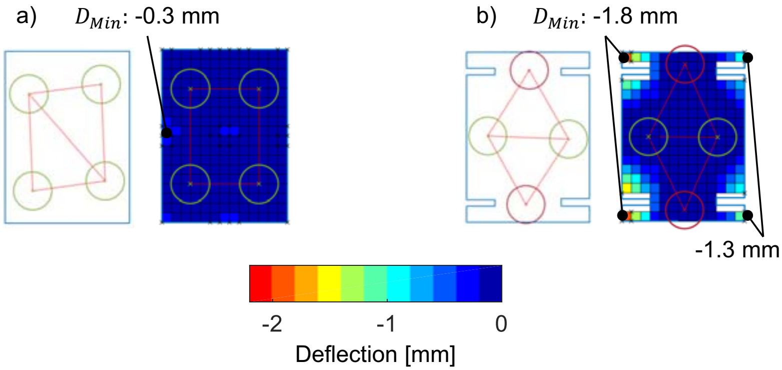

Figure 7-39: Adaptation of the gripper configuration for part IR001 (a) and IR002 (b) with four grippers

7.3.3 Conclusion for gripper configuration adjustment

The examples in 7.3.2 show that the gripper configurations can be considerably improved with the method presented. It should be noted, however, that the general shape of the gripper configuration does not change in this adjustment process. Also, the algorithm adjusts the gripper configuration towards a local optimum without reaching it. This effect was already explained and illustrated in Figure 7-34.

7.4 Number of grippers to maintain a user defined deflection

The implemented gripper configuration process is now able to place a defined number of grippers on an any shaped part and generate an initial gripper configuration by the algorithm in Figure 7-11. This initial gripper configurations then improved by the algorithm in Figure 7-30. How many grippers must be used in the initial gripper configuration to maintain a user defined amount of deflection depends on the geometry of the part and its material. This necessary number of grippers is therefore difficult to estimate at the beginning of the gripper configuration process.

In order to determine the necessary number of grippers, the procedure presented here start with the smallest possible number of two grippers. For these two grippers an initial gripper configuration is at first generated by the algorithm in Figure 7-11 and then improved by the algorithm in Figure 7-30. If the amount of deflection is not in the limits defined by the user, the whole procedure is repeated with an additional gripper.

8 Solution composition

The last steps in the generation of a finished handling solution are the combination of the different solutions into one and the implementation of these on the modular handling device from chapter 5.1. As already mentioned before the handling device should be able to transport the different parts one after another. Therefore, it must be possible to combine the gripper configurations in such a way the same grippers are used in as many gripper configurations as possible to minimize the total number of grippers.

8.1 Combination of solutions to one gripper configuration

For this process a master configuration is defined. This master configuration is the configuration containing the most grippers. An example of a set of different parts and their gripper configurations is shown in Figure 8-1.

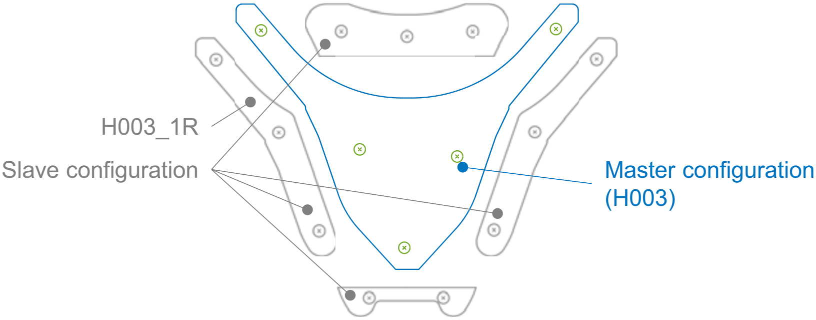

Figure 8-1: Master and slave configurations

Now the slave configurations will be aligned to the master configuration to find a compromise. The aim is to combine as many grippers as possible. The first step in this process is to find out how the master configuration could be matched with the individual slave configurations. However, for this task some boundary conditions must be defined.

The modular handling device is mounted on the end effector of the robot in such a way that its reach is not affected negatively. On the other hand, this limits the freedom of rotation over the cut layers. It is therefore assumed that the handling device always grips the parts from the same orientation. This means that the parts always remain in the same orientation relative to the handling device. Thus, only translations have to be carried out but no rotations.

The following considerations should be discussed using the example in Figure 8-1. In this example, part H003 with five grippers should be combined with part H003_1R with three grippers.

Accordingly, the first attempt is to fit the three grippers of the slave configuration to the master. For this it must be decided on which three grippers of the master configuration it should be fitted. It would not be a problem for a human to identify suitable grippers at a glance. However, since this process should also be programmable and automatable, the computing power is used to test all possible variations. For this purpose, all variations for three out of five are calculated for the grippers of the master. This results in ten different combination possibilities which now have to be tested. Figure 8-2 shows three of them.

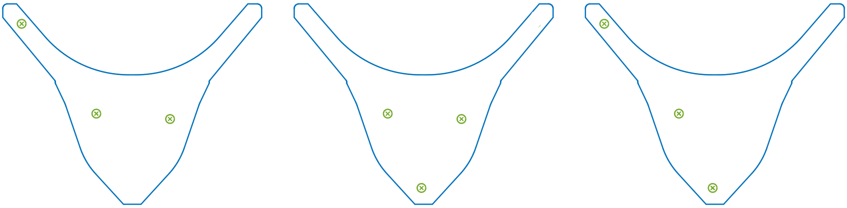

Figure 8-2: Three of ten different variation of the master configuration

The slave grippers must now be fitted to each of these possible variations. This fitting is done using vector quantization. Each gripper of the master configuration identifies the slave gripper that is closest and the slave gripper is then pulled towards this master gripper according to Equation 2-3. Likewise, all other grippers of the slave configuration are now moving in the same direction as well. All adjustments are done with the same vector. This action has the effect that the arrangement of the slave grippers, in regard to each other, does not change. The process is performed a defined number of iterations and then terminated. Then an error value is calculated based on the remaining distance between the closest slave and master gripper. Using this error, the different variations can be compared with each other.

This procedure is carried out for the ten possible variations for “H003 + H003_1R”, where the three variations shown in Figure 8-2 are presented with a fitted slave configuration in Figure 8-3 as an example. The best combination is the one with the smallest summarized distance between the gripper of the master and slave configuration. In Figure 8-2 the best combination is the one on the right side.

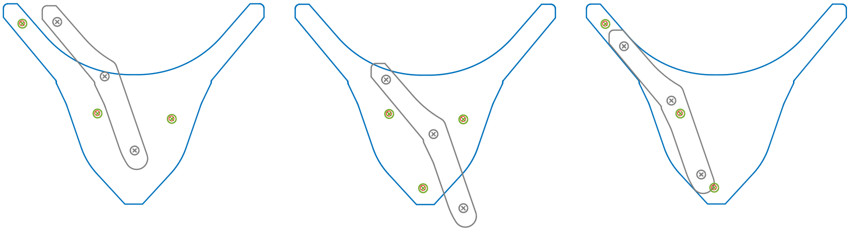

Figure 8-3: Three of the ten different variation of master configuration with a fitted slave configuration

Nonetheless, even with the best fitting, the grippers of the two configurations remain too far apart from each other. Therefore, the process has to be repeated, but this time only two grippers of the slave configuration are fitted to the master in order to achieve a better match. This is done by determining all variations two out of five in the master configuration and repeating the process the same way as before. The result of this is displayed in Figure 8-4 for H003_1L, H003_1R, H003_2 and H003_3 for H003. At the same time alternative gripper positions are generated by calculating the mean values between the nearest master and slave gripper.

The gripper configurations must now be combined. This combination process starts with a gripper configuration that requires only small adjustments. A gripper configuration is only considered as valid for a combination if the calculated alternative gripper position of each gripper in the configuration is less than half a gripper diameter away. In Figure 8-4 an evaluation of the different fittings has been made and highlighted by color.

The handling of configurations in which two or more grippers of master and slave do not fit together remains open until now. In such a situation, only one gripper in each configuration from master and slave can be brought together. It must therefore be decided which gripper is selected for this in each configuration. To decide this, the matching result of the slave part in question and the master with the most grippers is selected. In this situation, the largest number of grippers was tried to match, resulting in a very large overlap between the two parts.

Thus, the gripper of the slave configuration with the largest error is selected and fitted onto the master gripper, which has the smallest distance to it. This procedure ensures that the non-fitted grippers of the slave configuration are significantly away from the existing grippers of the master configuration. These grippers of the slave configuration must be integrated to the master configuration as new grippers and must not be located too close to existing grippers, otherwise implementation may become difficult or even impossible. The results of this method applied to all gripper configurations from Figure 8-1 is shown in Figure 8-4.

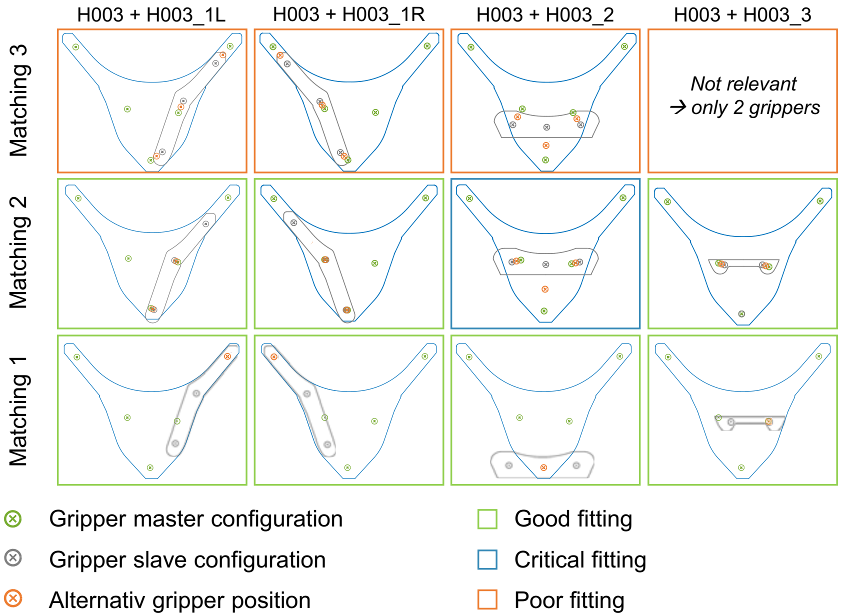
H003 + H003_1L
H003 + H003_1R
H003 + H003_2
H003 + H003_3
Matching 3
Matching 2
Matching 1
Not relevant
→ only 2 grippers
Gripper master configuration
Gripper slave configuration
Alternativ gripper position
Good fitting
Critical fitting
Poor fitting

Figure 8-4: Best fitting of H003 with different other gripper configurations using two and three grippers

The result with the smallest error between the master and slave configuration must now be selected from the matching in Figure 8-4. It is assumed that at least a smaller error than half a gripper diameter per gripper must be reached for a combination to make sense at all. First, the matching results with only one gripper from master and slave are ignored, since they can generally always be integrated and thus are uncritical.

In Figure 8-4 the best matching result is between “H003 + H003_1R” with two grippers (Matching 2 in Figure 8-4). The necessary adjustments between the two configurations are only a few millimeters and can be implemented almost without hesitation. The third gripper of the slave configuration has not been fitted and thus can be used as a new gripper. The advantage is that it is located on both H003 and H003_1R and can be used to transport both parts in the future. The new gripper configuration as a result of the combination is shown in Figure 8-5.

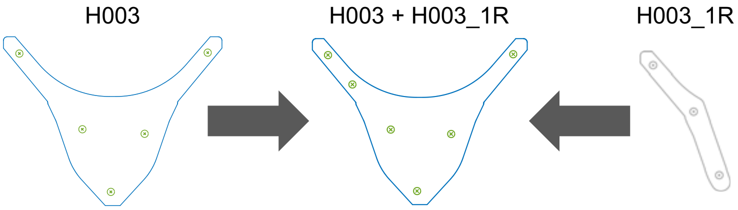

Figure 8-5: Combination of best match between H003 and H003_1R

The changes of both gripper configurations for the result in Figure 8-5 are very small and therefore it can hardly be assumed that the deflection will change significantly. Nevertheless, after each combination of gripper configurations, the deflection is simulative checked within a systematic process to determine whether a critical value is exceeded while creating the gripper configuration. This is not the case here.

The process is now repeated for the remaining slave configurations, but the new combination of "H003 + H003_1R" serves as new master configuration. One after another, the remaining slave gripper configurations are integrated by the same procedure. The last one is H003_2 since it has in every variation the largest error. Due to the various adjustments that the master configuration undergoes by integrating the other slave gripper configurations (H003_1L and H003_3), H003_2 can also be integrated into the gripper configuration with a minimum of error. Figure 8-6 shows the matching of H003_2 and the final master gripper configuration.

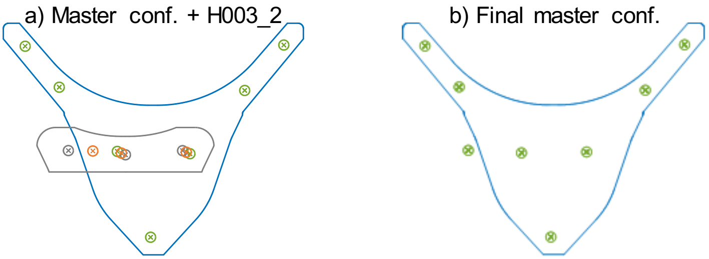
a) Master conf. + H003_2

b) Final master conf.

Figure 8-6: Last matching of master conf. (a) with H003_2
and the final master conf. (b)

8.2 Implementation on the modular handling device

With the procedure described in chapter 8.1 it is now possible to combine different gripper configurations with each other. These gripper configurations must now be implemented on the modular handling device from chapter 5.1. The modular handling device is divided in a basic frame element and an adjustable one (Figure 5-6).

How the gripper configuration can be implemented on the modular frame depends on the geometry and kinematic of the gripper module. In Figure 8-7 the geometry and kinematic of the gripper module is simplified by a two-dimensional representation.

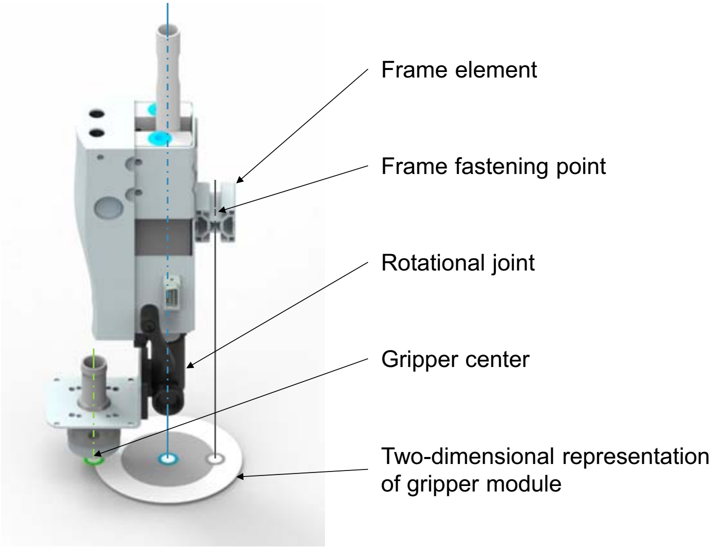

Figure 8-7: Two-dimensional representation of the gripper module

In Figure 8-8 (a) a gripper module is pictured from below together with the two-dimensional representation. The gripper module is fastened on the frame element. From this frame fastening point the rotational joint is 35 mm away. With the rotational joint the gripper center can be rotated freely in the plane. The radius of the rotation is 55 mm. With these dimensions in mind an arrangement element for the frame is designed (Figure 8-8, b). It has a square dimension of 180 mm x 180 mm. Because a gripper module has a maximum reach of 90 mm all points in this arrangement element could be reached. Since the gripper module can not only be placed in the center of every frame element, it is also possible to place the gripper center in the corner of the arrangement element.

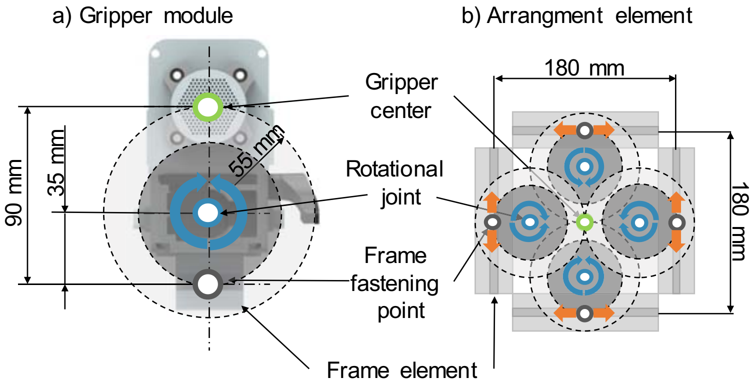
a) Gripper module
b) Arrangment element
90 mm
35 mm
55 mm
Gripper center
Rotational joint
Frame fastening point
Frame element
180 mm
180 mm

Figure 8-8: Geometry of a gripper module (a) and arrangement element (b)

The frame structure of the modular handling device is now divided into sections of these arrangement elements (Figure 8-9). An arrangement section is defined by the frame points on the edge, the ideal gripper point in the middle and the ideal fastening points in the middle of each frame element. Now the gripper configuration from Figure 8-6 can be implemented on the frame.

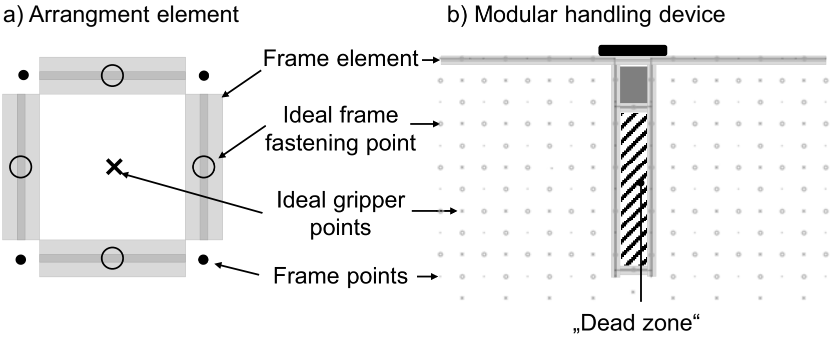
a) Arrangement element
b) Modular handling device
Frame element
Ideal frame fastening point
Ideal gripper points
Frame points
„Dead zone“

Figure 8-9: Arrangement element (a) and modular handling device divided into arrangement elements sections (b)

The modular handling device has hereby a “dead zone” in the middle of the structure. This is because an additional frame element in this area adds stiffness to structure and is therefore occupying this space (see Figure 5-6 for details).

A first alignment is done of frame and gripper configuration by aligning the X center of gripper arrangment and frame. The X center of the gripper arrangment is the mean value of all grippers in the arrangement. Likewise, all grippers of the gripper configuration are displaced in such a way that the smallest Y value in the gripper configuration is 90 mm. The result of this process is displayed in Figure 8-10.

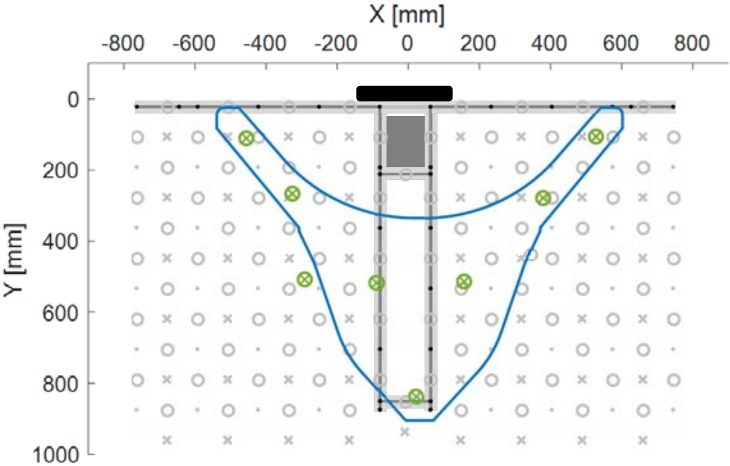

Figure 8-10: Result of a first alignment of gripper configuration and frame

The next step is fitting grippers of the gripper configuration to the ideal gripper positions of the modular handling device. For each gripper in the gripper configuration the distance to each ideal gripper spot is calculated. The gripper with the closest ideal gripper spot adjusts its own position first and also the position of every other gripper, by using Equation 2-3.

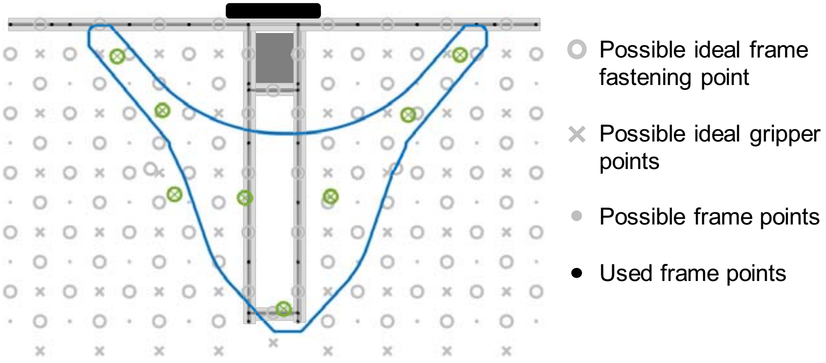
○ Possible ideal frame fastening point
× Possible ideal gripper points
● Possible frame points
● Used frame points

Figure 8-11: Result of the adjustment of the gripper position by fitting them to the closest ideal gripper spot of the handling device

In every iteration a gripper, as well as an ideal gripper spot, can just be selected once. This process is repeated for a defined number of iterations. For this example 100 iterations are used. Since every gripper is looking for the closest ideal gripper spot the adjustments made to the positioning of the grippers are rather small (adjustment for X: -3.2 mm, Y: 2.6 mm). Now it has to be decided on which frame element a gripper module should be fastened. Therefore, every gripper identifies the closest ideal frame fastening point (Figure 8-12).

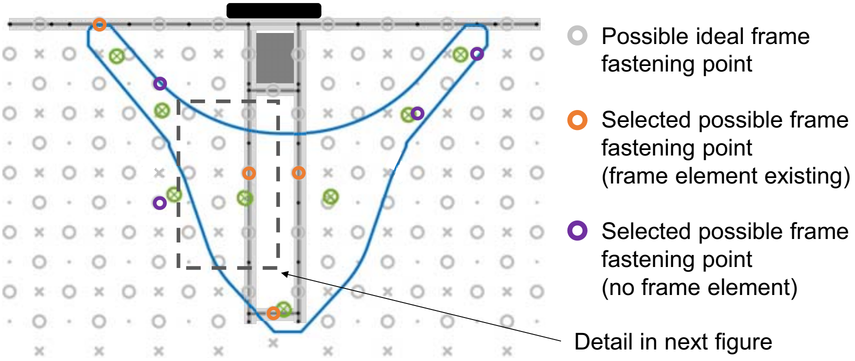
○ Possible ideal frame fastening point
○ Selected possible frame fastening point (frame element existing)
○ Selected possible frame fastening point (no frame element)
Detail in next figure

Figure 8-12: Grippers and the closest ideal frame fastening point

In this selection those must be preferred, which are already implemented by a frame element. In Figure 8-12 some of these selected frame fastening points have already existing frame elements and some do not. The ideal fastening point does not define the exact position of the gripper module, it just defines the frame element section on which the gripper module will be placed.

Figure 8-13 is a detail view of Figure 8-12. A gripper point should be implemented by installing a gripper module on the marked frame element section. The gripper position is known and so is the kinematic of the gripper module. The marked frame element section then represents the possible solution space for an inverse kinematic problem. By solving this, the fastening point is calculated.

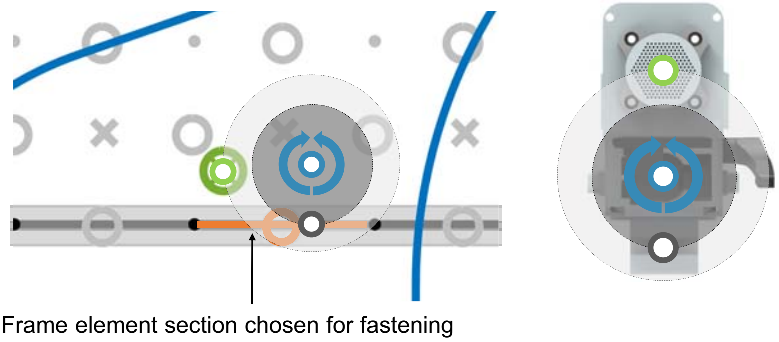

Figure 8-13: Installing of gripper module on the frame to implement a gripper point

When all gripper modules are placed that can be placed to the existing frame, new elements are added to the handling device which were not considered so far. These elements are diagonal stiffening frame elements which are necessary so that the far out hanging frame elements do not vibrate due to fast acceleration and deceleration in the handling process. These elements are added at the second last frame point of the frame elements (Figure 8-14). Since they are made out of the same aluminum profiles used for the rest of the frame, grippers can be fastened on them too (“New gripper position for module” in Figure 8-14). In this case one more gripper module can now be implemented. The remaining gripper point is slightly too far away from the new frame elements so it could not be implemented.

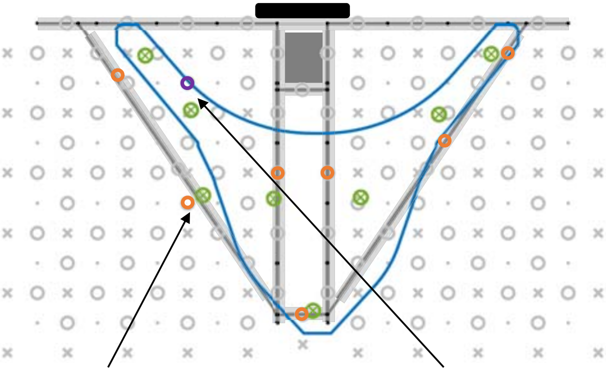

Figure 8-14: Adding diagonal stiffening frame elements to the handling device

The next step is adding additional new frame elements, so that the remaining not connected fastening point in Figure 8-14 can be connected to the handling device. This is done by searching the shortest way through the defined frame points until an already connected frame point is reached (Figure 8-15). In this process already installed grippers with their body dimensions have to be considered, because fastening points could be blocked.

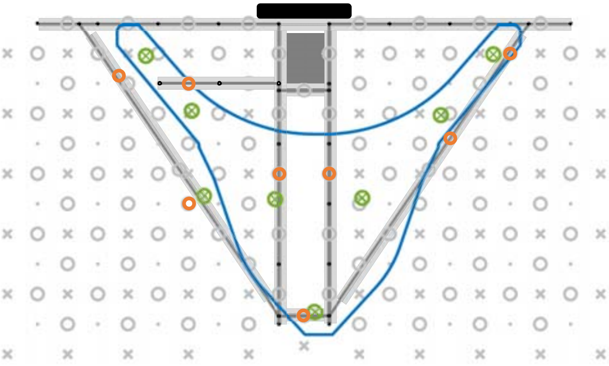

Figure 8-15: Installation of gripper modules on the modular handling device

This configuration was implemented on the modular handling device (Figure 8-16) to test the usability of the discussed systematic presented in this chapter. In addition, the reference objects are placed on the frame in Figure 8-16.

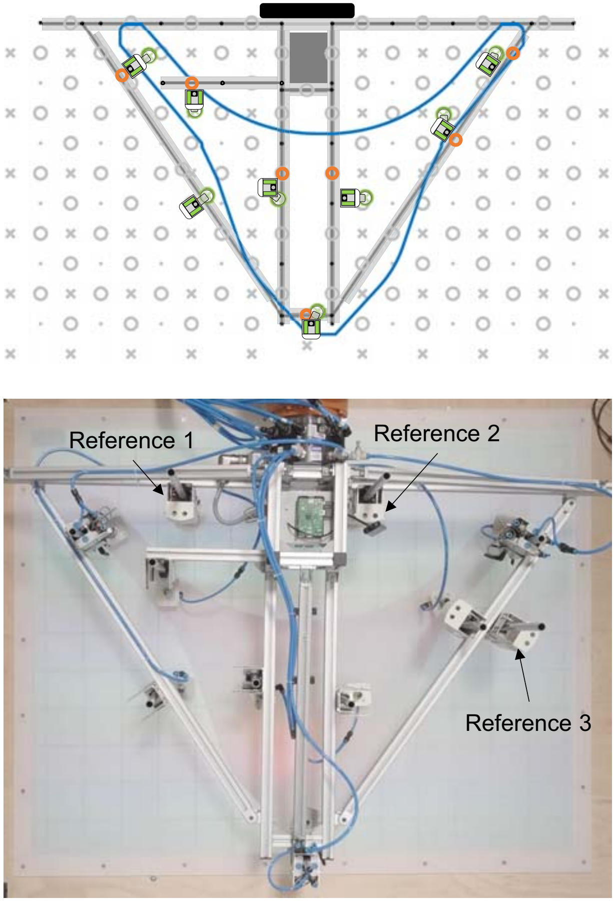
Reference 1
Reference 2
Reference 3

Figure 8-16: Implementation of the presented gripper configuration on the modular handling device

9 Summary and Outlook

9.1 Summary and conclusion

The automation of production processes is crucial for the economic production in high developing countries. Usually a product must go through several process steps which add value to the product by generating features. Such process steps are executed by different machines and could include an assembly step, milling, welding, heat treatment, painting and many more. An automated production on the other side also needs machines which link the different value-adding machines together.

This so-called handling process is often performed by industrial robots with a handling device on the TCP. The handling device can be realized with a wide range of different gripper technologies. Which gripper technology should be used, how much grippers are necessary and where the grippers should hold the object is mostly influenced by the geometry and properties of the object. The larger the object is and the lower the stiffness of the material used, the easier it can lead to deflections in the handling process. This is especially the case with flat objects like textiles, since they have only a small expansion in the thickness direction. As a result, the arrangement of the grippers on such an object is important to avoid unwanted deflections of the object which could lead to collisions with surrounding or folding edges.

The dimensioning of such a handling device can therefore become complicated and is often driven by human intuition. In such a situation human tend to add more grippers than necessary and the result is an oversized handling device. At the same time this increases the weight which causes the robot to consume more energy. Also, the handling device itself will need more energy to operate the grippers. Furthermore, it is not sure if the handling device will fulfill defined target conditions like a maximum amount of deflection of the handling part. If the same handling device should be able to handle different parts the design of the handling device becomes even more complicated. This thesis has therefore presented a systematic and also programmable approach to design handling devices which considers all these conditions. The result of this approach is a gripper arrangement on a modular handling device which is using a reduced number of grippers to fulfill the handling task of different shaped parts.

To achieve this at first a modular handling device was developed in chapter 5. The development was hereby based on the boundary conditions of the lightweight productions process using SMC and RTM. This handling device allows the free arrangement of gripper modules on a frame, to enable a wide range of different gripper arrangements. Also use-cases for the RTM and SMC process were defined to verify the next steps.

To consider the deflection of the part in the handling process a simulation model was implemented in chapter 6 which can interact with a design logic for the gripper arrangement. This design logic for the gripper arrangement is then working in four different steps.

The first step in the investigation for a systematic and programmable approach was to find a way to arrange grippers on a part considering only the shape. The general goal was to produce so-called initial gripper configurations. Various approaches were considered and evaluated for this purpose. The selected approach was based on the GNG algorithm. This algorithm enables to place a specific number of grippers on a randomly shaped part but tends to set grippers in cut-outs. This algorithm was then improved adding LOS checks so that no grippers are placed in cut-outs anymore. Also, since the GNG has a large number of parameters influencing the result of the gripper arrangement a systematic analysis of the GNG parameters and their influence on the result was performed.

The result of this investigation was a set of parameter values that were applied to different use-cases defined in in chapter 5. The algorithm can create gripper configurations for a wide set of different shapes and gripper numbers. Especially for a small number of grippers the algorithm sometimes tends not to distribute the grippers wide enough to cover the whole part with the initial gripper configuration.

The second step was the improvement of the initial gripper configuration considering the deflection. In this improvement step, each gripper represents a design degree of freedom, which makes the improvement task complex. Therefore, an iterative process of simulations and adaption steps was developed. The adaptation steps follow the rules of SOM and GNG using competitive learning, vector quantization and Hebbian learning. This process continues until a defined user-defined deflection value is reached or the arrangement cannot be further improved. With this process initial gripper configurations for different parts could be improved.

The examples with the use-cases from chapter 5 show that the gripper configurations can be considerably improved with the method presented. However, the general shape of the gripper configuration does not change in this adjustment process. Also, the algorithm adjusts the gripper configuration towards a local optimum without reaching it.

The third step was the development of a systematic method for the combination of different gripper arrangements to one final gripper arrangement. To achieve this an algorithm fits the different gripper configuration is such a way, that only small changes on each gripper configuration are necessary to combine them.

This method was tested with the defined RTM use-case. It was assumed that the components would always be picked up from the cutter table with the same orientation. Actually, the parts on the cutter table cannot be provided in any orientation, since the fiber orientation of the parts is important for the mechanical properties. For a plain weave fabric, however, changes in 90° steps are possible and for a UD fabric in 180° steps. This is not covered by the method so far.

The last and final step was the development of an implementation method for the final gripper arrangement on the modular handling device which was developed at the start of this thesis. Therefore, the modular handling device is divided into gripper arrangement elements. These gripper arrangement elements consider the dimensions and kinematic of the gripper modules which are fastened on the handling device frame. Every gripper arrangement element is defining ideal gripper points which can be fitted with the real gripping points of the final gripper arrangement. After this fitting the gripper module position on the frame can be calculated and the configuration process of the handling device is finished.

The planned gripper configuration was then implemented on the real handling device and worked well for the RTM use-case. However, it is conceivable that the algorithm could place grippers in the “dead zone” for other applications, so that a gripper configuration cannot be implemented. In the presented use-case this did not occur but cannot be excluded for any case.

In summary, a systematic and thus programmable method was developed and tested for each necessary sub step of the configuration of customized handling solutions on a modular handling device.

9.2 Outlook

The used simulation model in this thesis which predicts the deflection of the handling part is using a set of simplifications to describe the material behavior. These simplifications cause for larger deflections differences between reality and simulation. For this thesis these differences are not critical because deflections with a significant error are also indicate spots with such a large deflection that it is a general problem for the handling process. However, the interface between MATLAB and ABAQUS used in this thesis allows the adaption and extension of simulation models without problems, which is important for further developments. Also, the model calculates not the influence of the draft and was so far only tested for vertical accelerations. This aspect of draft could be improved by adding a CFD simulation. For all these simulative improvements, however, the relationship between effort and benefit must always be taken into account. Especially when the simulation is used iteratively like in chapter 7.3 it is important that a single simulation does not take hours to calculate. Most of the simulative calculation presented here need only a few minutes depending on the size of the part. Last but not least the simulation so far is based on a completely linear elastic material behavior. The measurements in Figure 6-3 have already shown that this is a simplification which cannot be accepted for higher accelerations. Accordingly, a further development of the model would make sense.

Another important aspect for the gripper arrangement is the gripping force. Already today the simulation model can predict the gripping force which is at least necessary to hold the part. What is missing is the relationship between the simulated necessary gripping forces and realizable gripping forces by the real low-pressure surface grippers. This relationship would then allow to adjust the gripping force at the low-pressure surface grippers in such a way that they would also consume only a minimum of energy. Also, the contact between the gripper and the part is modelled as a fixed interaction. Therefore, there is now shifting between the gripper and the part due to handling forces. But especially for lower gripping forces this could be an issue and should considered in further investigations. In addition, the systematic presented here could be extended to other grippers and materials. Larger adjustments would be necessary in the simulation but not in the general systematic.

The method shown here can create gripper configurations for various parts. However, the process can take up a large amount of time due to the necessary simulations. One main reason for this is that the number of necessary grippers is not estimated in advance. Up to now, the method starts with the lowest number of grippers (two) improves the gripper arrangement and increases the number of grippers if the improved gripper arrangement is not maintaining a user-defined deflection value. Here there is a great potential to save simulations by using a method Ito predetermine a rough guide value of necessary grippers. On the other side in each iteration step evaluable information is generated. The part shape, arrangement of the grippers and the material data are already available machine-readable. Together with the simulation results the arrangement of the grippers can be quantitatively evaluated. Thus, the method generates a large amount of rated data material with which other neural networks can be trained. Therefore, this method would then enable other neuronal networks to solve the problems described here even faster in the future.

So far, the systematic reduces the overall deflection of the gripped part. This is because the weight of a point defining the part depends on the deflection in the negative Z direction relatively to a target value zero. But not in every case deflection is unwanted. Especially for the draping process it could be interesting to deform the part already in the handling step. In further development it must be tested if the systematic can also find gripper arrangements for such a case by defining different target values for every spot of the part not equal to zero.

This work was part of the international research and training group “Integrated engineering of continuous discontinuous long fiber reinforced polymer structures” GRK 2078 presented within Kräger et al. (2015).

10 References

A_Abderrahman, A. (2017), *Machine Learning for the placement of Grippers on flat Parts*. Master thesis, KIT Karlsruhe Institute for Technology, Karlsruhe, wbk Institute of Production Science.

A_Dmytruk, T. (2017), *Verknüpfte Simulation flächiger textiler Halbzeuge mit Abaqus und MATLAB*. Master thesis, KIT Karlsruhe Institute for Technology, Karlsruhe, wbk Institute of Production Science.

A_Hörrmann, U. (2016), *3D-Scan basierte Parameterschätzung textiler Halbzeugeunter Anwendung der Finite-Elemente-Methode*. Master thesis, KIT Karlsruhe Institute for Technology, Karlsruhe, wbk Institute of Production Science.

A_Jenkel, S. (2016), *Optimierung einer Subpreform-Montagestation für den Automobilbau*. Master thesis, KIT Karlsruhe Institute for Technology, Karlsruhe, wbk Institute of Production Science.

A_Steinlein, M. (2017), *Entwicklung eines rekonfigurierbaren Greifsystems mit adaptiver Steuerung für die flexible Anwendung*. Master thesis, KIT Karlsruhe Institute for Technology, Karlsruhe, wbk Institute of Production Science.

Allen, R. C. (2017), 'Lessons from history for the future of work', *Nature*, vol. 550, no. 7676, pp. 321–324. DOI: 10.1038/550321a.

Angerer, A.; Ehinger, C.; Hoffmann, A.; Reif, W. & Reinhart, G. (2011), 'Design of an automation system for preforming processes in aerospace industries'. *2011 IEEE International Conference on Automation Science and Engineering,* pp. 557–562. ISBN: 978-1-4577-1732-1. DOI: 10.1109/CASE.2011.6042411.

Angerer, A.; Ehinger, C.; Hoffmann, A.; Reif, W.; Reinhart, G. & Strasser, G. (2010), 'Automated cutting and handling of carbon fiber fabrics in aerospace industries'. *2010 IEEE International Conference on Automation Science and Engineering,* pp. 861–866. ISBN: 978-1-4244-5447-1. DOI: 10.1109/COASE.2010.5584262.

Arnold, D. & Furmans, K. (2009), *Materialfluss in Logistiksystemen,* Springer-Verlag Berlin Heidelberg, Berlin, Heidelberg. ISBN: 978-3-642-01405-5.

Assmann, W. & Witten, E. (2013), *Handbuch Faserverbundkunststoffe/Composites,* Springer Fachmedien Wiesbaden, Wiesbaden. ISBN: 978-3-658-02754-4.

Balas, E. (1965), 'An additive algorithm for solving linear programs with zero-one variables', *Operations research*, vol. 13, no. 4, pp. 517–546. https://doi.org/10.1287/opre.13.4.517 [23.09.2018].

Bergmann, J.; Dörmann, H. & Lange, R. (2015), 'Interpreting process data of wet pressing process. Part 1. Theoretical approach', *Journal of Composite Materials*, vol. 50, no. 17, pp. 2399–2407. DOI: 10.1177/0021998315604728.

Biermann, D.; Hufenbach, W. & Seliger, G. (2008), *Serientaugliche Bearbeitung und Handhabung moderner faserverstärkter Hochleistungswerkstoffe*. *(sefawe) ; Untersuchung zum Forschungs- und Handlungsbedarf,* Progressmedia Verl. & Werbeagentur, Dresden. ISBN: 9783000262173.

Böger, T. (1997), *Beitrag zur Projektierung von Greifelementen für die Handhabung flächiger, biegeweicher Materialien*. Dissertation, Universität Dortmund, Dortmund, Lehrstuhls für Förder- und Lagerwesen.

Boisse, P.; Aimène, Y.; Dogui, A.; Dridi, S.; Gatouillat, S.; Hamila, N.; Aurangzeb Khan, M.; Mabrouki, T.; Morestin, F. & Vidal-Sallé, E. (2010), 'Hypoelastic, hyperelastic, discrete and semi-discrete approaches for textile composite reinforcement forming', *International Journal of Material Forming*, vol. 3, no. 2, pp. 1229–1240. DOI: 10.1007/s12289-009-0664-9.

Bruns, C.; Micke-Camuz, M.; Bohne, F. & Raatz, A. (unpubl. 2018), 'Process design and modelling methods for automated handling and draping strategies for composite components', *CIRP Annals*, vol. 67, no. 1, pp. 1–4. DOI: 10.1016/j.cirp.2018.04.014.

Bücheler, D. (2018), *Locally Continuous-fiber Reinforced Sheet Molding Compound*. Dissertation, KIT Karlsruhe Institute for Technology. DOI: 10.5445/IR/1000079163.

Castro, J. M. & Griffith, R. M. (1989), 'Sheet molding compound compression-molding flow', *Polymer Engineering & Science*, vol. 29, no. 10, pp. 632–638. DOI: 10.1002/pen.760291004.

Ceglarek, D.; Li, H. F. & Tang, Y. (2001), 'Modeling and Optimization of End Effector Layout for Handling Compliant Sheet Metal Parts', *Journal of Manufacturing Science and Engineering*, vol. 123, no. 3, p. 473. DOI: 10.1115/1.1366682.

Chemnitz, M.; Schreck, G. & Krüger, J. (2011), 'Analyzing energy consumption of industrial robots'. *ETFA2011,* pp. 1–4. DOI: 10.1109/ETFA.2011.6059221.

Chen, B. & Govindaraj, M. (1996), 'A Parametric Study of Fabric Drape', *Textile Research Journal*, vol. 66, no. 1, pp. 17–24. DOI: 10.1177/004051759606600103.

Chen, D.-L.; Chiu, T.-C.; Chen, T.-C.; Chung, M.-H.; Yang, P.-F. & Lai, Y.-S. (2014), 'Using DMA to Simultaneously Acquire Young's Relaxation Modulus and Time-dependent Poisson's Ratio of a Viscoelastic Material', *Procedia Engineering*, vol. 79, pp. 153–159. DOI: 10.1016/j.proeng.2014.06.324.

Chen, S.; Amid, D.; Shir, O. M.; Limonad, L.; Boaz, D.; Anaby-Tavor, A. & Schreck, T. (eds.) (2013), *Self-organizing maps for multi-objective pareto frontiers*. 2013 IEEE Pacific Visualization Symposium (PacificVis). ISBN: 2165-8765.

Cherif, C. (2011), *Textile Werkstoffe für den Leichtbau,* Springer Berlin Heidelberg, Berlin, Heidelberg. ISBN: 978-3-642-17991-4.

Cherif, C. (2016), *Textile Materials for Lightweight Constructions,* Springer Berlin Heidelberg, Berlin, Heidelberg. ISBN: 978-3-662-46340-6.

Christiano Silva, T. & Zhao, L. (2016), *Machine Learning in Complex Networks,* Springer International Publishing, Cham. ISBN: 978-3-319-17289-7.

Dickert, M. (2014), *Einfluss von Binder auf die Herstellung von Faserkunststoffverbunden*. Dissertation, Universität Clausthal-Zellerfeld, Clausthal-Zellerfeld.

Diebold, J. (1952), 'Automation. The advent of the automatic factory', *Institution of Production Engineers Journal*, vol. 32, no. 9, p. 415. DOI: 10.1049/ipej:19530056.

DIN 53362 (2003), *Prüfung von Kunststoff-Folien und von textilen Flächengebilden (außer Vliesstoffe), mit oder ohne Deckschicht aus Kunststoff*. *Bestimmung der Biegesteifigkeit ; Verfahren nach Cantilever ; DIN 53362 deutsche Norm,* Beuth, Berlin.

Dubbel, H. (2007), *Taschenbuch für den Maschinenbau*. *Mit Tabellen,* Springer, Berlin u.a. ISBN: 978-3-540-49714-1.

Ehinger, C. A. (2013), *Automatisierte Montage von Faserverbund-Vorformlingen*. Zugl.: München, Techn. Univ., Diss., 2012, Utz, München. ISBN: 978-3-8316-4233-5.

Fang, G. & Liang, J. (2011), 'A review of numerical modeling of three-dimensional braided textile composites', *Journal of Composite Materials*, vol. 45, no. 23, pp. 2415–2436. DOI: 10.1177/0021998311401093.

Fantoni, G.; Capiferri, S. & Tilli, J. (2014), 'Method for Supporting the Selection of Robot Grippers', *Procedia CIRP*, vol. 21, pp. 330–335. DOI: 10.1016/j.procir.2014.03.152.

Fantoni, G.; Santochi, M.; Dini, G.; Tracht, K.; Scholz-Reiter, B.; Fleischer, J.; Kristoffer Lien, T.; Seliger, G.; Reinhart, G.; Franke, J.; Nørgaard Hansen, H. & Verl, A. (2014), 'Grasping devices and methods in automated production processes', *CIRP Annals*, vol. 63, no. 2, pp. 679–701. DOI: 10.1016/j.cirp.2014.05.006.

Fette, M.; Hentschel, M.; Köhler, F.; Wulfsberg, J. & Herrmann, A. (2016), 'Automated and Cost-efficient Production of Hybrid Sheet Moulding Compound Aircraft Components', *Procedia Manufacturing*, vol. 6, pp. 132–139. http://www.sciencedirect.com/science/article/pii/S2351978916301536. DOI: 10.1016/j.promfg.2016.11.017.

Flixeder, S.; Glück, T. & Kugi, A. (2017), 'Force-based cooperative handling and lay-up of deformable materials. Mechatronic design, modeling, and control of a demonstrator', *Mechatronics*, vol. 47, pp. 246–261. DOI: 10.1016/j.mechatronics.2016.10.003.

Förster, F. (2016), *Geregeltes Handhabungssystem zum zuverlässigen und energieeffizienten Handling textiler Kohlenstofffaserzuschnitte*. Dissertation, KIT Karlsruhe Institute for Technology, Karlsruhe, wbk Institute for Production Science.

Förster, F.; Ballier, F.; Coutandin, S.; Defranceski, A. & Fleischer, J. (2017), 'Manufacturing of Textile Preforms with an Intelligent Draping and Gripping System', *Procedia CIRP*, vol. 66, pp. 39–44. DOI: 10.1016/j.procir.2017.03.370.

Friedrich, H. E. (2017), *Leichtbau in der Fahrzeugtechnik,* Springer Fachmedien Wiesbaden, Wiesbaden. ISBN: 978-3-658-12294-2.

Friedrich, K. (2016), 'Carbon fiber reinforced thermoplastic composites for future automotive applications' in *VIII International Conference on "Times of Polymers and Composites" - from aerospace to nanotechnology. Naples, Italy, 19-23 June 2016,* eds A. D'Amore, D. Acierno & L. Grassia, AIP Publishing, Melville, New York, Melville, New York, p. 20001. ISBN: 9780735413900. DOI: 10.1063/1.4949575.

Fritzke, B. (1994), 'Growing cell structures—A self-organizing network for unsupervised and supervised learning', *Neural Networks*, vol. 7, no. 9, pp. 1441–1460. DOI: 10.1016/0893-6080(94)90091-4.

Fritzke, B. (1995), 'A Growing Neural Gas Network Learns Topologies', vol. 7.

Fritzke, B. (1998), *Vektorbasierte neuronale Netze*. Zugl.: Erlangen-Nürnberg, Univ., Habil.-Schr., 1998, Shaker, Aachen. ISBN: 3826544587.

Gebauer, I.; Dörsch, C.; Thoben, K.-D. & Müller, D. H. , 'Automated Assembly of Fibre Preforms for Economical Production of High Performance Composite Parts' in *Proceedings of the ASME International Mechanical Engineering Congress,* pp. 17–23. DOI: 10.1115/IMECE2007-41820.

Gerngross, T. & Nieberl, D. (2016), 'Automated manufacturing of large, three-dimensional CFRP parts from dry textiles', *CEAS Aeronautical Journal*, vol. 7, no. 2, pp. 241–257. DOI: 10.1007/s13272-016-0184-5.

Glorieux, E. (2017), *Multi-Robot Motion Planning Optimisation for Handling Sheet Metal Parts*. Dissertatiom, University West, Trollhättan, Sweden, Department of Engineering Science.

Gutsche, C. (1993), *Beitrag zur automatisierten Montage technischer Textilien*. Zugl.: Berlin, Techn. Univ., Diss., 1992, Hanser, München. ISBN: 9783446174856.

Hamila, N.; Boisse, P.; Sabourin, F. & Brunet, M. (2009), 'A semi-discrete shell finite element for textile composite reinforcement forming simulation', *International Journal for Numerical Methods in Engineering*, vol. 79, no. 12, pp. 1443–1466. DOI: 10.1002/nme.2625.

Hebb, D. O. (1949), *The organization of behavior*. *A neuropsychological theory,* John Wiley & Sons, New York, London, Sydney. ISBN: 9780471367277.

Henning, F. & Moeller, E. (2011), *Handbuch Leichtbau*. *Methoden, Werkstoffe, Fertigung,* Hanser, München. ISBN: 978-3-446-42891-1.

Hesse, S. (2011), *Greifertechnik*. *Effektoren für Roboter und Automaten,* Hanser, München. ISBN: 9783446424227.

Hesse, S. (2016), *Grundlagen der Handhabungstechnik,* Hanser, Müchen. ISBN: 978-3446444324.

Hoffmann, H. & Kohnhäuser, M. (2002), 'Strategies to Optimize the Part Transport in Crossbar Transfer Presses', *CIRP Annals*, vol. 51, no. 1, pp. 27–32. http://www.sciencedirect.com/science/article/pii/S0007850607614589. DOI: 10.1016/S0007-8506(07)61458-9.

Hua-tie, K. (1987), 'Determination of the orientation of short glass fibers in sheet molding compound (SMC)', *Polymer Composites*, vol. 8, no. 2, pp. 82–93. DOI: 10.1002/pc.750080204.

Ishikawa, T.; Amaoka, K.; Masubuchi, Y.; Yamamoto, T.; Yamanaka, A.; Arai, M. & Takahashi, J. (2018), 'Overview of automotive structural composites technology developments in Japan', *Composites Science and Technology*, vol. 155, pp. 221–246. DOI: 10.1016/j.compscitech.2017.09.015.

Jodin, D. (1992), *Untersuchungen zur Handhabung von biegeweichen Flächenzuschnitten aus Leder mit pneumatischen Greifern*. Dissertation, Universität Dortmund, Dortmund, Förder- und Lagerwesen.

Kang, T. J. & Yu, W. R. (1995), 'Drape Simulation of Woven Fabric by Using the Finite-element Method', *Journal of the Textile Institute*, vol. 86, no. 4, pp. 635–648. DOI: 10.1080/00405009508659040.

Karakerezis, A.; Doulgeri, Z. & Petridis, V. (1994), 'A gripper for handling flat non-rigid materials' in *Automation and Robotics in Construction Xi,* ed D. A. Chamberlain, Elsevier, Oxford, pp. 593–601. ISBN: 978-0-444-82044-0. DOI: 10.1016/B978-0-444-82044-0.50082-5.

Kienzler, R. & Schröder, R. (2009), *Einführung in die Höhere Festigkeitslehre,* Springer Berlin, Berlin. ISBN: 9783540893257.

King, M. J.; Jearanaisilawong, P. & Socrate, S. (2005), 'A continuum constitutive model for the mechanical behavior of woven fabrics', *International Journal of Solids and Structures*, vol. 42, no. 13, pp. 3867–3896. DOI: 10.1016/j.ijsolstr.2004.10.030.

Klingele, J. (2014), *Produktorientierte Auswahl von Verfahren zur Vorfixierung textiler Preforms*. Dissertation, Shaker, Aachen. ISBN: 978-3-8440-2918-5.

Koch, S. F. (2017), *Ein Beitrag zur fertigungsgerechten intrinsischen Hybridisierung*. Dissertation, KIT Karlsruhe Institute for Technology, Karlsruhe, wbk Institue of production science.

Kohonen, T. (1982), 'Self-organized formation of topologically correct feature maps', *Biological Cybernetics*, vol. 43, no. 1, pp. 59–69. DOI: 10.1007/BF00337288.

Kohonen, T. (1990), 'The self-organizing map', *Proceedings of the IEEE*, vol. 78, no. 9, pp. 1464–1480. DOI: 10.1109/5.58325.

Kolluru, R.; Valavanis, K. P. & Hebert, T. M. (1998), 'Modeling, analysis, and performance evaluation of a robotic gripper system for limp material handling', *IEEE Transactions on Systems, Man, and Cybernetics, Part B (Cybernetics)*, vol. 28, no. 3, pp. 480–486. DOI: 10.1109/3477.678660.

Kolluru, R.; Valavanis, K. P.; Smith, S. S. & Tsourveloudis, N. (2000), 'Design fundamentals of a reconfigurable robotic gripper system', *IEEE Transactions on Systems, Man, and Cybernetics - Part A: Systems and Humans*, vol. 30, no. 2, pp. 181–187. DOI: 10.1109/3468.833099.

Körber, M. & Frommel, C. (2018), 'Sensor-Supported Gripper Surface for Optical Monitoring of Draping Processes' in *SAMPE Europe Conference & Exhibition 2017 Stuttgart. Stuttgart, Germany, 14-16 November 2017,* Curran Associates Inc, Red Hook, NY.

Körber, M.; Gänswürger, P. & Gerngross, T. (2014), *Endeffektor zur schonenden Drapierung von textilen Zuschnitten für Faserverbundbauteile,* Deutsche Gesellschaft für Luft- und Raumfahrt - Lilienthal-Oberth e.V, Bonn.

Kordi, M. T.; Husing, M. & Corves, B. (2007), 'Development of a multifunctional robot end- effector system for automated manufacture of textile preforms'. *2007 IEEE/ASME international conference on advanced intelligent mechatronics,* IEEE, pp. 1–6. ISBN: 978-1-4244-1263-1. DOI: 10.1109/AIM.2007.4412527.

Korte, B. & Vygen, J. (2012), *Kombinatorische Optimierung*. *Theorie und Algorithmen,* Springer Spektrum, Berlin. ISBN: 978-3-642-25400-0.

Kruse, R.; Borgelt, C.; Braune, C.; Mostaghim, S. & Steinbrecher, M. (2016), *Computational Intelligence*. *A Methodological Introduction,* Springer-Verlag, s.l. ISBN: 9781447172949.

Lammering, R.; Gabbert, U.; Sinapius, M.; Schuster, T. & Wierach, P. (2018), *Lamb-Wave Based Structural Health Monitoring in Polymer Composites,* Springer International Publishing; Imprint; Springer, Cham. ISBN: 9783319497150.

Lengsfeld, H.; Altstädt, V.; Wolff-Fabris, F. & Krämer, J. (2014), *Composite Technologien,* Carl Hanser Verlag GmbH & Co. KG, München. ISBN: 978-3-446-43300-7.

Leung, Y.-W. & Wang, Y. (2001), 'An orthogonal genetic algorithm with quantization for global numerical optimization', *IEEE Transactions on Evolutionary Computation*, vol. 5, no. 1, pp. 41–53. DOI: 10.1109/4235.910464.

Li, H. F.; Ceglarek, D. & Shi, J. (2002), 'A Dexterous Part-Holding Model for Handling Compliant Sheet Metal Parts', *Journal of Manufacturing Science and Engineering*, vol. 124, no. 1, p. 109. DOI: 10.1115/1.1406953.

Lien, T. & Davis, P. (2008), 'A novel gripper for limp materials based on lateral Coanda ejectors', *CIRP Annals*, vol. 57, no. 1, pp. 33–36. DOI: 10.1016/j.cirp.2008.03.119.

Lin, H.; Long, A. C.; Sherburn, M. & Clifford, M. J. (2008), 'Modelling of mechanical behaviour for woven fabrics under combined loading', *International Journal of Material Forming*, vol. 1, S1, pp. 899–902. DOI: 10.1007/s12289-008-0241-7.

Link, M. (2014), *Finite Elemente in der Statik und Dynamik,* Springer. ISBN: 9783658035563.

M. Kordi, M. Hüsing, B. Corves (2007), *Development of a Multifunctional Robot End-Effector System for Automated Manufacture of Textile Preforms*. *4 - 7 Sept. 2007, Zurich, Switzerland,* IEEE Service Center, Piscataway, NJ. ISBN: 9781424412631.

Magnaud, H. (2016), *Design For Success*. *A design & technology manual for SMC BMC Design for Success*, European Alliance for SMC/BMC. https://smcbmc-europe.org/design_for_success/rapport_design_for_success.pdf [08.07.2018].

Makhoul, J.; Roucos, S. & Gish, H. (1985), 'Vector quantization in speech coding', *Proceedings of the IEEE*, vol. 73, no. 11, pp. 1551–1588. DOI: 10.1109/PROC.1985.13340.

Mantriota, G. (2007), 'Optimal grasp of vacuum grippers with multiple suction cups', *Mechanism and Machine Theory*, vol. 42, no. 1, pp. 18–33. DOI: 10.1016/j.mechmachtheory.2006.02.007.

Marsh, P. (2012), *The new industrial revolution*. *Consumers, globalization and the end of mass production,* Yale University Press, New Haven. ISBN: 978-0-300-11777-6.

Martinetz, T. & Schulten, K. (1994), 'Topology representing networks', *Neural Networks*, vol. 7, no. 3, pp. 507–522. DOI: 10.1016/0893-6080(94)90109-0.

Martinetz, T. M.; Berkovich, S. G. & Schulten, K. J. (1993), '`Neural-gas' network for vector quantization and its application to time-series prediction', *IEEE Transactions on Neural Networks*, vol. 4, no. 4, pp. 558–569. DOI: 10.1109/72.238311.

Mohammad Dadkhah; Zhanyue Zhao; Nicholas Wettels & Matthew Spenko (2016), *A Self-Aligning Gripper Using an Electrostatic/Gecko-Like Adhesive,* IEEE, Piscataway, NJ. ISBN: 9781509037636.

Mohammed, A.; Schmidt, B.; Wang, L. & Gao, L. (2014), 'Minimizing Energy Consumption for Robot Arm Movement', *Procedia CIRP*, vol. 25, pp. 400–405. DOI: 10.1016/j.procir.2014.10.055.

Monkman, G. (2003), 'Electroadhesive microgrippers', *Industrial Robot: An International Journal*, vol. 30, no. 4, pp. 326–330. DOI: 10.1108/01439910310479595.

Monkman, G. J. (1995), 'Robot Grippers for Use With Fibrous Materials', *The International Journal of Robotics Research*, vol. 14, no. 2, pp. 144–151. DOI: 10.1177/027836499501400204.

Monkman, G. J. & Shimmin, C. (1991), 'Use if Permanently Pressure-sensitive Chemical Adhesives in Robot Gripping Devices', *International Journal of Clothing Science and Technology*, vol. 3, no. 2, pp. 6–11. DOI: 10.1108/eb002971.

Neitzel, M. (2014), *Handbuch Verbundwerkstoffe,* Carls Hanser Verlag, Müchen. ISBN: 978-3-446-43696-1.

Ochs, A. (2013), *Ultraschall-Strömungsgreifer für die Handhabung textiler Halbzeuge bei der automatisierten Fertigung von RTM-Bauteilen*. Dissertation, KIT Karlsruhe Institute for Technology, Karlsruhe, wbk Institute of Production Technology.

Paryanto; Brossog, M.; Kohl, J.; Merhof, J.; Spreng, S. & Franke, J. (2014), 'Energy Consumption and Dynamic Behavior Analysis of a Six-axis Industrial Robot in an Assembly System', *Procedia CIRP*, vol. 23, pp. 131–136. DOI: 10.1016/j.procir.2014.10.091.

Pham, D. T. & Yeo S. H. (1991), 'Strategies for gripper design and selection in robotic assembly', *International Journal of Production Research*, vol. 29, no. 2, pp. 303–316. DOI: 10.1080/00207549108930072.

Potter, K. (2002), 'Beyond the pin-jointed net. Maximising the deformability of aligned continuous fibre reinforcements', *Composites Part A: Applied Science and Manufacturing*, vol. 33, no. 5, pp. 677–686. DOI: 10.1016/S1359-835X(02)00014-3.

Prudent, Y. & Ennaji, A. (2005), 'An incremental growing neural gas learns topologies'. *Proceedings. 2005 IEEE International Joint Conference on Neural Networks, 2005,* IEEE, pp. 1211–1216. ISBN: 0-7803-9048-2. DOI: 10.1109/IJCNN.2005.1556026.

Rassõlkin, A.; Hõimoja, H. & Teemets, R. (2011), *Energy Saving Possibilities in the Industrial Robot IRB 1600 Control*. *1 - 3 June 2011, Tallinn, Estonia ; conference proceedings,* IEEE, Piscataway, NJ. ISBN: 9781424488070.

Reiff-Stephan, J. (2006), 'Greifer für biegeschlaffe Materialien', *A&D Kompendium 2005/2006*.

Reinhart, G. & Straßer, G. (2011), 'Flexible gripping technology for the automated handling of limp technical textiles in composites industry', *Production Engineering*, vol. 5, no. 3, pp. 301–306. https://doi.org/10.1007/s11740-011-0306-1. DOI: 10.1007/s11740-011-0306-1.

Reinhart, G.; Straβer, G. & Ehinger, C. (2009), 'Highly Flexible Automated Manufacturing of Composite Structures Consisting of Limp Carbon Fibre Textiles', *SAE International Journal of Aerospace*, vol. 2, no. 1, pp. 181–187. DOI: 10.4271/2009-01-3213.

Robertson, R.; Chu, T.-J.; Gerard, R.; Kim, J.-H.; Park, M.; Kim, H.-G. & Peterson, R. (2000), 'Three-dimensional fiber reinforcement shapes obtainable from flat, bidirectional fabrics without wrinkling or cutting. Part 1. A single four-sided pyramid', *Composites Part A: Applied Science and Manufacturing*, vol. 31, no. 7, pp. 703–715. DOI: 10.1016/S1359-835X(00)00013-0.

Rosenberg, P.; Chaudhari, R.; Karcher, M.; Henning, F. & Elsner, P. (2014), 'Investigating cavity pressure behavior in high-pressure RTM process variants', *AIP Conference Proceedings*, vol. 1593, no. 1, pp. 463–466. DOI: 10.1063/1.4873822.

Saadat, M. & Nan, P. (2002), 'Industrial applications of automatic manipulation of flexible materials', *Industrial Robot: An International Journal*, vol. 29, no. 5, pp. 434–442. DOI: 10.1108/01439910210440255.

Schmalz, J.; Giering, L.; Hölzle, M.; Huber, N. & Reinhart, G. (2016), 'Method for the Automated Dimensioning of Gripper Systems', *Procedia CIRP*, vol. 44, pp. 239–244. DOI: 10.1016/j.procir.2016.02.106.

Schmalz, J. & Reinhart, G. (2014), 'Automated Selection and Dimensioning of Gripper Systems', *Procedia CIRP*, vol. 23, pp. 212–216. DOI: 10.1016/j.procir.2014.10.080.

Seliger, G.; Gutsche, C. & Hsieh, L. H. (1992), 'Process Planning and Robotic Assembly System Design for Technical Textile Fabrics', *CIRP Annals*, vol. 41, no. 1, pp. 33–36. DOI: 10.1016/S0007-8506(07)61146-9.

Seliger, G.; Szimmat, F.; Niemeier, J. & Stephan, J. (2003), 'Automated Handling of Non-Rigid Parts', *CIRP Annals*, vol. 52, no. 1, pp. 21–24. DOI: 10.1016/S0007-8506(07)60521-6.

SGL Catalog (2016), *Textile Materials Made from Carbon, Glass, and Aramid Fibers*. https://www.sglgroup.com/cms/_common/downloads/products/product-groups/cm/textile-products/Textile_Materials_made_from_Carbon_Glass_Aramid_Fibers_e.pdf [23.09.2018].

Siebenpfeiffer, W. (2014), *Leichtbau-Technologien im Automobilbau*. *Werkstoffe - Fertigung - Konzepte,* Springer Fachmedien, Wiesbaden. ISBN: 978-3-658-04025-3.

Sirtautas, J.; Pickett, A. K. & Lépicier, P. (2013), 'A mesoscopic model for coupled drape-infusion simulation of biaxial Non-Crimp Fabric', *Composites Part B: Engineering*, vol. 47, pp. 48–57. DOI: 10.1016/j.compositesb.2012.09.088.

Stephan, J. (2001), *Beitrag zum Greifen von Textilien*. Dissertation, Technische Universität Berlin, Berlin, Institut für Werkzeugmaschinen und Fabrikbetrieb.

Stephens, M. P. & Meyers, F. E. (2013), *Manufacturing facilities design and material handling,* Purdue University Press, West Lafayette, Ind. http://site.ebrary.com/lib/alltitles/docDetail.action?docID=10714297. ISBN: 9781557536501.

Stewart, R. (2009), 'Carbon fibre composites poised for dramatic growth', *Reinforced Plastics*, vol. 53, no. 4, pp. 16–21. DOI: 10.1016/S0034-3617(09)70148-1.

Straßer, G. (2012), *Greiftechnologie für die automatisierte Handhabung von technischen Textilien in der Faserverbundfertigung*. Zugl.: München, Techn. Univ., Diss., 2011, Utz, München. ISBN: 9783831641611.

Stühm, K.; Tornow, A.; Schmitt, J.; Grunau, L.; Dietrich, F. & Dröder, K. (2014), 'A Novel Gripper for Battery Electrodes based on the Bernoulli-principle with Integrated Exhaust Air Compensation', *Procedia CIRP*, vol. 23, pp. 161–164. DOI: 10.1016/j.procir.2014.10.065.

Suhl, L. & Mellouli, T. (2013), *Optimierungssysteme*. *Modelle, Verfahren, Software, Anwendungen,* Springer Gabler, Berlin. http://dx.doi.org/10.1007/978-3-642-38937-5. ISBN: 978-3-642-38936-8.

Syerko, E.; Comas-Cardona, S. & Binetruy, C. (2012), 'Models of mechanical properties/behavior of dry fibrous materials at various scales in bending and tension. A review', *Composites Part A: Applied Science and Manufacturing*, vol. 43, no. 8, pp. 1365–1388. DOI: 10.1016/j.compositesa.2012.03.012.

Szimmat, F. (2007), *Beitrag zum Vereinzeln flächiger biegeschlaffer Bauteile*. Dissertation, Fraunhofer-IRB-Verl., Stuttgart. ISBN: 978-3-8167-7424-2.

Tai, K.; El-Sayed, A.-R.; Shahriari, M.; Biglarbegian, M. & Mahmud, S. (2016), 'State of the Art Robotic Grippers and Applications', *Robotics*, vol. 5, no. 2, p. 11. DOI: 10.3390/robotics5020011.

Uchiyama, T. & Arbib, M. A. (1994), 'Color image segmentation using competitive learning', *IEEE Transactions on Pattern Analysis and Machine Intelligence*, vol. 16, no. 12, pp. 1197–1206. DOI: 10.1109/34.387488.

VDI 2206 (2004), *Design methodology for mechatronic systems,* VDI-Verl., Düsseldorf.

Wagner, H. (2016), *Featurebasierte Technologieplanung zum Preforming von textilen Halbzeugen*. Dissertation, KIT Karlsruhe Institute for Technology, Karlsruhe, wbk Institute for production science.

Witten, E. & Schuster, A. , 'Der Composites-Markt Europa: Marktentwicklungen, Herausforderungen und Chancen'.

Wulfsberg, J.; Fette, M.; Schwake, K.; Neuhaus, F. & Brandt, M. (2015), 'Modular Lightweight Gripper System', *ZWF Zeitschrift für wirtschaftlichen Fabrikbetrieb*, vol. 110, 7-8, pp. 455–459. DOI: 10.3139/104.111375.

Zhang, Y.; Liu, G.; Fang, X. & Chen, B. (eds.) (2009), *Medial Axis Extraction Using Growing Neural Gas*. 2009 International Conference on Artificial Intelligence and Computational Intelligence.

Zhu, S. (2015), *An automated method for the layup of fiberglass fabric*. Dissertation, Iowa State University, Ames, Iowa.

Zoumponos, G. T. & Aspragathos, N. A. (2008), 'Fuzzy logic path planning for the robotic placement of fabrics on a work table', *Robotics and Computer-Integrated Manufacturing*, vol. 24, no. 2, pp. 174–186. DOI: 10.1016/j.rcim.2006.10.001.

List of figures

Figure 1-1: Example of an oversized (left) and a customized handling solution (right) 2

Figure 2-1: Own extended representation of force, information and energy flow based on Hesse (2011, p 16) 5

Figure 2-2: Co- and Dico-material in the demonstrator of GRK 2078 6

Figure 2-3: Structure of a plain weave fabric (a) and real fabric (b) 7

Figure 2-4: Structure of a sheet molding compound(a) and real material (b) 8

Figure 2-5: Functions of the VDI 2860 8

Figure 2-6: Example for competitive learning 11

Figure 2-7: Example of vector quantization 11

Figure 2-8: Example of Hebbian learning 12

Figure 2-9: Algorithm of GNG 15

Figure 2-10: Example of the GNG algorithm for two neurons and two input points 16

Figure 3-1: Layout of an automated RTM process chain 18

Figure 3-2: Layout of an automated SMC process chain 20

Figure 3-3: Different investigations in the field of handling devices according to Straßer (2012, pp 38–39) 27

Figure 4-1: Example of a customized handling device 36

Figure 4-2: Systematic for the design of handling device for lightweight production processes 37

Figure 4-3: Approach for the design of handling device in lightweight productions 39

Figure 5-1: Procedure of a handling test illustrated by VDI 2860 40

Figure 5-2: Design method of mechatronic systems by the V-model according to VDI 2206 (own representation) 41

Figure 5-3: Summary of parameters from the state of the art which have an impact on the design of a handling device 42

Figure 5-4: Three main components of the handling device 48

Figure 5-5: Concept for modular handling system 50

Figure 5-6: Basic frame structure and adjustable frame structure of the handling system 51

Figure 5-7: Mechanical elements of the gripper module 52

Figure 5-8: CCU to DCU communication and the control of the normal and proportional valves by the DCU in the gripper module (Own representation based on A_Steinlein (2017, p 53)) 53

Figure 5-9: GUI for gripper configuration 54

Figure 5-10: Final design for the handling device 55

Figure 5-11: Test setup to project the shape of the part and the gripper onto a surface 56

Figure 5-12: Complete setup for the handling tests 57

Figure 5-13: Test procedure of a handling test to measure the deflection 58

Figure 5-14: Two SMC sheets for the demonstrator of GRK 2078 60

Figure 5-15: Self-supporting rear diffusor in the automotive industry 61

Figure 6-1: Vertical movement of the robot with the modular handling device 63

Figure 6-2: Acceleration and velocity of a vertical handling process (T2 100 %) of KUKA KR180 63

Figure 6-3: Deflection of a rectangle part after different vertical movements 64

Figure 6-4: Schematic diagram of the test setup to measure the time behavior 65

Figure 6-5: Measurement of the deflection over time by camera 66

Figure 6-6: Deflection over time of three SMC specimens with a length of 10.5 mm 67

Figure 6-7: Deflection over time of four Sigratex C W160-PL1/1 textile specimens 67

Figure 6-8: Gripper configuration 1 and 2 69

Figure 6-9: Results of the sensitivity analysis (A_Hörrmann 2016, p 50) 70

Figure 6-10: Cut out of stripes from SMC roll with different directions 71

Figure 6-11: Maximum deflection of a Cantilever test of the SMC material in 0° and 90° direction (left) and resulting effect on a cut out triangle (right) 71

Figure 6-12: Test setup to measure the bending stiffness of fabrics an plastic materials defined by DIN 53362 73

Figure 6-13: Program structure for the simulation and comparison of simulation and scan data 77

Figure 6-14: Processing steps of deflection scans in MATLAB 79

Figure 6-15: Definition of the reference objects ($\boldsymbol{REF1}$, $\boldsymbol{REF2}$, $\boldsymbol{REF3}$) and the reference vector ($\boldsymbol{REFVector}$) in the experiment description 80

Figure 6-16: Result of a scan data clustering by the MATLAB function “clusterdata” 81

Figure 6-17: Matching of the scan data and the description of the experiment by aligning the $\boldsymbol{REFVector}$ and $\boldsymbol{REFCenter}$ 82

Figure 6-18: Example of the processing of scan or simulation data by interpolate data at the mesh grid points 83

Figure 6-19: Geometry RA001 83

Figure 6-20: Simulated deflection (a) and measured deflection (b) for three grippers on RA001 84

Figure 6-21: Simulated deflection (a) and measured deflection (b) for part H003 85

Figure 6-22: Simulated deflection (a) and measured deflection (b) for a triangle with different fiber orientations 87

Figure 6-23: Simulated deflection (a) and measured deflection (b) for part RA001S 88

Figure 7-1: Different approaches to generate an initial gripper configuration 90

Figure 7-2: Design diagram for the arrangement of grippers based on pre-simulated basic geometries 92

Figure 7-3: Arrangement of grippers on a part to achieve a maximum deflection of 30 mm 93

Figure 7-4: Deflection of an initial gripper configuration with a fiber orientation of 0° (a) and 30° (b) 94

Figure 7-5: Points defining the geometry of the part 95

Figure 7-6: Initial gripper configuration generated by using the GNG algorithm by Fritzke (1995) 97

Figure 7-7: A shape with inner cut-outs causing problems for GNG 98

Figure 7-8: Gripper configuration with higher weight of points defining the outer contour of the part 101

Figure 7-9: Gripper placed by standard GNG (a) and by implementing a line of sight (LOS) rule (b) 102

Figure 7-10: Connection of two grippers by standard GNG (a) and LOS rule (b) 102

Figure 7-11: Flowchart to create initial gripper configurations 105

Figure 7-12: Gripper surface represented by nine points 107

Figure 7-13: Variation of the parameters to investigate the influence of ϵb 108

Figure 7-14: Results for parameter setup in Figure 7-13 to investigate the influence of ϵb 109

Figure 7-15: Error of gripper configurations generated ϵb= 0.5 and ϵb= 0.005 (Number of iterations cut by 15) 110

Figure 7-16: Variation of the parameters to investigate the influence of $M\epsilon n$ 111

Figure 7-17: Error of gripper configurations generated $M\epsilon n$= 0 and $M\epsilon n$= 0.1 112

Figure 7-18: Error of gripper configurations generated by $PointWeight$ 113

Figure 7-19: Gripper configuration using only points on the edge of the part (a) and all points (b) 114

Figure 7-20: Variation of parameters to investigate the influence of $PointWeight$ 115

Figure 7-21: Test of the use of a final value ϵb_Final and $M\epsilon n\_Final$ 116

Figure 7-22: Final parameter setting of this chapter and influence of the T parameter 117

Figure 7-23: Adjustments to the algorithm relative to Figure 7-23 (marked blue) 118

Figure 7-24: Generated initial gripper configurations for part IR001 with a different number of grippers 119

Figure 7-25: Generated initial gripper configurations for part IR002 with a different number of grippers 119

Figure 7-26: Generated initial gripper configurations for part H003 with a different number of grippers 120

Figure 7-27: Generated initial gripper configurations for part H003_1L with a different number of grippers 121

Figure 7-28: Generated initial gripper configurations for part H003_2 and H003_3 with a different number of grippers 121

Figure 7-29: Geometry and generated initial gripper configurations for part RA001 with a different number of grippers 122

Figure 7-30: Flowchart for making adjustments to gripper configuration 126

Figure 7-31: Adjustment steps to an initial gripper configuration 128

Figure 7-32: Side view on the part in Figure 7-31 step four 128

Figure 7-33: Development of ϵb_FEM and deflection in Z-direction 129

Figure 7-34: Gripper arrangement with the use of $DZ\_Threshold$ (a) and without (b) 130

Figure 7-35: Adaptation of the gripper configuration for three grippers for part H003 131

Figure 7-36: Adaptation of the gripper configuration for four grippers for part H003 132

Figure 7-37: Adaptation of the gripper configuration for part H003 with different number of grippers 133

Figure 7-38: Adaptation of the gripper configuration for part H003_2 (a), H003_1L (b) and H003_3 (c) with different amount of grippers 134

Figure 7-39: Adaptation of the gripper configuration for part IR001 (a) and IR002 (b) with four grippers 135

Figure 8-1: Master and slave configurations 136

Figure 8-2: Three of ten different variation of the master configuration 137

Figure 8-3: Three of the ten different variation of master configuration with a fitted slave configuration 138

Figure 8-4: Best fitting of H003 with different other gripper configurations using two and three grippers 139

Figure 8-5: Combination of best match between H003 and H003_1R 140

Figure 8-6: Last matching of master conf. (a) with H003_2 and the final master conf. (b) 140

Figure 8-7: Two-dimensional representation of the gripper module 141

Figure 8-8: Geometry of a gripper module (a) and arrangement element (b) 142

Figure 8-9: Arrangement element (a) and modular handling device divided into arrangement elements sections (b) 142

Figure 8-10: Result of a first alignment of gripper configuration and frame 143

Figure 8-11: Result of the adjustment of the gripper position by fitting them to the closest ideal gripper spot of the handling device 144

Figure 8-12: Grippers and the closest ideal frame fastening point 144

Figure 8-13: Installing of gripper module on the frame to implement a gripper point 145

Figure 8-14: Adding diagonal stiffening frame elements to the handling device 146

Figure 8-15: Installation of gripper modules on the modular handling device 146

Figure 8-16: Implementation of the presented gripper configuration on the modular handling device 147

List of tables

Table 2-1: A small selection of function from VDI 2860 9

Table 3-1: Energy consumption of handling systems 26

Table 3-2: Evaluation of existing approaches 34

Table 5-1: Boundary conditions for the development of a modular handling device 47

Table 6-1: Measured vertical acceleration and calculated vertical velocity for different robot modes 64

Table 6-2: Measurement of bending stiffness of Sigratex C W160-PL1/1 (based on A_Hörrmann (2016, p 67)) 74

Table 6-3: Calculation of the elastic modulus for textile based on Equation 6-4 75

Table 6-4: Calculation of the elastic modulus for SMC based on Equation 6-4 76

Table 6-5: Deflection of P1 to P4 in Figure 6-20 85

Table 6-6: Deflection of P1 to P4 in Figure 6-21 86

Table 6-7: Deflection value for different points of a triangle with different fiber orientations 86

Table 6-8: Deflection of P1 to P4 in Figure 6-23 88

Table 7-1: Maximum length l for the different geometries and a maximum deflection of 30 mm 93

Table 7-2: Comparison of different derivates of SOM 96

Table 7-3: Parameter set for GNG to generate gripper arrangement in Figure 7-6 97

List of source code

Source text 5-1: JSON file describing an experiment 59

Source text 5-2: JSON file describing a gripper and a reference arrangement 59

Appendix

gng.m

```
function net = 
gng(PP,XinReal,params,ot,GNGDir,AppDir,HistoryOfConfig,Experiment,setting)

    TargetValue = params.TargetValue;

    %% Load Data
    XData = XinReal;
    XDataZmax = max(XData(:,3));
    XDataZmin = min(XData(:,3));

    nData = size(XData,1);
    nDim = size(XData,2);

    ShuffelSeed = randperm(nData);
    XData = XData(ShuffelSeed, :);

    if ot >= 2
        for i = 1:size(HistoryOfConfig,2)
            HistoryOfConfig(1).deflection = …
HistoryOfConfig(1).deflection(ShuffelSeed);
        end
    end

    %% Parameters
    GripperExisting = params.GripperExisting;
    ErrorCritAbort = params.ErrorCritAbort;
    N = params.N;
    MaxIt = params.MaxIt;
    E_Alternativ_Try = params.E_Alternativ_Try;
    epsilon_b = params.epsilon_b;
    epsilon_n = params.epsilon_n;
    epsilon_n_UR = epsilon_n;
    epsilon_b_UR = epsilon_b;
    params.epsilon_n_in_use = epsilon_n;
    params.epsilon_b_in_use = epsilon_b;
    PointWeight = params.PointWeight;
    alpha = params.alpha;
    delta = params.delta;
    T = params.T;
    GripperNextID = params.GripperNextID;
    AdjENatEnd = params.AdjENatEnd;
    AdjEBatEnd = params.AdjEBatEnd;

    %% Initialization
    Ni = size(GripperExisting,1);
    w = zeros(Ni, nDim+1);
    E = zeros(Ni,1);
    for i = 1:Ni
        w(i,:) = GripperExisting(i,:);
    end
    C = params.C;
    t = params.t;

    warning('off')
    poly = polyshape(PP);
    warning('on')
```

```
%% Loop
nx = 0;
ErrorCrit = inf;
TriggerReduceP = 0;

% Update weight
[XDataWeight,DifferenceSum] = weightData(XData,TargetValue,ot);

for it = 1:MaxIt
    TextInCommand = ['Iteration GNG: ' num2str(it) '\n'];
    fprintf(TextInCommand)
    tic

    E_Alternativ_Try = zeros(size(w,1),1);
    EReal = zeros(N,1);

    for l = 1:nData
        if XData(l,3)~= 0
            nx = nx + 1;
            x = XData(l,:);
            x(3) = 0;
            d = pdist2(x, w(:,1:3));
            [~, SortOrder] = sort(d);

            if setting.StandardGNG == false
                % Test of LineOfSight between X and all grippers
                i = 0;
                %Groersse = size(SortOrder,2)
                while i < size(SortOrder,2)
                    i = i + 1;

                    lineseg = [x(1) x(2);w(SortOrder(i),1) w(SortOrder(i),2)];

                    [in,out] = intersect(poly,lineseg);

                    if isempty(out)
                        % Nothing
                    else
                        SortOrder(i) = [];
                        i = i - 1;
                    end
                end
            end


            if size(SortOrder,2) >= 1
                s1 = SortOrder(1);


                if size(SortOrder,2) >= 2
                    s2 = SortOrder(2);
                end

                t = t + 1;

                % Adaptation
                Deflection = XDataWeight(l,3);
```

```
                    if ot < 2 % Normaly first round without sim results
                        epsilon_b_weight = epsilon_b/PointWeight * …
                                     d(s1)^2; %d(s1)*  UserValue * Distance *…
                                     Deflection(relativ to TargetValue)
                    else % With simulation results
                        epsilon_b_weight = epsilon_b/PointWeight * Deflection;
                    end

                    E_Alternativ_Try(s1) = E_Alternativ_Try(s1) + …
                                     ((epsilon_b_weight/epsilon_b));
                    E(s1) = E(s1) + d(s1).^2;

                    epsilon_b_result = epsilon_b_weight*(x-w(s1,1:3))/…
                                 norm((x-w(s1,1:3)));
                    w(s1,1:3) = w(s1,1:3) + epsilon_b_result;

                    if setting.StandardGNG == false && size(w,1) < N
                        Ns1 = find(C(s1,:)==1);
                        for j=Ns1
                            lineseg = [w(s1,1) w(s1,2); w(j,1) w(j,2)];
                            [in,out] = intersect(poly,lineseg);
                            if isempty(out)
                                DoN = 1;
                            else
                                DoN = 0;
                                w(s1,1:3) = w(s1,1:3) - epsilon_b_result;
                            end
                        end
                    else
                        DoN = 1;
                    end


                    if DoN == 1
                        Ns1 = find(C(s1,:)==1);
                        for j=Ns1
                             if ot <= 2
                                epsilon_n_weight = epsilon_n/PointWeight*…
                                                 d(j)^2;
                                epsilon_n_result = epsilon_n_weight*(x-w(j,1:3))…
                                                 /norm((x-w(j,1:3)));
                             else %
                                epsilon_n_weight = epsilon_n/PointWeight*…
                                                 Deflection;
                                epsilon_n_result = epsilon_n_weight*(x-w(j,1:3))…
                                                 /norm((x-w(j,1:3)));
                             end
                             w(j,1:3) = w(j,1:3) + epsilon_n_result;
                             lineseg = [w(s1,1) w(s1,2); w(j,1) w(j,2)];

                             if setting.StandardGNG == false
                                 [in,out] = intersect(poly,lineseg);
                                 if isempty(out)
                                    % Nothing
                                 else
                                    w(j,1:3) = w(j,1:3)  - epsilon_n_result;
                                 end
                             end
                        end
                        % Create Link
                        if size(SortOrder,2) >= 2
                           C(s1,s2) = 1;
                           C(s2,s1) = 1;
                           t(s1,s2) = 0;
                           t(s2,s1) = 0;
                        end


                        % Remove Links if to old
                        if size(w,1) >= 2
                            C(t>T) = 0;
                            t(t>T) = 0;
                            nNeighbor = sum(C);
                            AloneNodes = (nNeighbor==0);
                            C(AloneNodes, :) = [];
                            C(:, AloneNodes) = [];
                            t(AloneNodes, :) = [];
                            t(:, AloneNodes) = [];
                            w(AloneNodes, :) = [];
                            E_Alternativ_Try(AloneNodes) = [];
                            E(AloneNodes) = [];
                        end
                end
                else
                    % Nothing
                end
            end
        end


        % Add New Nodes
        if size(w,1) < N && ErrorCrit <= ErrorCritAbort
            [~, q] = max(E_Alternativ_Try);
            [~, f] = max(C(:,q).*E_Alternativ_Try);
            r = size(w,1) + 1;
            w(r,:) = (w(q,:) + w(f,:))/2;
            w(r,4) = GripperNextID;

            C(q,r) = 1;
            C(r,q) = 1;
            C(r,f) = 1;
            C(f,r) = 1;
            t(r,:) = 0;
            t(:, r) = 0;
            E_Alternativ_Try = zeros(size(w,1),1);
            ErrorCrit = inf;
            E(q) = alpha*E(q);
            E(f) = alpha*E(f);
            E(r) = E(q);
            GripperNextID = GripperNextID + 1;
        end

        % Decrease Errors
        E = delta*E;


        % Calc Error real
        for i = 1:nData
            x = XData(i,:);
            d = pdist2(x, w(:,1:3));
            [~, SortOrder] = sort(d);
            s1 = SortOrder(1);
            EReal(s1) = EReal(s1) + (d(s1)*XDataWeight(i,3));
        end


        % Calc Error crit
        EAlternativHistory(it) = sum(E_Alternativ_Try(:));
        EOriginalHistory(it) = sum(E(:));
        ERealHistory(it) = sum(EReal(:));
        params.ERealHistory = ERealHistory(it);

        if it > 3
            AverageErrorPast3 = (EAlternativHistory(it-3) + …
                              EAlternativHistory(it-2) + …
                              EAlternativHistory(it-1))/3;
            ErrorCrit = abs(abs(AverageErrorPast3) – …
                      abs(EAlternativHistory(it)));
        end

        if AdjENatEnd < 1 && ot < 2

            if ErrorCrit <= ErrorCritAbort && size(w,1) == N && …
                         epsilon_n ~= AdjENatEnd*epsilon_n_UR
                ErrorCrit = ErrorCritAbort + 1; % Prevent abort
                epsilon_b = AdjEBatEnd*epsilon_b;
                epsilon_n = AdjENatEnd*epsilon_n;
                params.epsilon_n_in_use = epsilon_n;
                params.epsilon_b_in_use = epsilon_b;
            end
        end

        if setting.PlotByStep == true | it == MaxIt | (size(w,1) == N && …
                              ErrorCrit <= ErrorCritAbort)
            close all
            if setting.PlotFlag == true
                figure('visible','on');
            else
                figure('visible','off');
            end

            State = 'GNG';

            plotResultsGNG(XinReal,XDataWeight,w,C,it,ot,Experiment,State,…
            params,setting);

            if setting.PrintFlag == 1
                cd(GNGDir)
                TimeSig = datestr(now,'ddmmyyyyHHMMSS');
                imgname = strcat(TimeSig,'.png');
                img = imgname;

                try
                 s=hgexport('readstyle',setting.PlotStyle);
                 fnam=img; % your file name
                 s.Format = 'png';
                 hgexport(gcf,fnam,s);
                 figname = strcat(TimeSig,'.fig');
                 savefig(figname);
                catch
                end
```

```
          end
          cd(AppDir)
        end

        TimeForIrreration(it) = toc;
        TextInCommand = ['--> Time for itteration needed: ' …
                      num2str(TimeForIrreration(it)) '\n'];
        fprintf(TextInCommand)
        ErrorCritProgress = 100*(ErrorCritAbort/ErrorCrit);
        if ErrorCritProgress >= 100
            ErrorCritProgress = 100;
        end
        TextInCommand = ['--> Epsilon B used: ' num2str(epsilon_b) '\n'];
        fprintf(TextInCommand)
        TextInCommand = ['--> Epsilon N used: ' num2str(epsilon_n) '\n'];
        fprintf(TextInCommand)
        TextInCommand = ['--> TargetValue used: ' num2str(TargetValue) '\n'];
        fprintf(TextInCommand)
        TextInCommand = ['--> ErrorCrit progress: ' …
                      num2str(ErrorCritProgress) '\n'];
        fprintf(TextInCommand)
        TextInCommand = ['--> Gripper: ' num2str(size(w,1)) '\n'];
        fprintf(TextInCommand)


        %% Export Results
        if ErrorCrit <= ErrorCritAbort && size(w,1) == N
            wg = w;
            net.w = wg;
            net.C = C;
            net.t = t;
            net.it = it;
            net.E_Alternativ_Try = E_Alternativ_Try;
            net.E = E;
            net.GripperNextID = GripperNextID;
            net.ERealHistory(:,1) = ERealHistory;
            net.EOriginalHistory(:,1)  = EOriginalHistory;
            net.EAlternativHistory(:,1) = EAlternativHistory;
            net.epsilon_b = epsilon_b;
            net.epsilon_n = epsilon_n;
            return
        end
    end


    %% Export Results
    wg = w;
    net.w = wg;
    net.C = C;
    net.t = t;
    net.it = it;
    net.E_Alternativ_Try = E_Alternativ_Try;
    net.E = E;
    net.GripperNextID = GripperNextID;
    net.ERealHistory(:,1) = ERealHistory;
    net.EOriginalHistory(:,1)  = EOriginalHistory;
    net.EAlternativHistory(:,1) = EAlternativHistory;
    net.epsilon_b = epsilon_b;
    net.epsilon_n = epsilon_n;
    return
end
```

Forschungsberichte aus dem wbk
Institut für Produktionstechnik
Karlsruher Institut für Technologie (KIT)

Bisher erschienene Bände:

Band 0
Dr.-Ing. Wu Hong-qi

Adaptive Volumenstromregelung mit Hilfe von drehzahlgeregelten Elektroantrieben

Band 1
Dr.-Ing. Heinrich Weiß

Fräsen mit Schneidkeramik - Verhalten des System Werkzeugmaschine-Werkzeug-Werkstück und Prozessanalyse

Band 2
Dr.-Ing. Hans-Jürgen Stierle

Entwicklung und Untersuchung hydrostatischer Lager für die Axialkolbenmaschine

Band 3
Dr.-Ing. Herbert Hörner

Untersuchung des Geräuschverhaltens druckgeregelter Axialkolbenpumpen

Band 4
Dr.-Ing. Rolf-Dieter Brückbauer

Digitale Drehzahlregelung unter der besonderen Berücksichtigung von Quantisierungseffekten

Band 5
Dr.-Ing. Gerhard Staiger

Graphisch interaktive NC-Programmierung von Drehteilen im Werkstattbereich

Band 6
Dr.-Ing. Karl Peters

Ein Beitrag zur Berechnung und Kompensation von Positionierfehlern an Industrierobotern

Band 7
Dr.-Ing. Paul Stauss

Automatisierte Inbetriebnahme und Sicherung der Zuverlässigkeit und Verfügbarkeit numerisch gesteuerter Fertigungseinrichtungen

Band 8
Dr.-Ing. Günter Möckesch

Konzeption und Realisierung eines strategischen, integrierten Gesamtplanungs- und -bearbeitungssystems zur Optimierung der Drehteilorganisation für auftragsbezogene Drehereien

Band 9
Dr.-Ing. Thomas Oestreicher

Rechnergestützte Projektierung von Steuerungen

Band 10
Dr.-Ing. Thomas Selinger

Teilautomatisierte werkstattnahe NC-Programmerstellung im Umfeld einer integrierten Informationsverarbeitung

Band 11
Dr.-Ing. Thomas Buchholz

Prozessmodell Fräsen, Rechnerunterstützte Analyse, Optimierung und Überwachung

Band 12
Dr.-Ing. Bernhard Reichling

Lasergestützte Positions- und Bahnvermessung von Industrierobotern

Band 13
Dr.-Ing. Hans-Jürgen Lesser

Rechnergestützte Methoden zur Auswahl anforderungsgerechter Verbindungselemente

Band 14
Dr.-Ing. Hans-Jürgen Lauffer

Einsatz von Prozessmodellen zur rechnerunterstützten Auslegung von Räumwerkzeugen

Band 15
Dr.-Ing. Michael C. Wilhelm

Rechnergestützte Prüfplanung im Informationsverbund moderner Produktionssysteme

Band 16
Dr.-Ing. Martin Ochs

Entwurf eines Programmsystems zur wissensbasierten Planung und Konfigurierung

Band 17
Dr.-Ing. Heinz-Joachim Schneider

Erhöhung der Verfügbarkeit von hochautomatisierten Produktionseinrichtungen mit Hilfe der Fertigungsleittechnik

Band 18
Dr.-Ing. Hans-Reiner Ludwig

Beanspruchungsanalyse der Werkzeugschneiden beim Stirnplanfräsen

Band 19
Dr.-Ing. Rudolf Wieser

Methoden zur rechnergestützten Konfigurierung von Fertigungsanlagen

Band 20
Dr.-Ing. Edgar Schmitt

Werkstattsteuerung bei wechselnder Auftragsstruktur

Band 21
Dr.-Ing. Wilhelm Enderle

Verfügbarkeitssteigerung automatisierter Montagesysteme durch selbsttätige Behebung prozessbedingter Störungen

Band 22
Dr.-Ing. Dieter Buchberger

Rechnergestützte Strukturplanung von Produktionssystemen

Band 23
Prof. Dr.-Ing. Jürgen Fleischer

Rechnerunterstützte Technologieplanung für die flexibel automatisierte Fertigung von Abkantteilen

Band 24
Dr.-Ing. Lukas Loeffler

Adaptierbare und adaptive Benutzerschnittstellen

Band 25
Dr.-Ing. Thomas Friedmann

Integration von Produktentwicklung und Montageplanung durch neue rechnergestützte Verfahren

Band 26
Dr.-Ing. Robert Zurrin

Variables Formhonen durch rechnergestützte Hornprozesssteuerung

Band 27
Dr.-Ing. Karl-Heinz Bergen

Langhub-Innenrundhonen von Grauguss und Stahl mit einem elektromechanischem Vorschubsystem

Band 28
Dr.-Ing. Andreas Liebisch

Einflüsse des Festwalzens auf die Eigenspannungsverteilung und die Dauerfestigkeit einsatzgehärteter Zahnräder

Band 29
Dr.-Ing. Rolf Ziegler

Auslegung und Optimierung schneller Servopumpen

Band 30
Dr.-Ing. Rainer Bartl

Datenmodellgestützte Wissensverarbeitung zur Diagnose und Informationsunterstützung in technischen Systemen

Band 31
Dr.-Ing. Ulrich Golz

Analyse, Modellbildung und Optimierung des Betriebsverhaltens von Kugelgewindetrieben

Band 32
Dr.-Ing. Stephan Timmermann

Automatisierung der Feinbearbeitung in der Fertigung von Hohlformwerkzeugen

Band 33
Dr.-Ing. Thomas Noe

Rechnergestützter Wissenserwerb zur Erstellung von Überwachungs- und Diagnoseexpertensystemen für hydraulische Anlagen

Band 34
Dr.-Ing. Ralf Lenschow

Rechnerintegrierte Erstellung und Verifikation von Steuerungsprogrammen als Komponente einer durchgängigen Planungsmethodik

Band 35
Dr.-Ing. Matthias Kallabis

Räumen gehärteter Werkstoffe mit kristallinen Hartstoffen

Band 36
Dr.-Ing. Heiner-Michael Honeck

Rückführung von Fertigungsdaten zur Unterstützung einer fertigungsgerechten Konstruktion

Band 37
Dr.-Ing. Manfred Rohr

Automatisierte Technologieplanung am Beispiel der Komplettbearbeitung auf Dreh-/Fräszellen

Band 38
Dr.-Ing. Martin Steuer

Entwicklung von Softwarewerkzeugen zur wissensbasierten Inbetriebnahme von komplexen Serienmaschinen

Band 39
Dr.-Ing. Siegfried Beichter

Rechnergestützte technische Problemlösung bei der Angebotserstellung von flexiblen Drehzellen

Band 40
Dr.-Ing. Thomas Steitz

Methodik zur marktorientierten Entwicklung von Werkzeugmaschinen mit Integration von funktionsbasierter Strukturierung und Kostenschätzung

Band 41
Dr.-Ing. Michael Richter

Wissensbasierte Projektierung elektrohydraulischer Regelungen

Band 42
Dr.-Ing. Roman Kuhn

Technologieplanungssystem Fräsen. Wissensbasierte Auswahl von Werkzeugen, Schneidkörpern und Schnittbedingungen für das Fertigingsverfahren Fräsen

Band 43
Dr.-Ing. Hubert Klein

Rechnerunterstützte Qualitätssicherung bei der Produktion von Bauteilen mit frei geformten Oberflächen

Band 44
Dr.-Ing. Christian Hoffmann

Konzeption und Realisierung eines fertigungsintegrierten Koordinatenmessgerätes

Band 45
Dr.-Ing. Volker Frey

Planung der Leittechnik für flexible Fertigungsanlagen

Band 46
Dr.-Ing. Achim Feller

Kalkulation in der Angebotsphase mit dem selbsttätig abgeleiteten Erfahrungswissen der Arbeitsplanung

Band 47
Dr.-Ing. Markus Klaiber

Produktivitätssteigerung durch rechnerunterstütztes Einfahren von NC-Programmen

Band 48
Dr.-Ing. Roland Minges

Verbesserung der Genauigkeit beim fünfachsigen Fräsen von Freiformflächen

Band 49
Dr.-Ing. Wolfgang Bernhart

Beitrag zur Bewertung von Montagevarianten: Rechnergestützte Hilfsmittel zur kostenorientierten, parallelen Entwicklung von Produkt und Montagesystem

Band 50
Dr.-Ing. Peter Ganghoff

Wissensbasierte Unterstützung der Planung technischer Systeme: Konzeption eines Planungswerkzeuges und exemplarische Anwendung im Bereich der Montagesystemplanung

Band 51
Dr.-Ing. Frank Maier

Rechnergestützte Prozessregelung beim flexiblen Gesenkbiegen durch Rückführung von Qualitätsinformationen

Band 52
Dr.-Ing. Frank Debus

Ansatz eines rechnerunterstützten Planungsmanagements für die Planung in verteilten Strukturen

Band 53
Dr.-Ing. Joachim Weinbrecht

Ein Verfahren zur zielorientierten Reaktion auf Planabweichungen in der Werkstattregelung

Band 54
Dr.-Ing. Gerd Herrmann

Reduzierung des Entwicklungsaufwandes für anwendungsspezifische Zellenrechnersoftware durch Rechnerunterstützung

Band 55
Dr.-Ing. Robert Wassmer

Verschleissentwicklung im tribologischen System Fräsen: Beiträge zur Methodik der Prozessmodellierung auf der Basis tribologisher Untersuchungen beim Fräsen

Band 56
Dr.-Ing. Peter Uebelhoer

Inprocess-Geometriemessung beim Honen

Band 57
Dr.-Ing. Hans-Joachim Schelberg

Objektorientierte Projektierung von SPS-Software

Band 58
Dr.-Ing. Klaus Boes

Integration der Qualitätsentwicklung in featurebasierte CAD/CAM-Prozessketten

Band 59
Dr.-Ing. Martin Schreiber

Wirtschaftliche Investitionsbewertung komplexer Produktionssysteme unter Berücksichtigung von Unsicherheit

Band 60
Dr.-Ing. Ralf Steuernagel

Offenes adaptives Engineering-Werkzeug zur automatisierten Erstellung von entscheidungsunterstützenden Informationssystemen

Band 62
Dr.-Ing. Uwe Schauer

Qualitätsorientierte Feinbearbeitung mit Industrierobotern: Regelungsansatz für die Freiformflächenfertigung des Werkzeug- und Formenbaus

Band 63
Dr.-Ing. Simone Loeper

Kennzahlengestütztes Beratungssystem zur Verbesserung der Logistikleistung in der Werkstattfertigung

Band 64
Dr.-Ing. Achim Raab

Räumen mit hartstoffbeschichteten HSS-Werkzeugen

Band 65,
Dr.-Ing. Jan Erik Burghardt

Unterstützung der NC-Verfahrenskette durch ein bearbeitungselementorientiertes, lernfähiges Technologieplanungssystem

Band 66
Dr.-Ing. Christian Tritsch

Flexible Demontage technischer Gebrauchsgüter: Ansatz zur Planung und (teil-)automatisierten Durchführung industireller Demontageprozesse

Band 67
Dr.-Ing. Oliver Eitrich

Prozessorientiertes Kostenmodell für die entwicklungsbegleitende Vorkalkulation

Band 68
Dr.-Ing. Oliver Wilke

Optimierte Antriebskonzepte für Räummaschinen - Potentiale zur Leistungssteigerung

Band 69
Dr.-Ing. Thilo Sieth

Rechnergestützte Modellierungsmethodik zerspantechnologischer Prozesse

Band 70
Dr.-Ing. Jan Linnenbuerger

Entwicklung neuer Verfahren zur automatisierten Erfassung der geometrischen Abweichungen an Linearachsen und Drehschwenkköpfen

Band 71
Dr.-Ing. Mathias Klimmek

Fraktionierung technischer Produkte mittels eines frei beweglichen Wasserstrahlwerkzeuges

Band 72
Dr.-Ing. Marko Hartel

Kennzahlenbasiertes Bewertungssystem zur Beurteilung der Demontage- und Recyclingeignung von Produkten

Band 73
Dr.-Ing. Jörg Schaupp

Wechselwirkung zwischen der Maschinen- und Hauptspindelantriebsdynamik und dem Zerspanprozess beim Fräsen

Band 74
Dr.-Ing. Bernhard Neisius

Konzeption und Realisierung eines experimentellen Telemanipulators für die Laparoskopie

Band 75
Dr.-Ing. Wolfgang Walter

Erfolgsversprechende Muster für betriebliche Ideenfindungsprozesse. Ein Beitrag zur Steigerung der Innovationsfähigkeit

Band 76
Dr.-Ing. Julian Weber

Ein Ansatz zur Bewertung von Entwicklungsergebnissen in virtuellen Szenarien

Band 77
Dr.-Ing. Dipl. Wirtsch.-Ing. Markus Posur

Unterstützung der Auftragsdurchsetzung in der Fertigung durch Kommunikation über mobile Rechner

Band 78
Dr.-Ing. Frank Fleissner

Prozessorientierte Prüfplanung auf Basis von Bearbeitungsobjekten für die Kleinserienfertigung am Beispiel der Bohr- und Fräsbearbeitung

Band 79
Dr.-Ing. Anton Haberkern

Leistungsfähigere Kugelgewindetriebe durch Beschichtung

Band 80
Dr.-Ing. Dominik Matt

Objektorientierte Prozess- und Strukturinnovation (OPUS)

Band 81
Dr.-Ing. Jürgen Andres

Robotersysteme für den Wohnungsbau: Beitrag zur Automatisierung des Mauerwerkabaus und der Elektroinstallation auf Baustellen

Band 82
Dr.-Ing. Dipl.Wirtschaftsing. Simone Riedmiller

Der Prozesskalender - Eine Methodik zur marktorientierten Entwicklung von Prozessen

Band 83
Dr.-Ing. Dietmar Tilch

Analyse der Geometrieparameter von Präzisionsgewinden auf der Basis einer Least-Squares-Estimation

Band 84
Dr.-Ing. Dipl.-Kfm. Oliver Stiefbold

Konzeption eines reaktionsschnellen Planungssystems für Logistikketten auf Basis von Software-Agenten

Band 85
Dr.-Ing. Ulrich Walter

Einfluss von Kühlschmierstoff auf den Zerspanprozess beim Fräsen: Beitrag zum Prozessverständniss auf Basis von zerspantechnischen Untersuchungen

Band 86
Dr.-Ing. Bernd Werner

Konzeption von teilautonomer Gruppenarbeit unter Berücksichtigung kultureller Einflüsse

Band 87
Dr.-Ing. Ulf Osmers

Projektieren Speicherprogrammierbarer Steuerungen mit Virtual Reality

Band 88
Dr.-Ing. Oliver Doerfel

Optimierung der Zerspantechnik beim Fertigungsverfahren Wälzstossen: Analyse des Potentials zur Trockenbearbeitung

Band 89
Dr.-Ing. Peter Baumgartner

Stufenmethode zur Schnittstellengestaltung in der internationalen Produktion

Band 90
Dr.-Ing. Dirk Vossmann

Wissensmanagement in der Produktentwicklung durch Qualitätsmethodenverbund und Qualitätsmethodenintegration

Band 91
Dr.-Ing. Martin Plass

Beitrag zur Optimierung des Honprozesses durch den Aufbau einer Honprozessregelung

Band 92
Dr.-Ing. Titus Konold

Optimierung der Fünfachsfräsbearbeitung durch eine kennzahlenunterstützte CAM-Umgebung

Band 93
Dr.-Ing. Jürgen Brath

Unterstützung der Produktionsplanung in der Halbleiterfertigung durch risikoberücksichtigende Betriebskennlinien

Band 94
Dr.-Ing. Dirk Geisinger

Ein Konzept zur marktorientierten Produktentwicklung

Band 95
Dr.-Ing. Marco Lanza

Entwurf der Systemunterstützung des verteilten Engineering mit Axiomatic Design

Band 96
Dr.-Ing. Volker Hüntrup

Untersuchungen zur Mikrostrukturierbarkeit von Stählen durch das Fertigungsverfahren Fräsen

Band 97
Dr.-Ing. Frank Reinboth

Interne Stützung zur Genauigkeitsverbesserung in der Inertialmesstechnik: Beitrag zur Senkung der Anforderungen an Inertialsensoren

Band 98
Dr.-Ing. Lutz Trender

Entwicklungsintegrierte Kalkulation von Produktlebenszykluskosten auf Basis der ressourcenorientierten Prozesskostenrechnung

Band 99
Dr.-Ing. Cornelia Kafka

Konzeption und Umsetzung eines Leitfadens zum industriellen Einsatz von Data-Mining

Band 100
Dr.-Ing. Gebhard Selinger

Rechnerunterstützung der informellen Kommunikation in verteilten Unternehmensstrukturen

Band 101
Dr.-Ing. Thomas Windmüller

Verbesserung bestehender Geschäftsprozesse durch eine mitarbeiterorientierte Informationsversorgung

Band 102
Dr.-Ing. Knud Lembke

Theoretische und experimentelle Untersuchung eines bistabilen elektrohydraulischen Linearantriebs

Band 103
Dr.-Ing. Ulrich Thies

Methode zur Unterstützung der variantengerechten Konstruktion von industriell eingesetzten Kleingeräten

Band 104
Dr.-Ing. Andreas Schmälzle

Bewertungssystem für die Generalüberholung von Montageanlagen –Ein Beitrag zur wirtschaftlichen Gestaltung geschlossener Facility- Managment-Systeme im Anlagenbau

Band 105
Dr.-Ing. Thorsten Frank

Vergleichende Untersuchungen schneller elektromechanischer Vorschubachsen mit Kugelgewindetrieb

Band 106
Dr.-Ing. Achim Agostini

Reihenfolgeplanung unter Berücksichtigung von Interaktionen: Beitrag zur ganzheitlichen Strukturierung und Verarbeitung von Interaktionen von Bearbeitungsobjekten

Band 107
Dr.-Ing. Thomas Barrho

Flexible, zeitfenstergesteuerte Auftragseinplanung in segmentierten Fertigungsstrukturen

Band 108
Dr.-Ing. Michael Scharer

Quality Gate-Ansatz mit integriertem Risikomanagement

Band 109
Dr.-Ing. Ulrich Suchy

Entwicklung und Untersuchung eines neuartigen Mischkopfes für das Wasser Abrasivstrahlschneiden

Band 110
Dr.-Ing. Sellal Mussa

Aktive Korrektur von Verlagerungsfehlern in Werkzeugmaschinen

Band 111
Dr.-Ing. Andreas Hühsam

Modellbildung und experimentelle Untersuchung des Wälzschälprozesses

Band 112
Dr.-Ing. Axel Plutowsky

Charakterisierung eines optischen Messsystems und den Bedingungen des Arbeitsraums einer Werkzeugmaschine

Band 113
Dr.-Ing. Robert Landwehr

Konsequent dezentralisierte Steuerung mit Industrial Ethernet und offenen Applikationsprotokollen

Band 114
Dr.-Ing. Christoph Dill

Turbulenzreaktionsprozesse

Band 115
Dr.-Ing. Michael Baumeister

Fabrikplanung im turbulenten Umfeld

Band 116
Dr.-Ing. Christoph Gönnheimer

Konzept zur Verbesserung der Elektromagnetischen Verträglichkeit (EMV) in Produktionssystemen durch intelligente Sensor/Aktor-Anbindung

Band 117
Dr.-Ing. Lutz Demuß

Ein Reifemodell für die Bewertung und Entwicklung von Dienstleistungsorganisationen: Das Service Management Maturity Modell (SMMM)

Band 118
Dr.-Ing. Jörg Söhner

Beitrag zur Simulation zerspanungstechnologischer Vorgänge mit Hilfe der Finite-Element-Methode

Band 119
Dr.-Ing. Judith Elsner

Informationsmanagement für mehrstufige Mikro-Fertigungsprozesse

Band 120
Dr.-Ing. Lijing Xie

Estimation Of Two-dimension Tool Wear Based On Finite Element Method

Band 121
Dr.-Ing. Ansgar Blessing

Geometrischer Entwurf mikromechatronischer Systeme

Band 122
Dr.-Ing. Rainer Ebner

Steigerung der Effizienz mehrachsiger Fräsprozesse durch neue Planungsmethoden mit hoher Benutzerunterstützung

Band 123
Dr.-Ing. Silja Klinkel

Multikriterielle Feinplanung in teilautonomen Produktionsbereichen – Ein Beitrag zur produkt- und prozessorientierten Planung und Steuerung

Band 124
Dr.-Ing. Wolfgang Neithardt

Methodik zur Simulation und Optimierung von Werkzeugmaschinen in der Konzept- und Entwurfsphase auf Basis der Mehrkörpersimulation

Band 125
Dr.-Ing. Andreas Mehr

Hartfeinbearbeitung von Verzahnungen mit kristallinen diamantbeschichteten Werkzeugen beim Fertigungsverfahren Wälzstoßen

Band 126
Dr.-Ing. Martin Gutmann

Entwicklung einer methodischen Vorgehensweise zur Diagnose von hydraulischen Produktionsmaschinen

Band 127
Dr.-Ing. Gisela Lanza

Simulative Anlaufunterstützung auf Basis der Qualitätsfähigkeiten von Produktionsprozessen

Band 128
Dr.-Ing. Ulf Dambacher

Kugelgewindetrieb mit hohem Druckwinkel

Band 129
Dr.-Ing. Carsten Buchholz

Systematische Konzeption und Aufbau einer automatisierten Produktionszelle für pulverspritzgegossene Mikrobauteile

Band 130
Dr.-Ing. Heiner Lang

Trocken-Räumen mit hohen Schnittgeschwindigkeiten

Band 131
Dr.-Ing. Daniel Nesges

Prognose operationeller Verfügbarkeiten von Werkzeugmaschinen unter Berücksichtigung von Serviceleistungen

Im Shaker Verlag erschienene Bände:

Band 132
Dr.-Ing. Andreas Bechle

Beitrag zur prozesssicheren Bearbeitung beim Hochleistungsfertigungsverfahren Wälzschälen

Band 133
Dr.-Ing. Markus Herm

Konfiguration globaler Wertschöpfungsnetzwerke auf Basis von Business Capabilities

Band 134
Dr.-Ing. Hanno Tritschler

Werkzeug- und Zerspanprozessoptimierung beim Hartfräsen von Mikrostrukturen in Stahl

Band 135
Dr.-Ing. Christian Munzinger

Adaptronische Strebe zur Steifigkeitssteigerung von Werkzeugmaschinen

Band 136
Dr.-Ing. Andreas Stepping

Fabrikplanung im Umfeld von Wertschöpfungsnetzwerken und ganzheitlichen Produktionssystemen

Band 137
Dr.-Ing. Martin Dyck

Beitrag zur Analyse thermische bedingter Werkstückdeformationen in Trockenbearbeitungsprozessen

Band 138
Dr.-Ing. Siegfried Schmalzried

Dreidimensionales optisches Messsystem für eine effizientere geometrische Maschinenbeurteilung

Band 139
Dr.-Ing. Marc Wawerla

Risikomanagement von Garantieleistungen

Band 140
Dr.-Ing. Ivesa Buchholz

Strategien zur Qualitätssicherung mikromechanischer Bauteile mittels multisensorieller Koordinatenmesstechnik

Band 141
Dr.-Ing. Jan Kotschenreuther

Empirische Erweiterung von Modellen der Makrozerspanung auf den Bereich der Mikrobearbeitung

Band 142
Dr.-Ing. Andreas Knödel

Adaptronische hydrostatische Drucktascheneinheit

Band 143
Dr.-Ing. Gregor Stengel

Fliegendes Abtrennen räumlich gekrümmter Strangpressprofile mittels Industrierobotern

Band 144
Dr.-Ing. Udo Weismann

Lebenszyklusorientiertes interorganisationelles Anlagencontrolling

Band 145
Dr.-Ing. Rüdiger Pabst

Mathematische Modellierung der Wärmestromdichte zur Simulation des thermischen Bauteilverhaltens bei der Trockenbearbeitung

Band 146
Dr.-Ing. Jan Wieser

Intelligente Instandhaltung zur Verfügbarkeitssteigerung von Werkzeugmaschinen

Band 147
Dr.-Ing. Sebastian Haupt

Effiziente und kostenoptimale Herstellung von Mikrostrukturen durch eine Verfahrenskombination von Bahnerosion und Laserablation

Band 148
Dr.-Ing. Matthias Schlipf

Statistische Prozessregelung von Fertigungs- und Messprozess zur Erreichung einer variabilitätsarmen Produktion mikromechanischer Bauteile

Band 149
Dr.-Ing. Jan Philipp Schmidt-Ewig

Methodische Erarbeitung und Umsetzung eines neuartigen Maschinenkonzeptes zur produktflexiblen Bearbeitung räumlich gekrümmter Strangpressprofile

Band 150
Dr.-Ing. Thomas Ender

Prognose von Personalbedarfen im Produktionsanlauf unter Berücksichtigung dynamischer Planungsgrößen

Band 151
Dr.-Ing. Kathrin Peter

Bewertung und Optimierung der Effektivität von Lean Methoden in der Kleinserienproduktion

Band 152
Dr.-Ing. Matthias Schopp

Sensorbasierte Zustandsdiagnose und -prognose von Kugelgewindetrieben

Band 153
Dr.-Ing. Martin Kipfmüller

Aufwandsoptimierte Simulation von Werkzeugmaschinen

Band 154
Dr.-Ing. Carsten Schmidt

Development of a database to consider multi wear mechanisms within chip forming simulation

Band 155
Dr.-Ing. Stephan Niggeschmidt

Ausfallgerechte Ersatzteilbereitstellung im Maschinen- und Anlagenbau mittels lastabhängiger Lebensdauerprognose

Band 156
Dr.-Ing. Jochen Conrad Peters

Bewertung des Einflusses von Formabweichungen in der Mikro-Koordinatenmesstechnik

Band 157
Dr.-Ing. Jörg Ude

Entscheidungsunterstützung für die Konfiguration globaler Wertschöpfungsnetzwerke

Band 158
Dr.-Ing. Stefan Weiler

Strategien zur wirtschaftlichen Gestaltung der globalen Beschaffung

Band 159
Dr.-Ing. Jan Rühl

Monetäre Flexibilitäts- und Risikobewertung

Band 160
Dr.-Ing. Daniel Ruch

Positions- und Konturerfassung räumlich gekrümmter Profile auf Basis bauteilimmanenter Markierungen

Band 161
Dr.-Ing. Manuel Tröndle

Flexible Zuführung von Mikrobauteilen mit piezoelektrischen Schwingförderern

Band 162
Dr.-Ing. Benjamin Viering

Mikroverzahnungsnormal

Band 163
Dr.-Ing. Chris Becke

Prozesskraftrichtungsangepasste Frässtrategien zur schädigungsarmen Bohrungsbearbeitung an faserverstärkten Kunststoffen

Band 164
Dr.-Ing. Patrick Werner

Dynamische Optimierung und Unsicherheitsbewertung der lastabhängigen präventiven Instandhaltung von Maschinenkomponenten

Band 165
Dr.-Ing. Martin Weis

Kompensation systematischer Fehler bei Werkzeugmaschinen durch self-sensing Aktoren

Band 166
Dr.-Ing. Markus Schneider

Kompensation von Konturabweichungen bei gerundeten Strangpressprofilen durch robotergestützte Führungswerkzeuge

Band 167
Dr.-Ing. Ester M. R. Ruprecht

Prozesskette zur Herstellung schichtbasierter Systeme mit integrierten Kavitäten

Band 168
Dr.-Ing. Alexander Broos

Simulationsgestützte Ermittlung der Komponentenbelastung für die Lebensdauerprognose an Werkzeugmaschinen

Band 169
Dr.-Ing. Frederik Zanger

Segmentspanbildung, Werkzeugverschleiß, Randschichtzustand und Bauteileigenschaften: Numerische Analysen zur Optimierung des Zerspanungsprozesses am Beispiel von Ti-6Al-4V

Band 170
Dr.-Ing. Benjamin Behmann

Servicefähigkeit

Band 171
Dr.-Ing. Annabel Gabriele Jondral

Simulationsgestützte Optimierung und Wirtschaftlichkeitsbewertung des Lean-Methodeneinsatzes

Band 172
Dr.-Ing. Christoph Ruhs

Automatisierte Prozessabfolge zur qualitätssicheren Herstellung von Kavitäten mittels Mikrobahnerosion

Band 173
Dr.-Ing. Steven Peters

Markoffsche Entscheidungsprozesse zur Kapazitäts- und Investitionsplanung von Produktionssystemen

Band 174
Dr.-Ing. Christoph Kühlewein

Untersuchung und Optimierung des Wälzschälverfahrens mit Hilfe von 3D-FEM-Simulation – 3D-FEM Kinematik- und Spanbildungssimulation

Band 175
Dr.-Ing. Adam-Mwanga Dieckmann

Auslegung und Fertigungsprozessgestaltung sintergefügter Verbindungen für µMIM-Bauteile

Band 176
Dr.-Ing. Heiko Hennrich

Aufbau eines kombinierten belastungs- und zustandsorientierten Diagnose- und Prognosesystems für Kugelgewindetriebe

Band 177
Dr.-Ing. Stefan Herder

Piezoelektrischer Self-Sensing-Aktor zur Vorspannungsregelung in adaptronischen Kugelgewindetrieben

Band 178
Dr.-Ing. Alexander Ochs

Ultraschall-Strömungsgreifer für die Handhabung textiler Halbzeuge bei der automatisierten Fertigung von RTM-Bauteilen

Band 179
Dr.-Ing. Jürgen Michna

Numerische und experimentelle Untersuchung zerspanungsbedingter Gefügeumwandlungen und Modellierung des thermo-mechanischen Lastkollektivs beim Bohren von 42CrMo4

Band 180
Dr.-Ing. Jörg Elser

Vorrichtungsfreie räumliche Anordnung von Fügepartnern auf Basis von Bauteilmarkierungen

Band 181
Dr.-Ing. Katharina Klimscha

Einfluss des Fügespalts auf die erreichbare Verbindungsqualität beim Sinterfügen

Band 182
Dr.-Ing. Patricia Weber

Steigerung der Prozesswiederholbarkeit mittels Analyse akustischer Emissionen bei der Mikrolaserablation mit UV-Pikosekundenlasern

Band 183
Dr.-Ing. Jochen Schädel

Automatisiertes Fügen von Tragprofilen mittels Faserwickeln

Band 184
Dr.-Ing. Martin Krauße

Aufwandsoptimierte Simulation von Produktionsanlagen durch Vergrößerung der Geltungsbereiche von Teilmodellen

Band 185
Dr.-Ing. Raphael Moser

Strategische Planung globaler Produktionsnetzwerke
Bestimmung von Wandlungsbedarf und Wandlungszeitpunkt mittels multikriterieller Optimierung

Band 186
Dr.-Ing. Martin Otter

Methode zur Kompensation fertigungsbedingter Gestaltabweichungen für die Montage von Aluminium Space-Frame-Strukturen

Band 187
Dr.-Ing. Urs Leberle

Produktive und flexible Gleitförderung kleiner Bauteile auf phasenflexiblen Schwingförderern mit piezoelektrischen 2D-Antriebselementen

Band 188
Dr.-Ing. Johannes Book

Modellierung und Bewertung von Qualitätsmanagementstrategien in globalen Wertschöpfungsnetzwerken

Band 189
Dr.-Ing. Florian Ambrosy

Optimierung von Zerspanungsprozessen zur prozesssicheren Fertigung nanokristalliner Randschichten am Beispiel von 42CrMo4

Band 190
Dr.-Ing. Adrian Kölmel

Integrierte Messtechnik für Prozessketten unreifer Technologien am Beispiel der Batterieproduktion für Elektrofahrzeuge

Band 191
Dr.-Ing. Henning Wagner

Featurebasierte Technologieplanung zum Preforming von textilen Halbzeugen

Band 192
Dr.-Ing. Johannes Gebhardt

Strukturoptimierung von in FVK eingebetteten metallischen Lasteinleitungselementen

Band 193
Dr.-Ing. Jörg Bauer

Hochintegriertes hydraulisches Vorschubsystem für die Bearbeitung kleiner Werkstücke mit hohen Fertigungsanforderungen

Band 194
Dr.-Ing. Nicole Stricker

Robustheit verketteter Produktionssysteme
Robustheitsevaluation und Selektion des Kennzahlensystems der Robustheit

Band 195
Dr.-Ing. Anna Sauer

Konfiguration von Montagelinien unreifer Produkttechnologien am Beispiel der Batteriemontage für Elektrofahrzeuge

Band 196
Dr.-Ing. Florian Sell-Le Blanc

Prozessmodell für das Linearwickeln unrunder Zahnspulen
Ein Beitrag zur orthozyklischen Spulenwickeltechnik

Band 197
Dr.-Ing. Frederic Förster

Geregeltes Handhabungssystem zum zuverlässigen und energieeffizienten Handling textiler Kohlenstofffaserzuschnitte

Band 198
Dr.-Ing. Nikolay Boev

Numerische Beschreibung von Wechselwirkungen zwischen Zerspanprozess und Maschine am Beispiel Räumen

Band 199
Dr.-Ing. Sebastian Greinacher

Simulationsgestützte Mehrzieloptimierung schlanker und ressourceneffizienter Produktionssysteme

Band 200
Dr.-Ing. Benjamin Häfner

Lebensdauerprognose in Abhängigkeit der Fertigungsabweichungen bei Mikroverzahnungen

Band 201
Dr.-Ing. Stefan Klotz

Dynamische Parameteranpassung bei der Bohrungsherstellung in faserverstärkten Kunststoffen unter zusätzlicher Berücksichtigung der Einspannsituation

Band 202
Dr.-Ing. Johannes Stoll

Bewertung konkurrierender Fertigungsfolgen mittels Kostensimulation und stochastischer Mehrzieloptimierung
Anwendung am Beispiel der Blechpaketfertigung für automobile Elektromotoren

Band 203
Dr.-Ing. Simon-Frederik Koch

Fügen von Metall-Faserverbund-Hybridwellen im Schleuderverfahren
ein Beitrag zur fertigungsgerechten intrinsischen Hybridisierung

Band 204
Dr.-Ing. Julius Ficht

Numerische Untersuchung der Eigenspannungsentwicklung für sequenzielle Zerspanungsprozesse

Band 205
Dr.-Ing. Manuel Baumeister

Automatisierte Fertigung von Einzelblattstapeln in der Lithium-Ionen-Zellproduktion

Band 206
Dr.-Ing. Daniel Bertsch

Optimierung der Werkzeug- und Prozessauslegung für das Wälzschälen von Innenverzahnungen

Band 207
Dr.-Ing. Kyle James Kippenbrock

Deconvolution of Industrial Measurement and Manufacturing Processes for Improved Process Capability Assessments

Band 208
Dr.-Ing. Farboud Bejnoud

Experimentelle Prozesskettenbetrachtung für Räumbauteile am Beispiel einer einsatzgehärteten PKW-Schiebemuffe

Band 209
Dr.-Ing. Steffen Dosch

Herstellungsübergreifende Informationsübertragung zur effizienten Produktion von Werkzeugmaschinen am Beispiel von Kugelgewindetrieben

Band 210
Dr.-Ing. Emanuel Moser

Migrationsplanung globaler Produktionsnetzwerke
Bestimmung robuster Migrationspfade und risiko-effizienter Wandlungsbefähiger

Band 211
Dr.-Ing. Jan Hochdörffer

Integrierte Produktallokationsstrategie und Konfigurationssequenz in globalen Produktionsnetzwerken

Band 212
Dr.-Ing. Tobias Arndt

Bewertung und Steigerung der Prozessqualität in globalen Produktionsnetzwerken

Band 213
Dr.-Ing. Manuel Peter

Unwuchtminimale Montage von Permanentmagnetrotoren durch modellbasierte Online-Optimierung

Band 214
Dr.-Ing. Robin Kopf

Kostenorientierte Planung von Fertigungsfolgen additiver Technologien

Band 215
Dr.-Ing. Harald Meier

Einfluss des Räumens auf den Bauteilzustand in der Prozesskette Weichbearbeitung – Wärmebehandllung – Hartbearbeitung

Band 216
Dr.-Ing. Daniel Brabandt

Qualitätssicherung von textilen Kohlenstofffaser-Preforms mittels optischer Messtechnik

Band 217
Dr.-Ing. Alexandra Schabunow

Einstellung von Aufnahmeparametern mittels projektionsbasierter Qualitätskenngrößen in der industriellen Röntgen-Computertomographie

Band 218
Dr.-Ing. Jens Bürgin

Robuste Auftragsplanung in Produktionsnetzwerken
Mittelfristige Planung der variantenreichen Serienproduktion unter Unsicherheit der Kundenauftragskonfigurationen

Band 219
Dr.-Ing. Michael Gerstenmeyer

Entwicklung und Analyse eines mechanischen Oberflächenbehandlungsverfahrens unter Verwendung des Zerspanungswerkzeuges

Band 220
Dr.-Ing. Jacques Burtscher

Erhöhung der Bearbeitungsstabilität von Werkzeugmaschinen durch semi-passive masseneinstellbare Dämpfungssysteme

Band 221
Dr.-Ing. Dietrich Berger

Qualitätssicherung von textilen Kohlenstofffaser-Preforms mittels prozessintegrierter Wirbelstromsensor-Arrays

Band 222

Dr.-Ing. Fabian Johannes Ballier

Systematic gripper arrangement for a handling device in lightweight production processes